UNIVERSITY OF MILANO-BICOCCA

SCHOOL OF MEDICINE AND FACULTY OF SCIENCE

PH.D. PROGRAM IN MOLECULAR AND TRANSLATIONAL MEDICINE (DIMET)

Embryonic Vessel-Associated Progenitors in Skeletal Muscle Development and in Tissue Repair.

Dr. Valentina Conti

Matr. No. 050540

Tutor: Prof. Silvia Brunelli

XXV CYCLE

Academic Year 2011-2012

A te amore mio,

che sei la mia anima gemella.

Life and dreams are leaves of the same book: reading them in order is living, skimming through them is dreaming / La vita e i sogni sono fogli di uno stesso libro. Leggerli in ordine è vivere, sfogliarli a caso è sognare.

Arthur Schopenhauer

Table of Contents

Chapter I. General Introduction

1.1. The embryonic origin of skeletal muscle

1.1.1. The onset of myogenesis in the embryo

The development of skeletal muscle is a complex process. All vertebrate skeletal muscles (apart from head ones) are derived from mesodermal precursor cells originating from the somites. Somites are transient segments of paraxial mesoderm that form progressively on either side of the neural tube, following an anterior-to-posterior developmental gradient [1]. Within hours of somite epithelialization, dorsoventral orientation becomes established by the formation of the epithelial dermomyotome (in the dorsal domain) and the mesenchymal sclerotome (in the ventral domain). Cells of the dermomyotome are specified as myoblasts and dermal fibroblasts, while cells of the sclerotome will form cartilage and bone.

As development proceeds, the dermomyotome of each somite expands along the dorso-ventral axis, and develops specialized zones at the dorsomedial (DML) and ventrolateral (VLL) lips. The DML provides myoblasts for all epaxial muscles, while the VLL is the source of myoblasts for the hypaxial muscles [2, 3]. The epaxial myotome, which gives rise to the deep back muscle, is formed when progenitor cells of the DML extend beneath the dermomyotome, exit the cell cycle, elongate and terminally differentiate [1, 4, 5]. Similarly, the VLL establishes the ventral non-migratory hypaxial myotome, which gives rise to the lateral trunk muscles (Fig.1).

The formation of head and limb muscles differ from this general process. The head muscles originate from three sources of mesoderm: occipital somites (that give rise to the tongue and

laryngeal muscles) and paraxial head mesoderm and prechordal mesoderm (that give rise to all the craniofacial muscles) [3, 6, 7]. The limb myogenic progenitors, unlike other hypaxial muscles, delaminate directly from the VLL of limb adjacent somites and undergo a long-range of migration towards the target sites in the limb [5, 8]. The migrated cells then proliferate to amplify their numbers [9] and differentiate into fusion competent myoblasts which will fuse to form multinucleated myotubes (Fig.1).

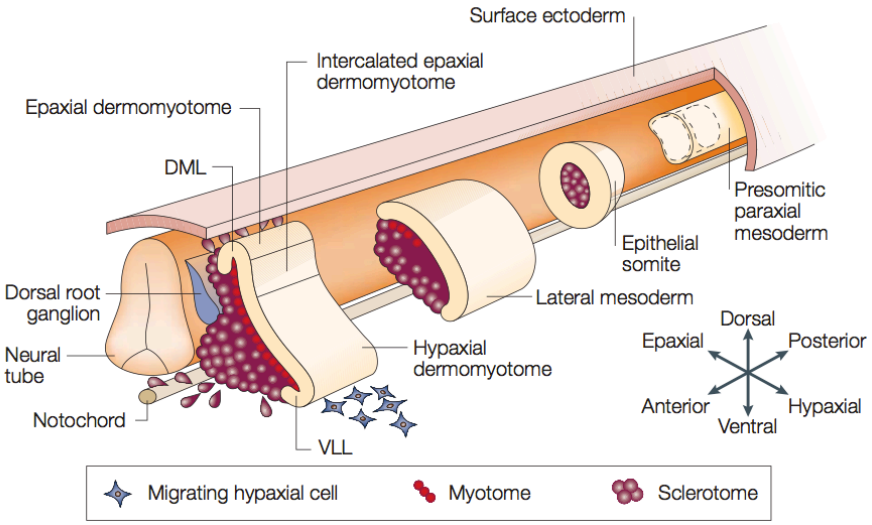

Fig.1. The embryonic origin of limb and trunk skeletal muscle.

1.1.2. Specification of myogenic identity: From signaling molecules to downstream genes

The determination of the somitic myogenic compartment is largely influenced by the interplay of diffusible signals secreted by neighboring tissues [10] (Fig. 2). Axial structures such as the notochord and the neural tube [11-13] secrete signaling molecules such as Sonic Hedgehog (Shh) and Wnts, that act

as positive effectors of epaxial myogenic progenitor cells (MPCs) determination [14-21]. Hypaxial MPCs are subjected to the effects of Wnt signaling from the dorsal ectoderm, in addition to negative bone morphogenetic protein (BMP) signaling from the lateral mesoderm in limb-level somites [22-24].

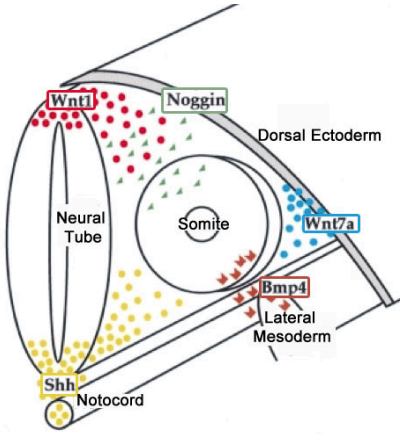

Fig.2. Signaling molecules in newly formed epithelial somite.

Activation of myogenesis is controlled by a series of complex transcriptional regulatory networks that control the expression of members of the bHLH transcription factors known as the myogenic regulatory factors (MRFs) [25]. This family includes Myf5, Mrf4 (also known as Myf6), MyoD, and myogenin (Myog) and control muscle cell determination and differentiation [26]. MRFs, together with other cofactors, control the expression of genes required to generate the contractile properties of a mature skeletal muscle cell. Experimental studies about the MRF family have suggested that Myf5 and MyoD act redundantly and upstream of Myog. Combined inactivation of Myf5 and MyoD results in a complete lack of skeletal muscle formation, whereas inactivation of either gene alone results in relatively normal myogenesis after transient defects [27]. Myog

mutants initiate myogenesis normally but show defects in the differentiation of myocytes and myofibers [28, 29]. Initial studies of the Mrf4 knockout mouse suggested that, similarly to Myog, Mrf4 acts downstream of the redundant activities of Myf5 and MyoD. However, recently, it has emerged that the original gene targeting of the Myf5 locus resulted in the concomitant loss of function of the neighboring Mrf4 gene [30]. Rescue of Mrf4 function in Myf5;MyoD double mutant embryos partially restore embryonic myogenesis, suggesting that Mrf4 may have some role also in myogenic determination.

Together, these experiments demonstrate that redundancy can act through the existence of two distinct lineages of muscle cells, one specified by MyoD and the other by Myf5; either of them can compensate for the loss of the other.

Currently, the idea is that Myf5, MyoD and Mrf4 are essential for skeletal muscle determination and acquisition of a myoblast precursor fate; while Myog, MyoD and Mrf4 are required for terminal differentiation (Fig.3).

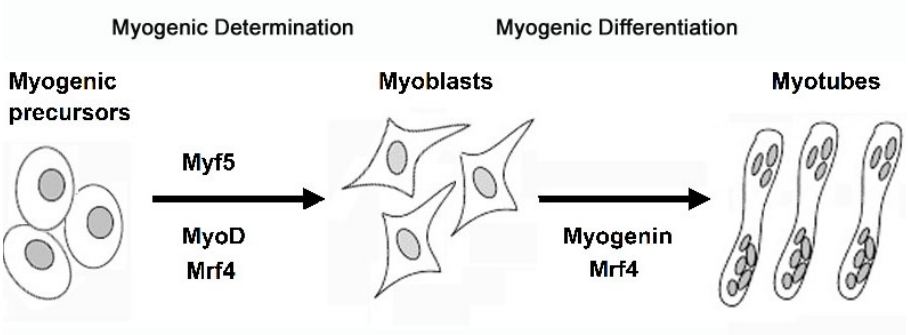

Fig.3. Involvement of Myogenic Regulatory Factors in Myogenesis. Myf5 and MyoD are involved in specification / commitment of muscle progenitors into skeletal muscle lineage. Mrf4 also plays a role as a determination gene in addition to directing terminal differentiation with myogenin.

Genetic studies have provided insight into the regulatory genes that act upstream of the MRFs. These studies have shown that MRFs act downstream of (or in parallel with) the paired domain and homeobox containing transcription factors paired box gene 3 (Pax3) and 7 (Pax7), in different phases of myogenesis in the embryo and in the adult [31]. Pax3 is first expressed in the presomitic mesoderm [32, 33] and at the onset of dorso-ventral somite compartmentalization, it is expressed throughout the entire epithelial dermomyotome. Expression of Pax3 is subsequently down regulated in the DML, becoming regionalized to the hypaxial VLL domain [34]. The Pax7 expression domain is partially overlapping to that of Pax3 during the early epithelial dermomyotome stage [35, 36]. Pax3 is required for myogenic specification upstream of MyoD [34], somite segmentation and dermomyotome formation [26, 37], limb musculature development [38, 39] and MyoD and Myf5 expression [40, 41]. Most of the functions of Pax3 can be replaced by its paralogue Pax7 [16, 42]. However, Pax7 was shown to be necessary only for the maintenance of adult satellite cells [43, 44], indeed, unlike Pax3, Pax7 deficiency does not affect embryonic myogenesis [45].

During maturation of the somite, starting from E10.5, the central region of the dermomyotome loses its epithelial structure and Pax3/Pax7 positive cells enter the myotome [46-49]. Such Pax3/Pax7 positive cells are present in all developing skeletal muscle masses at late embryonic and fetal stages [47-50]. Most of these cells are proliferating and do not express skeletal muscle markers. However, they give rise to myogenic cells, marked by the expression of Myf5 and MyoD, and to subsequent muscle fibers, thus providing a reserve of myogenic progenitor cells during embryonic and fetal

development.

‘‘Embryonic’’ or primary fibers appear at E11 in the mouse and establish the basic muscle pattern. “Fetal” or secondary myogenesis occurs between E14.5 and E17.5 and involves the fusion of fetal myoblasts either with each other to form secondary fibers (initially smaller and surrounding primary fibers), or with primary fibers. At E16, satellite cells appear as mononucleated cells underneath the newly formed basal lamina of each individual fiber (Fig. 4).

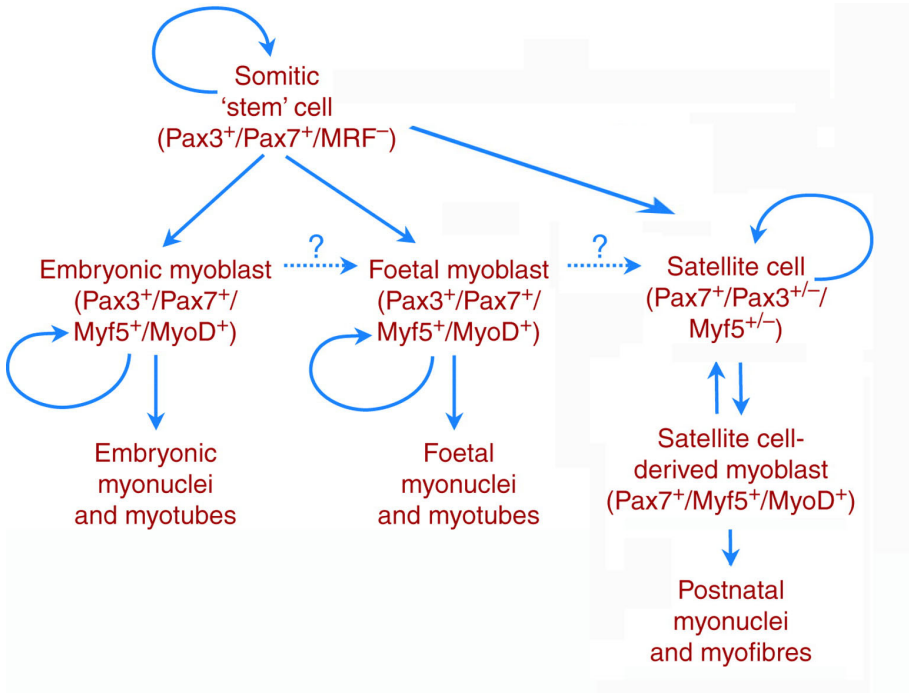

Fig.4. Schematic summary of normal myogenesis from uncommitted mesoderm to myotube. Pax3/Pax7 positive somitic stem cells give rise to muscle precursors during development (embryonic, fetal myoblasts and satellite cells). Embryonic and fetal myoblasts give rise to 1° and 2° fibers, respectively. Satellite cells appear at the end of gestation and are responsible for postnatal growth and regeneration.

1.2. Adult Skeletal Muscle Biology

1.2.1. Structural Organization of Skeletal Muscle Tissue

The histological and functional cellular units of adult mammalian skeletal muscles are the muscle fibers (myofibers), multinucleated syncytia with their post-mitotic myonuclei located in a subsarcolemmal position [51, 52]. Myofibers stretch along the entire length of the muscle and their cytoplasm (sarcoplasm) contains myofibrils (composed of sarcomeres) and mitochondria. Sarcomeres consists of thick myosin-rich filaments and thin actin-rich filaments and generate force by contraction. The basic mechanism of muscle contraction is the result of a "sliding mechanism" of the myosin-rich thick filament over the actin-rich thin filament, after neuronal activation [53].

Skeletal muscle tissue is characterized by the richness in connective tissue, that provides the framework to transform contraction force into movement, and the high degree of vascularization, fundamental to provide essential nutrients and oxygen for muscle function.

The individual myofibers are bound together by a connective tissue structure composed of three levels of sheaths: the epimysium is the fibrous outer layer that surrounds the complete muscle and is contiguous with the tendons (that link muscle to bone), the perimysium surrounds the bundles of myofibers, and the endomysium (also referred to as basal lamina or basement membrane) surrounds individual myofibers.

Myofibers are heterogeneous with respect to their contractile properties, ranging from slow/oxidative to fast/glycolytic types and the proportion of each fiber type within a muscle

determines its overall contractile property [3] (Fig. 5).

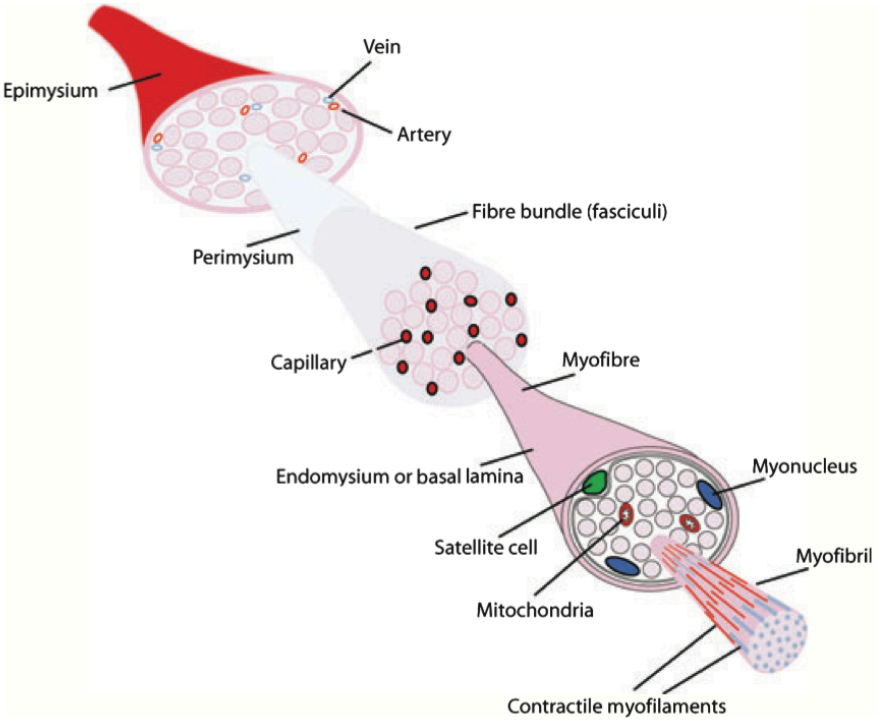

Fig.5. Skeletal muscle and associated structures.

1.2.2. Satellite Cells: the Adult Resident Muscular Stem Cells

Half a century ago, Alexander Mauro observed by electron microscopy the presence of mononucleated cells intimately associated with skeletal muscle fibers of the frog [54]. He called these cells “satellite cells” (SCs) due to their peripheral, sub-laminar position. SCs were subsequently identified in skeletal muscles of other vertebrates, including humans. The direct juxtaposition of SCs with myofibers immediately raised a hypothesis about their involved in skeletal muscle growth and regeneration [55].

Typically mitotically quiescent (G0 phase), SCs are present throughout skeletal muscle but show an unequal distribution

between different muscle groups and fiber types (slow twitch fibers with higher number of SCs). The unequal distribution of SCs is also apparent along individual myofibers with higher numbers of SCs associating with the neuromuscular junction as well as adjacent to capillaries.

SCs are rare in uninjured muscles: at birth, they account for 20–30% of sublaminar nuclei in mouse skeletal muscle. As mice grow and mature this number rapidly declines to approximately 5% at two months of age and to 2% in senile mice. Nevertheless, SCs have a remarkable proliferative potential and can efficiently repair even severely damaged muscles. Upon exposure to signals from a damaged environment, SCs become activated, undergo proliferative expansion and generate myoblasts that terminally differentiate by fusing to each other or with damaged fibers. Similarly, in growing muscles, SC progeny fuse with existing fibers. Interestingly, the SC compartment is maintained after multiple rounds of degeneration and regeneration. A fraction of activated SCs, indeed, do not terminally differentiate, but restore the SC pool by self-renewal, re-occupying a position under the basal lamina. By definition, stem cells found in adult tissues can both replicate themselves (self-renew) and give rise to functional progeny (differentiate). Thus SCs can be properly considered the adult stem cells of skeletal muscle [45, 56].

1.2.2.1. Satellite Cell Molecular Markers

SCs were considered to be a homogeneous population of committed muscle progenitors [57]. However, recent evidence demonstrated that they represent a heterogeneous population of cells. This heterogeneity is evident for a series of different

criteria, such as gene expression signatures, myogenic differentiation propensity, stemness, and lineage potential to assume nonmyogenic fates [58, 59].

Classically, SCs were identified by electron microscopy based on their anatomical location as well as on other morphological characteristics such as large nuclear-to-cytoplasmic ratio, few organelles, small nucleus, and condensed interphase chromatin.

Over the past decades, several molecular markers of SCs have been found, allowing their identification by fluorescence microscopy in muscle sections or in single fiber preparations. In adult skeletal muscle, all or most of SCs express characteristic, although not unique, markers (Fig. 6).

Pax7 is the canonical biomarker as it is specifically expressed in all quiescent and proliferating SCs [45] across multiple species, including human [60], monkey [60], mouse [45], pig [61], chick [62], salamander [63], and zebrafish [64].

Some of these markers are membrane proteins and are therefore used for large scale isolation of SCs by fluorescent-activated cell sorting (FACS), usually with a combination of positive (satellite cell-specific cell surface markers) and negative (definitive cell surface markers for non-satellite cell populations) selection. Mutant mice in which the expression of reporter genes is under the control of satellite cell-specific genes are also available and represent another way to identify and isolate SCs.

Marker	Species[a]	Expression Q	A	D
Cell surface				
c-met	m, h	+	+	+
Caveolin-1	m	+	–	–
CD34	m	+	+	+
CTR	m	+	–	–
CXCR4/SDF-1	m, h	+	+	+
ErbB receptor	m	–	+	+
Igsf4a	m	+	+	–
Integrin α_7	m, h	+	+	+
Integrin β_1	m, h	+	+	+
M-cadherin	m, h	+	+	+
Necdin	m	–	+	+
Megf10	m	+/–	+	–
NCAM	m, h	+	+	+
Neuritin-1	m	+	+	–
p75NTR/BDNF	m	+	+	–
Pb99	m	+	+	–
SM/C-2.6	m	+	+	–
Sphingomyelin	m	+	–	–
Syndecan 3/4	m	+	+	+
TcRβ	m	+	+	–
VCAM-1/VLA-4	m	+	+	+
Transcription factor				
Foxk1	m	+	+	+
HoxC10	m	+	+	+
Lbx1	m	–	+	+
Myf5	m, h	+	+	+
MyoD	m, h	–	+	+
Msx1	m	+	–	–
Pax3	m	+/–	+/–	–
Pax7	m, h	+	+	–
Sox8/9	m	+	+	–
Other				
Desmin	m, h	+/–	+	+
Myostatin/ACVR2	m, h?	+	+	+
Nestin	m, h	+	–	–

Fig.6. Satellite cell markers. Abbreviations used: Q, quiescent satellite cell; A, activated (cycling) satellite cell; D, differentiating myoblast. Species column includes mouse (m) and human (h).

1.2.2.2. Satellite Cell Niche

According to the stem cell niche concept, behaviors of tissue-specific stem cells are determined by structural and biochemical cues emanating from the surrounding microenvironment.

SCs are present in a highly specified niche, which consists of the extracellular matrix (ECM), vascular and neural networks, different types of surrounding cells, and various diffusible molecules (Fig. 7). The dynamic interactions between SCs and

their niche specifically regulate their quiescence, self-renewal, proliferation and differentiation [59, 65, 66].

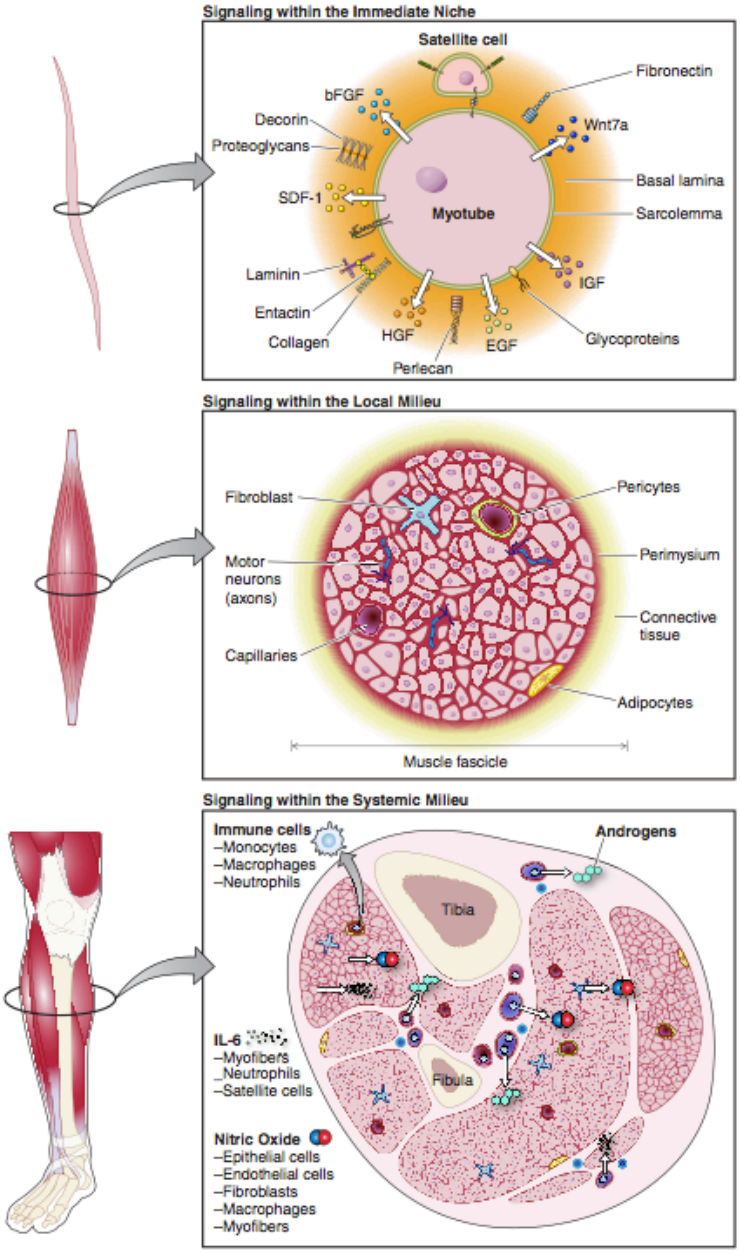

Fig.7. The satellite cell niche.

The myofibers are the primary component of the immediate niche due to their direct contact with SCs. Numerous extracellular matrix (ECM) components and cellular receptors are present either on the surface of the sarcolemma, on SCs or contained within the basal lamina. The basal lamina of the skeletal muscle is composed of different ECM molecules (including type IV collagen, laminin, fibronectin, elastin and proteoglycans) that directly contacts the SC and separates it from the muscle interstitium. These molecules are mainly synthesized and excreted by interstitial fibroblasts but can also be produced and remodeled by myoblasts during muscle development and regeneration.

Proteoglycans reside on the surface of SCs and function as receptors to bind a group of secreted, yet inactive, growth factor precursors, including HGF, basic fibroblast growth factor (bFGF), epidermal growth factor (EGF), insulin-like growth factor isoforms (IGF-I, IGF-II) and various Wnt glycoproteins, that originate from either SCs, myofibers, interstitial cells, or serum. All these physical interactions are crucial for SC activation as they allow the transduction of extracellular mechanical force into intracellular chemical signals.

The muscle fascicle defines the extremities of the local milieu, an environment composed of several myofibers in addition to local interstitial cells, blood vessels and motor neurons. Each of these cell types influences the surrounding environment and thereby affects SCs.

Interstitial cells are the major component of the stromal tissue between the basal lamina and epimysial sheath surrounding skeletal muscle and fibroblasts represent the dominant cell population. Fibroblasts secrete growth factors, such as FGFs, and also contribute to skeletal muscle ECM molecules

deposition [67].

The importance of motor neurons for SCs is revealed by the higher incidence of SCs observed in the proximity of the motor endplate. It is known that long-term denervation results in progressive skeletal muscle atrophy and in a drastic decline in the number of SCs, due to their decreased proliferation and increased apoptosis. Moreover, it has been shown that neurotrophins, such as nerve growth factor (NGF) and brain-derived neurotrophic factor (BDNF), function in an autocrine fashion to regulate SC behavior.

The microvascular network is of primary importance for SCs. Most SCs remain in close proximity to capillaries regardless of their state of quiescence, proliferation and differentiation. In adult human muscles 88% of SCs are found within a 21-micron distance of a capillary.

The systemic milieu contains the greatest diversity of cells and factors by which SCs are influenced. SCs are exposed to the host immune system and to circulating hormones. Changes that occur in the systemic milieu affect SCs gradually and the prolonged exposure of signals from the systemic milieu plays an important role in the regulation of the behavior of SCs.

1.3. Skeletal Muscle Regeneration

1.3.1. Morphological Features of Skeletal Muscle Regeneration

Adult mammalian skeletal muscle is a relatively stable tissue with little turnover of nuclei [68]. Minor lesions caused by normal everyday activity elicit only a slow turnover of its constituent multinucleated muscle fibers. It is estimated that in a normal adult rat muscle, no more than 1–2% of myonuclei are replaced every week. Nevertheless, skeletal muscle has the

ability to complete a rapid and extensive regeneration in response to severe damage.
Whether the muscle injury is inflicted by a direct trauma or innate genetic defects, muscle regeneration is invariably characterized by two phases: a degenerative phase and a regenerative one [69, 70] (Fig. 8).

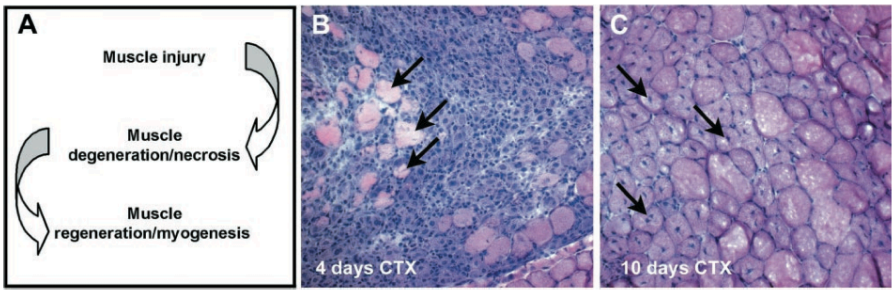

Fig.8. The Skeletal muscle repair process. A: After muscle injury there is a degenerative phase followed by a regenerative phase. B: injury due to cardiotoxin (CTX) injection results in the rapid necrosis of myofibers and the activation of an inflammatory response. C: myofiber regeneration is characterized by the activation of myogenic cells to proliferate and differentiate. Regenerating fibers are characterized by their small caliber and their centrally located myonuclei (arrows).

The process of muscle regeneration follows a centripetal gradient (from the outer regions to the inner regions), which results in the formation of different zones within a regenerating muscle, each zone possibly being in a different phase of degeneration or regeneration. *In vivo*, muscle regeneration can be followed by histological analyses of muscle cross-sections. A regenerating muscle is indeed characterized by a series of typical and well-defined morphological features. On muscle cross-sections, newly formed myofibers can be readily distinguished by their small caliber and centrally located

myonuclei. These myofibers are often basophilic (reflecting high protein synthesis) and express embryonic/developmental forms of MHC (reflecting *de novo* fiber formation) [71, 72]. Fiber splitting or branching is also a typical feature of muscle regeneration and is probably due to the incomplete fusion of fibers regenerating within the same basal lamina [73].

1.3.2. Satellite Cells in Skeletal Muscle Regeneration

The initial event of muscle degeneration is characterized by necrosis of muscle fibers, generally triggered by disruption of the sarcolemma resulting in increased myofiber permeability and increased calcium influx. The loss of calcium homeostasis and the subsequent activation of calcium-activated proteases (calpains) that cleave myofibrillar and cytoskeletal proteins, lead to a process of autolysis of myofibers [74]. Immediately after injury, cytokines and growth factors are released from both the injured myofibers, blood vessels and inflammatory cells. These factors stimulate the chemotactic recruitment of circulating leukocytes to the site of injury.

Neutrophils are the first inflammatory cells to invade the injured muscle and their number significantly increases as early as 1-6 hours after damage [75]. Following neutrophil infiltration, macrophages become the predominant inflammatory cells and two distinct subpopulations that sequentially invade the injured muscle can be defined [76-79]. The early invading macrophages, the classically activated (or type I), reach their highest concentration in damaged muscle at 24 h after damage and thereafter rapidly decline. These macrophages secrete proinflammatory cytokines, such as tumor necrosis factor-α (TNF-α) and interleukin-1 (IL-1), and are responsible for the phagocytosis of cellular debris. The second population

of macrophages, the alternatively activated (or type II) reaches their peak at 2–4 days after injury. These cells are involved in wound healing, have immunoregulatory functions secreting anti-inflammatory cytokines, such as IL-10, and persist in damaged muscle until the resolution of inflammation [80, 81]. Macrophages are essential element for the regeneration process. They produce a vast array of signals involved in matrix remodeling, neovessel formation and activation of SCs and it has been shown that monocyte/macrophage depletion at the time of injury totally prevents spontaneous muscle regeneration [78, 79, 82-87].

Myogenic cell proliferation is another important event necessary for muscle regeneration. The expansion of myogenic cells provides a sufficient source of new myonuclei for muscle repair [88-92].

Upon damage, quiescent SCs are activated and initiate multiple rounds of proliferation. The descendants of activated SCs are referred to as myogenic precursor cells (mpcs) or adult myoblasts. SCs appear to form a population of stem cells that are distinct from their daughter mpcs as defined by biological and biochemical criteria [57, 93].

Some of the activated cells then exit from the cell cycle and return to their niche as quiescent satellite cells to replenish the SC pool for subsequent muscle repair [52]. Other SCs migrate reach the site of injury, exit from the cell cycle and undergo differentiation. These differentiated myoblasts can either form multinucleated myofibers (hyperplasia) or fuse to the damaged myofibers (hypertrophy) for muscle regeneration [88]. During these later stages of muscle regeneration, muscle nuclei align along the longitudinal axis of the muscle fiber, becoming central nuclei. Upon completion of terminal differentiation, the

central nuclei migrate to the surface of the muscle fiber (Fig. 9).

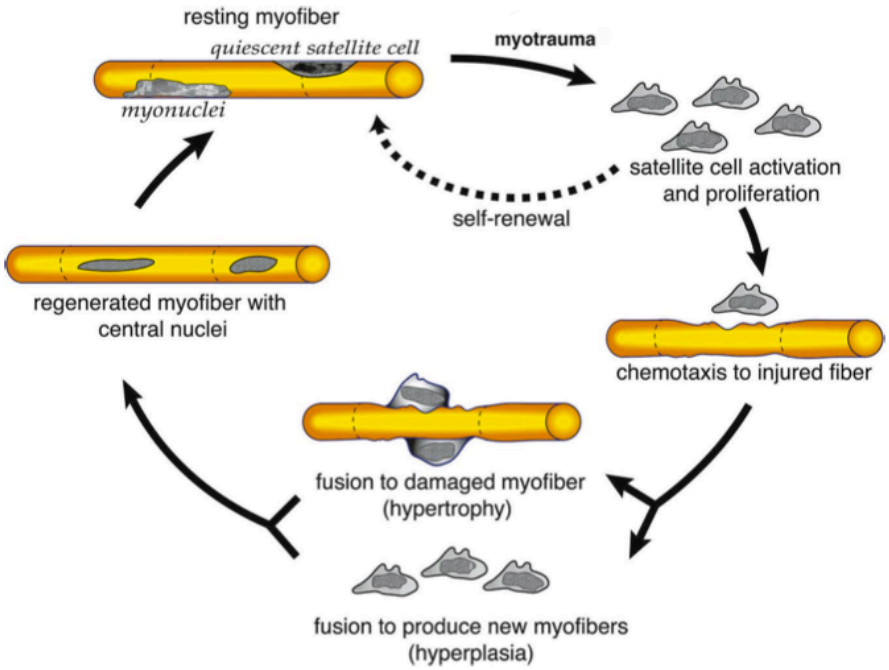

Fig.9. Schematic representation of the cycle of satellite cell activation, proliferation, and differentiation following muscle injury

At the molecular level, activation of mpc is characterized by the rapid up regulation of two MRFs, Myf5 and MyoD in a program analogous to the one occurring during the embryonic development of skeletal muscle. Quiescent satellite cells express no detectable levels of MRFs. Upon activation, MyoD is rapidly up-regulated within 12h of muscle injury and is detectable prior to expression of proliferating cell nuclear antigen (PCNA), a marker for cell proliferation [94]. SCs activated after CTX injury [95] first express either Myf5 or MyoD, followed soon after by co-expression of these two markers. Following proliferation, myogenin and MRF4 are

expressed in cells beginning their terminal differentiation program.

SC self-renewal, fundamental to maintain the pool of SCs for subsequent round of regeneration, may result from an asymmetric division generating two different daughter cells, one committed to myogenic differentiation and one identical to the original stem cell. Alternatively, SCs may undergo symmetric division with one daughter cell being able to withdraw from the differentiation program and return to quiescence. Recent research demonstrated that SCs can undergo both kind of divisions within their natural niche environment [96, 97]. The choice of asymmetric versus symmetric division is largely correlated to the mitotic spindle orientation relative to the longitude axis of the myofiber and Notch signaling has been shown to play an important role of asymmetric division [98]. Members of the canonical/β-catenin-dependent and of the non-canonical Wnt pathways appear to be relevant for SC self-renewal, the latter involving Wnt7a, its receptor Frizzled7 (Fzd7) and Vangl2, the mammalian homologue of the Drosophila Vangl2/Stbm [99-106].

1.3.3. Contribution of non-satellite cells in Muscle Regeneration

During the last decades stem cells isolated from various tissues have been shown to differentiate *in vitro* and *in vivo* upon transplantation into multiple lineages, depending on environmental cues, and this is true also for skeletal muscle. It has been unequivocally demonstrated the existence of myogenic progenitors (distinct from SCs) originating from skeletal muscle or other tissues. For example, progenitor cells isolated from the bone marrow [107], the adult musculature,

the neuronal compartment and various mesenchymal tissues can differentiate into the myogenic lineage.
Upon transplantation, these cells have been shown to participate in muscle regeneration in wild-type and/or dystrophic mice, eventually entering the SC pool.
When identified, the anatomical niche of these cells has been often associated with blood vessels (Fig. 10).

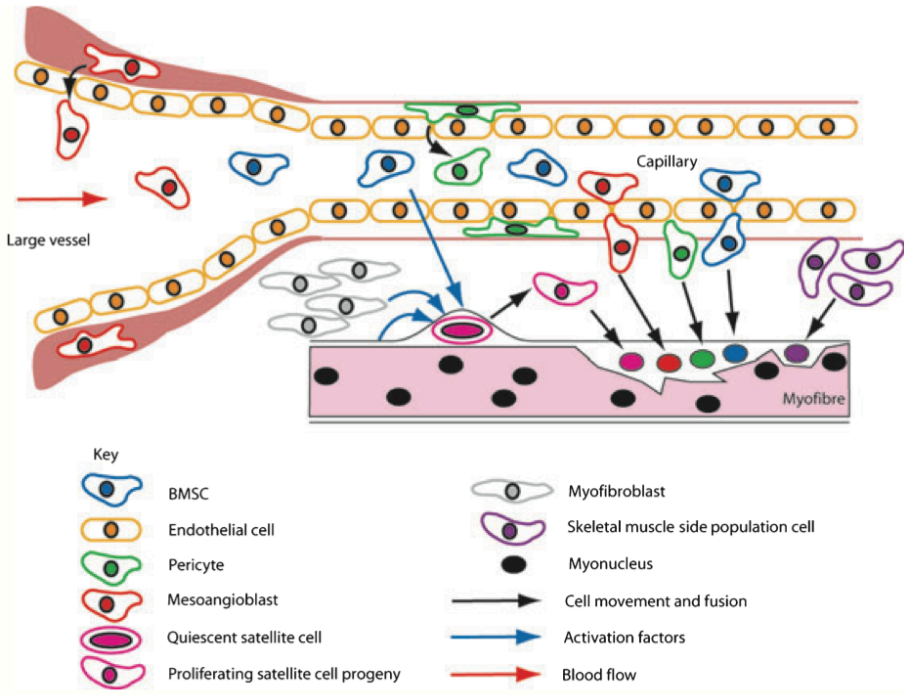

Fig.10. Schematic representation of the major cell types that has been shown to engraft into regenerating skeletal muscle.

Recently, it has been demonstrated that SCs are indispensable for adult skeletal muscle regeneration and that other cell types with regenerative potential depend on their presence [108]. However, the interest in these non-satellite stem cells remains high, due to their peculiar characteristics, such as higher stem

cell-like properties, ability to migrate extensively in the muscle bed, cross vascular tissue from the circulation and self renew with significantly higher capacity than SCs [109-112]. Below, a brief description of some of these unorthodox myogenic cells.

Bone marrow (BM) stem cells. Upon transplantation (either BM transplantation [BMT] or direct injection into skeletal muscle), these cells are incorporated into newly formed myofibers within regenerating muscles [113-115].

Lineage tracing experiments have demonstrated that BM cells were able to reconstitute the SC niche and these BM-derived SCs can undergo myogenic differentiation *in vitro* and give rise to myofibers when injected into damaged muscles [116].

Adult BM contains hematopoietic stem cells (HSC) and stromal cells (also called mesenchymal stem cells, MSC) and conflicting results exist regarding the exact BM-derived progenitor cell type(s) contributing to muscle regeneration. HSC are able to incorporate into newly forming myofibers, although it is unclear whether they occupy the SC niche [117-120]. MSC are able to incorporate into myofibers in injured muscles and give rise to SCs, which can support multiple rounds of muscle regeneration [121, 122].

These results opened the possibility of treating muscular dystrophies by BMT, but work in mice indicated that, unfortunately, the frequency of this event was too low [115, 123]. Future studies are required to define the subpopulation(s) of BM cells, which have long-term myogenic potential *in vivo* in order to enrich their specific fraction.

Muscle side population cells. Similarly to other tissues, including BM, an enriched population of adult stem cells can be isolated from skeletal muscles by FACS analysis on the

basis of the exclusion of Hoechst 33342 staining and this is called muscle side population (mSP). Early experiments demonstrated that mSP cells have the ability, upon intramuscular transplantation, to give rise to both differentiated muscle cells and SCs [115]. In addition mSP cells transplanted intravenously are able to engraft in the skeletal muscle of dystrophic mice [125]. Moreover, when host mice were lethally irradiated, mSP cells appeared to provide short-term hematopoietic reconstitution of the BM [115]. As described for other SPs [126, 127], CD45 expression defined two different mSP subsets: a main population of CD45- cells and a minor population of CD45+ cells [128]. Subsequent studies have indicated that the hematopoietic potential of mSP cells resides in a small fraction that expresses the hematopoietic cell marker CD45, whereas the "myogenic" fraction is negative for CD45. Accordingly, lineage tracing experiments have revealed that only the main population of CD45- mSP cells arise from the somites, suggesting the minor CD45+ mSP cells might have distinct origins, possibly from endothelial, hematopoietic stem, or bone marrow cells [50].

The majority of mSP cells reside in the skeletal muscle interstitium juxtaposed to blood vessels, which make them distinct from satellite cells and bone marrow-derived SP cells. mSP increases in number following muscle injury [129, 130]; it is not clear if these cells migrate into the injured muscle, or expand within the muscle as a response to injury (or both).

PW1+ interstitial cells (PICs). It has been reported that some interstitial cells, characterized by their expression of PW1 (also called peg3), might be involved in perinatal skeletal muscle growth [131]. Moreover, it has been reported that adult stem cells/progenitors residing in multiple tissues/organs can be

directly identified and isolated from PW1-reporter mice [132]. PW1 is strongly transcribed in skeletal muscle in both embryonic and postnatal stages [133, 134] and within skeletal muscle, PW1 expression was detected in both SCs and a group of non-satellite interstitial cells called PICs (PW1+ interstitial cells) [135, 136]. PICs have myogenic potential when cultured *in vitro* and, when transplanted into injured muscles, they give rise to both interstitial cells and SCs [137]. Although not directly assessed by lineage tracing, recent observations support the hypothesis that PICs may contribute to the SC population during postnatal muscle growth and during adult muscle regeneration. Of note, Pax3 lineage tracing experiments further indicated that PICs do not arise from embryonic Pax3+ myogenic progenitor cells, indicating a distinct developmental lineages between PICs and SCs.

Muscle-derived stem cells. A series of studies have demonstrated that a distinct cell population, termed muscle-derived stem cells (MDSCs), can be isolated from skeletal muscles based on their weak adhesion characteristics and long-term proliferation behaviours in culture [138-140]. Marker expression characterization of MDSCs indicated that these cells are distinct from SCs and hematopoietic cells but more similar to mSP. A unique characteristic of MDSCs is their multipotency, indeed they can differentiate into myogenic, adipogenic, osteogenic, chondrogenic and hematopoietic lineages. After intra-arterial transplantation, MDSCs contribute to regenerated myofibers, incorporate into the SC niche, and also give rise to endothelial and neural cells. Like mSP, MDSCs can repopulate the hematopoietic lineage in irradiated murine hosts, and the reconstituted BM can in turn contribute to muscle regeneration. It has been shown that MDSCs are more

efficient than myoblasts at forming dystrophin-positive myofibers when directly transplanted into mdx mice [141, 142].

Multipotent adipose-derived stem cells. Adipose tissue is composed primarily of adipocytes, but also multipotent progenitor cells are present. MADS have been shown to differentiate into cells of the mesodermal lineage including adipocytes, chondrocytes, osteoblasts, osteoclasts, and myoblasts [143]. Recently, the myogenic and muscle repair capacities of human MADS cells have been enhanced by transient expression of MyoD [144]. Because of their plasticity and accessibility, adipose-derived stem cells could be an important tool for cell-mediated therapy for skeletal muscle disorders.

Pericytes. Pericytes (also called Rouget cells or mural cells) are contractile connective tissue cells residing beneath the microvascular basement membrane. Pericytes originate from the embryonic sclerotome and are believed to regulate the blood flow in capillaries [145, 146]. As a multipotent stem cell population, they can differentiate into adipocytes [147], chondrocytes [147] and osteoblasts [148, 149] *in vitro* and into skeletal muscles both *in vitro* and *in vivo* [112, 150]. These cells do not express Pax7, Myf5, or MyoD, suggesting that pericyte-mediated myogenesis may follow a myogenic differentiation program distinct from that of SCs. Pericytes display a specific cell surface marker combination, which makes them distinct from other cell types [151-153]. Cells carrying the same surface markers can be isolated from various tissues, including pancreas, adipose tissue and placenta and, regardless of their origins, were able to differentiate into skeletal muscle cells when cultured *in vitro*

[154]. Transplantation of pericytes into combined immune deficient-X-linked, mouse muscular dystrophy (scid-mdx) mice through the femoral artery gave rise to numerous myofibers expressing dystrophin and a small portion of transplanted pericytes incorporated beneath the basal lamina of myofibers, indicating the ability to occupy the SC niche [112]. The myogenic potential, together with their abilities to be cultured *in vitro* and penetrate the blood vessel wall, makes pericytes another promising candidate for future cell-based therapies to treat muscular dystrophy.

Mesoangioblasts. Mesoangioblasts (MABs) are vessel-associated progenitors that were originally isolated from the wall of the mouse embryonic dorsal aorta [155, 156]. These cells express early endothelial (as well as several pericyte) markers, are highly proliferative when cultured *in vitro* and are multipotent, being able to give rise to multiple mesodermal lineages, such as bone, cartilage, smooth, cardiac and skeletal muscle following transplantation [156]. MABs-like cells were later isolated from vessels of post-natal tissues in the mouse, rat, dog and human. Post-natal MABs generally express pericyte rather than endothelial cell markers but are similar to their embryonic counterparts in terms of proliferation and differentiation potency. While rodent derived MABs eventually become aneuploid and immortal, MABs isolated from dogs and humans proliferate to a limited extent and undergo senescence, remaining euploid.

Although the contribution of MABs to normal muscle development is not yet established, multiple studies have demonstrated that they can be employed via intra-artery injection to improve muscle regeneration, also for dystrophic mice and dogs [110, 111]. MABs can extravasate and reach to

regenerating muscles via the bloodstream and it has been shown that they can release immunosuppressive and tolerogenic molecules [157]. Several reports demonstrated that factors involved in normal muscle regeneration also facilitate MABs-based muscle regeneration. For example, HMGB1, CXCR4, SDF-1 and alpha4-integrin have been shown to enhance the migration of MABs from blood vessels toward injured muscles [158, 159]. Similarly, pre-treatment of MABs with nitric oxide before transplantation also stimulated alpha-sarcoglycan expression in MABs-derived myofibers [160]. Taken together, investigations on MABs have revealed great therapeutic potential for the structural and functional amelioration of human dystrophic diseases.

CD133+ cells (AC133). Recent studies demonstrated that a fraction of CD133+ (also called AC133) mononucleated cells in adult peripheral blood have myogenic potential. Freshly isolated human CD133+ cells can undergo myogenic differentiation when co-cultured with myogenic cells or exposed to Wnt-producing cells *in vitro*. Importantly, when transplanted via intra-arterial or intramuscular injection, they can fuse with regenerating muscles in dystrophic mice. Moreover, after transplantation, these cells are able to reconstitute the SC niche [161]. A small subpopulation of CD133+ cells, expressing also CD34, can be identified in the blood and skeletal muscle interstitium [162, 163]. Similar to blood-derived CD133+ cells, human muscle-derived CD133+ cells manifested remarkable myogenic differentiation capacity in regenerating muscle [164]. As CD133+ cells can be readily isolated from the blood, manipulated *in vitro* and delivered through the circulation, some studies have explored their application to treat dystrophic mice, demonstrating an

improved muscle morphology and function as well as dystrophin expression. Future studies are needed to verify the long-term effect of this treatment.

Embryonic and induced pluripotent stem cells. Embryonic stem cells (ESCs) are pluripotent stem cells, which can differentiate into all three germ layers and hence have been extensively studied for cell-based therapies. Induced pluripotent stem cells (iPSCs) result from the direct reprogramming of adult somatic cells to become pluripotent hES-like cells. ESCs and iPSCs differentiate at low efficiency into skeletal muscle cells; thus, specific protocols had to be designed for both murine and human PSCs [165]. Among these methods, some allow the generation of SCs or myoblasts from murine and human iPSCs and ESCs [166-168].

For cell therapy purposes, among the various mesoderm stem cells that have been shown to contribute to skeletal muscle regeneration, some can be generated from mouse and human ESC/iPSC-derived embryoid bodies [169-172]. Interestingly, recent work demonstrated amelioration of limb ischemia using mesenchymal stem cells/vasculogenic pericytes derived from human ESCs/iPSCs [173, 174]. It has been recently demonstrated that human skeletal muscle pericytes/MABs derived from iPSCs can be utilized to generate, genetically correct and restore pericyte/MAB-like cells from limb-girdle muscular dystrophy [175].

1.3.4. Animal Models of Acute Skeletal Muscle Injury

To unravel the normal regeneration process, several groups took advantage of different animal models, in which different methods were used to induce an acute damage and the

resulting myofiber degradation. Among them are injection of myotoxins such as bupivacaine, snake venoms like cardiotoxin (CTX) or notexin, physical trauma like freezing, whole muscle free graft, crushing, or denervation-devascularization [176-182]. All of these insults result in muscle injury, resulting in a phase of degeneration, followed by the induction of regeneration. Although the degenerative and regenerative phases of muscle regeneration are similar, the selection of the method of injury greatly influences the kinetics and the extension of each phase. Moreover the dynamics of these phases may vary also depending on the extent of the injury, the involved muscle and the animal model (and also, the mouse strain) [183].

The use of myotoxins is perhaps the easiest and most controlled and reproducible way to induce muscle regeneration [52, 184-186]. These toxins have a broad spectrum of biological activities, which are not entirely understood.

Cardiotoxins (CTX), small molecular weight all β-sheet proteins, act as a protein kinase C-specific inhibitor. Moreover CTX stimulate calcium transport and ATP hydrolysis by inhibiting sarcolemmal Ca/Mg-ATPase. As a result there is an induction of depolarization and contraction of muscle fibers, disruption of membrane organization and severe mitochondrial damage. These effects occur as early as 30 min after intra-muscular injection. The compromised sarcolemmal integrity allows the uptake by the damaged myofiber of low-molecular-weight dyes, such as Evans blue or procion orange, and this is a reliable indication of sarcolemmal damage [187-189].

Injection of 50 μL of 15 μM CTX in adult mouse tibialis anterior muscle results in a very reproducible damage that immediately

leads to a wound coagulum with mononuclear cell infiltration. Inflammatory response and mononuclear cell proliferation is most active within the first 4 days after injection. Myogenic cell differentiation and new myotube formation is observed 5-6 days post injection. The overall architecture of the muscle is restored 14 days after the injection, although most regenerated myofibers are smaller and display central myonuclei. The return to a morphologically and histochemically normal mature muscle is seen at 3-4 wk post injection.

Regarding other biological effects, it has been demonstrated that the internal structure of the muscle, i.e. basal lamina or microvasculature, is less affected after CTX injection than after other injuries, such as crushing [177, 190], but the impact of CTX on the different muscle cell types, including SCs, is not fully assessed yet.

1.4. Chronic Skeletal Muscle Damage

1.4.1. The Muscular Dystrophies

The muscular dystrophies (MD) are a group of inherited disorders characterized by progressive muscle wasting and weakness, leading to mobility limitations and, in the most severe forms, heart and/or respiratory failure [191].

MD are generally characterized by histological alterations in the muscle, which typically includes variations in fiber size, areas of muscle necrosis, presence of inflammatory infiltrate (mainly composed by macrophages) and, ultimately, increased amounts of fat and connective tissue.

The original classification of MD was based on the distribution of predominant muscle weakness (whether mainly proximal or distal and whether facial muscles were affected) and on the

mode of inheritance. On those basis, six principal groups of MD were identified, with the addition of congenital dystrophies, in which muscle weakness is more generalized (Fig. 11).

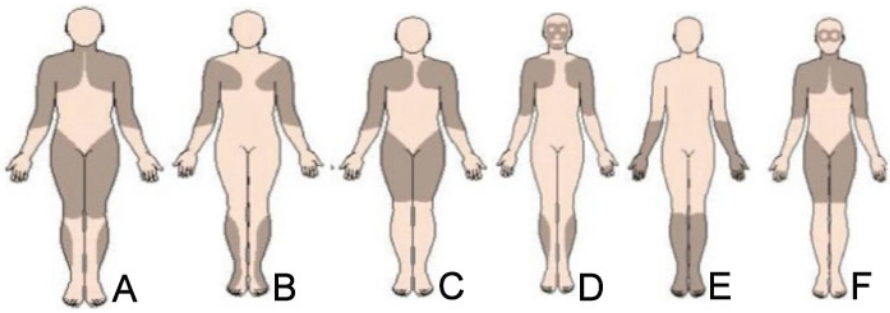

Fig.11. Distribution of predominant muscle weakness in different types of dystrophy. Shaded=affected areas. From left to right: A. Duchenne-type, B. Emery-Dreifuss, C. Limb girdle, D. Facioscapulohumeral, E. Distal, F. Oculopharyngeal

Duchenne muscular dystrophy (DMD) is a devastating X-linked disorder and is one of the most prevalent forms of muscular dystrophies afflicting one out of every 3,500 male births [191]. The deficient gene product, dystrophin, is a membrane-associated protein that provides a link between the intracellular F-actin of the cytoskeleton and the extracellular matrix [192].
In DMD, the protein is completely or partially lost. A less severe phenotype is observed in Becker MD, in which mutations still affect the dystrophin gene, but myofibers retain a truncated and low-active isoform of the protein.
Dystrophin interacts with a number of membrane proteins forming the dystrophin glycoprotein complex (DGC), whose function is to stabilize muscle cell membrane during cycles of contraction and relaxation [193]. It seems that the absence of any one of these proteins would interfere with the integrity and the strength of the membrane, thus resulting in muscle weakness [194]. For example, mutations in the sarcoglycan

complex proteins, such as α- or β-sarcoglycan (αsg or βsg) result in different forms of limb-girdle muscular dystrophy (LGMD2) (Fig. 12).

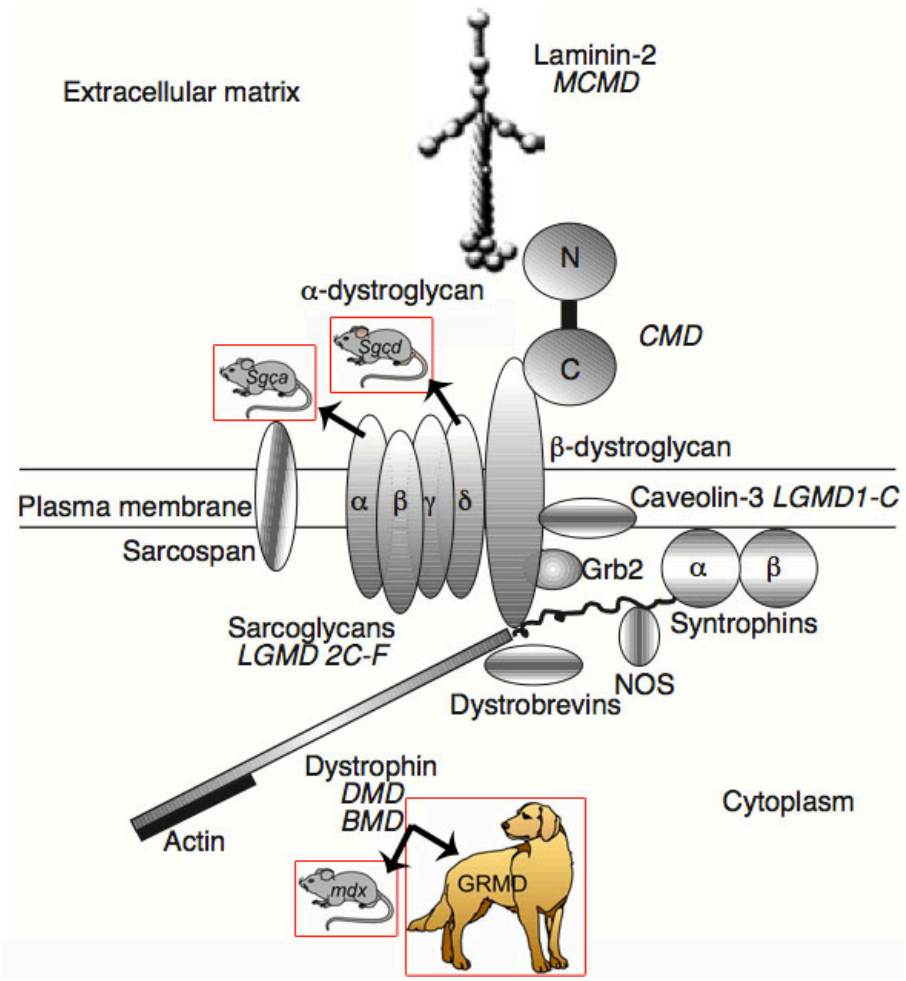

Fig.12. Dystrophin-glycoprotein complex (DGC). Many muscular dystrophies arise from mutations in DGC components. Similar mutation are present in murine and canine models. The most used in preclinical trials are shown.

1.4.2. Animal Models for Muscular Dystrophies

Several animal models have been developed to study MD. The

most widely used model for MD is the mdx mouse, existing both on wild type or on the nude mouse background. mdx mice carries a naturally occurring X-linked point mutation in the dystrophin gene, which leads to the absence of full-length dystrophin [195]. Thus mdx mice mimic, at least in principle, the DMD genotype in humans, but pathology is less severe in mice and is thought to be attenuated by the presence of relatively high numbers of revertant fibers (1–3%) and an up regulation of utrophin, a smaller (autosomal) analogue of the dystrophin [196-198]. Although mdx mice are normal at birth, skeletal muscles show extensive signs of muscle degeneration by 3–5 weeks of age. This acute muscle degeneration phase is accompanied by an effective regeneration process leading to a transient muscle hypertrophy. After this period, the degeneration/regeneration activity continues at lower and relatively constant levels throughout the life span of the animal. In the older animals (around 15 months) muscle regeneration process is defective and the mice become extremely weak and die before wild-type littermates [199].

Feasible models of LGMD2 are α-sg and β-sg-knockout mice, generated by disruption of region encompassing the relative genes. Sarcoglycans are a group of single pass transmembrane glycoproteins, which form a complex with the DGC. In contrast to other sarcoglycans (β, γ, δ), expression of α-sg is specifically restricted to striated muscle fibers. LGMD mice are considered a better animal model than mdx mice because of their lack of revertant fibers. Moreover, their phenotypes are very close to the human one, as they show chronic skeletal muscle degeneration and, in the case of βsg-KO mice, dilatative cardiomyopathy [200-202]. Histological

changes in these mice appear at 1 week of age and extend to most skeletal muscles, including extensive central nucleation, connective tissue proliferation, increasing variability of muscle fiber diameter and presence of necrotic fibers.

Canine models of DMD are being extensively studied as large animal models of MD [203, 204]. At present, there are two major colonies of dystrophic dogs all over the world, bearing the same mutation in different genetic backgrounds: a colony of Golden Retrievers (GRMD) and one of Beagle dogs. These animals are both derived through cross-breeding of a naturally born, affected founder. The mutation lies in intron 6 of dystrophin gene and results in a premature transcription stop codon and in complete absence of the protein [204]. In these models, revertant fibers are also almost undetectable, thus providing a good model to analyze regeneration effects of cell and genetic therapies [111].

Dystrophic dogs, from both varieties, show extremely affected motility, posing, salivation, severe chronic scar infiltrations and skeletal muscle degeneration and, although variability exists between individuals, by 8 months of age most dogs walk with great difficulty. In these animals, not only limb, respiratory and heart muscles are affected, but also tongue and pharyngeal, masticatory and trunk muscles, resulting in a severe involvement of the digestive tract [205]. Myocardial involvement is much more evident in dog models than in mice models, and this aspect resembles very closely the cardiac complications present in DMD patients.

1.4.3. Strategies for Muscular Dystrophy Therapy

MD are among the most difficult diseases to treat, even though the underlying molecular defects are now known. Actually,

there is no resolutive treatment for these diseases and those employed are generally aimed at controlling the onset of symptoms and at delaying the progression of the disease, in order to maximize the quality of life.

Any therapeutic protocol used to improve muscle regeneration in MD has to face some problems. One of the major hurdles is the large volume and wide distribution of the target tissue. Skeletal muscle may constitute up to 40% of the human body, and some muscles, such as the diaphragm and intercostal muscles, are not easily accessible to a route of administration such as intramuscular injections. In addition, the heart is affected in DMD and in a subset of LGMD patients. Thus the systemic delivery of the therapeutic agent appears a necessity. One of the goals of MD research is to understand how sarcolemmal damage is initiated, how it is repaired, and how the sarcolemma can be protected (or the damage minimized) by pharmacologic or therapeutic interventions.

There have been studies of possible treatments that function at the molecular, cellular and pharmacological level [206, 207] (Fig. 13).

1.4.3.1. Pharmacological Therapy

The current therapeutic approach to MD involve glucocorticoid corticosteroids, administered in various protocols. These therapies are effective in slowing the progression of DMD and their use has significantly reduced mortality and lengthened life expectancies. However, long term treatment is associated with clinically significant adverse effects [208-210].

The potential beneficial effects of these treatments include inhibition of muscle proteolysis, stimulation of myoblast proliferation, increase in myogenic repair, anti-inflammatory

and immunosuppressive effects, and reduction of cytosolic calcium concentrations and up regulation of utrophin [211, 212].

Over the last years, several pharmacological treatments have been proposed in order to counteract the consequences of the dystrophic process, including administration of protease inhibitors, and drugs that regulate calcium homeostasis or act on protein and lipid metabolism. The majority of these treatments have yielded no favorable outcomes in clinical trials, mainly due to high systemic toxicity [213].

Other pharmacological strategies aim at increase muscle strength, up-regulate compensatory proteins, suppress stop codon (by using aminoglycoside antibiotics) and/or decrease inflammation.

Drugs that stimulate muscle growth and regeneration will not cure the genetic defect of MD, but they may provide functional benefits by increasing size and strength of minimally affected muscle or by improving the quality of the composition of dystrophic muscle. Postnatal growth and regeneration are regulated by a variety of endogenous growth factors, such as insulin-like growth factor-1 (IGF-1) and members of the transforming growth factor-β (TGF-β) superfamily, such as myostatin (a negative regulator of muscle growth). In mdx mice that over-expressed IGF-1 the dystrophic phenotype was attenuated [214]. Similarly, when neutralizing antibodies against myostatin were systemically delivered to dystrophic mice, muscle wasting was dramatically delayed [215].

A number of studies have tested the hypothesis that the over expression of utrophin (a protein with genetic and functional similarities with dystrophin) in dystrophin-deficient muscles may correct dystrophic symptoms. It has been shown that

even the expression of truncated utrophin led to significant improvements in mechanical functions and prevention of the dystrophic pathology [216, 217]. It has also been reported that heregulin can induce utrophin expression in skeletal muscle [218]. Moreover, several other 'booster' proteins were identified that stimulated muscle regeneration and ameliorated dystrophy [219]. For example, increasing the expression levels of other genes, such as nitric oxide synthase (NOS), calpastatin, L-arginine (a NOS substrate), $\alpha 7\beta 1$-integrin and a disintegrin and metalloprotease ADAM12, was successful in improving the pathology of dystrophic mice. Following the over expression of many of these genes, it was observed an increase also in the levels of utrophin and many dystrophin-associated proteins. A large-scale search for small molecules that may up-regulate utrophin and these other proteins currently is under way.

It is known that treating cultured cells with aminoglycoside (i.e. gentamycin and negamycin) can cause suppression of stop codons by extensive misreading of RNA codes [220] and insertion of alternative amino acids in place of the stop codon. Since the defect in the mdx mouse is caused by a mutation that introduces a premature stop codon, it has be investigated whether treatment of mdx mice with these antibiotics could lead to the synthesis of dystrophin in muscle fibers. Encouraging preliminary results showed that restoration of dystrophin levels to 10–20% of normal was detected in skeletal muscle of mdx mice after subcutaneous injections of gentamicin [220], supporting functional benefits to treated muscles. Of course, further investigations are needed to assess the side effects due to aminoglycoside antibiotic treatment, even if such treatment is expected to be long lasting, due to the extended half-life of dystrophin.

Inflammation is a clear hallmark of dystrophic muscle and contributes to myofiber necrosis. Early inflammation is important to remove dead myofibers and to activate muscle repair program; however a chronic inflammatory state is established in dystrophic muscle. It has been recently proved that pharmacological inhibition of IkB kinase (IKK), a direct upstream positive regulator of NF-kB, resulted in improved pathology and muscle function in mdx mice [221]. In addition, drugs with an anti-cytokine action, such as those contrasting TNFα, have been proven to protect mdx muscle against early necrosis and to induce long-term benefits [222].

Classical non-steroidal anti-inflammatory drugs (NSAIDs), such as ibuprofen and flurbiporfen, have been found to ameliorate function and disease course in mdx, especially if combined with or linked to a nitric oxide (NO)-donating moiety which has been shown also to enhance SCs activation and myogenic program [223, 224]. Clinical trials in DMD boys with various anti-inflammatory agents are under considerations [225].

Pharmacological treatment remains attractive and of significant value mainly for the fact that this approach can address all patients (not only those with a specific genetic defect) and that the costs are relatively affordable. The major disadvantage is that if used singly, pharmacological approaches might improve only a specific and limited component of secondary pathology, rather than the overall phenotype. Moreover, the combinatorial use of multiple drugs could help increase the therapeutic benefit, but might result in adverse interactions between them.

1.4.3.2. Gene Therapy

The task of replacing a missing gene in at least a good proportion of the post-mitotic nuclei of skeletal muscle is

challenging. Furthermore, for DMD the gene to be replaced is the largest known, with a cDNA of 14 Kb [226].

Gene therapy entails the delivery of genes to somatic cells using vectors derived from viruses or constructed using non-viral elements (non-viral vectors). The gene vector is introduced to an intact organism by injection into a blood vessel or directly into a target tissue.

Gene therapy for MD targets the genetic defects, attempting to overcome the pathological mutation by providing the muscle with the correct form of the gene. One problem that might be encountered during the expression of a previously missing gene product is the onset of an immunological reaction. However, recent investigations [227] suggest that this should not be a problem in humans because of revertant fibres, which are muscle fibres that express a smaller, but functional, dystrophin protein due to exon skipping. It remains to take into account the immune response caused by the vector used to deliver the transgene [228, 229]. A further barrier to clinical application involves the development of technologies to produce adequate amounts of gene therapy vectors for the conversion to large human application.

The simplest form of gene therapy consists in injecting naked DNA plasmids encoding dystrophin directly into muscle. In 1990 it has been shown for the first time that a direct gene transfer of naked plasmid DNA or RNA resulted in transgene expression in skeletal muscle fibers [230]. Naked DNA transfer have the advantage to be safe and non-toxic, but the efficiency of the transgene delivery is low. More recently, more efficient delivery strategies have been developed. Intravascular injection of plasmid DNA under high hydrostatic pressure has been shown to lead to high efficiency of reporter gene product

expression in several muscle groups of rat hind limbs [231]. In addition, high-level and long-lasting gene expression of reporter gene products has been obtained by optimized electroporation conditions [232]. Nowadays, a clinical trial that uses high pressure intravascular delivery of plasmid DNA containing full length human dystrophin is ongoing. However, further studies are necessary to unravel the mechanisms for uptake of naked plasmid DNA that have not been clarified.

An alternative gene therapy approach for delivering the dystrophin gene to dystrophic fibers is through the use of viral vectors. Skeletal muscle is composed of post-mitotic, non dividing cells, thus for the *in vivo* muscle gene transfer the attention has been focused on adenovirus (Ad) and adeno-associate virus (AAV). Adenoviral vectors were successful in delivering dystrophin to a very large fraction of muscle fibers in newborn dystrophic mice [233]. However, the treatment caused a strong immune reaction against the vector, observed only when adult mice were treated, due to the tolerance of newborn mice. Improved adenoviral vectors, the so-called gutted adenovirus, have then emerged. These vectors can accommodate the full-length cDNA for dystrophin, but do not carry genes encoding viral proteins. They induce a much weaker immune reaction, but the efficiency of transduction was greatly reduced [229]. Further modification of adenoviral vectors are needed to enhance muscle cell transduction or to promote genomic integration.

Adeno-associated vectors (AAVs) are derived from a non-pathogenic replication-deficient virus with a small single-stranded DNA genome. AAVs hold great promise because of their low immunogenicity and their potential for integration. In addition, transduction of mature myofibers is achieved

effectively with AAVs, especially if delivered systemically together with factors that increase vascular permeability [234]. Unfortunately, AAV gene transfer is only possible for a restricted number of MDs since they can only accommodate up to 5 kb of exogenous DNA, thus excluding their use for gene transfer of the dystrophin genes. A successful clinical trial of gene transfer of α–sarcoglycan gene with an AAV vectors in patients with LGMD2D was recently performed (Mendell 2009), and others are ongoing. To fit the AAV packaging limitations, truncated versions of the dystrophin gene (the micro- and mini-dystrophin) have been engineered (Harper 2002) and tested for their ability to rescue dystrophic muscle. Several versions of these minigenes successfully improved the phenotype in mdx mice and are expected to convert a DMD phenotype into a milder BMD phenotype.

Taken together, these studies show that gene therapy through the use of viral vectors appears promising in the treatment of DMD. Improvements in vector design and/or delivery will hopefully result in more efficient gene replacement therapies.

For diseases caused by point mutations, an alternative to gene replacement is to correct the point mutations, changing the mutant nucleotide to the correct one *in vivo*. This can be achieved through the use of short fragments or chimaeraplasts (double-stranded RNA-DNA chimaeric oligonucleotides), which are designed to contain the correct nucleotide. It has been shown that chimaeraplasts can target and change single nucleotides in genomic DNA of somatic cells of intact animals [235]. This strategy takes advantage of the endogenous DNA mismatch repair machinery within the cell to accomplish the desired base change. The potential feasibility of this approach to treat MD patients was demonstrated in both mdx mouse and

GRMD dog [236]. Expression of dystrophin nevertheless was restricted to myofibers directly surrounding the injection site and it thus appears that other delivery methods may need to be investigated, in particular systemic delivery, which is theoretically feasible.

An alternative strategy for gene therapy involves “exon skipping”, that prevents the transcription of the exon containing the mutation thus restoring the reading frame of the mutated gene to allow the expression of internally deleted but partially functional dystrophin proteins. Apart from the use of chimeraplast [237], skipping can be achieved through the use of antisense oligonucleotides (that target transcribed RNA molecules) or by small RNAs that hybridize with the donor and/or acceptor sites of the mutated exon, causing its exclusion from the otherwise intact transcript [238, 239]. Because the skipped exon usually does not encode a functionally essential domain, the resulting protein is shorter but functional. The main disadvantages of this approach are that it requires repetitive administrations (since it modifies only the process of mRNA splicing) and that different antisense oligonucleotides are required for different mutations.

1.4.3.3. Cell Therapy

Cell therapy is a procedure where the active therapeutic agent is represented by cells. When the cells are derived from another individual of the same species the donor cells are considered heterologous and the transplant is define allogeneic. In this case cell express the normal copy of the mutated gene but induce an immune rejection unless the patient is permanently under immunesuppression. Donor cells derived from the same patient are considered autologous and,

in this case, immune suppression is not required. If cells are also genetically manipulated during their *in vitro* expansion (for example to introduce a normal copy of the mutated gene though a viral vector), the procedure represents a form of *in vitro* or *ex-vivo* gene therapy.

Of course, the first hope for treating MD with cells that can make new muscle arose from the identification of SCs in 1961. SCs and cell lines derived from them have been used since the late 1970s, mainly through intra-muscular injection. A first pivotal study involved the injection of wild-type myoblasts into mdx mice and resulted in the conversion of muscles from dystrophin-negative to dystrophin-positive [240]. This study led to a series of clinical trials in the early 1980s that failed for several reasons, the most important of which were the poor survival and the very limited migratory capacity of injected donor cells, together with the immune response of the patient that was not suppressed at that time. Nowadays, the current consensus is that intra-muscular injection of SC-derived myoblasts could be the elective treatment for localized forms of MD. For example, in oculopharyngeal MD, characterized by a typical distribution localized to eyelid and pharyngeal muscles, autologous transplantation of unmodified SCs isolated from nonaffected muscles has shown good results in preclinical work and has entered clinical experimentation [241].

For other forms of MD affecting the majority of skeletal muscles this approach would still be inefficient and impractical. In these cases, the possible systemic delivery of cells with myogenic potential and able to cross the endothelial layer was the obvious choice. Some of these progenitor cells have been recently tested in large preclinical models [131, 137]. Mesoangioblasts (MABs) (or pericytes) are the most promising

and indeed the only cell type (in addition to SCs) that has reached clinical experimentation.

Considering the advantages in the use of autologous cells, several research have been made in order to improve efficacy and safety of ex-vivo genetic modification. Lentiviruses are ideal to introduce genes into stem cells, as they infect post-mitotic or quiescent cells and become integrated in the host genome, resulting in stable long-term gene expression both *in vitro* and *in vivo* [242, 243]. Their main limitations are the relatively small gene insert and the possible insertional mutagenesis in the host genome. The choice of an appropriate promoter, so that the gene of interest is only switched on in muscle fibres [244] and maintains long-term expression *in vivo* [244, 245] is also fundamental. In addition to viral vectors, recently developed non-viral vectors such as transposons [246] and human artificial chromosomes (HACs) are possible alternative gene delivery tools for future clinical applications. A transposon-based vector has the capacity of both stable integration of target genes into the host genome and high gene expression level over long period of time in cells such as hematopoietic stem cells, mesenchymal stem cells, muscle progenitor cells and iPS cells [247]; while HACs enable a stable episomal maintenance that avoids insertional mutations and in addition, have the ability to carry large gene inserts including regulatory elements [248]. The use of HACs to introduce a full length dystrophin gene into iPS cells derived from DMD patients has been reported [249]. It has been recently reported the amelioration of the dystrophic phenotype in mdx mouse via transplantation of autologous MABs genetically corrected with a HAC vector containing the entire human dystrophin genetic locus [250].

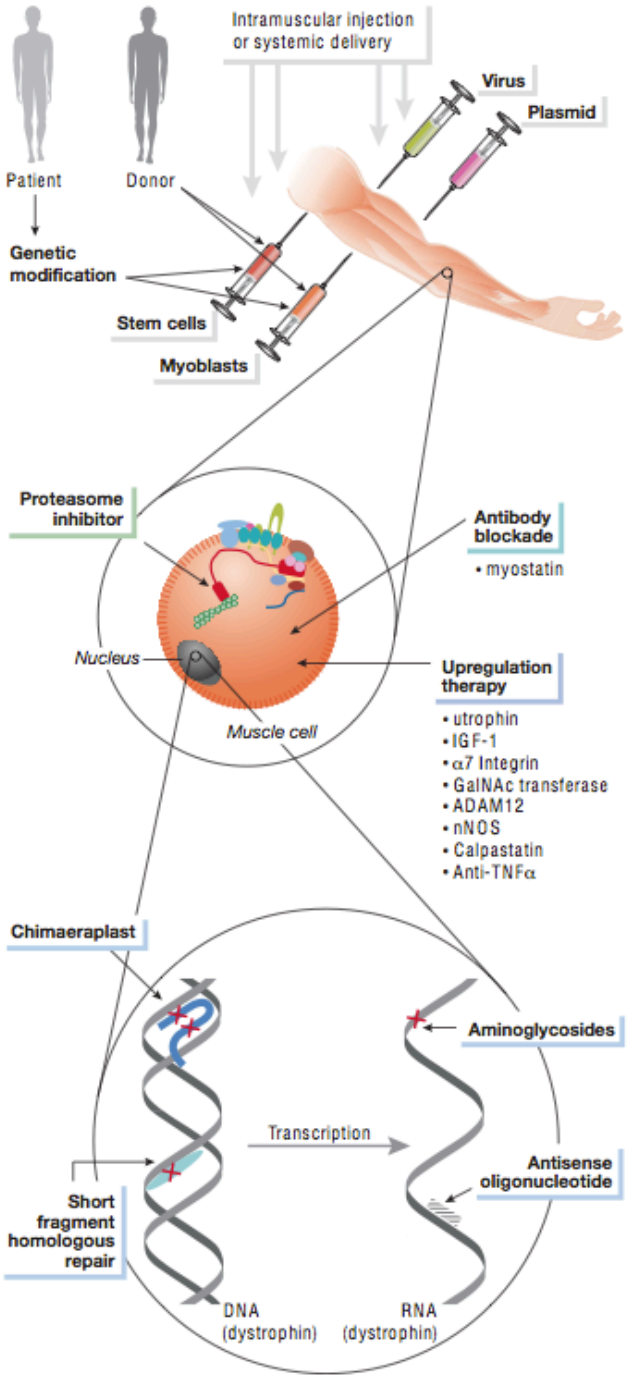

Fig.13. Summary of the wide range of approaches being used to treat Duchenne muscular dystrophy.

1.5. The Vascular Network in Skeletal Muscle Tissue

1.5.1. Hallmarks of Vessel Growth

Recent work demonstrates that dystrophin (the missing protein in DMD patients) is also found in the vasculature [251, 252] and its absence results in vascular deficiency and abnormal blood flow, that induce a state of ischemia. The absence of dystrophin in the vasculatures of mdx mice [253] results in the vascular abnormalities that may impair blood flow. This is through decreased vascular density, lower expression of endothelial and neuronal nitric oxide synthases and reduced flow (shear stress)-induced endothelium-dependent dilation [254, 255]. It appears evident that any effective form of therapy for MD needs to restore both the muscle and the vasculature defects. So far, most of therapeutic options for dystrophic patients focus on repairing the mechanoinstability of the muscle. Recently, it has been shown that alleviating the problems associated with vasculature can drastically improve the diseased phenotype of mdx mice [251, 256, 257].

The growth of blood vessels is a tightly controlled process: endothelial differentiation occurs during normal vascular development in the embryo. This process is recapitulated in the adult when endothelial progenitor cells are generated in the BM and can contribute to vascular repair or angiogenesis at sites of vascular injury or ischemia.

The development of blood vessels from endothelial cells is achieved by two mechanisms: vasculogenesis and angiogenesis. Vasculogenesis is defined as the de novo formation of primitive blood vessels resulting by proliferation and differentiation of the angioblasts, mesenchymal vascular endothelial cell precursors [258]. Angiogenesis occurs

subsequently and is the result of sprouting, branching, cell division, migration and assembly of endothelial cells derived from preexisting vessels, leading to the growth of the vascular network [259, 260] (Fig. 14).

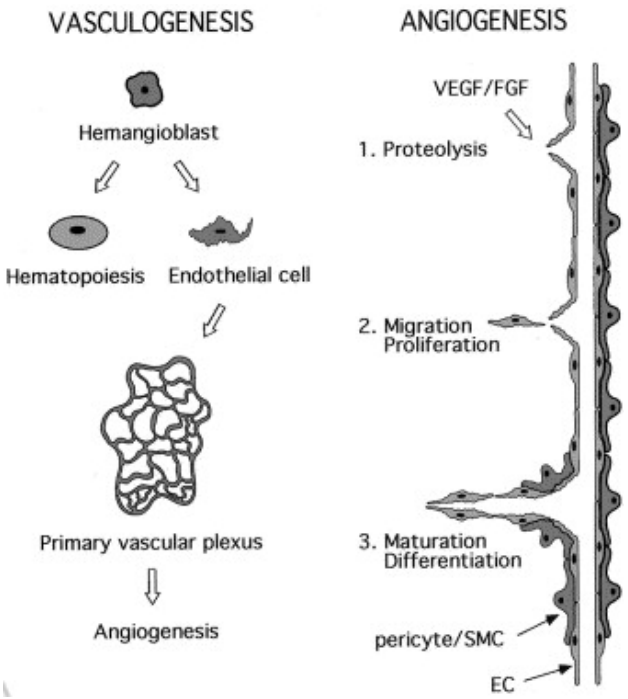

Fig.14. Schematic outline of vasculogenesis, formation of the vascular tree, and angiogenesis, formation of new vessels from pre-existing ones. In vasculogenesis, angioblastic stem cells in primitive organs develop into endothelial cells and hematopoietic cells. The endothelial cells form the primitive vascular plexus, which is further developed and processed to form the mature vascular system. Angiogenesis can be divided into a series of temporally regulated responses, including protease induction, migration, proliferation and differentiation.

Later vascular development involves the acquisition of organ-specific properties as well as several other processes including vascular remodeling, the establishment of artero-venous identity and mural cell recruitment. Newly formed blood vessels are indeed initially free of smooth muscle cells,

pericytes and other associated cells [261]. Mural cell coverage is required for the stabilization of immature endothelial tubes and the structural support provided by mural cells is physiologically relevant [262].

Various signaling molecules are involved in all these processes. Most of them are protein ligands that bind to and modulate the activity of transmembrane receptor tyrosine kinases [263]. Vascular endothelial growth factor (VEGF) family members and their receptors are known to be involved in various aspects of blood vessel development including vasculogenesis and angiogenesis, both physiological and pathological [264-267]. Besides VEGF, other growth factors have been shown to have a significant proangiogenic effect, like fibroblast growth factor (FGF), transforming growth factors, hepatocyte growth factor, angiopoietin-1, platelet-derived growth factors (PDGF) and others [268]. Some of these factors have also been implicated in specific phases. For example PDGFB-PDGFB receptor axis is important for pericyte recruitment [269-271].

The acquisition and maintenance of specialized properties by endothelial cells is important in the functional homeostasis of the different organs [272]. Another important determinant of endothelial cell differentiation is the local environment, and especially the interaction with surrounding cells, that occur through the release of soluble cytokines, cell-to-cell adhesion and communication, and the synthesis of matrix proteins on which the endothelium adheres and grows.

1.5.2. Embryological Origin of Vascular Cells

The vascular system is one of the earliest functional organs formed in a developing embryo and the main reason is to meet

the nutritional needs of the developing organism [260, 273, 274]. At E7.5 in the mouse, the extra embryonic mesodermal cells of the yolk sac aggregate into clusters that constitute the initial stage of blood island (BI) formation. Shortly thereafter, BI differentiate into an external layer of endothelial cells and an inner core of blood cells [275]. The close developmental link between these two cell types led to the hypothesis of the existence of a common progenitor, the hemangioblast [276, 277]. An alternative theory was that hematopoietic cells originate from a specific type of endothelium, the hemogenic endothelium [278]. In mammalian embryos, the concept of the hemangioblast and the hematogenic endothelium have both received experimental confirmation, and a recent report has reconciled these two pathways by proposing that the Flk1+ hemangioblast first generates the hematogenic endothelium (Scl-dependent stage), which then produces hematopoietic cells (Runx1-dependent stage) [279, 280] (Fig. 15).

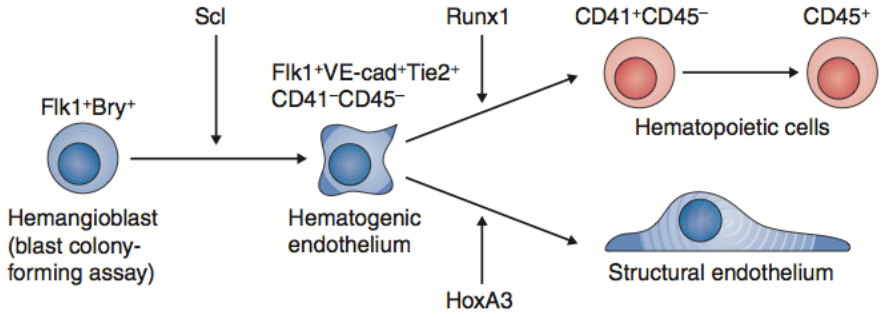

Fig.15. The hemangioblast to hematogenic endothelium lineage pathway. Hemangioblast transits through the hematogenic endothelium stage prior to generating hematopoietic cells. Hematogenic endothelium can generate both hematopoietic cells and structural endothelium. The formation of the hematogenic endothelium is Scl-dependent and that of hematopoietic cells is Runx1-dependent. HoxA3 antagonizes the hematopoietic program and maintains the endothelial characteristics of cells.

Morphological analyses showed that cells in the hematopoietic clusters form tight junctions with the endothelial cells of the aorta and appear to be budding from the endothelium [281, 282]. Immunohistological analyses revealed an extensive overlap in the expression of hematopoietic and endothelial markers in the clusters, suggestive of a close developmental relationship [275, 283].

In addition, other evidences indicated that also smooth muscle cells, other than arising from local mesenchyme and the neural crest [284], may originate from the common precursor of endothelial and hematopoietic cells. Thus, the existence of a general vascular progenitor cell was hypothesized [285]. Later, these results were confirmed by the demonstration that endothelial cells and smooth muscle cells, derived from a single embryonic progenitor, integrate into pre-existing vasculature [286].

Postnatally, such common vascular progenitors have not been described yet. However, reciprocal plasticity between endothelial and mesenchymal lineages has been suggested. The first description of endothelial to mesenchymal transdifferentiation (EndMT) was the process of heart valves formation during embryonic development. This process has been shown in mammals to be largely dependent on TGF-β signaling and on β-catenin [287, 288].

The *in vivo* postnatal role of EndMT has long been unclear. Recent evidences support a role for EndMT in cardiovascular and renal fibrosis, fibrodysplasia ossificans progressiva (FOP), in atherosclerosis, pulmonary hypertension and cancer [289-291].

1.5.3. Regeneration of the Adult Vascular Compartment

Endothelial cells are a crucial component of the normal vascular wall, providing an interface between the bloodstream and surrounding tissue of the blood vessel wall. Endothelial cells are also involved in physiological events including angiogenesis, inflammation and prevention of thrombosis. Wound healing and tumor growth require active endothelial proliferation, a process referred to as neo-angiogenesis. Neo-angiogenesis involves the recruitment of endothelial cells to the site of injury. In addition to the endothelial cells that compose the vasculature, non-hematologic endothelial progenitor cells (EPCs) circulate in the blood [292-294] and migrate to regions of the circulatory system with injured endothelia [295, 296]. EPCs showed similar antigenic characteristic to embryonic angioblasts [297, 298]. Both EPCs and mature endothelial cells may express similar endothelial-specific markers, including vascular endothelial growth factor receptor-2 (VEGFR-2), Tie-1, Tie-2 and vascular endothelial (VE)-cadherin. Moreover, hematopoietic stem and progenitor cells express markers similar to those of endothelial cells, such as VEGFR-1 (Flt-1), CD34, platelet endothelial cell adhesion molecule (PECAM/CD31), Tie-1, Tie-2, and von Willebrand's factor (vWF). Thus, it has been so far really difficult to specifically identify this population.

1.6. Nitric Oxide in Myogenesis and Muscle Repair

1.6.1. NO Biogenesis and Mechanisms of Action

In 1987, the free radical nitric oxide (NO) was identified as the gaseous messenger accounting for the vasodilating activity of the endothelium-derived relaxing factor [299]. In 1992 NO was

awarded the title of “molecule of the year” [300].
Despite its structural simplicity, NO has a complex chemistry and is an important mediator of functions in a variety of physiological systems [301], including the skeletal muscle tissue, where NO has a protective role regulating key functions, such as excitation-contraction coupling, vasodilatation, glucose uptake, mitochondrial function and biogenesis.
Endogenous NO is synthesized from the enzymatic conversion of L-arginine to L-citrulline by NO synthase (NOS). The reaction requires molecular O2 and nicotinamide adenine dinucleotide phosphate (NADPH) as co-substrates (Fig. 16).

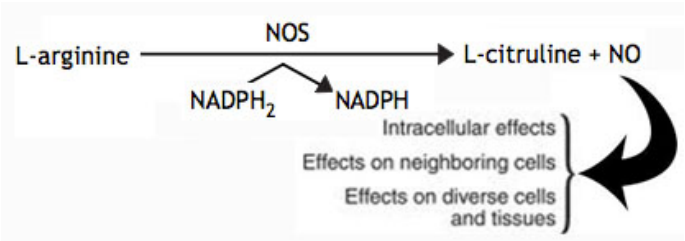

Fig.16. Biochemical synthesis of Nitric Oxide. NO diffuses freely across cell membranes and acts in a paracrine or even autocrine fashion, affecting only cells near its point of synthesis.

NOS are present in almost all mammalian cells and tissues [302]. Three distinct isoforms of NOS have been identified, two of which, namely the neuronal (nNOS or typeI) and endothelial (eNOS or type III) isoforms, are constitutively expressed and require the Ca2+/calmodulin complex for their activation, whereas one is inducible by cytokines and bacterial products (iNOS or type II) (Fig. 17).
Typically, iNOS mRNA is absent or present at very low levels under physiological conditions in skeletal muscles and is transcriptionally unregulated by cytokines. All isoforms may be transcriptionally regulated by hypoxia. In skeletal muscle nNOS

expression is increased by crush injury, muscle activity, and the ageing process, whereas it decreases following denervation [303-306]. Changes in the expression of skeletal muscle eNOS are induced by chronic exercise [307, 308]. These changes are usually of small extent and, moreover, both nNOS and eNOS produce NO at low, physiological levels (in the pico to nanomolar range) for short periods. Conversely, iNOS is highly expressed in skeletal muscle primarily under severe inflammatory conditions, such as in the course of autoimmune inflammatory myopathies and after crash injury [304, 309]. The activity of iNOS is independent of the Ca2+/calmodulin complex and generates NO at high concentrations (micromolar range) for prolonged periods.

NOS isoform	Type I	Type II	Type III
Alternate name	Neuronal	Inducible	Endothelial
Molecular weight	160 kDa	130 kDa	130 kDa
Constitutive expression	Yes	No	Yes
Stimulus for induction	Exercise	Cytokines	Exercise
Localization within myocyte	Sarcolemma	Cytosol	Mitochondria
Fibre type specificity	Fast fibres	Not tested	No
Expression by other cell types	Neuronal axons	Macrophages	Vascular endothelium
Regulation of enzyme activity	Ca^{2+} – calmodulin	Transcription	Ca^{2+} – calmodulin
Pattern of NO synthesis	Low rate, intermittent	High rate, continuous	Low rate, intermittent
Physiological role	Mediate contractile function? Cell–cell interactions?	Antimicrobial action	Modulate mitochondrial respiration?

Fig.17. Nitric Oxide Synthase (NOS) isoforms in skeletal muscle

NOSs are also susceptible to post-translational modifications including phosphorylation, nitrosylation (cysteine and iron), and oxygen concentration. In particular, nNOS and iNOS activities are directly coupled to oxygen concentration.

All major nitric oxide synthase (NOS) isoforms are expressed in skeletal muscles of all mammals, including a muscle-specific splice variant of nNOS called nNOSμ. This isoform, being the more abundant in normal physiological conditions, is considered the main source of NO during skeletal muscle

contraction [310].

Each NOS isoform has a specific localization in different compartments of muscle fibers. In adult skeletal muscle, nNOS is largely targeted to specialized structures at the surface membrane and is anchored to the sarcolemma via the DGC. This specific localization is a key aspect that explains the coupling of NO generation with muscle contractile activity and nNOS displacement from the sarcolemma has been shown to be involved in the pathological evolution of MD. It has been demonstrated that nNOS is enriched at neuromuscular junctions and shows a fast-twitch muscle fiber predominance.

eNOS is localized to the caveolae, microdomains of the plasmalemmal membrane that are implicated in a variety of cellular functions including signal transduction events. The caveolin proteins are the major coat proteins of caveolae and eNOS establishes specific interactions with caveolin-1 and caveolin-3. Caveolin binding to eNOS in skeletal muscle, inhibited NO synthesis, and this inhibition is reversed by calcium-calmodulin. Further analysis showed that eNOS colocalized also with mitochondrial markers in a subset of fibers [311].

NO exerts its effects in skeletal muscle by three main mechanisms of action: activation of the NO-dependent guanylyl cyclase, with formation of cyclic GMP (cGMP), inhibition of cytochrome c (cyt c) oxidase in the mitochondrial respiratory chain and/or S-nitrosylation [311].

Generation of cGMP appears of particular relevance. Alongside mediating most of NO effects on myogenesis, cyclic GMP-dependent signaling plays a major role in NO-dependent vasodilation and vascular responses and presides over complex intracellular crosstalk events involving calcium and

sphingolipids, which are key players in muscle homeostasis [312]. In addition, cGMP mediates the NO-dependent biogenesis of mitochondria [313]. Increased mitochondrial biogenesis leads to an enhanced ability by the skeletal muscle to generate ATP via mitochondrial respiration. Such an effect is complemented by NO-dependent stimulation of glucose transport [307], both in the case of insulin and exercise-stimulated glucose uptake.

The interaction of NO with heme-containing proteins is exemplified in the binding to cyt c oxidase, the terminal enzyme in the mitochondrial electron-transport chain. Inhibition of cyt c oxidase in mitochondria occurs at physiological concentrations of NO. The binding of NO to cyt c oxidase is reversible, occurs in competition with oxygen and results in inhibition of enzyme activity and thus cell respiration. The observation that nNOS is also localized in close proximity with mitochondria suggests a tight coupling between NO generation and regulation of mitochondrial respiration and metabolism. As a consequence of cyt c oxidase regulation, NO controls the generation of reactive oxygen species preventing their excessive generation and ensuing toxicity. This is particularly relevant since small concentrations of these radicals, generated physiologically under NO control, may be beneficial and contribute to the maintenance of an antioxidant defense in tissues [314]. A significant contribution to regulation of NO concentrations in muscle, with consequence also on its bioenergetic role, comes from myoglobin that acts as a NO scavenger in skeletal muscle, thus regulating its delivery [315].

S-nitrosylation, the covalent attachment of a nitrogen monoxide group to the thiol side chain of cysteine, is the process by which NO regulates the activity of several enzymes that are

important in skeletal muscle physiology, among which are phosphatases, caspases and oxidoreductases as well as several transcription factors, such as p53 and NF-κB. It has recently been demonstrated that NO inhibits the activity of class IIa histone deacetylases via S-nitrosylation. Of importance, the nitrosylation state of class IIa histone deacetylases has been shown to influence the expression of specific microRNAs genes important for muscle regeneration. Another important S-nitrosylation-dependent effect is the regulation of oxygen binding to, and release from, haemoglobin and thus the modulation of oxygen supply to mitochondria.

1.6.2. NO Action in Skeletal Muscle Physiology

Several studies in the last decade have shown that NO regulates SCs through a variety of actions, mediated by different signal transduction pathways and downstream effectors. Of importance, it also appears that such regulation can be sustained by NO generated endogenously by these same cells, although NO produced by myofibres or endothelial cells may also play a role.

One of the initial reports about a role of NO in myogenesis was on its ability to induce activation of SCs immediately upon damage [316]. Blocking NO signal in the early phase of injury impairs muscle repair, favoring fibrotic scar tissue production. The mechanism by which NO influences SC activation involves release of the hepatocyte growth factor (HGF) from extracellular matrix through metalloproteinases induction [317]. In agreement with previous reports about the mitogenic action of NO [318-320], it has been recently demonstrated that NO

stimulates proliferation of SCs via generation of cGMP [321]. Moreover NO acts on the maintenance of SC reserve pool and this effect depends on the Vangl2-dependent Wnt non-canonical pathway and treatment with molsidomine (a NO donor drug) has been shown to prevents the exhaustion of the SC pool in case of severe muscle damage or MD. The effect of NO on Vangl2 signaling suggests that this regulation could also act during embryonic muscle development. Indeed the non-canonical Wnt pathway plays a role in differential activation of genes in epaxial or hypaxial progenitors [322, 323], but the effect of NO on embryonic myogenesis needs to be investigated further.

Besides the control by NO of mitochondrial biogenesis and respiration, it has been recently described the inhibition by NO of mitochondrial fission, an event that allows myogenesis to occur. During myogenic differentiation the short mitochondria of the myoblasts change into the extensive elongated network observed in the myotubes. Such an effect appears to initiate already in differentiating myoblasts prior to their fusion. Physiological generation of NO was found to inhibit the activity of the dynamin-related protein 1 (Drp-1), a protein playing a key role in the process of mitochondrial fission [324].

The effect of NO on myogenic precursor cell fusion was firstly described in chicken myoblast, in which NOS activity showed a peak in cell competent for fusion, but not in proliferating myoblasts or in myotubes. In these experiments NO was shown to induce early fusion, whereas inhibition of NO production delayed the time of fusion. Of importance, this effect was observed not only on adult SCs but also on the presomitic mesoderm, further indicating that NO has an effect, still to be characterized in full detail, at critical stages of pre-

postnatal muscle developmental life (Fig. 18).

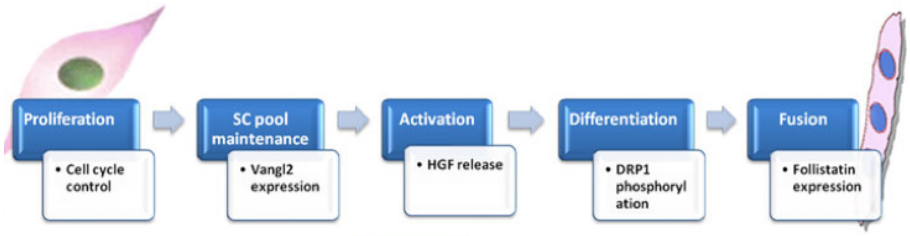

Fig.18. NO check points on myogenesis. White boxes indicate the mechanisms of NO-dependent control.

1.6.3. Modulating Nitric Oxide as a Therapy

During the 1980s, the free radical NO was discovered to be a crucial signaling molecule, with wide-ranging functions in the cardiovascular, nervous and immune systems. The large body of evidence that show that NO plays a critical role under a variety of physiologic and pathologic conditions has opened up the possibility of designing new drugs that are capable of delivering NO into tissues and the blood-stream in a sustained and controlled manner.

Inhibition of the synthesis of NO may be necessary in situations in which there is overproduction of NO, as a result of over activity of the constitutive or induction of the calcium-independent NO synthase. This is obtained by using inhibitors of nitric oxide synthases (such as L-NAME, 7-nitroindazole, aminoguanidine) as well as inhibitors of the guanylate cyclase (oxadiazoloquinoxalinone (ODQ) and methylene blue) or the protein kinase G (KT5823).

On the other hand, NO deficiency has been implicated in many pathologic processes, including MD, thus providing the basis for the use of NO replacement therapy. In these situations it may be desirable to mimic or enhance the physiological

generation of NO. This may be achieved in several ways, including direct administration of NO, increasing the action of endogenous NOS (by increasing intracellular Ca2+ or by stimulating the iNOS) or providing additional substrate for NO synthesis (L-arginine, L-ornitine) as well as stimulating the cGMP-dependent pathway, such as activators of soluble guanylate cyclase (YC-1, BAY41-2272, BAY58-2667) or inhibitors of phosphodiesterase (sildenafil, tadalafil, vardenafil).
Although the use of NO as a therapeutic gas is recent, NO donor drugs have been used in patients for more than a century. The organic nitrates are the most commonly used NO donor drugs. These can be divided in short acting drugs such as glyceryl trinitrate (GTN; also known as nitroglycerin), isosorbide dinitrate and sodium nitroprusside and long acting drugs such as isosorbide mononitrate, pentaerythritol tetranitrate and molsidomine [325].
Recently, a wide range of novel NO donor classes have emerged. Some of these drug classes appear to be of interest for their potential therapeutic applications because they allow the deliver of NO into tissues and the bloodstream in a sustained and controlled manner. There are excellent reviews available describing both the chemistry and the pharmacology of the new NO donor compounds, including the so-called hybrid NO donors that combine a nitrate moiety with pharmacologically active structures [326-331].
The efficacy of therapies based on the administration of NO has been intensively investigated in mouse models of muscular dystrophy [311]. Some positive results have been demonstrated in dystrophic animal models and humans, even if a strategy based on NO donation alone appears insufficient to yield a full therapeutic benefit.

An alternative strategy, that is to combine the properties of NO with the anti-inflammatory activity of NSAIDs, has been shown to effectively provide higher clinical efficacy [223-225, 332, 333]. From these experiments an important consideration emerged, that is that several mechanisms synergized to yield the therapeutic effect of this combined therapy: significant reduction in both fiber damage and inflammation and increases in the myogenic precursor cells number and differentiation capacity, which preserve the long-term regeneration capacity of muscle. Other actions of NO such as vasodilation and increased angiogenesis (and thus reduction of the ischemia), increase in glucose uptake and in energy generation may also have contributed to muscle repair. In addition, the observation that these therapies significantly enhance the homing of exogenously administered myogenic stem cells to dystrophic muscles suggests the possibility of obtaining synergic effects by combining pharmacological with cell therapy approaches [160, 223].

1.7. Aims of the thesis

A - Identify and characterize the *in vivo* counterpart of embryonic mesoangioblasts as a sub-population of endothelial progenitor cells, defining their identity and developmental ontogeny (see Chapter II)

B - Characterize the role of nitric oxide on vascular-associated progenitors during development as well as during skeletal muscle regeneration, in order to define conditions to enhance the recruitment and therapeutic efficacy of these endogenous cells in muscle repair (see Chapter III)

C - Investigate whether a genetic modification (i.e. the over expression of the MAGE protein Necdin) could be exploited to improve the performance of mesoangioblasts in dystrophic skeletal muscle regeneration (see Chapter IV)

1.8. References

1. Christ, B. and C.P. Ordahl, *Early stages of chick somite development.* Anat Embryol (Berl), 1995. **191**(5): p. 381-96.
2. Stockdale, F.E., W. Nikovits, Jr., and B. Christ, *Molecular and cellular biology of avian somite development.* Dev Dyn, 2000. **219**(3): p. 304-21.
3. Wigmore, P.M. and D.J. Evans, *Molecular and cellular mechanisms involved in the generation of fiber diversity during myogenesis.* Int Rev Cytol, 2002. **216**: p. 175-232.
4. Ordahl, C.P. and N.M. Le Douarin, *Two myogenic lineages within the developing somite.* Development, 1992. **114**(2): p. 339-53.
5. Cinnamon, Y., et al., *The sub-lip domain--a distinct pathway for myotome precursors that demonstrate rostral-caudal migration.* Development, 2001. **128**(3): p. 341-51.
6. Noden, D.M., *The embryonic origins of avian cephalic and cervical muscles and associated connective tissues.* Am J Anat, 1983. **168**(3): p. 257-76.
7. Huang, R., et al., *Origin and development of the avian tongue muscles.* Anat Embryol (Berl), 1999. **200**(2): p. 137-52.
8. Christ, B. and B. Brand-Saberi, *Limb muscle development.* Int J Dev Biol, 2002. **46**(7): p. 905-14.
9. Nikovits, W., Jr., et al., *Patterning of fast and slow fibers within embryonic muscles is established independently of signals from the surrounding mesenchyme.* Development, 2001. **128**(13): p. 2537-44.
10. Brent, A.E. and C.J. Tabin, *Developmental regulation of somite derivatives: muscle, cartilage and tendon.* Curr Opin Genet Dev, 2002. **12**(5): p. 548-57.
11. Brand-Saberi, B., et al., *The ventralizing effect of the notochord on somite differentiation in chick embryos.* Anat Embryol (Berl), 1993. **188**(3): p. 239-45.
12. Pourquie, O., et al., *Control of dorsoventral patterning of somitic derivatives by notochord and floor plate.* Proc Natl Acad Sci U S A, 1993. **90**(11): p. 5242-6.
13. Fan, C.M. and M. Tessier-Lavigne, *Patterning of mammalian somites by surface ectoderm and notochord: evidence for sclerotome induction by a hedgehog homolog.* Cell, 1994. **79**(7): p. 1175-86.
14. Munsterberg, A.E., et al., *Combinatorial signaling by Sonic hedgehog and Wnt family members induces myogenic bHLH gene expression in the somite.* Genes Dev, 1995. **9**(23): p. 2911-22.
15. Borycki, A.G., L. Mendham, and C.P. Emerson, Jr., *Control of somite patterning by Sonic hedgehog and its downstream signal response genes.* Development, 1998. **125**(4): p. 777-90.
16. Borycki, A.G., et al., *Sonic hedgehog controls epaxial muscle determination through Myf5 activation.* Development, 1999. **126**(18): p. 4053-63.
17. Capdevila, J., C. Tabin, and R.L. Johnson, *Control of dorsoventral somite patterning by Wnt-1 and beta-catenin.* Dev Biol, 1998. **193**(2): p. 182-94.
18. Tajbakhsh, S. and R. Sporle, *Somite development: constructing the vertebrate body.* Cell, 1998. **92**(1): p. 9-16.
19. Olivera-Martinez, I., et al., *Dorsal dermis development depends on a signal from the dorsal neural tube, which can be substituted by Wnt-1.* Mech Dev, 2001. **100**(2): p. 233-44.
20. Fan, C.M., C.S. Lee, and M. Tessier-Lavigne, *A role for WNT proteins in induction of dermomyotome.* Dev Biol, 1997. **191**(1): p. 160-5.

21. Fan, C.M., et al., *Long-range sclerotome induction by sonic hedgehog: direct role of the amino-terminal cleavage product and modulation by the cyclic AMP signaling pathway.* Cell, 1995. **81**(3): p. 457-65.
22. Marcelle, C., M.R. Stark, and M. Bronner-Fraser, *Coordinate actions of BMPs, Wnts, Shh and noggin mediate patterning of the dorsal somite.* Development, 1997. **124**(20): p. 3955-63.
23. Reshef, R., M. Maroto, and A.B. Lassar, *Regulation of dorsal somitic cell fates: BMPs and Noggin control the timing and pattern of myogenic regulator expression.* Genes Dev, 1998. **12**(3): p. 290-303.
24. Sela-Donenfeld, D. and C. Kalcheim, *Localized BMP4-noggin interactions generate the dynamic patterning of noggin expression in somites.* Dev Biol, 2002. **246**(2): p. 311-28.
25. Parker, M.H., P. Seale, and M.A. Rudnicki, *Looking back to the embryo: defining transcriptional networks in adult myogenesis.* Nat Rev Genet, 2003. **4**(7): p. 497-507.
26. Tajbakhsh, S. and M. Buckingham, *The birth of muscle progenitor cells in the mouse: spatiotemporal considerations.* Curr Top Dev Biol, 2000. **48**: p. 225-68.
27. Rudnicki, M.A., et al., *Inactivation of MyoD in mice leads to up-regulation of the myogenic HLH gene Myf-5 and results in apparently normal muscle development.* Cell, 1992. **71**(3): p. 383-90.
28. Nabeshima, Y., et al., *Myogenin gene disruption results in perinatal lethality because of severe muscle defect.* Nature, 1993. **364**(6437): p. 532-5.
29. Hasty, P., et al., *Muscle deficiency and neonatal death in mice with a targeted mutation in the myogenin gene.* Nature, 1993. **364**(6437): p. 501-6.
30. Kassar-Duchossoy, L., et al., *Mrf4 determines skeletal muscle identity in Myf5:Myod double-mutant mice.* Nature, 2004. **431**(7007): p. 466-71.
31. Pownall, M.E., M.K. Gustafsson, and C.P. Emerson, Jr., *Myogenic regulatory factors and the specification of muscle progenitors in vertebrate embryos.* Annu Rev Cell Dev Biol, 2002. **18**: p. 747-83.
32. Daston, G., et al., *Pax-3 is necessary for migration but not differentiation of limb muscle precursors in the mouse.* Development, 1996. **122**(3): p. 1017-27.
33. Williams, B.A. and C.P. Ordahl, *Pax-3 expression in segmental mesoderm marks early stages in myogenic cell specification.* Development, 1994. **120**(4): p. 785-96.
34. Tajbakhsh, S. and G. Cossu, *Establishing myogenic identity during somitogenesis.* Curr Opin Genet Dev, 1997. **7**(5): p. 634-41.
35. Horst, D., et al., *Comparative expression analysis of Pax3 and Pax7 during mouse myogenesis.* Int J Dev Biol, 2006. **50**(1): p. 47-54.
36. Jostes, B., C. Walther, and P. Gruss, *The murine paired box gene, Pax7, is expressed specifically during the development of the nervous and muscular system.* Mech Dev, 1990. **33**(1): p. 27-37.
37. Schubert, F.R., et al., *Early mesodermal phenotypes in splotch suggest a role for Pax3 in the formation of epithelial somites.* Dev Dyn, 2001. **222**(3): p. 506-21.
38. Goulding, M., A. Lumsden, and A.J. Paquette, *Regulation of Pax-3 expression in the dermomyotome and its role in muscle development.* Development, 1994. **120**(4): p. 957-71.
39. Bober, E., et al., *Pax-3 is required for the development of limb muscles: a possible role for the migration of dermomyotomal muscle progenitor cells.* Development, 1994. **120**(3): p. 603-12.

40. Maroto, M., et al., *Ectopic Pax-3 activates MyoD and Myf-5 expression in embryonic mesoderm and neural tissue.* Cell, 1997. **89**(1): p. 139-48.
41. Bajard, L., et al., *A novel genetic hierarchy functions during hypaxial myogenesis: Pax3 directly activates Myf5 in muscle progenitor cells in the limb.* Genes Dev, 2006. **20**(17): p. 2450-64.
42. Relaix, F., et al., *Divergent functions of murine Pax3 and Pax7 in limb muscle development.* Genes Dev, 2004. **18**(9): p. 1088-105.
43. Oustanina, S., G. Hause, and T. Braun, *Pax7 directs postnatal renewal and propagation of myogenic satellite cells but not their specification.* EMBO J, 2004. **23**(16): p. 3430-9.
44. Relaix, F., et al., *Pax3 and Pax7 have distinct and overlapping functions in adult muscle progenitor cells.* J Cell Biol, 2006. **172**(1): p. 91-102.
45. Seale, P. and M.A. Rudnicki, *A new look at the origin, function, and "stem-cell" status of muscle satellite cells.* Dev Biol, 2000. **218**(2): p. 115-24.
46. Ben-Yair, R. and C. Kalcheim, *Lineage analysis of the avian dermomyotome sheet reveals the existence of single cells with both dermal and muscle progenitor fates.* Development, 2005. **132**(4): p. 689-701.
47. Gros, J., et al., *A common somitic origin for embryonic muscle progenitors and satellite cells.* Nature, 2005. **435**(7044): p. 954-8.
48. Kassar-Duchossoy, L., et al., *Pax3/Pax7 mark a novel population of primitive myogenic cells during development.* Genes Dev, 2005. **19**(12): p. 1426-31.
49. Relaix, F., et al., *A Pax3/Pax7-dependent population of skeletal muscle progenitor cells.* Nature, 2005. **435**(7044): p. 948-53.
50. Schienda, J., et al., *Somitic origin of limb muscle satellite and side population cells.* Proc Natl Acad Sci U S A, 2006. **103**(4): p. 945-50.
51. Schmalbruch, H. and D.M. Lewis, *Dynamics of nuclei of muscle fibers and connective tissue cells in normal and denervated rat muscles.* Muscle Nerve, 2000. **23**(4): p. 617-26.
52. Charge, S.B. and M.A. Rudnicki, *Cellular and molecular regulation of muscle regeneration.* Physiol Rev, 2004. **84**(1): p. 209-38.
53. Huxley, A.F., *Cross-bridge action: present views, prospects, and unknowns.* J Biomech, 2000. **33**(10): p. 1189-95.
54. Mauro, A., *Satellite cell of skeletal muscle fibers.* J Biophys Biochem Cytol, 1961. **9**: p. 493-5.
55. Bischoff, R., *Interaction between satellite cells and skeletal muscle fibers.* Development, 1990. **109**(4): p. 943-52.
56. Scharner, J. and P.S. Zammit, *The muscle satellite cell at 50: the formative years.* Skelet Muscle, 2011. **1**(1): p. 28.
57. Bischoff, R. and C. Heintz, *Enhancement of skeletal muscle regeneration.* Dev Dyn, 1994. **201**(1): p. 41-54.
58. Biressi, S. and T.A. Rando, *Heterogeneity in the muscle satellite cell population.* Semin Cell Dev Biol, 2010. **21**(8): p. 845-54.
59. Yin, H., F. Price, and M.A. Rudnicki, *Satellite cells and the muscle stem cell niche.* Physiol Rev, 2013. **93**(1): p. 23-67.
60. McLoon, L.K. and J. Wirtschafter, *Activated satellite cells in extraocular muscles of normal adult monkeys and humans.* Invest Ophthalmol Vis Sci, 2003. **44**(5): p. 1927-32.
61. Patruno, M., et al., *Expression of the paired box domain Pax7 protein in myogenic cells isolated from the porcine semitendinosus muscle after birth.* Tissue Cell, 2008. **40**(1): p. 1-6.

62. Halevy, O., et al., *Pattern of Pax7 expression during myogenesis in the posthatch chicken establishes a model for satellite cell differentiation and renewal.* Dev Dyn, 2004. **231**(3): p. 489-502.
63. Morrison, J.I., et al., *Salamander limb regeneration involves the activation of a multipotent skeletal muscle satellite cell population.* J Cell Biol, 2006. **172**(3): p. 433-40.
64. Hammond, C.L., et al., *Signals and myogenic regulatory factors restrict pax3 and pax7 expression to dermomyotome-like tissue in zebrafish.* Dev Biol, 2007. **302**(2): p. 504-21.
65. Boonen, K.J. and M.J. Post, *The muscle stem cell niche: regulation of satellite cells during regeneration.* Tissue Eng Part B Rev, 2008. **14**(4): p. 419-31.
66. Kuang, S., M.A. Gillespie, and M.A. Rudnicki, *Niche regulation of muscle satellite cell self-renewal and differentiation.* Cell Stem Cell, 2008. **2**(1): p. 22-31.
67. Murphy, M.M., et al., *Satellite cells, connective tissue fibroblasts and their interactions are crucial for muscle regeneration.* Development, 2011. **138**(17): p. 3625-37.
68. Schmalbruch, H. and U. Hellhammer, *The number of nuclei in adult rat muscles with special reference to satellite cells.* Anat Rec, 1977. **189**(2): p. 169-75.
69. Grefte, S., et al., *Skeletal muscle development and regeneration.* Stem Cells Dev, 2007. **16**(5): p. 857-68.
70. Jarvinen, T.A., et al., *Muscle injuries: biology and treatment.* Am J Sports Med, 2005. **33**(5): p. 745-64.
71. Hall-Craggs, E.C. and H.S. Seyan, *Histochemical changes in innervated and denervated skeletal muscle fibers following treatment with bupivacaine (marcain).* Exp Neurol, 1975. **46**(2): p. 345-54.
72. Whalen, R.G., et al., *Expression of myosin isoforms during notexin-induced regeneration of rat soleus muscles.* Dev Biol, 1990. **141**(1): p. 24-40.
73. Blaveri, K., et al., *Patterns of repair of dystrophic mouse muscle: studies on isolated fibers.* Dev Dyn, 1999. **216**(3): p. 244-56.
74. Crews, L., et al., *Expression and activity of the newt Msx-1 gene in relation to limb regeneration.* Proc Biol Sci, 1995. **259**(1355): p. 161-71.
75. Tidball, J.G., *Inflammatory cell response to acute muscle injury.* Med Sci Sports Exerc, 1995. **27**(7): p. 1022-32.
76. Chazaud, B., et al., *Dual and beneficial roles of macrophages during skeletal muscle regeneration.* Exerc Sport Sci Rev, 2009. **37**(1): p. 18-22.
77. Robertson, T.A., et al., *The role of macrophages in skeletal muscle regeneration with particular reference to chemotaxis.* Exp Cell Res, 1993. **207**(2): p. 321-31.
78. Merly, F., et al., *Macrophages enhance muscle satellite cell proliferation and delay their differentiation.* Muscle Nerve, 1999. **22**(6): p. 724-32.
79. Lescaudron, L., et al., *Blood borne macrophages are essential for the triggering of muscle regeneration following muscle transplant.* Neuromuscul Disord, 1999. **9**(2): p. 72-80.
80. Mantovani, A., et al., *Regulatory pathways in inflammation.* Autoimmun Rev, 2007. **7**(1): p. 8-11.
81. Mantovani, A., A. Sica, and M. Locati, *Macrophage polarization comes of age.* Immunity, 2005. **23**(4): p. 344-6.
82. Mantovani, A., et al., *The chemokine system in diverse forms of macrophage activation and polarization.* Trends Immunol, 2004. **25**(12): p. 677-86.

83. Cantini, M. and U. Carraro, *Macrophage-released factor stimulates selectively myogenic cells in primary muscle culture.* J Neuropathol Exp Neurol, 1995. **54**(1): p. 121-8.
84. Cantini, M., et al., *Macrophage-secreted myogenic factors: a promising tool for greatly enhancing the proliferative capacity of myoblasts in vitro and in vivo.* Neurol Sci, 2002. **23**(4): p. 189-94.
85. Sonnet, C., et al., *Human macrophages rescue myoblasts and myotubes from apoptosis through a set of adhesion molecular systems.* J Cell Sci, 2006. **119**(Pt 12): p. 2497-507.
86. Sun, D., et al., *Bone marrow-derived cell regulation of skeletal muscle regeneration.* FASEB J, 2009. **23**(2): p. 382-95.
87. Arnold, L., et al., *Inflammatory monocytes recruited after skeletal muscle injury switch into antiinflammatory macrophages to support myogenesis.* J Exp Med, 2007. **204**(5): p. 1057-69.
88. Hawke, T.J. and D.J. Garry, *Myogenic satellite cells: physiology to molecular biology.* J Appl Physiol, 2001. **91**(2): p. 534-51.
89. Quinlan, J.G., et al., *Radiation inhibition of mdx mouse muscle regeneration: dose and age factors.* Muscle Nerve, 1995. **18**(2): p. 201-6.
90. Pietsch, P., *Differentiation in regeneration. I. The development of muscle and cartilage following deplantation of of regenerating limb blastemata of Amblystoma larvae.* Dev Biol, 1961. **3**: p. 255-64.
91. Grounds, M.D., et al., *The role of stem cells in skeletal and cardiac muscle repair.* J Histochem Cytochem, 2002. **50**(5): p. 589-610.
92. Mann, C.J., et al., *Aberrant repair and fibrosis development in skeletal muscle.* Skelet Muscle, 2011. **1**(1): p. 21.
93. Grounds, M.D. and Z. Yablonka-Reuveni, *Molecular and cell biology of skeletal muscle regeneration.* Mol Cell Biol Hum Dis Ser, 1993. **3**: p. 210-56.
94. Beauchamp, J.R., et al., *Dynamics of myoblast transplantation reveal a discrete minority of precursors with stem cell-like properties as the myogenic source.* J Cell Biol, 1999. **144**(6): p. 1113-22.
95. Cooper, R.N., et al., *In vivo satellite cell activation via Myf5 and MyoD in regenerating mouse skeletal muscle.* J Cell Sci, 1999. **112 (Pt 17)**: p. 2895-901.
96. Kuang, S., et al., *Asymmetric self-renewal and commitment of satellite stem cells in muscle.* Cell, 2007. **129**(5): p. 999-1010.
97. Shinin, V., et al., *Asymmetric division and cosegregation of template DNA strands in adult muscle satellite cells.* Nat Cell Biol, 2006. **8**(7): p. 677-87.
98. Conboy, I.M. and T.A. Rando, *The regulation of Notch signaling controls satellite cell activation and cell fate determination in postnatal myogenesis.* Dev Cell, 2002. **3**(3): p. 397-409.
99. Perez-Ruiz, A., et al., *beta-Catenin promotes self-renewal of skeletal-muscle satellite cells.* J Cell Sci, 2008. **121**(Pt 9): p. 1373-82.
100. Brack, A.S., et al., *Increased Wnt signaling during aging alters muscle stem cell fate and increases fibrosis.* Science, 2007. **317**(5839): p. 807-10.
101. Brack, A.S., et al., *A temporal switch from notch to Wnt signaling in muscle stem cells is necessary for normal adult myogenesis.* Cell Stem Cell, 2008. **2**(1): p. 50-9.
102. Brack, A.S., et al., *BCL9 is an essential component of canonical Wnt signaling that mediates the differentiation of myogenic progenitors during muscle regeneration.* Dev Biol, 2009. **335**(1): p. 93-105.

103. Le Grand, F., et al., *Wnt7a activates the planar cell polarity pathway to drive the symmetric expansion of satellite stem cells.* Cell Stem Cell, 2009. **4**(6): p. 535-47.
104. Seale, P., A. Polesskaya, and M.A. Rudnicki, *Adult stem cell specification by Wnt signaling in muscle regeneration.* Cell Cycle, 2003. **2**(5): p. 418-9.
105. Otto, A., et al., *Canonical Wnt signalling induces satellite-cell proliferation during adult skeletal muscle regeneration.* J Cell Sci, 2008. **121**(Pt 17): p. 2939-50.
106. Ou, C.Y., et al., *Requirement of cell cycle and apoptosis regulator 1 for target gene activation by Wnt and beta-catenin and for anchorage-independent growth of human colon carcinoma cells.* J Biol Chem, 2009. **284**(31): p. 20629-37.
107. Cossu, G., *Unorthodox myogenesis: possible developmental significance and implications for tissue histogenesis and regeneration.* Histol Histopathol, 1997. **12**(3): p. 755-60.
108. Sambasivan, R., et al., *Pax7-expressing satellite cells are indispensable for adult skeletal muscle regeneration.* Development, 2011. **138**(17): p. 3647-56.
109. Cossu, G. and P. Bianco, *Mesoangioblasts — vascular progenitors for extravascular mesodermal tissues.* Current Opinion in Genetics & Development, 2003. **13**(5): p. 537-542.
110. Sampaolesi, M., et al., *Cell therapy of alpha-sarcoglycan null dystrophic mice through intra-arterial delivery of mesoangioblasts.* Science, 2003. **301**(5632): p. 487-92.
111. Sampaolesi, M., et al., *Mesoangioblast stem cells ameliorate muscle function in dystrophic dogs.* Nature, 2006. **444**(7119): p. 574-9.
112. Dellavalle, A., et al., *Pericytes of human skeletal muscle are myogenic precursors distinct from satellite cells.* Nat Cell Biol, 2007. **9**(3): p. 255-67.
113. Ferrari, G., *Muscle Regeneration by Bone Marrow-Derived Myogenic Progenitors.* Science, 1998. **279**(5356): p. 1528-1530.
114. Bittner, R.E., et al., *Recruitment of bone-marrow-derived cells by skeletal and cardiac muscle in adult dystrophic mdx mice.* Anat Embryol (Berl), 1999. **199**(5): p. 391-6.
115. Gussoni, E., et al., *Dystrophin expression in the mdx mouse restored by stem cell transplantation.* Nature, 1999. **401**(6751): p. 390-4.
116. LaBarge, M.A. and H.M. Blau, *Biological progression from adult bone marrow to mononucleate muscle stem cell to multinucleate muscle fiber in response to injury.* Cell, 2002. **111**(4): p. 589-601.
117. Corbel, S.Y., et al., *Contribution of hematopoietic stem cells to skeletal muscle.* Nat Med, 2003. **9**(12): p. 1528-32.
118. Yoshimoto, M., et al., *Two different roles of purified CD45+c-Kit+Sca-1+Lin- cells after transplantation in muscles.* Stem Cells, 2005. **23**(5): p. 610-8.
119. Camargo, F.D., et al., *Single hematopoietic stem cells generate skeletal muscle through myeloid intermediates.* Nat Med, 2003. **9**(12): p. 1520-7.
120. Abedi, M., et al., *Robust conversion of marrow cells to skeletal muscle with formation of marrow-derived muscle cell colonies: a multifactorial process.* Exp Hematol, 2004. **32**(5): p. 426-34.
121. Shi, D., et al., *Myogenic fusion of human bone marrow stromal cells, but not hematopoietic cells.* Blood, 2004. **104**(1): p. 290-4.
122. Dezawa, M., et al., *Bone marrow stromal cells generate muscle cells and repair muscle degeneration.* Science, 2005. **309**(5732): p. 314-7.

123. Ferrari, G., A. Stornaiuolo, and F. Mavilio, *Failure to correct murine muscular dystrophy.* Nature, 2001. **411**(6841): p. 1014-5.
124. !!! INVALID CITATION !!!
125. Bachrach, E., et al., *Muscle engraftment of myogenic progenitor cells following intraarterial transplantation.* Muscle Nerve, 2006. **34**(1): p. 44-52.
126. Asakura, A. and M.A. Rudnicki, *Side population cells from diverse adult tissues are capable of in vitro hematopoietic differentiation.* Exp Hematol, 2002. **30**(11): p. 1339-45.
127. Challen, G.A. and M.H. Little, *A side order of stem cells: the SP phenotype.* Stem Cells, 2006. **24**(1): p. 3-12.
128. Polesskaya, A., P. Seale, and M.A. Rudnicki, *Wnt signaling induces the myogenic specification of resident CD45+ adult stem cells during muscle regeneration.* Cell, 2003. **113**(7): p. 841-52.
129. Tanaka, K.K., et al., *Syndecan-4-expressing muscle progenitor cells in the SP engraft as satellite cells during muscle regeneration.* Cell Stem Cell, 2009. **4**(3): p. 217-25.
130. Uezumi, A., et al., *Functional heterogeneity of side population cells in skeletal muscle.* Biochem Biophys Res Commun, 2006. **341**(3): p. 864-73.
131. Mitchell, K.J., et al., *Identification and characterization of a non-satellite cell muscle resident progenitor during postnatal development.* Nat Cell Biol, 2010. **12**(3): p. 257-66.
132. Besson, V., et al., *PW1 gene/paternally expressed gene 3 (PW1/Peg3) identifies multiple adult stem and progenitor cell populations.* Proc Natl Acad Sci U S A, 2011. **108**(28): p. 11470-5.
133. Nicolas, N., et al., *Embryonic deregulation of muscle stress signaling pathways leads to altered postnatal stem cell behavior and a failure in postnatal muscle growth.* Dev Biol, 2005. **281**(2): p. 171-83.
134. Relaix, F., et al., *Pw1, a novel zinc finger gene implicated in the myogenic and neuronal lineages.* Dev Biol, 1996. **177**(2): p. 383-96.
135. Coletti, D., et al., *TNFalpha inhibits skeletal myogenesis through a PW1-dependent pathway by recruitment of caspase pathways.* EMBO J, 2002. **21**(4): p. 631-42.
136. Schwarzkopf, M., et al., *Muscle cachexia is regulated by a p53-PW1/Peg3-dependent pathway.* Genes Dev, 2006. **20**(24): p. 3440-52.
137. Rouger, K., et al., *Systemic delivery of allogenic muscle stem cells induces long-term muscle repair and clinical efficacy in duchenne muscular dystrophy dogs.* Am J Pathol, 2011. **179**(5): p. 2501-18.
138. Gharaibeh, B., et al., *Isolation of a slowly adhering cell fraction containing stem cells from murine skeletal muscle by the preplate technique.* Nat Protoc, 2008. **3**(9): p. 1501-9.
139. Gharaibeh, B., et al., *Terminal differentiation is not a major determinant for the success of stem cell therapy - cross-talk between muscle-derived stem cells and host cells.* Stem Cell Res Ther, 2011. **2**(4): p. 31.
140. Qu-Petersen, Z., et al., *Identification of a novel population of muscle stem cells in mice: potential for muscle regeneration.* J Cell Biol, 2002. **157**(5): p. 851-64.
141. Usas, A. and J. Huard, *Muscle-derived stem cells for tissue engineering and regenerative therapy.* Biomaterials, 2007. **28**(36): p. 5401-6.
142. Ikezawa, M., et al., *Dystrophin delivery in dystrophin-deficient DMDmdx skeletal muscle by isogenic muscle-derived stem cell transplantation.* Hum Gene Ther, 2003. **14**(16): p. 1535-46.

143. Meliga, E., et al., *Adipose-derived cells.* Cell Transplant, 2007. **16**(9): p. 963-70.
144. Goudenege, S., et al., *Enhancement of myogenic and muscle repair capacities of human adipose-derived stem cells with forced expression of MyoD.* Mol Ther, 2009. **17**(6): p. 1064-72.
145. Pouget, C., K. Pottin, and T. Jaffredo, *Sclerotomal origin of vascular smooth muscle cells and pericytes in the embryo.* Dev Biol, 2008. **315**(2): p. 437-47.
146. Wiegreffe, C., et al., *Remodeling of aortic smooth muscle during avian embryonic development.* Dev Dyn, 2009. **238**(3): p. 624-31.
147. Farrington-Rock, C., et al., *Chondrogenic and adipogenic potential of microvascular pericytes.* Circulation, 2004. **110**(15): p. 2226-32.
148. Doherty, M., et al., *Identification of genes expressed during the osteogenic differentiation of vascular pericytes in vitro.* Biochem Soc Trans, 1998. **26**(1): p. S4.
149. Collett, G.D. and A.E. Canfield, *Angiogenesis and pericytes in the initiation of ectopic calcification.* Circ Res, 2005. **96**(9): p. 930-8.
150. Morgan, J. and F. Muntoni, *Mural cells paint a new picture of muscle stem cells.* Nat Cell Biol, 2007. **9**(3): p. 249-51.
151. Armulik, A., G. Genove, and C. Betsholtz, *Pericytes: developmental, physiological, and pathological perspectives, problems, and promises.* Dev Cell, 2011. **21**(2): p. 193-215.
152. Ozerdem, U., et al., *NG2 proteoglycan is expressed exclusively by mural cells during vascular morphogenesis.* Dev Dyn, 2001. **222**(2): p. 218-27.
153. Lindahl, P., et al., *Pericyte loss and microaneurysm formation in PDGF-B-deficient mice.* Science, 1997. **277**(5323): p. 242-5.
154. Crisan, M., et al., *A perivascular origin for mesenchymal stem cells in multiple human organs.* Cell Stem Cell, 2008. **3**(3): p. 301-13.
155. De Angelis, L., et al., *Skeletal myogenic progenitors originating from embryonic dorsal aorta coexpress endothelial and myogenic markers and contribute to postnatal muscle growth and regeneration.* J Cell Biol, 1999. **147**(4): p. 869-78.
156. Minasi, M.G., et al., *The meso-angioblast: a multipotent, self-renewing cell that originates from the dorsal aorta and differentiates into most mesodermal tissues.* Development, 2002. **129**(11): p. 2773-83.
157. Guttinger, M., et al., *Allogeneic mesoangioblasts give rise to alpha-sarcoglycan expressing fibers when transplanted into dystrophic mice.* Exp Cell Res, 2006. **312**(19): p. 3872-9.
158. Galvez, B.G., et al., *Complete repair of dystrophic skeletal muscle by mesoangioblasts with enhanced migration ability.* J Cell Biol, 2006. **174**(2): p. 231-43.
159. Palumbo, R., et al., *Extracellular HMGB1, a signal of tissue damage, induces mesoangioblast migration and proliferation.* J Cell Biol, 2004. **164**(3): p. 441-9.
160. Sciorati, C., et al., *Ex vivo treatment with nitric oxide increases mesoangioblast therapeutic efficacy in muscular dystrophy.* J Cell Sci, 2006. **119**(Pt 24): p. 5114-23.
161. Torrente, Y., et al., *Human circulating AC133(+) stem cells restore dystrophin expression and ameliorate function in dystrophic skeletal muscle.* J Clin Invest, 2004. **114**(2): p. 182-95.
162. Peichev, M., et al., *Expression of VEGFR-2 and AC133 by circulating human CD34(+) cells identifies a population of functional endothelial precursors.* Blood, 2000. **95**(3): p. 952-8.
163. Cao, B. and J. Huard, *Muscle-derived stem cells.* Cell Cycle, 2004. **3**(2): p. 104-7.

164. Benchaouir, R., et al., *Restoration of human dystrophin following transplantation of exon-skipping-engineered DMD patient stem cells into dystrophic mice.* Cell Stem Cell, 2007. **1**(6): p. 646-57.
165. Tedesco, F.S., et al., *Repairing skeletal muscle: regenerative potential of skeletal muscle stem cells.* J Clin Invest, 2010. **120**(1): p. 11-9.
166. Barberi, T., et al., *Derivation of engraftable skeletal myoblasts from human embryonic stem cells.* Nat Med, 2007. **13**(5): p. 642-8.
167. Mizuno, Y., et al., *Generation of skeletal muscle stem/progenitor cells from murine induced pluripotent stem cells.* FASEB J, 2010. **24**(7): p. 2245-53.
168. Chang, H., et al., *Generation of transplantable, functional satellite-like cells from mouse embryonic stem cells.* FASEB J, 2009. **23**(6): p. 1907-19.
169. Quattrocelli, M., et al., *Intrinsic cell memory reinforces myogenic commitment of pericyte-derived iPSCs.* J Pathol, 2011. **223**(5): p. 593-603.
170. Darabi, R., et al., *Functional skeletal muscle regeneration from differentiating embryonic stem cells.* Nat Med, 2008. **14**(2): p. 134-43.
171. Darabi, R., et al., *Assessment of the myogenic stem cell compartment following transplantation of Pax3/Pax7-induced embryonic stem cell-derived progenitors.* Stem Cells, 2011. **29**(5): p. 777-90.
172. Sakurai, H., et al., *Paraxial mesodermal progenitors derived from mouse embryonic stem cells contribute to muscle regeneration via differentiation into muscle satellite cells.* Stem Cells, 2008. **26**(7): p. 1865-73.
173. Lian, Q., et al., *Future perspective of induced pluripotent stem cells for diagnosis, drug screening and treatment of human diseases.* Thromb Haemost, 2010. **104**(1): p. 39-44.
174. Dar, A., et al., *Multipotent vasculogenic pericytes from human pluripotent stem cells promote recovery of murine ischemic limb.* Circulation, 2012. **125**(1): p. 87-99.
175. Tedesco, F.S., et al., *Transplantation of genetically corrected human iPSC-derived progenitors in mice with limb-girdle muscular dystrophy.* Sci Transl Med, 2012. **4**(140): p. 140ra89.
176. Benoit, P.W. and W.D. Belt, *Destruction and regeneration of skeletal muscle after treatment with a local anaesthetic, bupivacaine (Marcaine).* J Anat, 1970. **107**(Pt 3): p. 547-56.
177. Couteaux, R., J.C. Mira, and A. d'Albis, *Regeneration of muscles after cardiotoxin injury. I. Cytological aspects.* Biol Cell, 1988. **62**(2): p. 171-82.
178. Harris, J.B. and C.A. MacDonell, *Phospholipase A2 activity of notexin and its role in muscle damage.* Toxicon, 1981. **19**(3): p. 419-30.
179. Vracko, R. and E.P. Benditt, *Basal lamina: the scaffold for orderly cell replacement. Observations on regeneration of injured skeletal muscle fibers and capillaries.* J Cell Biol, 1972. **55**(2): p. 406-19.
180. Carlson, B.M. and E. Gutmann, *Regneration in free grafts of normal and denervated muscles in the rat: morphology and histochemistry.* Anat Rec, 1975. **183**(1): p. 47-62.
181. Bassaglia, Y. and J. Gautron, *Fast and slow rat muscles degenerate and regenerate differently after whole crush injury.* J Muscle Res Cell Motil, 1995. **16**(4): p. 420-9.
182. Anderson, J.E., *Dystrophic changes in mdx muscle regenerating from denervation and devascularization.* Muscle Nerve, 1991. **14**(3): p. 268-79.
183. Roberts, P., J.K. McGeachie, and M.D. Grounds, *The host environment determines strain-specific differences in the timing of skeletal muscle regeneration: cross-*

transplantation studies between SJL/J and BALB/c mice. J Anat, 1997. **191 (Pt 4)**: p. 585-94.
184. d'Albis, A., et al., *Regeneration after cardiotoxin injury of innervated and denervated slow and fast muscles of mammals. Myosin isoform analysis.* Eur J Biochem, 1988. **174**(1): p. 103-10.
185. Hall-Craggs, E.C., *Rapid degeneration and regeneration of a whole skeletal muscle following treatment with bupivacaine (Marcain).* Exp Neurol, 1974. **43**(2): p. 349-58.
186. Harris, J.B. and M.A. Johnson, *Further observations on the pathological responses of rat skeletal muscle to toxins isolated from the venom of the Australian tiger snake, Notechis scutatus scutatus.* Clin Exp Pharmacol Physiol, 1978. **5**(6): p. 587-600.
187. Palacio, J., et al., *Procion orange tracer dye technique vs. identification of intrafibrillar fibronectin in the assessment of sarcolemmal damage.* Eur J Clin Invest, 2002. **32**(6): p. 443-7.
188. Hamer, P.W., et al., *Evans Blue Dye as an in vivo marker of myofibre damage: optimising parameters for detecting initial myofibre membrane permeability.* J Anat, 2002. **200**(Pt 1): p. 69-79.
189. Matsuda, R., A. Nishikawa, and H. Tanaka, *Visualization of dystrophic muscle fibers in mdx mouse by vital staining with Evans blue: evidence of apoptosis in dystrophin-deficient muscle.* J Biochem, 1995. **118**(5): p. 959-64.
190. Harris, J.B., *Myotoxic phospholipases A2 and the regeneration of skeletal muscles.* Toxicon, 2003. **42**(8): p. 933-45.
191. Emery, A.E.H., *The muscular dystrophies.* The Lancet, 2002. **359**(9307): p. 687-695.
192. Ibraghimov-Beskrovnaya, O., et al., *Primary structure of dystrophin-associated glycoproteins linking dystrophin to the extracellular matrix.* Nature, 1992. **355**(6362): p. 696-702.
193. Ervasti, J.M., *Dystrophin, its interactions with other proteins, and implications for muscular dystrophy.* Biochim Biophys Acta, 2007. **1772**(2): p. 108-17.
194. Emery, A.E., *The muscular dystrophies.* BMJ, 1998. **317**(7164): p. 991-5.
195. Sicinski, P., et al., *The molecular basis of muscular dystrophy in the mdx mouse: a point mutation.* Science, 1989. **244**(4912): p. 1578-80.
196. Grady, R.M., et al., *Skeletal and cardiac myopathies in mice lacking utrophin and dystrophin: a model for Duchenne muscular dystrophy.* Cell, 1997. **90**(4): p. 729-38.
197. Weir, A.P., et al., *A- and B-utrophin have different expression patterns and are differentially up-regulated in mdx muscle.* J Biol Chem, 2002. **277**(47): p. 45285-90.
198. Hirst, R.C., K.J. McCullagh, and K.E. Davies, *Utrophin upregulation in Duchenne muscular dystrophy.* Acta Myol, 2005. **24**(3): p. 209-16.
199. Pastoret, C. and A. Sebille, *mdx mice show progressive weakness and muscle deterioration with age.* J Neurol Sci, 1995. **129**(2): p. 97-105.
200. Duclos, F., et al., *Progressive muscular dystrophy in alpha-sarcoglycan-deficient mice.* J Cell Biol, 1998. **142**(6): p. 1461-71.
201. Duclos, F., et al., *Beta-sarcoglycan: genomic analysis and identification of a novel missense mutation in the LGMD2E Amish isolate.* Neuromuscul Disord, 1998. **8**(1): p. 30-8.

202. Durbeej, M., et al., *Disruption of the beta-sarcoglycan gene reveals pathogenetic complexity of limb-girdle muscular dystrophy type 2E.* Mol Cell, 2000. **5**(1): p. 141-51.
203. Cooper, B.J., et al., *The homologue of the Duchenne locus is defective in X-linked muscular dystrophy of dogs.* Nature, 1988. **334**(6178): p. 154-6.
204. Sharp, N.J., et al., *An error in dystrophin mRNA processing in golden retriever muscular dystrophy, an animal homologue of Duchenne muscular dystrophy.* Genomics, 1992. **13**(1): p. 115-21.
205. Kornegay, J.N., et al., *The cranial sartorius muscle undergoes true hypertrophy in dogs with golden retriever muscular dystrophy.* Neuromuscul Disord, 2003. **13**(6): p. 493-500.
206. Chakkalakal, J.V., et al., *Molecular, cellular, and pharmacological therapies for Duchenne/Becker muscular dystrophies.* FASEB J, 2005. **19**(8): p. 880-91.
207. Nowak, K.J. and K.E. Davies, *Duchenne muscular dystrophy and dystrophin: pathogenesis and opportunities for treatment.* EMBO Rep, 2004. **5**(9): p. 872-6.
208. Manzur, A.Y., et al., *Glucocorticoid corticosteroids for Duchenne muscular dystrophy.* Cochrane Database Syst Rev, 2004(2): p. CD003725.
209. Urtizberea, J.A., *Therapies in muscular dystrophy: current concepts and future prospects.* Eur Neurol, 2000. **43**(3): p. 127-32.
210. Manzur, A.Y., et al., *Glucocorticoid corticosteroids for Duchenne muscular dystrophy.* Cochrane Database Syst Rev, 2008(1): p. CD003725.
211. Vandebrouck, C., et al., *The effect of methylprednisolone on intracellular calcium of normal and dystrophic human skeletal muscle cells.* Neurosci Lett, 1999. **269**(2): p. 110-4.
212. Pasquini, F., et al., *The effect of glucocorticoids on the accumulation of utrophin by cultured normal and dystrophic human skeletal muscle satellite cells.* Neuromuscul Disord, 1995. **5**(2): p. 105-14.
213. Skuk, D., J.T. Vilquin, and J.P. Tremblay, *Experimental and therapeutic approaches to muscular dystrophies.* Curr Opin Neurol, 2002. **15**(5): p. 563-9.
214. Barton, E.R., et al., *Muscle-specific expression of insulin-like growth factor I counters muscle decline in mdx mice.* J Cell Biol, 2002. **157**(1): p. 137-48.
215. Bogdanovich, S., et al., *Functional improvement of dystrophic muscle by myostatin blockade.* Nature, 2002. **420**(6914): p. 418-21.
216. Tinsley, J.M., et al., *Amelioration of the dystrophic phenotype of mdx mice using a truncated utrophin transgene.* Nature, 1996. **384**(6607): p. 349-53.
217. Tinsley, J., et al., *Expression of full-length utrophin prevents muscular dystrophy in mdx mice.* Nat Med, 1998. **4**(12): p. 1441-4.
218. Gramolini, A.O., et al., *Induction of utrophin gene expression by heregulin in skeletal muscle cells: role of the N-box motif and GA binding protein.* Proc Natl Acad Sci U S A, 1999. **96**(6): p. 3223-7.
219. Engvall, E. and U.M. Wewer, *The new frontier in muscular dystrophy research: booster genes.* FASEB J, 2003. **17**(12): p. 1579-84.
220. Barton-Davis, E.R., et al., *Aminoglycoside antibiotics restore dystrophin function to skeletal muscles of mdx mice.* J Clin Invest, 1999. **104**(4): p. 375-81.
221. Acharyya, S., et al., *Interplay of IKK/NF-kappaB signaling in macrophages and myofibers promotes muscle degeneration in Duchenne muscular dystrophy.* J Clin Invest, 2007. **117**(4): p. 889-901.
222. Radley, H.G., M.J. Davies, and M.D. Grounds, *Reduced muscle necrosis and long-term benefits in dystrophic mdx mice after cV1q (blockade of TNF) treatment.* Neuromuscul Disord, 2008. **18**(3): p. 227-38.

223. Brunelli, S., et al., *Nitric oxide release combined with nonsteroidal antiinflammatory activity prevents muscular dystrophy pathology and enhances stem cell therapy.* Proc Natl Acad Sci U S A, 2007. **104**(1): p. 264-9.
224. Sciorati, C., et al., *Co-administration of ibuprofen and nitric oxide is an effective experimental therapy for muscular dystrophy, with immediate applicability to humans.* Br J Pharmacol, 2010. **160**(6): p. 1550-60.
225. D'Angelo, M.G., et al., *Nitric oxide donor and non steroidal anti inflammatory drugs as a therapy for muscular dystrophies: evidence from a safety study with pilot efficacy measures in adult dystrophic patients.* Pharmacol Res, 2012. **65**(4): p. 472-9.
226. Blake, D.J., et al., *Function and genetics of dystrophin and dystrophin-related proteins in muscle.* Physiol Rev, 2002. **82**(2): p. 291-329.
227. Ferrer, A., et al., *Long-term expression of full-length human dystrophin in transgenic mdx mice expressing internally deleted human dystrophins.* Gene Ther, 2004. **11**(11): p. 884-93.
228. Yang, Y., et al., *Immunology of gene therapy with adenoviral vectors in mouse skeletal muscle.* Hum Mol Genet, 1996. **5**(11): p. 1703-12.
229. DelloRusso, C., et al., *Functional correction of adult mdx mouse muscle using gutted adenoviral vectors expressing full-length dystrophin.* Proc Natl Acad Sci U S A, 2002. **99**(20): p. 12979-84.
230. Wolff, J.A., et al., *Direct gene transfer into mouse muscle in vivo.* Science, 1990. **247**(4949 Pt 1): p. 1465-8.
231. Budker, V., et al., *The efficient expression of intravascularly delivered DNA in rat muscle.* Gene Ther, 1998. **5**(2): p. 272-6.
232. Vicat, J.M., et al., *Muscle transfection by electroporation with high-voltage and short-pulse currents provides high-level and long-lasting gene expression.* Hum Gene Ther, 2000. **11**(6): p. 909-16.
233. Ragot, T., et al., *Efficient adenovirus-mediated transfer of a human minidystrophin gene to skeletal muscle of mdx mice.* Nature, 1993. **361**(6413): p. 647-50.
234. Herzog, R.W., *AAV-mediated gene transfer to skeletal muscle.* Methods Mol Biol, 2004. **246**: p. 179-94.
235. Cole-Strauss, A., et al., *Correction of the mutation responsible for sickle cell anemia by an RNA-DNA oligonucleotide.* Science, 1996. **273**(5280): p. 1386-9.
236. Rando, T.A., M.H. Disatnik, and L.Z. Zhou, *Rescue of dystrophin expression in mdx mouse muscle by RNA/DNA oligonucleotides.* Proc Natl Acad Sci U S A, 2000. **97**(10): p. 5363-8.
237. Bertoni, C., C. Lau, and T.A. Rando, *Restoration of dystrophin expression in mdx muscle cells by chimeraplast-mediated exon skipping.* Hum Mol Genet, 2003. **12**(10): p. 1087-99.
238. Lu, Q.L. and T.A. Partridge, *Antisense therapy corrects nonsense mutation by exon skipping.* Discov Med, 2003. **3**(19): p. 39-44.
239. Lu, Q.L., et al., *Massive idiosyncratic exon skipping corrects the nonsense mutation in dystrophic mouse muscle and produces functional revertant fibers by clonal expansion.* J Cell Biol, 2000. **148**(5): p. 985-96.
240. Partridge, T.A., et al., *Conversion of mdx myofibres from dystrophin-negative to -positive by injection of normal myoblasts.* Nature, 1989. **337**(6203): p. 176-9.
241. Perie, S., et al., *Premature proliferative arrest of cricopharyngeal myoblasts in oculo-pharyngeal muscular dystrophy: Therapeutic perspectives of autologous myoblast transplantation.* Neuromuscul Disord, 2006. **16**(11): p. 770-81.

242. Kimura, E., et al., *Dystrophin delivery to muscles of mdx mice using lentiviral vectors leads to myogenic progenitor targeting and stable gene expression.* Mol Ther, 2010. **18**(1): p. 206-13.
243. Escors, D. and K. Breckpot, *Lentiviral vectors in gene therapy: their current status and future potential.* Arch Immunol Ther Exp (Warsz), 2010. **58**(2): p. 107-19.
244. Larochelle, A., K.W. Peng, and S.J. Russell, *Lentiviral vector targeting.* Curr Top Microbiol Immunol, 2002. **261**: p. 143-63.
245. Dunant, P., et al., *Expression of dystrophin driven by the 1.35-kb MCK promoter ameliorates muscular dystrophy in fast, but not in slow muscles of transgenic mdx mice.* Mol Ther, 2003. **8**(1): p. 80-9.
246. Ivics, Z. and Z. Izsvak, *Transposons for gene therapy!* Curr Gene Ther, 2006. **6**(5): p. 593-607.
247. Izsvak, Z., et al., *Efficient stable gene transfer into human cells by the Sleeping Beauty transposon vectors.* Methods, 2009. **49**(3): p. 287-97.
248. Hoshiya, H., et al., *A highly stable and nonintegrated human artificial chromosome (HAC) containing the 2.4 Mb entire human dystrophin gene.* Mol Ther, 2009. **17**(2): p. 309-17.
249. Kazuki, Y., et al., *Complete genetic correction of ips cells from Duchenne muscular dystrophy.* Mol Ther, 2010. **18**(2): p. 386-93.
250. Tedesco, F.S., et al., *Stem cell-mediated transfer of a human artificial chromosome ameliorates muscular dystrophy.* Sci Transl Med, 2011. **3**(96): p. 96ra78.
251. Ito, K., et al., *Smooth muscle-specific dystrophin expression improves aberrant vasoregulation in mdx mice.* Hum Mol Genet, 2006. **15**(14): p. 2266-75.
252. Miyatake, M., et al., *Possible systemic smooth muscle layer dysfunction due to a deficiency of dystrophin in Duchenne muscular dystrophy.* J Neurol Sci, 1989. **93**(1): p. 11-7.
253. Cullen, M.J. and E. Jaros, *Ultrastructure of the skeletal muscle in the X chromosome-linked dystrophic (mdx) mouse. Comparison with Duchenne muscular dystrophy.* Acta Neuropathol, 1988. **77**(1): p. 69-81.
254. Loufrani, L., B.I. Levy, and D. Henrion, *Defect in microvascular adaptation to chronic changes in blood flow in mice lacking the gene encoding for dystrophin.* Circ Res, 2002. **91**(12): p. 1183-9.
255. Loufrani, L., et al., *Absence of dystrophin in mice reduces NO-dependent vascular function and vascular density: total recovery after a treatment with the aminoglycoside gentamicin.* Arterioscler Thromb Vasc Biol, 2004. **24**(4): p. 671-6.
256. Messina, S., et al., *VEGF overexpression via adeno-associated virus gene transfer promotes skeletal muscle regeneration and enhances muscle function in mdx mice.* FASEB J, 2007. **21**(13): p. 3737-46.
257. Verma, M., et al., *Flt-1 haploinsufficiency ameliorates muscular dystrophy phenotype by developmentally increased vasculature in mdx mice.* Hum Mol Genet, 2010. **19**(21): p. 4145-59.
258. Risau, W., *Embryonic angiogenesis factors.* Pharmacol Ther, 1991. **51**(3): p. 371-6.
259. Noden, D.M., *Embryonic origins and assembly of blood vessels.* Am Rev Respir Dis, 1989. **140**(4): p. 1097-103.
260. Risau, W. and I. Flamme, *Vasculogenesis.* Annu Rev Cell Dev Biol, 1995. **11**: p. 73-91.

261. Drake, C.J., *Embryonic and adult vasculogenesis.* Birth Defects Res C Embryo Today, 2003. **69**(1): p. 73-82.
262. Gerhardt, H. and C. Betsholtz, *Endothelial-pericyte interactions in angiogenesis.* Cell Tissue Res, 2003. **314**(1): p. 15-23.
263. Mustonen, T. and K. Alitalo, *Endothelial receptor tyrosine kinases involved in angiogenesis.* J Cell Biol, 1995. **129**(4): p. 895-8.
264. Carmeliet, P., et al., *Role of tissue factor in embryonic blood vessel development.* Nature, 1996. **383**(6595): p. 73-5.
265. Ferrara, N., *Vascular endothelial growth factor.* Eur J Cancer, 1996. **32A**(14): p. 2413-22.
266. Ferrara, N., *Vascular endothelial growth factor and the regulation of angiogenesis.* Recent Prog Horm Res, 2000. **55**: p. 15-35; discussion 35-6.
267. Koch, S., et al., *Signal transduction by vascular endothelial growth factor receptors.* Biochem J, 2011. **437**(2): p. 169-83.
268. Ferrara, N., *The role of VEGF in the regulation of physiological and pathological angiogenesis.* EXS, 2005(94): p. 209-31.
269. Hoch, R.V. and P. Soriano, *Roles of PDGF in animal development.* Development, 2003. **130**(20): p. 4769-84.
270. Betsholtz, C., *Insight into the physiological functions of PDGF through genetic studies in mice.* Cytokine Growth Factor Rev, 2004. **15**(4): p. 215-28.
271. Chantrain, C.F., et al., *Mechanisms of pericyte recruitment in tumour angiogenesis: a new role for metalloproteinases.* Eur J Cancer, 2006. **42**(3): p. 310-8.
272. Dyer, L.A. and C. Patterson, *Development of the endothelium: an emphasis on heterogeneity.* Semin Thromb Hemost, 2010. **36**(3): p. 227-35.
273. Wilting, J. and B. Christ, *Embryonic angiogenesis: a review.* Naturwissenschaften, 1996. **83**(4): p. 153-64.
274. Wilting, J., et al., *Development of the embryonic vascular system.* Cell Mol Biol Res, 1995. **41**(4): p. 219-32.
275. Palis, J. and M.C. Yoder, *Yolk-sac hematopoiesis: the first blood cells of mouse and man.* Exp Hematol, 2001. **29**(8): p. 927-36.
276. Choi, K., et al., *A common precursor for hematopoietic and endothelial cells.* Development, 1998. **125**(4): p. 725-32.
277. Kabrun, N., et al., *Flk-1 expression defines a population of early embryonic hematopoietic precursors.* Development, 1997. **124**(10): p. 2039-48.
278. Zape, J.P. and A.C. Zovein, *Hemogenic endothelium: origins, regulation, and implications for vascular biology.* Semin Cell Dev Biol, 2011. **22**(9): p. 1036-47.
279. Lancrin, C., et al., *The haemangioblast generates haematopoietic cells through a haemogenic endothelium stage.* Nature, 2009. **457**(7231): p. 892-5.
280. Medvinsky, A., S. Rybtsov, and S. Taoudi, *Embryonic origin of the adult hematopoietic system: advances and questions.* Development, 2011. **138**(6): p. 1017-31.
281. North, T., et al., *Cbfa2 is required for the formation of intra-aortic hematopoietic clusters.* Development, 1999. **126**(11): p. 2563-75.
282. Tavian, M., et al., *Aorta-associated CD34+ hematopoietic cells in the early human embryo.* Blood, 1996. **87**(1): p. 67-72.
283. Marshall, C.J. and A.J. Thrasher, *The embryonic origins of human haematopoiesis.* Br J Haematol, 2001. **112**(4): p. 838-50.

284. Hellstrom, M., et al., *Role of PDGF-B and PDGFR-beta in recruitment of vascular smooth muscle cells and pericytes during embryonic blood vessel formation in the mouse.* Development, 1999. **126**(14): p. 3047-55.
285. Yamashita, J., et al., *Flk1-positive cells derived from embryonic stem cells serve as vascular progenitors.* Nature, 2000. **408**(6808): p. 92-6.
286. Ferreira, L.S., et al., *Vascular progenitor cells isolated from human embryonic stem cells give rise to endothelial and smooth muscle like cells and form vascular networks in vivo.* Circ Res, 2007. **101**(3): p. 286-94.
287. Liebner, S., et al., *Beta-catenin is required for endothelial-mesenchymal transformation during heart cushion development in the mouse.* J Cell Biol, 2004. **166**(3): p. 359-67.
288. Camenisch, T.D., et al., *Temporal and distinct TGFbeta ligand requirements during mouse and avian endocardial cushion morphogenesis.* Dev Biol, 2002. **248**(1): p. 170-81.
289. Wosczyna, M.N., et al., *Multipotent progenitors resident in the skeletal muscle interstitium exhibit robust BMP-dependent osteogenic activity and mediate heterotopic ossification.* J Bone Miner Res, 2012. **27**(5): p. 1004-17.
290. Zeisberg, E.M., et al., *Discovery of endothelial to mesenchymal transition as a source for carcinoma-associated fibroblasts.* Cancer Res, 2007. **67**(21): p. 10123-8.
291. Arciniegas, E., et al., *Perspectives on endothelial-to-mesenchymal transition: potential contribution to vascular remodeling in chronic pulmonary hypertension.* Am J Physiol Lung Cell Mol Physiol, 2007. **293**(1): p. L1-8.
292. Asahara, T., A. Kawamoto, and H. Masuda, *Concise review: Circulating endothelial progenitor cells for vascular medicine.* Stem Cells, 2011. **29**(11): p. 1650-5.
293. Dome, B., et al., *Circulating endothelial cells, bone marrow-derived endothelial progenitor cells and proangiogenic hematopoietic cells in cancer: From biology to therapy.* Crit Rev Oncol Hematol, 2009. **69**(2): p. 108-24.
294. Shi, Q., et al., *Evidence for circulating bone marrow-derived endothelial cells.* Blood, 1998. **92**(2): p. 362-7.
295. Kalka, C., et al., *Vascular endothelial growth factor(165) gene transfer augments circulating endothelial progenitor cells in human subjects.* Circ Res, 2000. **86**(12): p. 1198-202.
296. Kalka, C., et al., *Transplantation of ex vivo expanded endothelial progenitor cells for therapeutic neovascularization.* Proc Natl Acad Sci U S A, 2000. **97**(7): p. 3422-7.
297. Asahara, T., et al., *Isolation of putative progenitor endothelial cells for angiogenesis.* Science, 1997. **275**(5302): p. 964-7.
298. Asahara, T., et al., *Bone marrow origin of endothelial progenitor cells responsible for postnatal vasculogenesis in physiological and pathological neovascularization.* Circ Res, 1999. **85**(3): p. 221-8.
299. Palmer, R.M., A.G. Ferrige, and S. Moncada, *Nitric oxide release accounts for the biological activity of endothelium-derived relaxing factor.* Nature, 1987. **327**(6122): p. 524-6.
300. Culotta, E. and D.E. Koshland, Jr., *NO news is good news.* Science, 1992. **258**(5090): p. 1862-5.
301. Moncada, S., *Nitric oxide gas: mediator, modulator, and pathophysiologic entity.* J Lab Clin Med, 1992. **120**(2): p. 187-91.

302. Moncada, S., R.M. Palmer, and E.A. Higgs, *Nitric oxide: physiology, pathophysiology, and pharmacology.* Pharmacol Rev, 1991. **43**(2): p. 109-42.
303. Gaston, B., *Nitric oxide and thiol groups.* Biochim Biophys Acta, 1999. **1411**(2-3): p. 323-33.
304. Rubinstein, I., et al., *Involvement of nitric oxide system in experimental muscle crush injury.* J Clin Invest, 1998. **101**(6): p. 1325-33.
305. Capanni, C., et al., *Increase of neuronal nitric oxide synthase in rat skeletal muscle during ageing.* Biochem Biophys Res Commun, 1998. **245**(1): p. 216-9.
306. Tews, D.S., et al., *Expression of different isoforms of nitric oxide synthase in experimentally denervated and reinnervated skeletal muscle.* J Neuropathol Exp Neurol, 1997. **56**(12): p. 1283-9.
307. Balon, T.W. and J.L. Nadler, *Evidence that nitric oxide increases glucose transport in skeletal muscle.* J Appl Physiol, 1997. **82**(1): p. 359-63.
308. Tidball, J.G., et al., *Mechanical loading regulates NOS expression and activity in developing and adult skeletal muscle.* Am J Physiol, 1998. **275**(1 Pt 1): p. C260-6.
309. Tews, D.S. and H.H. Goebel, *Cell death and oxidative damage in inflammatory myopathies.* Clin Immunol Immunopathol, 1998. **87**(3): p. 240-7.
310. Moncada, S. and E.A. Higgs, *Endogenous nitric oxide: physiology, pathology and clinical relevance.* Eur J Clin Invest, 1991. **21**(4): p. 361-74.
311. De Palma, C. and E. Clementi, *Nitric oxide in myogenesis and therapeutic muscle repair.* Mol Neurobiol, 2012. **46**(3): p. 682-92.
312. Clementi, E., *Role of nitric oxide and its intracellular signalling pathways in the control of Ca2+ homeostasis.* Biochem Pharmacol, 1998. **55**(6): p. 713-8.
313. Nisoli, E., et al., *Calorie restriction promotes mitochondrial biogenesis by inducing the expression of eNOS.* Science, 2005. **310**(5746): p. 314-7.
314. Taylor, C.T. and S. Moncada, *Nitric oxide, cytochrome C oxidase, and the cellular response to hypoxia.* Arterioscler Thromb Vasc Biol, 2010. **30**(4): p. 643-7.
315. Brunori, M., *Nitric oxide moves myoglobin centre stage.* Trends Biochem Sci, 2001. **26**(4): p. 209-10.
316. Anderson, J.E., *A role for nitric oxide in muscle repair: nitric oxide-mediated activation of muscle satellite cells.* Mol Biol Cell, 2000. **11**(5): p. 1859-74.
317. Wozniak, A.C., et al., *Signaling satellite-cell activation in skeletal muscle: markers, models, stretch, and potential alternate pathways.* Muscle Nerve, 2005. **31**(3): p. 283-300.
318. Lincoln, T.M., et al., *Regulation of vascular smooth muscle cell phenotype by cyclic GMP and cyclic GMP-dependent protein kinase.* Front Biosci, 2006. **11**: p. 356-67.
319. Pilz, R.B. and K.E. Broderick, *Role of cyclic GMP in gene regulation.* Front Biosci, 2005. **10**: p. 1239-68.
320. Sciorati, C., et al., *Nitric oxide effects on cell growth: GMP-dependent stimulation of the AP-1 transcription complex and cyclic GMP-independent slowing of cell cycling.* Br J Pharmacol, 1997. **122**(4): p. 687-97.
321. Buono, R., et al., *Nitric oxide sustains long-term skeletal muscle regeneration by regulating fate of satellite cells via signaling pathways requiring Vangl2 and cyclic GMP.* Stem Cells, 2012. **30**(2): p. 197-209.
322. Cossu, G. and U. Borello, *Wnt signaling and the activation of myogenesis in mammals.* EMBO J, 1999. **18**(24): p. 6867-72.

323. Brunelli, S., et al., *Beta catenin-independent activation of MyoD in presomitic mesoderm requires PKC and depends on Pax3 transcriptional activity.* Dev Biol, 2007. **304**(2): p. 604-14.
324. De Palma, C., et al., *Nitric oxide inhibition of Drp1-mediated mitochondrial fission is critical for myogenic differentiation.* Cell Death Differ, 2010. **17**(11): p. 1684-96.
325. Ahlner, J., et al., *Organic nitrate esters: clinical use and mechanisms of actions.* Pharmacol Rev, 1991. **43**(3): p. 351-423.
326. Gasco, A., R. Fruttero, and G. Sorba, *No-donors: an emerging class of compounds in medicinal chemistry.* Farmaco, 1996. **51**(10): p. 617-35.
327. Megson, I.L. and M.R. Miller, *NO and sGC-stimulating NO donors.* Handb Exp Pharmacol, 2009(191): p. 247-76.
328. Megson, I.L. and D.J. Webb, *Nitric oxide donor drugs: current status and future trends.* Expert Opin Investig Drugs, 2002. **11**(5): p. 587-601.
329. del Soldato, P., R. Sorrentino, and A. Pinto, *NO-aspirins: a class of new anti-inflammatory and antithrombotic agents.* Trends Pharmacol Sci, 1999. **20**(8): p. 319-23.
330. Burgaud, J.L., E. Ongini, and P. Del Soldato, *Nitric oxide-releasing drugs: a novel class of effective and safe therapeutic agents.* Ann N Y Acad Sci, 2002. **962**: p. 360-71.
331. Burgaud, J.L., J.P. Riffaud, and P. Del Soldato, *Nitric-oxide releasing molecules: a new class of drugs with several major indications.* Curr Pharm Des, 2002. **8**(3): p. 201-13.
332. Sciorati, C., et al., *A dual acting compound releasing nitric oxide (NO) and ibuprofen, NCX 320, shows significant therapeutic effects in a mouse model of muscular dystrophy.* Pharmacol Res, 2011. **64**(3): p. 210-7.
333. Archer, J.D., C.C. Vargas, and J.E. Anderson, *Persistent and improved functional gain in mdx dystrophic mice after treatment with L-arginine and deflazacort.* FASEB J, 2006. **20**(6): p. 738-40.

Chapter II

Hemogenic endothelium generates mesoangioblasts that contribute to several mesodermal lineages in vivo

Emanuele Azzoni[1,2], Valentina Conti[1,2], Lara Campana[2], Arianna Dellavalle[2], Ralf H. Adams[3], Giulio Cossu[2,4], Silvia Brunelli[1,2]

[1]Dept. of Experimental Medicine, University of Milano-Bicocca, 20052 Monza, Italy; [2]Division of Regenerative Medicine, H. San Raffaele Scientific Institute, 20132, Milan, Italy; [3]Max Planck Institute for Molecular Biomedicine, Department of Tissue Morphogenesis, and University of Muenster, Faculty of Medicine, D-48149 Münster, Germany. [4]Dept. of Cell and Developmental Biology, University College London, WC1E 6DE London, United Kingdom.

*Corresponding author
Silvia Brunelli
Tel, +390264488308; +390226435066; brunelli.silvia@hsr.it

Running title: Endothelial origin of mesoangioblasts
Keywords: VE-Cadherin, Hemogenic Endothelium, Mesoangioblasts, Muscle.

Submitted to PNAS

ABSTRACT

The embryonic endothelium is a known source of hematopoietic stem cells. Moreover, vessel-associated stem cells, endowed with multineage mesodermal differentiation potential, such as the embryonic mesoangioblasts, originate in vitro from the endothelium. Using a genetic lineage tracing approach, we show that early extraembryonic endothelium generates, in a narrow time-window, and prior to the hemogenic endothelium in the dorsal aorta and major embryonic arteries, hematopoietic cells that migrate to the embryo proper, and are subsequently found within the mesenchyme. A subpopulation of these cells, distict from embryonic macrophages, expresses mesenchymal markers. We also found that hemogenic endothelium derived cells contribute to skeletal and smooth muscle and to other mesodermal cells in vivo, and specifically display features of embryonic mesoangioblasts in vitro. Therefore, we provide new insights on the distinctive characteristics of the extraembryonic and embryonic hemogenic endothelium and we identify the in vivo counterpart of embryonic mesoangioblasts, suggesting their identity and developmental ontogeny.

INTRODUCTION

The vascular and the hematopoietic system are deeply entwined throughout embryonic development. The first endothelial cells (ECs) in the gastrulating embryo originate from the lateral and posterior mesoderm, migrate towards the yolk sac (YS), where they will eventually differentiate into ECs and hematopoietic cells (HCs) of the blood islands (1). This close anatomical and temporal relationship of HCs and ECs

during developmental life has suggested that they may share a common mesodermal ancestor, which has been called the hemangioblast. These progenitors have been initially identified in ES, where blast colony-forming cells (BL-CFU) gave rise to both HCs and ECs in vitro (2). Other studies associate the first HSCs with phenotypically differentiated ECs endowed with hematopoietic potential, the hemogenic endothelium. Indeed, fate mapping or in vivo time-lapse imaging in mouse and zebrafish revealed that HCs originate from VE-Cadherin (VE-Cad) positive ECs in the dorsal aorta (3-5), and insight have been given also on the different potential of hemogenic endothelial progenitors (6). A link has then been proposed between these two hypoteses, since it has been demonstrated that the hemangioblast generates HCs through the formation of a hemogenic endothelium intermediate that is transiently generated during BL-CFU development. This cell population is also present in gastrulating mouse embryos and generates HCs on further culture (7).

The embryonic dorsal aorta is the source of another population of progenitor cells, namely mesoangioblasts (MABs) (8). These culture-defined cells express hemangioblastic, hematopoietic, endothelial and some mesodermal markers (Flk-1, c-Kit, CD34, VE-Cad, α-SMA); possess self-renewal capacity and differentiation potency for different mesodermal lineages in vitro and in vivo (e.g. endothelium, skeletal muscle, smooth muscle, dermis, bone) (8-10); in vitro only, they display hematopoietic potential. These cells have been successfully used in cell transplantation protocols that led to a significant recovery of the structure and function of the skeletal muscle of dystrophic animals (11, 12). While MAB myogenic differentiation potency is undoubtedly useful for cell

transplantation protocols, only theoretical models have been proposed for their origin (13) and still no insights have been given on their origin, their role during normal development and tissue remodeling, and the correlation with recently identified cell types with therapeutic potential isolated from the perivascular space of perinatal and postnatal skeletal muscle (14) (15). These informations would be critical in order to optimize their in vivo recruitment and mobilization.

We decided to undertake a genetic lineage tracing analysis, combining pulses of induction of Cre recombinase with a time course evaluation of the reporter expression, to follow the fate of VE-Cad expressing ECs in the early and late embryo and in perinatal stages.

We show that extraembryonic VE-Cad+ endothelium generates the first wave of hemopoietic cells that colonize the embryo mesenchyme. Moreover, we identify the hemogenic endothelium as the source of progenitor cells that physiologically contribute to several mesodermal lineages in the embryo, including skeletal muscle, and whose features overlap those of embryonic MAB cell lines.

RESULTS

VE-Cadherin lineage tracer transgenic lines lead to efficient and endothelial specific Cre recombination.

To genetically label and follow the fate of different subsets of endothelial derived cell populations, we took advantage of transgenic mice expressing a tamoxifen (TAM) inducible form of Cre recombinase (CRE-ER^{T2}) under the control of VE-Cad regulatory sequences, highly specific for endothelial progenitors and differentiated ECs from early

developmental stages (16). To guarantee reproducibility, we used two transgenic lines. One is the Cdh5-CreER^{T2} transgenic mouse line, where CRE-ER^{T2} is inserted in a PAC construct encompassing the VE-Cad gene (17). We generated another transgenic mouse, using a construct, VE-Cadherin-CREER^{T2}, containing different specific sequences of the VE-Cad gene (Fig. S1A) that boost the activity of the promoter region while maintaining endothelial specificity (18).

We induced Cre recombination with one single intra-peritoneal TAM injection in the pregnant mother at E8.5 to avoid labeling the YS mesoderm, which transiently expresses VE-Cad at E7.5 (19). All transgenic lines displayed strong vascular labeling: Cdh5-CreER^{T2} (showing the strongest signal) and VE-Cadherin-CREER^{T2} line 9616 (Fig. S1B), were selected for further experiments.

FACS analysis on cells dissociated from E9.5 Cdh5-CreER^{T2}; R26R-EYFP embryos, (Fig. 1A), showed a higher percentage of EYFP+ cells in the YS, followed by placenta and embryo proper (Fig. 1A), thus reflecting the overall vascularization of these tissues.

The efficiency of Cre recombination was measured first by flow cytometry as the percentage of EYFP+ cells in the CD31+ population, and was found to be 60±5.78% in the embryo proper 24h after Cre induction (Fig. 1B).

Immunofluorescence (IF) analysis on Cdh5-CreER^{T2};R26R-EYFP and VE-Cadherin-CREER^{T2};R26R-EYFP E9.5 embryos revealed co-localization of EYFP with endothelial specific markers (VE-Cad and CD31/Pecam1) (Fig. 1C, Fig. S1C). At this stage no EYFP+CD31- or EYFP+VE-Cad- cells were detected. Cre recombination efficiency (estimated as the number of EYFP+ cells on the total of CD31+ or VE-Cadherin+

cells, counted on 10-20x fields) was approximately 80% for Cdh5-CreER^{T2} (Fig. 1A), and 30% for VE-Cadherin-CREER^{T2} 9616 (Fig. S1C).

Strict tissue specificity is a crucial issue for all lineage-tracing approaches. To exclude that Cre recombination could occur in VE-Cad- or paraxial mesoderm cells, TAM injection was performed at E8.5 in Cdh5-CreER^{T2};R26R-EYFP embryos and EYFP+ and EYFP- cells were separately sorted from the embryo proper and from the YS at E9.5 (gating depicted in Fig. 1A). Quantitative real-time PCR analysis was performed on RNA extracted from the different populations, to evaluate the amount of lineage specific transcripts (Fig. 1D). Pax3 (paraxial mesoderm, dermamyotome) and Paraxis (paraxial mesoderm) mRNAs were confined in the EYFP- population. VE-Cad and CD31 (endothelium) expressing cells were found almost entirely in the EYFP+ fraction in both embryo proper and YS. The absence of VE-Cadherin and CD31 transcripts in the EYFP- population also confirmed the efficiency of the recombination. Runx1 (expressed in hemogenic ECs and hematopoietic cells) was expressed mainly in the YS, and also in EYFP- cells. Interestingly Sox7, a gene found to regulate VE-Cad expression in the hemogenic endothelium (20) was expressed exclusively in EYFP+ cells in the embryo, while in both EYFP+ and EYFP- cells in the YS. These results confirmed that induction of Cre recombination at E8.5 resulted in labelling of cells that express VE-Cad (eVE-Cad+ for embryonic VE-Cadherin expressing cells), and have mainly an endothelial phenotype in the embryo, and also an hematopoietic phenotype in the YS, while completely lacking paraxial mesoderm characteristics.

Non-macrophage eVE-Cad+ derived hematopoietic cells are found within the embryonic mesenchyme.

The presence of abundant hematopoietic and hemogenic endothelium specific transcripts 24 h after induction in VE-Cad+ derived cells prompted us to investigate the hematopoietic nature and fate of these cells.

The endothelium in the embryo proper is able to contribute to definitive hematopoiesis (3, 4), starting at E10-E10.5 in the dorsal aorta, with very rare clusters appearing in the umbilical vein and vitelline artery as soon as E9.5 (21). Indeed at E10.5 and, more abundantly, at E11.5, we could detect EYFP+ intra-aortic clusters, expressing the hematopoietic markers CD41 or CD45, originating from EYFP+CD31+ hemogenic endothelium (Fig. S2). At E10.5 some clusters also expressed c-Kit, marker of HSCs and hematopoietic progenitors (Fig. S2). Most clusters remained positive for CD31.

On the other hand, at E9.5, both FACS and IF analysis confirmed that only very rare EYFP+ cells labeled at E8.5 were CD41+ or CD45+ in the embryo proper (Fig. 2A,D). EYFP+CD45+ and EYFP+CD41+ cells were found in the YS (Fig. 2B,D), and more scarsely in the placenta (Fig. 2C,D). EYFP+c-Kit+ cells were also found in the YS as early as E9 and E9.5 (Fig. S3,i-ii). This implies that the endothelium of YS, and at a lower extent of the placenta, are already hemogenic at E8.5, being able to generate cells bearing HSCs or HC progenitors features.

We have then investigated the fate of EYFP+ cells at later stages in the embryo. In addition to endothelial and intra-aortic hematopoietic clusters, starting from E10.5 we were able to detect EYFP+CD45+CD31- cells on the abluminal side of

vessels, which were localized in the surrounding mesenchyme (Fig. 3A). This was quite evident around the dorsal aorta (arrows in Fig. 3Ai,ii; Movie S1) but also around vessels in the limb bud (arrow in Fig. S4,i). Some EYFP+ cells expressing CD41+ were also seen in the mesenchyme (Fig. S4,ii). At E10.5 the frequency of EYFP+CD41+ and EYFP+CD45+ cells in the embryo proper was almost equivalent (graph in Fig. 3A).

CD45+ cells in the mesenchyme were not natively labeled since they did not express endothelial markers such as VE-Cadherin or CD31 (Fig. 3A,i-ii; Fig. S4,i), implying that their labeling had occurred at an earlier time, antecedent the establishment of the embryonic hemogenic endothelium; moreover, at E10.5 they were the only EYFP+VE-Cad- cells in the embryo. At this stage some EYFP+CD45+c-Kit+ cells appeared in the embryo mesenchyme (Fig. S3,iii).

At E11.5 EYFP+CD45+CD31- cells were present in the mesenchyme at higher frequency (Fig. 3A,iii; 3B,ii; graph in Fig. 3A; Fig. S4,iii); again, clusters of eVE-Cad+-derived CD45+ cells appeared in the subaortic mesenchyme (Fig. 3A,iii, Movie S2, Fig. S4,iii,). Also EYFP+CD41+ cells and EYFP+c-kit+ cells were seen in the embryo proper, outside EYFP+CD31+ vessels (Fig. S4,iv and S3,iv-v). These data indicate that mesenchymal cells expressing HC markers are generated from eVE-Cad+ cells.

At E12.5, EYFP+CD45+ cells in the mesenchyme were even more abundant and could be detected throughout the whole embryo (Fig. 3A,iv and Fig. S4B,; Movie S3). EYFP+CD41+ cells were rare in the mesenchyme (graph in Fig. 3A).

IF analysis in the placenta at E10.5-E12.5 also revealed the presence of EYFP+CD45+ and EYFP+CD41+ cells (Fig.

S5A). Their overall number did not increase significantly with time. FACS analysis demonstrated that EYFP+ cells on the total of CD45+ in the placenta accounted for a low percentage (1-2.5%) at E11.5-12.5 (Fig. S5B), respect to YS and embryo (20-30%). Alternate analysis revealed that at E11.5-E12.5 the percentage of CD45+ cells within the EYFP+ subset was higher in the yolk sac (30-40%), followed by the embryo (15-30%) and the placenta (5-15%) (Fig. 3C and not shown). Taking into account that many of placental CD45+ cells are of maternal origin, therefore EYFP-, these data suggest that a small but still significant number of hematopoietic cells in the placenta are of endothelial origin.

Primitive embryonic macrophages (MΦs) arise in the yolk sac as early as E7.5, before the appearance of definitive HSCs. While still differing from adult MΦs, they are characterized by the unambiguous expression of specific markers such as F4/80 and CD11b, and are thought to play important roles in tissue remodeling and organ development (22, 23). Recently, it has been shown that YS MΦs persist in the adult and contribute to several lineages of tissue MΦs such as liver Kupffer cells, epidermal Langerhans cells and microglia (24).

Indeed, IF and FACS analysis showed that a substantial percentage of EYFP+CD45+ cells in the mesenchyme were F4/80+ (Fig. 3B,iii-v). In particular at E12.5 the majority of EYFP+CD45+F4/80+ resided in the YS and in the embryo mesenchyme, while less numerous in the placenta and fetal liver (Fig. 3C).

Still, from E10.5 to E12.5 a significant portion of EYFP+CD45+ cells in the mesenchyme were not macrophages (F4/80-) (around 35% of the total EYFP+CD45+ cells at E10.5-

E12.5, as assessed by cell counting on sections for all stages, and around 20% by FACS analysis at E12.5 stage, in which the mesenchymal fraction of EYFP+ cells was enriched by removing fetal liver) (Fig. 3Biii,v, graphs in 3B, Fig. 3C, Movie S3).

Remarkably, at E10.5-E12.5 many isolated EYFP+CD45+ cells in the embryo mesenchyme also expressed α-SMA, that at these early stages is expressed in a range of cells of mesodermal origin (including smooth, skeletal, cardiac muscle cells, pericytes) (25, 26) but not in hematopoietic cells (Fig. 3B,i-ii,iv-v; Movie S4 and graph in Fig. 3D). These isolated EYFP+α-SMA+cells in the mesenchyme did not express F4/80 (Fig. 3B,iv and Fig. 3D). They were detected in various anatomical locations, mostly in a perivascular location in association with big vessels such as the dorsal aorta (Fig. 3B,i-ii,iv-v) but also in the developing limb (Fig. 3B,iii). These cells were invariably CD41- (Fig. S4,ii,iv).

The presence of EYFP+CD45+F4/80-CD11b-α-SMA+ cells was also confirmed by FACS analysis (Fig. 3E, top panels and graph), suggesting that eVE-Cad+ derived cells generate a mesenchymal population in which the expression of hematopoietic markers persists, but distinct from embryonic MΦs. α-SMA+ cells accounted for approximately 30% of the EYFP+CD45+ F4/80-CD11b- cells at E12.5 (Fig. 3E, top graph); α-SMA+ cells were also found within the EYFP+CD45+F4/80+CD11b+ subset (approx. 25%). We could also observe the presence of a EYFP+CD45+ F4/80- CD11b- cell population expressing high level of NG2 (NG2hi), therefore confirming the presence of hemopoietic derived mesenchymal cells (Fig. 3E, bottom panel and graph). NG2hicells were rare

in the EYFP+CD45+F4/80+CD11b+ population (Fig.3E, bottom panel and graph). Low levels of NG2 where found in both populations. Reports on MΦs expressing mesenchymal markers in pathological settings or specific culture conditions, but not during development, exist (27, 28). Still, many of them could be macrophages that have phagocyted mesenchymal cells, and transiently acquired or exposed their antigens (29, 30).

Extraembryonic origin of mesenchymal eVE-Cad+ derived cells.

Two possible origins of mesenchymal EYFP+CD45+ cells can be postulated. We may observe an endothelial to hematopoietic transition of hemogenic ECs, in a direction opposite to that of classical hematopoietic clusters, as reported during vascular remodeling of the vitelline artery (31) but not further confirmed (21).

On the other hand, these cells may originate from other VE-Cad expressing cells in the embryo or extra-embryonic tissue, that reach the embryo mesenchyme by extravasation, where some maintain an hematopoietic phenotype, while others start to co-express mesenchymal markers. To get insight in this phenomenon we performed an experiment in which pulses of Cre activation were induced at different time points: analysis of EYFP+ cells was carried on 12h and 24h after TAM injection, to immediately follow the fate of labeled cells.

Labeling at E9.5 with analysis at E10 and E10.5, revealed in the YS a lower number of EYFP+CD41+ cells (Fig. 4A,i-ii; 4C) respect to those detected with labeling at E8.5, while the number of EYFP+CD45+ was similar (Fig. 4A,iii; 4C). Rare EYFP+CD41+ and EYFP+CD45+ cells were seen in the

placenta at this time point (Fig. 4C, Fig. S5C). Interestingly EYFP+CD41+ and EYFP+CD45+ cells could be hardly detected in either YS or placenta when injection was performed at E10.5 and analysis performed at E11 and E11.5 (Fig. 4B,i-iii, 4C, Fig. S5C): this suggests that the hemogenic potency of the extraembryonic endothelium is indeed restricted to a short time-window, starting at E8.5 or before and progressively decreasing until E10.5, possibly ending shortly thereafter.

Importantly, when induction was performed at E9.5 and E10.5, no EYFP+ CD41+ or EYFP+CD45+ were observed in the mesenchyme of the embryo at E10.5 or E11.5 (Fig. 4A,iv-vii; 4B,iv-vi). As described before, these EYFP+ cells were seen in the embryo proper starting from E10.5 only when injection was performed at E8.5 (Fig. 3A-B and Fig. S4): at least 48h are therefore needed to allow EYFP+ labeled cells at E8.5 to be found in the embryonic mesenchyme. With the current induction protocol, expression of reporter genes is completed by 24h (32). If EYFP+CD45+ and if EYFP+CD41+ cells in the embryonic mesenchyme originated from the hemogenic endothelium in the embryo proper we would have been able to detect them at E10.5-E11.5 by labeling VE-Cad+ cells later in the E9.5-E10.5 time window, when embryonic endothelium starts to be hemogenic. As this is not the case EYFP+CD45+ and EYFP+CD41+ cells in the embryonic mesenchyme should therefore derive from cells that originate in the extraembryonic tissues, mostly in the YS, and become labeled in the E8.5-E9.5 time-window, since YS hemogenic activity decrease later on, as described above.

These results also imply that CD45+α-SMA+ cells in the mesenchyme have the same origin.

These unique characteristics of the extraembryonic endothelium, namely being hemogenic in a restricted time-window that scarcely overlaps to the one in the AGM, and generating CD45+ cells able to acquire a mesenchymal fate, suggests that this tissue bears characteristics different from those of the endothelium in the embryo proper, implying diverse responsiveness to distinct molecules and signaling pathways.

To investigate differences between EYFP+ populations that are labeled at different times and in different endothelial compartments, we carried on a gene expression profile analysis on eVE-Cad+ derived cells from either YS end embryo proper, focusing on a panel of genes mainly involved in stem cell-related signaling pathways and EC biology.

We sorted EYFP+ cells from E9.5 (TAM injection at E8.5) or E10.5 (TAM injection at E9.5) embryos and YS using the same gating strategy depicted in Fig. 1A. From previous data, at least 80-95% of these cells should be endothelial cells.

By comparing the gene expression profile of eVE-Cad+ derived cells from embryos or YS at E9.5 and E10.5 we found that groups of genes involved in signaling pathways were differentially expressed with a significant fold change (Fig. 5). In particular, FGF, Wnt, Hedgehog and, to a lesser extent, Notch related genes were more expressed in embryonic eVE-Cad+ derived cells. Of those supergroups, only one gene (Fzd8) was more expressed in YS cells, both at E9.5 and E10.5. TGF-β related genes were instead more expressed in the YS at E9.5; at E10.5, some of them became upregulated in the embryo. A number of other genes, including ECM and adhesion molecules, and genes involved in EC activation, angiogenesis or cytokine activity, were differentially expressed

in the embryo and YS, both at E9.5 and E10.5. Moreover, we compared gene expression profiles of eVE-Cad+ derived cells at E9.5 versus E10.5, in the embryo and YS (Fig. S6). We found that, within embryonic eVE-Cad+ cells, genes involved in FGF, Wnt and Hedgehog pathway are more expressed at E10.5 than E9.5. In the YS, no gene becomes upregulated at E10.5; several genes (mostly functional, rather than signalling related) are instead more expressed at E9.5.

These data indicate that YS ECs expression profile shows critical differences from the endothelium in the embryo proper both at E9.5 and E10.5, and this may reflect a functional distinction. These results also suggest that even within the same subset, between E9.5 and E10.5, events that crucially change the intrinsic properties of ECs in the embryo and YS take place.

eVE-Cad+ derived mesenchymal progenitors contribute to multiple mesodermal lineages during development.

We previously reported the isolation of vessel-associated stem cells in the embryo, the MABs, endowed with mesodermal multilineage potency (8) and expressing hemo-angioblastic and mesodermal markers (8, 9). These cells have been only characterized on the basis of in vitro culture or in vivo transplants and there is no hint of their in vivo origin. Our results indicate that such cells may correspond to the EYFP+CD45+α-SMA+F4/80- cells we observe in the embryo mesenchyme, suggesting that they may be generated by a common endothelial or hemogenic endothelial precursor giving rise to both hematopoietic and mesenchymal lineages.

We decided to evaluate the contribution of eVE-Cad+ derived cells to other mesodermal lineages.

At E12.5-E15.5, in the smooth muscle layer of big vessels (aorta, carotid artery, mesenteric artery), we detected EYFP+CD31- cells which were also α-SMA+ or NG2+, markers of the pericyte-smooth muscle lineage at those stages (0.5-3% of the total α-SMA+ or NG2+ peri-endothelial, smooth muscle cells). (Fig.6A). Interestingly, EYFP+NG2+ cells could also be found earlier at E10.5, where mostly were also CD31+, and at E11.5, where they were CD31- and mainly in a perivascular location (Fig. S4C). These data demonstrate in vivo a developmental relationship between endothelial progenitors and smooth muscle cells; to our knowledge only DiI labeling or in vitro experiments had previously suggested this possibility (33, 34).

We next examined the contribution of eVE-Cad+ derived progenitors to the skeletal muscle lineage. No EYFP+ cells were found to co-localize with markers of somitic populations such as Pax3, MyoD and Myf5 (Fig. S7A,i-iv and not shown) at E9.5-E11.5, suggesting that eVE-Cad+ derived progenitors do not give rise to cells within somites.

From E12.5, we observed EYFP+CD31- mononucleated cells expressing skeletal Myosin Heavy Chain (MyHC)(Fig. 6B,ii-iv) or α-SMA (Fig. 6B,i), that at this stage is transiently expressed by skeletal myoblasts. In E12.5 embryos those cells were still rare (Fig. 6B,i-ii, 6F). Importantly, at E12.5 and E13.5 we could observe the presence of myoblasts expressing Myogenin and EYFP, indicating that eVE-Cad+ derived cells can undergo at least some of the steps of canonical skeletal myogenesis. MyHC+EYFP+CD31- cells or EYFP+Desmin+CD31- were detected throughout the embryo until P0, last time point of our analysis (Fig. 6B-E and Fig. S7B-C). A graph summarizing the quantification of eVE-Cad+

derived myogenic cells during development is shown in Fig. 6F. We can conclude that cells expressing VE-Cad at E8.5 and/or their progeny enter the myogenic lineage, without going through somitic intermediates, as part of their normal, unperturbed fate.

At E15.5 the heart displayed a high degree of EYFP labeling in the endocardium (a VE-Cad+ endothelial subpopulation); however, we did not detect any EYFP+ cardiomyocytes (Fig. S8A). In addition we found that almost all the fibroblast-like CD31- cells of the endocardial cushions were EYFP+ (inset of Fig. S8A), thus confirming previous in vivo data showing that endocardial cushions, from which AV valves and part of the septum originate, arise from a subset of ECs that undergo endothelial to mesenchymal transition (35, 36).

At E17.5 we observed that the dermal layer surrounding the developing fingers contained a remarkably high number of EYFP+ cells (Fig. S8B). EYFP+CD31- Collagen I+ cells and EYFP+F4/80- Collagen I+ cells (Fig. S8B,iii, iv) were detected (both populations representing 2-4% of total Collagen I+ cells), indicating that eVE-Cad+ derived cells, distinct from embryonic MΦs, had entered the dermal lineage.

As expected, and described before by FACS analysis (Fig. 3C), eVE-Cad+ cells colonized fetal secondary hematopoietic organs (fetal liver, thymus and spleen) (Fig. S8C).

eVE-Cad+ derived CD45+ cells, distinct from ECs and MΦs, display MAB features.

MABs have been characterized only after isolation from explants of embryonic aorta and, not univocally expressing any specific gene, they are identified by a combination of

morphological and functional features (8, 10, 12). To verify whether cells derived from eVE-Cad+ precursors displayed, after isolation and culture, characteristics resembling embryonic MABs, we prepared aorta explant cultures from Cdh5-CreER^{T2}; R26R-EYFP E9.5-E11.5 embryos as described (37), 24 hours after TAM induction. As expected, cells within the aorta endothelium were initially EYFP+ (yellow arrow in Fig. 7A and Fig. S9A). At all time points, we observed after a week the emergence of round, weakly adhering refractile cells, distinct from the populations of fibroblasts and floating HCs, and displaying MAB morphology. The majority of these cells were EYFP+ and, most interestingly, also CD45+ (Fig. 7A, Fig. S9A). These data suggest that MABs originate from hemogenic endothelium, and, at least at early stages of ex vivo culture, display a hemopoietic phenotype.

We isolated endothelial derived EYFP+ cells by FACS from Cdh5-CreER^{T2}; R26R-EYFP E12.5 embryos, a time when CD45+ cells in the mesenchyme are abundant. The EYFP+ population accounted for approximately 1-2% of cells in the embryo (Fig. 7B).

Isolated cells were grown in culture in conditions suited for MABs . IF confirmed that after culture, they were indeed EYFP+. EYFP+ cells grew as a mixed population of spindle-shaped cells and small round-shaped cells, some of which were adherent and others in suspension (and smaller than the adherent ones).

eVE-Cad+ derived cells were exposed to several differentiating stimuli. When treated with VEGF, cells formed endothelial-like networks (Fig. 7C,i). TGF-β increased the number of α-SMA+ cells with smooth muscle phenotype (80% vs 10% of the untreated cells)(Fig. 7C,ii). EYFP+ cells

expressed alkaline phosphatase (AP, marker of pericytes and of initial osteblastic differentiation) when treated with BMP-2 (Fig. 7C,iii)(60-70% of AP+ cells vs 5% of the untreated). Culturing EYFP+ cells in adipogenic medium induced the appearance of adipocytes containing Oil Red O-positive fat droplets (Fig. 7C,iv).

When co-cultured with C2C12 murine myoblasts (after infection with a lentivirus directing expression of nLacZ), EYFP+ cells fused into multi-nucleated, MyHC+ myotubes (Fig. 7C,v-vi). Single mononucleated MyHC+β-Gal+ cells were also detectable (arrow in Fig. 7C,v), indicating that eVE-Cad+ derived cells were also able of differentiating directly into myogenic cells. nLacZ eVE-Cad+ derived cells were also injected into cardiotoxin injured tibialis anterior (TA) muscles of wt mice. We detected donor derived X-Gal+ nuclei inside myofibers (Fig. 7D,i-ii), preferentially localized in a central position typical of myonuclei inside regenerating myofibers (white arrow in Fig. 7D,ii) but also underneath the basal lamina in a peripheral position (purple arrow in Fig. 7D,ii). When injected into TA of immunosuppressed α-sarcoglycan (α-SG) KO mice, model of limb-girdle muscular dystrophy, this resulted in the appearance of clusters of α-SG positive, regenerating myofibers (Fig. 7D,iii-iv). We then concluded that cells derived from VE-Cad+ embryonic precursors are able to contribute to muscle regeneration in vivo.

From the previously performed in vivo analysis, it was clear that the EYFP+ population in the embryo became more heterogeneous with time; therefore we evaluated this heterogeneity in vitro to understand which of the populations carried MAB characteristics.

We separated different cell fractions of EYFP+ Cdh5-CreER^{T2}; R26R-EYFP E12.5 embryos (lacking the foetal liver) and analyzed the difference between the endothelial (CD31+CD45-), and the hematopoietic lineage (CD45+CD31-), that should contain the α-SMA+CD45+ "mesenchymal" like cells found in vivo (Fig. S9B,C). In MAB conditions only the CD45+CD31- cells displayed morphology similar to MABs (Fig. S9D).

To identify the progeny of sorted cells at the single cell level, we performed a colony forming cell (CFC) assay on methylcellulose. Only the "hematopoietic" CD31-CD45+ subset (35% of total EYFP+ cells) gave rise to varied hematopoietic colonies (Fig. S9E,i,iv), and very interestingly, mesenchymal-like cells started to appear in some of these colonies as adherent cells sprouting out from the hematopoietic colony, as early as day 2 (Fig. S9E,i'); by day 7, mesenchymal-like outgrowths grew quite extensively (Fig. S9E,iv'). When picked and cultured in MAB-like conditions, mixed hematopoietic-mesenchymal colonies gave rise to cells expressing EYFP and α-SMA, some of which also expressing CD45 (Fig. S9, vii-vii''). The "endothelial" CD31+CD45- fraction (approximately 55% of the total EYFP+ population) either did not form colonies with high efficiency or those that grew were mostly formed by endothelial-like cells (Fig. S9E,v): eVE-Cad+ derived cells retaining endothelial markers are not able to give rise directly to cells with mesenchymal features.

To further investigate which CD45+ fraction carried MAB characteristics, and to follow the fate of the embryonic MΦ population, we separately sorted the CD45+F4/80-CD11b- with the CD45+F4/80+CD11b+ and the CD45-F4/80-CD11b- subsets (Fig. 7E).

In MAB culture conditions only the CD45+F4/80-CD11b- non-MΦ subset was able to give rise to cells with uniformly small, adherent, triangular or spindle shape that closely resembled embryonic MABs (Fig. 7F). CD45+F4/80+CD11b+ and CD45-F4/80-CD11b- cells grew poorly (Fig. 7G); the latter were generally bigger and more heterogeneous in size and shape, and similar to the CD31+CD45- cells (Fig. S9D).

In CFC assays colonies started to form after 4 days, already displaying different morphology (Fig. 7G,iv,v,vi). Again, only CD45+F4/80-CD11b- cells were able to give rise to mesenchymal like colonies with high frequency (Fig. 7G).

Real time PCR assays on single colonies showed that mesenchymal markers such as α-SMA, PDGF-β and CD90, CD105, CD73, CD71, NG2 were exclusively or significantly more expressed by CD45+F4/80-CD11b- mesenchymal colonies. Hematopoietic CD45+F4/80-CD11b- colonies, likely containing HCs, specifically expressed Tie2 and c-Kit. Hematopoietic CD45+F4/80+CD11b+ colonies, containing embryonivc MΦs, expressed Ang1 but not Tie2 and did not express mesenchymal markers (Fig. 7H)

These data suggest that cells bearing characteristics of embryonic MABs originate from eVE-Cad+ derived CD45+ cells, distinct from MΦs and able to give rise both to hematopoietic cells and mesenchymal progenitor cells.

DISCUSSION

Endothelium has been shown to be a crossroad of several cell lineages during development. One of the most studied phenomena is the close relationship that exists between angiogenesis and definitive hematopoiesis, that led to the

postulation of a very early common mesodermal precursor, the hemangioblast. Recent work has shed light on the existence of hemogenic endothelium (3, 4), a specialized embryonic endothelial population that gives rise to the precursors of HSCs and therefore virtually to all the adult blood. It has also been demonstrated that HSCs and an earlier wave of definitive erythroid/myeloid progenitors differentiate from distinct hemogenic endothelial cells in the conceptus (6). The process by which ECs give rise to blood cells has been demonstrated to be not an asymmetric cell division but rather a unique type of cell transition. In mammals, almost without exception (31), cells in the aortic wall undergo endothelial to hematopoietic transition (EHT) in an intraluminal direction to generate HSCs precursors.

In this study we show that at early developmental stages, extraembryonic eVE-Cad+ progenitors, mainly in the YS, generate CD45+CD31- and CD41+CD31- cells, a subset of which are later found in the embryo mesenchyme. Without a live imaging approach of whole intact mouse embryos, not currently possible to our knowledge, we can only speculate that they reach the mesenchyme through the circulation.

It is known that E9-10 YS derived cells can provide long-term contribution to adult hematopoiesis (38), and that by E11.5 YS contains true multilineage dHCs (39). These cells are thought to derive from hemangioblasts that from the primitive streak migrate to the forming YS, and by the time they colonize it (E7.5) hemangioblasts segregate into endothelial and hematopoietic lineages, and possibly also smooth muscle cells (40), progressively losing their bi- or tri-potency. Nevertheless, it has been suggested that, from E8.25, cells in the YS bearing endothelial features may give rise to CD41+ definitive

hematopoietic progenitors (41). Still, a clear evidence of the emergence of HSCs in the YS has not been provided (42).

Likewise, the placenta is a hematopoietic organ that, even in absence of circulation, can generate multipotent HSCs de novo and support their expansion without promoting differentiation, and it contains a large population of HSCs that appear slightly later than in the YS and as early as in the AGM region (43, 44). A number of evidences point to the fact that at least some placental hematopoietic stem and progenitor cells are probably generated in situ by hemogenic endothelial cells (3) . We provide novel qualitative and quantitative informations about the dynamics of generation of CD41+ and CD45+ cells by placental VE-Cadherin+ hemogenic endothelium.

Here we show that a population of progenitors with mesodermal potency, including HCs, originates from VE-Cad+ ECs in the YS and in the placenta, in a very narrow temporal window (starting at E8.5 or before, progressively decreasing until E10.5 or shortly thereafter). It is noteworthy to notice that these ECs at this stage are the only ones that give rise to HCs that are later found within the embryo mesenchyme, since we confirm, by performing pulses of Cre activation, that the hemogenic endothelium in the embryo proper does not display this feature at early stages. This is the first evidence suggesting that the extraembryonic and embryonic hemogenic endothelia have a different timing of activity and possibly distinct biological characteristics.

This exclusive potency of extraembryonic hemogenic endothelium implies a specific sensitivity to different signaling pathways. Remarkably, little information is available on the nature and function of different endothelial populations in the early embryo, the fine understanding of which could open the

way to designing tools for in vivo manipulation of the fate of endothelial progenitors and possibly reprogramming in adult tissues. We have focused on a specific panel of genes that has allowed us to highlight not only significant differences between ECs of YS and embryo proper but also between cells labeled within a 24 h interval. Definitive hematopoiesis in the AGM region, but not the YS derived one, is Wnt- and Notch-dependent (45, 46): we found indeed that genes belonging to the Notch pathway are upregulated in the embryonic endothelium, suggesting that it is intrinsicly responsive to these signals. Other pathways whose components are upregulated in the embryo endothelium are Shh and Fgf. Hedgehog has been described to play a role in AGM hemopoiesis in zebrafish (47, 48), while the role of Fgf has not been fully explored in early hemopoiesis and endothelial development. On the other hand, the genes that appear upregulated in the YS belong to the BMP/TGF pathway. Interestingly, both these and Fzd8, the only Wnt related gene more expressed in the YS, are known to play important roles in the extraembryonic and early gastrulating embryo (49-51). Further studies will be required to unravel the role of these genes in the differential nature and function of YS and embryonic ECs.

The YS is also the source of an important cell type, the embryonic MΦs, that first appear around E8.5-9 and rapidily infiltrate the embryo via the vasculature (23). Recently it has been further confirmed that YS derived tissue MΦs are distinct from the HSC progeny, displaying different transcriptional requirements and persisting in the embryo and adult independently from the HSC-derived one (24). Here we suggest that F4/80+CD11b+ embryonic MΦs are generated from the hemogenic endothelium; we also show the presence

of another population of non MΦ CD45+ eVE-Cad+ derived cells in the mesenchyme that co-express α-SMA, a gene that in the embryo is transiently expressed by several solid mesoderm cells including pericytes, smooth muscle and skeletal muscle (25, 26). Several studies hinted to the possibility of existence of a common precursor that may give rise to both endothelium and blood cells or pericytes/mesenchymal cells (2, 33). The embryonic dorsal aorta contains indeed progenitors for multiple mesodermal tissues, the MABs, culture defined, vessel associated progenitors, that express hemo-angioblastic markers and are able, in vitro and in transplantation assays, to differentiate into most mesodermal tissues (8). Explant experiments have suggested that NG2+ expressing cells in the dorsal aorta could be recruited to either a skeletal or smooth muscle fate in a BMP dependent way (52). Now we show that perivascular and mesenchymal NG2+ cells derive as well from the hemogenic endothelium. Although we are not following a clonal population, the distribution and tissue contribution of the non-MΦs CD45+ eVE-Cad+ derived cells in the embryo overlaps the one observed with MAB cell line transplantation. This is also in agreement with the identification of mesenchymal stem/progenitor cells in the major hematopoietic sites during mouse development (53).

Experiments on aorta explants and on selected sorted populations, showed at midgestation that eVE-Cad+ derived cells could give rise to endothelium, blood and mesenchymal cells in the embryo, and that a fraction of these cells maintained hematopoietic (CD45) and mesenchymal markers (α-SMA). Furthermore the non-MΦ HCs subset of eVE-Cad+ derived cells (EYFP+CD45+CD11b-F4/80-) is the only one able to give rise to uniformly small, adherent, triangular or spindle-

shaped cells that closely resembled embryonic MABs, as well as the only subset that generate with high efficiency colonies expressing mesenchymal genes. These data therefore suggest that the non-MΦ CD45+ eVE-Cad+ derived cells bearing mesenchymal features are the in vivo counterparts of MABs. These observations also indicate that the contribution of the eVE-Cad+ derived MΦ to the multilineage differentiation in vivo and in vitro, by direct differentiation or fusion, is marginal. This is in agreement with reports that CD11b+ cells are not the cells that amongst the HSC derivatives are able to integrate into regenerating muscle fibers (54, 55) while some myelomonocytic progenitors c-Kit+ cells are. This is suggestive of a relationship between myelomonocytic cells and pericytes, MABs and other mesodermal precursors that will be extremely interesting to investigate.

In conclusion, we have demonstrated that extraembryonic hemogenic endothelium generates, in a narrow developmental time window, the first wave of CD41+ and CD45+ HCs that disseminate the mesenchyme in the embryo proper. Most importantly, we indicate for the first time the developmental origin of embryonic MABs as a subpopoulation of hemogenic endothelium derived cells, and support the idea that their in vitro and in vivo myogenic and multi-lineage differentiation capability are not a cell culture or transplantation artifact, but rather an expression of a differentiation potential that takes part also during normal development.

EXPERIMENTAL PROCEDURES

Transgenic mice and CRE-ERT2 induction. The generation of the VE-Cadherin-CREERT2 mice and genotyping of the transgenic lines is described in Supplementary Information. Cre activity was induced in the embryo by one

single intra-peritoneal injection of pregnant females with 2mg/25g body weight of Tamoxifen (TAM) (SIGMA; 10 mg/mL in corn oil).

Embryos. Mouse embryos were collected after natural overnight matings. Staging of E9-E11.5 embryos was performed by counting of somite pairs. For E12.5 and later stages, fertilization was considered to take place at 6 a.m.

Immunofluorescence and antibodies. Immunofluorescence on frozen section of embryos and muscles was carried out as in (11). A list of the antibodies that we used is provided in Supplementary Information. In all experiments, at least 6 embryos were analyzed for each condition (stage and TAM induction).

Statistical analysis Data were analyzed with Microsoft Excel 12.2.3 and GraphPad Prism 5. Values are expressed as means ± SEM. To assess statistical significance, two-tailed Student's t-tests were used (where not specified, *: $p<0.05$; **: $p<0.01$; ***: $p<0.001$).

Acknowledgements

This work has benefited from research funding from the European Community's Seventh Framework Programme in the project ENDOSTEM (Grant agreement number 241440) to SB, and OPTISTEM (Grant agreement number 223098) to GC. Part of this work has been carried out in the ALEMBIC imaging center (San Raffaele Scientific Institute). We are also grateful to Elisabetta Dejana and Patrizia Rovere-Querini for critical reading of the manuscript and fruitful discussion.

REFERENCES

1. Medvinsky A, Rybtsov S, & Taoudi S (2011) Embryonic origin of the adult hematopoietic system: advances and questions. *Development (Cambridge, England)* 138(6):1017-1031.
2. Yamashita J, *et al.* (2000) Flk1-positive cells derived from embryonic stem cells serve as vascular progenitors. *Nature* 408(6808):92-96.
3. Zovein AC, *et al.* (2008) Fate Tracing Reveals the Endothelial Origin of Hematopoietic Stem Cells. *Stem Cell* 3(6):625-636.
4. Boisset JC, *et al.* (2010) In vivo imaging of haematopoietic cells emerging from the mouse aortic endothelium. *Nature* 464(7285):116-120.
5. Bertrand JY, *et al.* (2010) Haematopoietic stem cells derive directly from aortic endothelium during development. *Nature* 464(7285):108-111.

6. Chen MJ, *et al.* (2011) Erythroid/Myeloid Progenitors and Hematopoietic Stem Cells Originate from Distinct Populations of Endothelial Cells. *Stem Cell* 9(6):541-552.
7. Lancrin C, *et al.* (2009) The haemangioblast generates haematopoietic cells through a haemogenic endothelium stage. *Nature* 457(7231):892-895.
8. Minasi MG, *et al.* (2002) The meso-angioblast: a multipotent, self-renewing cell that originates from the dorsal aorta and differentiates into most mesodermal tissues. *Development* 129(11):2773-2783.
9. Tagliafico E, *et al.* (2004) TGFbeta/BMP activate the smooth muscle/bone differentiation programs in mesoangioblasts. *J Cell Sci* 117(Pt 19):4377-4388.
10. Brunelli S, *et al.* (2004) Msx2 and necdin combined activities are required for smooth muscle differentiation in mesoangioblast stem cells. *Circ Res* 94(12):1571-1578.
11. Brunelli S, *et al.* (2007) Nitric oxide release combined with nonsteroidal antiinflammatory activity prevents muscular dystrophy pathology and enhances stem cell therapy. *Proc Natl Acad Sci U S A* 104(1):264-269.
12. Sampaolesi M, *et al.* (2003) Cell therapy of alpha-sarcoglycan null dystrophic mice through intra-arterial delivery of mesoangioblasts. *Science* 301(5632):487-492.
13. Cossu G & Bianco P (2003) Mesoangioblasts--vascular progenitors for extravascular mesodermal tissues. *Current opinion in genetics & development* 13(5):537-542.
14. Dellavalle A, *et al.* (2007) Pericytes of human skeletal muscle are myogenic precursors distinct from satellite cells. *Nat Cell Biol* 9(3):255-267.
15. Mitchell KJ, *et al.* (2010) Identification and characterization of a non-satellite cell muscle resident progenitor during postnatal development. *Nature cell biology* 12(3):257-266.
16. Breier G, *et al.* (1996) Molecular cloning and expression of murine vascular endothelial-cadherin in early stage development of cardiovascular system. *Blood* 87(2):630-641.
17. Wang Y, *et al.* (2010) Ephrin-B2 controls VEGF-induced angiogenesis and lymphangiogenesis. *Nature* 465(7297):483-486.
18. Hisatsune H, *et al.* (2005) High level of endothelial cell-specific gene expression by a combination of the 5' flanking region and the 5' half of the first intron of the VE-cadherin gene. *Blood* 105(12):4657-4663.
19. Drake CJ & Fleming PA (2000) Vasculogenesis in the day 6.5 to 9.5 mouse embryo. *Blood* 95(5):1671-1679.
20. Costa G, *et al.* (2012) SOX7 regulates the expression of VE-cadherin in the haemogenic endothelium at the onset of haematopoietic development. *Development (Cambridge, England)* 139(9):1587-1598.
21. Yokomizo T, Ng CE, Osato M, & Dzierzak E (2011) Three-dimensional imaging of whole midgestation murine embryos shows an intravascular localization for all hematopoietic clusters. *Blood* 117(23):6132-6134.
22. Bertrand JY, *et al.* (2005) Three pathways to mature macrophages in the early mouse yolk sac. *Blood* 106(9):3004-3011.
23. Ovchinnikov DA (2008) Macrophages in the embryo and beyond: Much more than just giant phagocytes. *Genesis (New York, NY : 2000)* 46(9):447-462.
24. Schulz C, *et al.* (2012) A Lineage of Myeloid Cells Independent of Myb and Hematopoietic Stem Cells. *Science (New York, NY)* 336(6077):86-90.

25. Sawtell NM & Lessard JL (1989) Cellular distribution of smooth muscle actins during mammalian embryogenesis: expression of the alpha-vascular but not the gamma-enteric isoform in differentiating striated myocytes. *The Journal of Cell Biology* 109(6 Pt 1):2929-2937.
26. Crawford K, *et al.* (2002) Mice lacking skeletal muscle actin show reduced muscle strength and growth deficits and die during the neonatal period. *Molecular and Cellular Biology* 22(16):5887-5896.
27. Secchiero P, *et al.* (2012) Activation of the p53 pathway induces α-smooth muscle actin expression in both myeloid leukemic cells and normal macrophages. *J Cell Physiol* 227(5):1829-1837.
28. Ninomiya K, Takahashi A, Fujioka Y, Ishikawa Y, & Yokoyama M (2006) Transforming growth factor-beta signaling enhances transdifferentiation of macrophages into smooth muscle-like cells. *Hypertension research : official journal of the Japanese Society of Hypertension* 29(4):269-276.
29. Barrio MM, *et al.* (2012) Human Macrophages and Dendritic Cells Can Equally Present MART-1 Antigen to CD8+ T Cells after Phagocytosis of Gamma-Irradiated Melanoma Cells. *PLoS One* 7(7):e40311.
30. Russo V, *et al.* (2000) Acquisition of intact allogeneic human leukocyte antigen molecules by human dendritic cells. *Blood* 95(11):3473-3477.
31. Zovein AC, *et al.* (2010) Vascular remodeling of the vitelline artery initiates extravascular emergence of hematopoietic clusters. *Blood* 116(18):3435-3444.
32. Park EJ, *et al.* (2007) System for tamoxifen-inducible expression of cre-recombinase from the Foxa2 locus in mice. *Dev Dyn* 237(2):447-453.
33. DeRuiter MC, *et al.* (1997) Embryonic endothelial cells transdifferentiate into mesenchymal cells expressing smooth muscle actins in vivo and in vitro. *Circulation Research* 80(4):444-451.
34. Moonen JR, *et al.* (2010) Endothelial progenitor cells give rise to pro-angiogenic smooth muscle-like progeny. *Cardiovascular research* 86(3):506-515.
35. Liebner S, *et al.* (2004) Beta-catenin is required for endothelial-mesenchymal transformation during heart cushion development in the mouse. *J Cell Biol* 166(3):359-367.
36. Rivera-Feliciano J, *et al.* (2006) Development of heart valves requires Gata4 expression in endothelial-derived cells. *Development* 133(18):3607-3618.
37. Tonlorenzi R, Dellavalle A, Schnapp E, Cossu G, & Sampaolesi M (2007) Isolation and characterization of mesoangioblasts from mouse, dog, and human tissues. *Curr Protoc Stem Cell Biol* Chapter 2:Unit 2B 1.
38. Yoder MC, Hiatt K, & Mukherjee P (1997) In vivo repopulating hematopoietic stem cells are present in the murine yolk sac at day 9.0 postcoitus. *Proceedings of the National Academy of Sciences of the United States of America* 94(13):6776-6780.
39. Kumaravelu P, *et al.* (2002) Quantitative developmental anatomy of definitive haematopoietic stem cells/long-term repopulating units (HSC/RUs): role of the aorta-gonad-mesonephros (AGM) region and the yolk sac in colonisation of the mouse embryonic liver. *Development* 129(21):4891-4899.
40. Huber TL, Kouskoff V, Fehling HJ, Palis J, & Keller G (2004) Haemangioblast commitment is initiated in the primitive streak of the mouse embryo. *Nature* 432(7017):625-630.

41. Li W, Ferkowicz MJ, Johnson SA, Shelley WC, & Yoder MC (2005) Endothelial cells in the early murine yolk sac give rise to CD41-expressing hematopoietic cells. *Stem cells and development* 14(1):44-54.
42. Wang LD & Wagers AJ (2011) Dynamic niches in the origination and differentiation of haematopoietic stem cells. *Nature Reviews Molecular Cell Biology* 12(10):643-655.
43. Dzierzak E & Robin C (2010) Placenta as a source of hematopoietic stem cells. *Trends in molecular medicine* 16(8):361-367.
44. Rhodes KE, *et al.* (2008) The Emergence of Hematopoietic Stem Cells Is Initiated in the Placental Vasculature in the Absence of Circulation. *Cell stem cell* 2(3):252-263.
45. Bertrand JY, Cisson JL, Stachura DL, & Traver D (2010) Notch signaling distinguishes 2 waves of definitive hematopoiesis in the zebrafish embryo. *Blood* 115(14):2777-2783.
46. Loeffler D, Kokkaliaris KD, & Schroeder T (2011) Wnt to notch relay signaling induces definitive hematopoiesis. *Cell stem cell* 9(1):2-4.
47. Peeters M, *et al.* (2009) Ventral embryonic tissues and Hedgehog proteins induce early AGM hematopoietic stem cell development. *Development* 136(15):2613-2621.
48. Wilkinson RN, *et al.* (2009) Hedgehog and Bmp polarize hematopoietic stem cell emergence in the zebrafish dorsal aorta. *Developmental cell* 16(6):909-916.
49. Singbrant S, *et al.* (2010) Canonical BMP signaling is dispensable for hematopoietic stem cell function in both adult and fetal liver hematopoiesis, but essential to preserve colon architecture. *Blood* 115:4689-4698.
50. Tremblay KD, Dunn NR, & Robertson EJ (2001) Mouse embryos lacking Smad1 signals display defects in extra-embryonic tissues and germ cell formation. *Development (Cambridge, England)* 128(18):3609-3621.
51. Lu CC, Robertson EJ, & Brennan J (2004) The mouse frizzled 8 receptor is expressed in anterior organizer tissues. *Gene Expr Patterns* 4(5):569-572.
52. Ugarte G, Cappellari O, Perani L, Pistocchi A, & Cossu G (2012) Noggin recruits mesoderm progenitors from the dorsal aorta to a skeletal myogenic fate. *Dev Biol*:1-10.
53. Mendes SC (2005) Mesenchymal progenitor cells localize within hematopoietic sites throughout ontogeny. *Development (Cambridge, England)* 132(5):1127-1136.
54. Doyonnas R, Labarge MA, Sacco A, Charlton C, & Blau HM (2004) Hematopoietic contribution to skeletal muscle regeneration by myelomonocytic precursors. *Proceedings of the National Academy of Sciences of the United States of America* 101(37):13507-13512.
55. Ojima K, *et al.* (2004) Mac-1(low) early myeloid cells in the bone marrow-derived SP fraction migrate into injured skeletal muscle and participate in muscle regeneration. *Biochemical and biophysical research communications* 321(4):1050-1061.

Figure 1. Efficiency and specificity of Cre recombination in Cdh5-CREERT2 mice

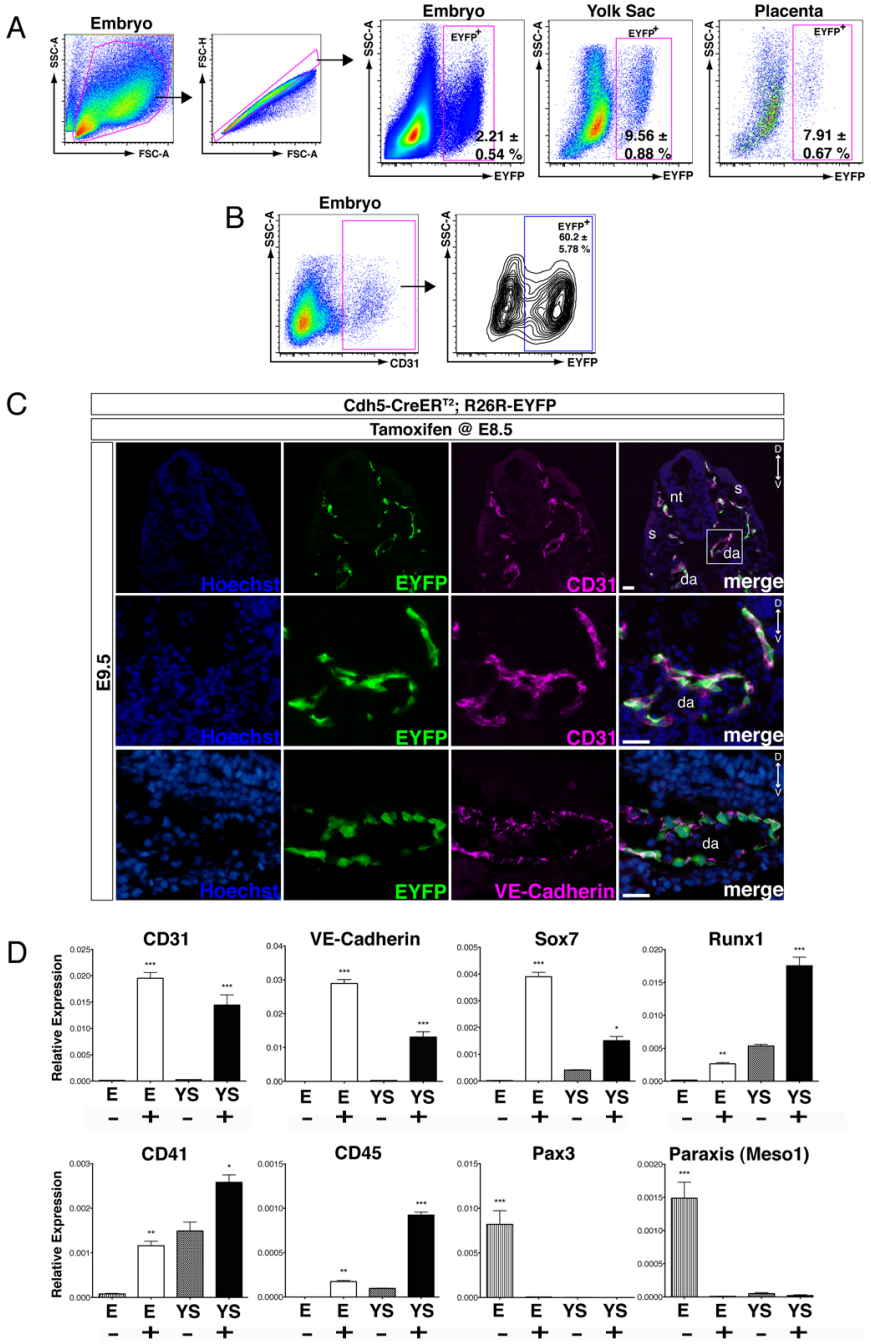

Figure 2. eVE-Cad+ cells in extraembryonic tissues generate hematopoietic cells at early stages

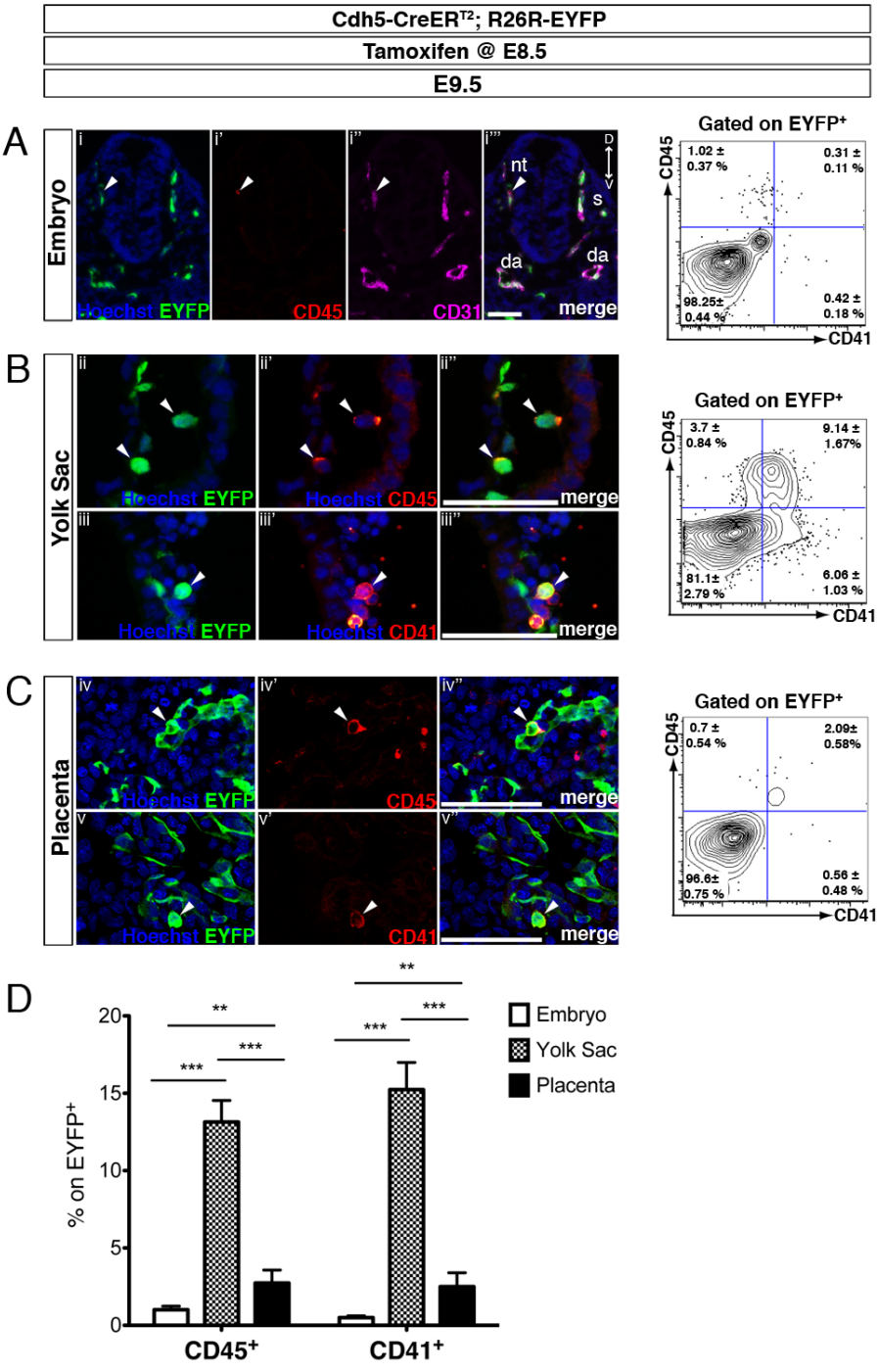

Figure 3. eVE-Cad+ derived non-MΦ hematopoietic cells emerge from vessels in an abluminal direction and express the mesenchymal marker α-SMA

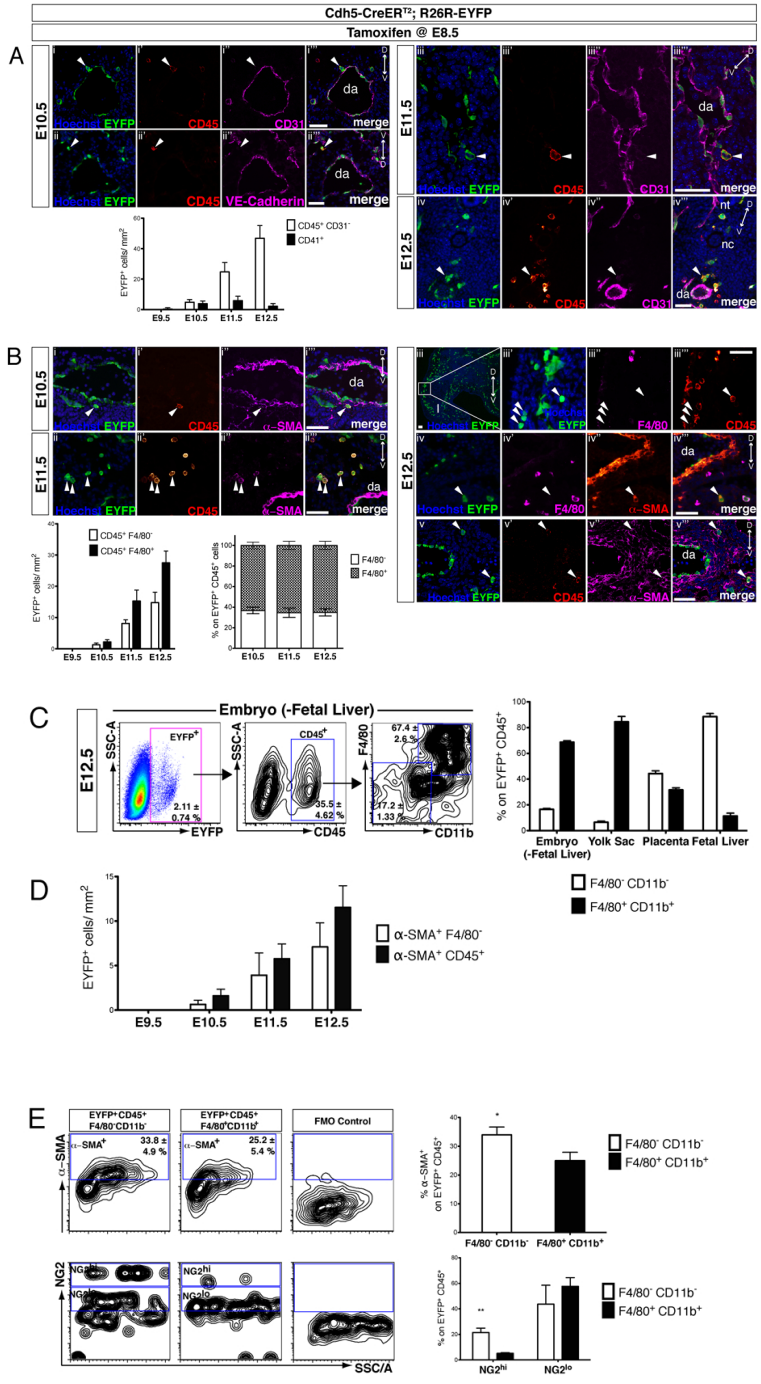

Figure 4. The first wave of eVe-Cad+ derived CD41+ and CD45+ cells in the mesenchyme originates from extraembryonic hemogenic endothelium

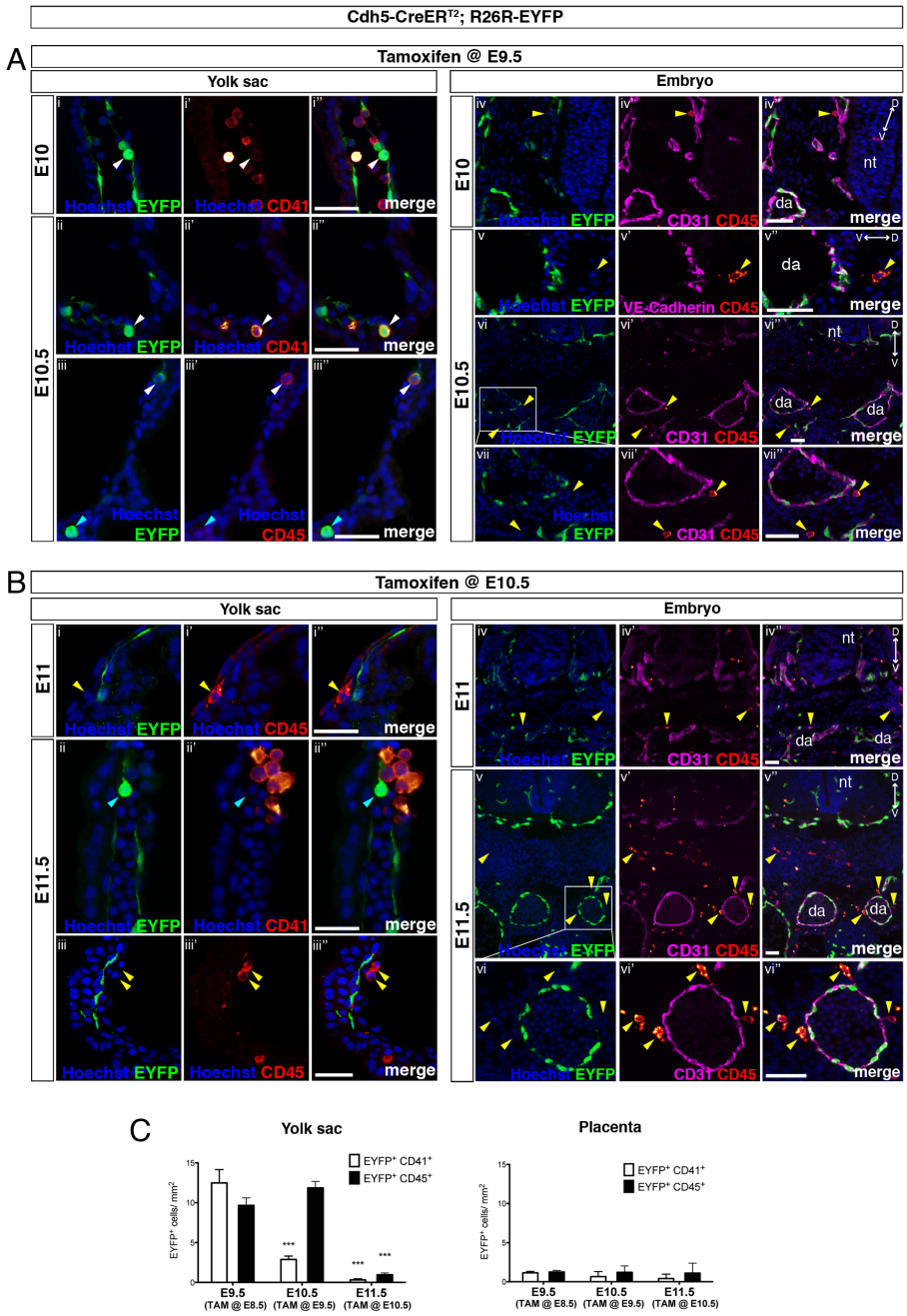

Figure 5. E9.5 and E10.5 VE-Cadherin+ cells in the embryo and YS express a non-overlapping set of genes

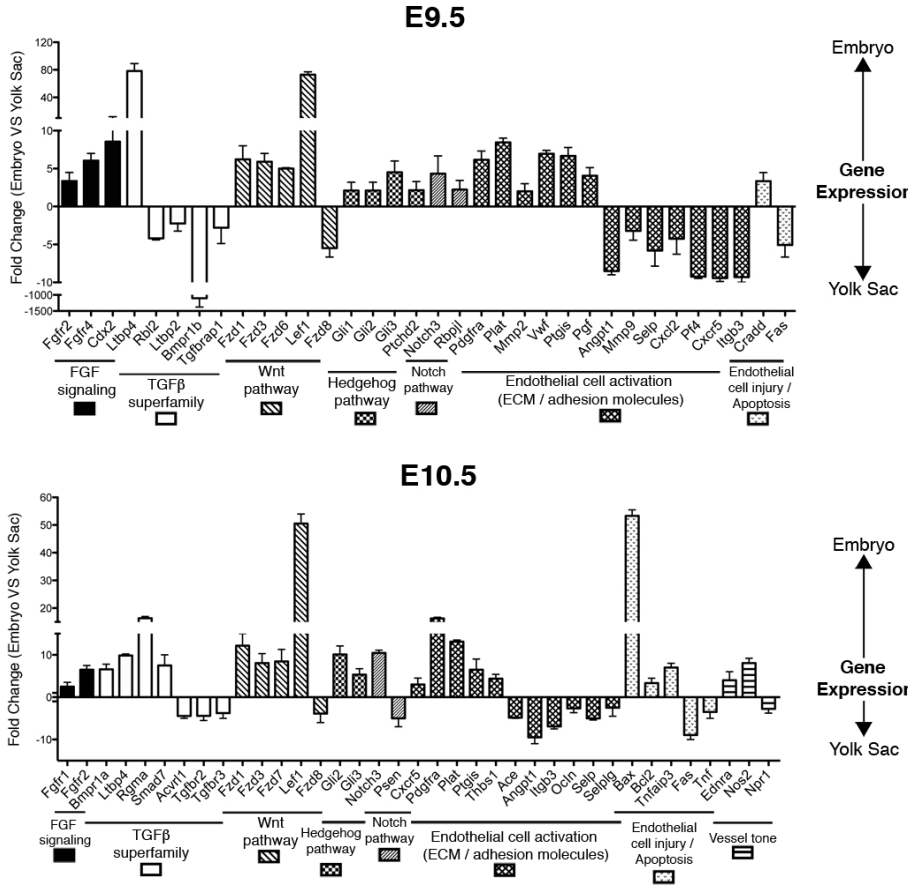

Figure 6. eVE-Cad+ derived cells contribute to smooth and skeletal muscle

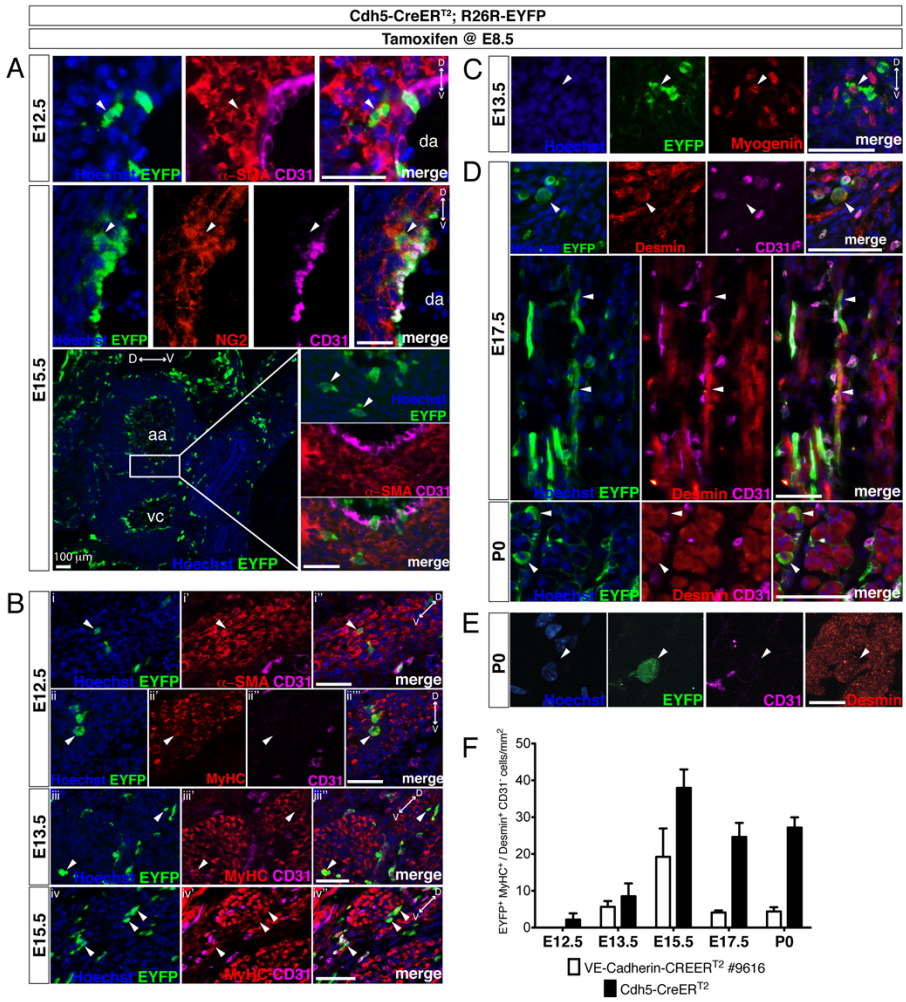

Figure 7. Isolation and in vitro characterization of eVE-Cad+ derived cells

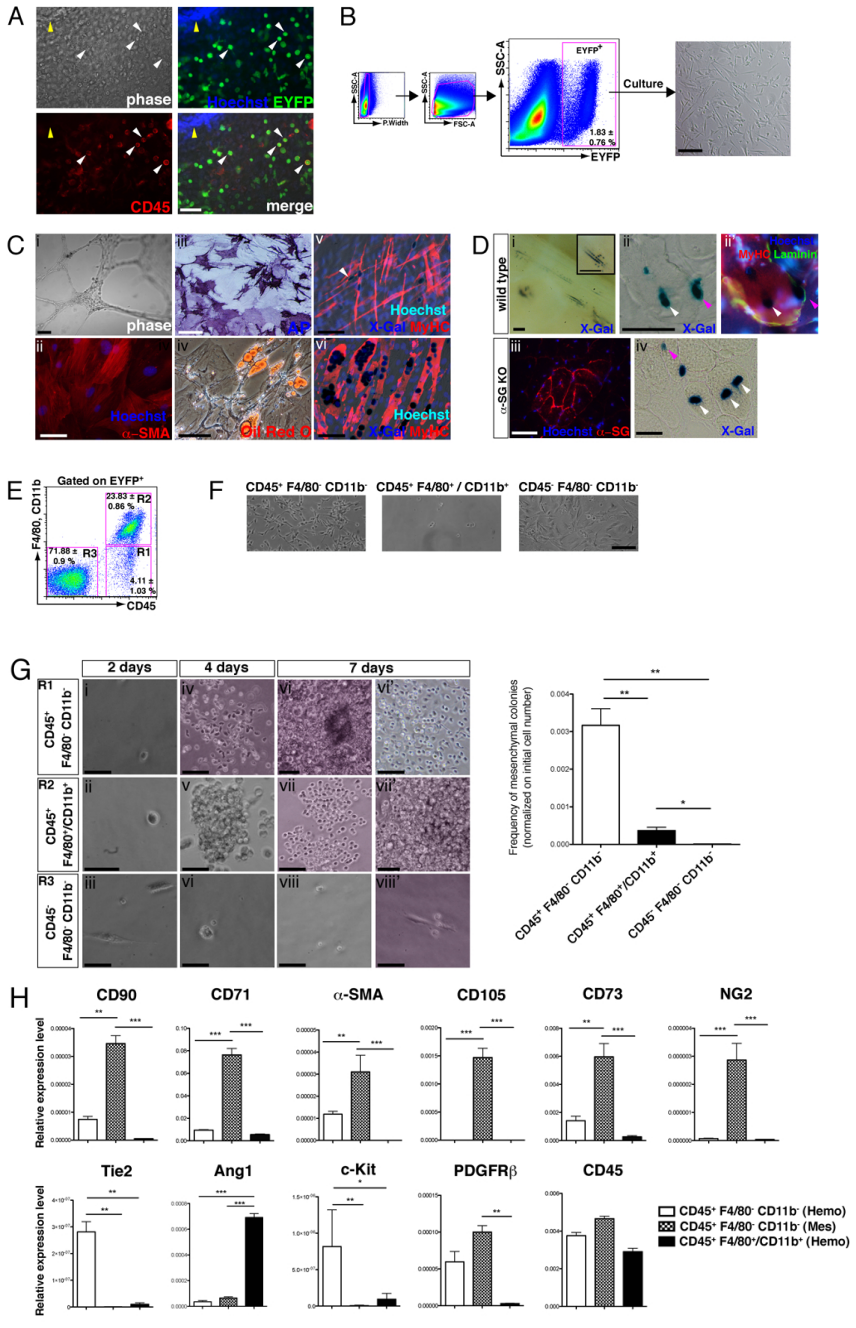

FIGURE LEGENDS

FIGURE 1. Efficiency and specificity of Cre recombination in Cdh5-CREERT2 mice. (**A**) FACS analysis of E9.5 Cdh5-CREER^{T2};R26R-EYFP embryos (1 single TAM I/P injection in the pregnant mother at E8.5) showing the percentage of EYFP^{+} cells. At least 8 embryos, YS, or placentas were pooled for each experiment. Dot plots show the gating strategy and doublet exclusion. Data representative of at least 3 independent experiments. (**B**) FACS analysis of E9.5 Cdh5-CREER^{T2};R26R-EYFP embryos showing Cre recombination efficiency, calculated as % of EYFP^{+} cells on total CD31^{+} cells, 24 hours after TAM injection. Data representative of 5 independent experiments. (**C**) Immunofluorescence (IF) using anti-EYFP, anti-CD31 and anti-VE-Cad specific antibodies (Abs) on transversal sections of E9.5 embryos. Nuclei were stained with Hoechst. da: dorsal aorta; nt: neural tube; s: somite. Dorso/Ventral orientation indicator is shown on the top right of each merged image. Scale bars, 50 μm. (**D**) EYFP^{+} cells were separately sorted from E9.5 Cdh5-CREER^{T2};R26R-EYFP embryos and yolk sac. Quantitative Real-Time PCR analysis was performed. At least 10 embryos, or YS were pooled for each experiment. All data points were calculated in triplicate as gene expression relative to endogenous 28S or cyclophilin A expression. Data representative of 3 independent experiments. Data are shown as mean ± SEM. * $p<0.05$; ** $p<0.01$; *** $p<0.001$ vs EYFP- cells of the same embryo compartment (Embryo proper, or YS)(for CD31, VE-Cad, Sox7, Runx1, CD41, CD45); or vs EYFP+ cells of the same embryo

compartment (for Pax3 and Paraxis). E+ : Embryo EYFP+; E-: Embryo EYFP-; YS+: Yolk sac EYFP+; YS-: Yolk sac EYFP-

FIGURE 2. eVE-Cad+ cells in extraembryonic tissues generate hematopoietic cells at early stages. (**A**) Left panels: IF using anti-EYFP, anti-CD31 and anti CD45 on transversal sections of a E9.5 embryo. A Dorso/Ventral orientation indicator is shown on the top right of merged image. Arrow indicates a unlabelled $CD45^+$ $CD31^+$ HC. da: dorsal aorta; nt: neural tube; s: somite. Dot plot on the right: FACS analysis showing the percentage of $CD41^+$ and $CD45^+$ cells within the $EYFP^+$ subset. (**B**) Left panels: IF using anti-EYFP, anti CD45 (ii) and anti-CD41 (iii) on sections of E9.5 yolk sacs. Arrows indicate EYFP+ CD45+ or $EYFP^+$ $CD41^+$ HCs. Dot plot on the right: FACS analysis showing the percentage of $CD41^+$ and $CD45^+$ cells within the $EYFP^+$ subset. (**C**) Left panels: IF using anti-EYFP, anti CD45 (iv) and anti-CD41 (v) on sections of E9.5 placentas. Arrows indicate $EYFP^+$ $CD45^+$ or $EYFP^+$ $CD41^+$ HCs. Dot plot on the right: FACS analysis showing the percentage of $CD41^+$ and $CD45^+$ cells within the $EYFP^+$ subset. Scale bars in (A) (B) and (C), 50 μm. At least 8 embryos, YS, placentas or fetal livers were pooled for each FACS experiment in (A), (B) and (C). Dot plots in (A), (B) and (C) are representative of at least n=3 independent experiments. (**D**) Graph showing the percentage of $CD45^+$ and $CD41^+$ cells within the $EYFP^+$ subset for each tissue, as quantification of FACS analyses. Data are shown as mean ± SEM. ** $p<0.01$; *** $p<0.001$ as specified by the bar.

FIGURE 3. eVE-Cad+ derived non-MΦ hematopoietic cells emerge from vessels in an abluminal direction and express the mesenchymal marker α-SMA. (**A**) IF using anti-EYFP, anti-CD45 and anti-CD31 (i,iii,iv) or anti-VE-Cadherin (ii) on transversal

sections of E10.5 (i,ii), E11.5 (iii) and E12.5 (iv) embryos. Arrows indicate EYFP^{+}CD45^{+}CD31$^{low/-}$ or EYFP^{+}CD45^{+}VE-Cadherin^{-} cells in an abluminal position. Graph shows quantification by histology of EYFP^{+}CD45^{+}CD31$^{low/-}$ and EYFP^{+}CD41^{+} cells in the embryo mesenchyme. (**B**) IF using anti-EYFP, anti-CD45 (i,ii,iii,v), anti α-SMA, (i,ii,iv,v) and anti-F4/80 (iii,iv) on transversal sections of E10.5 (i), E11.5 (ii) and E12.5 (iii-v) embryos. Arrows indicates EYFP^{+}CD45^{+}α-SMA^{+} cells in the mesenchyme surrounding dorsal aorta (i,ii,v); EYFP^{+}CD45^{+}F4/80^{-} cells in the developing limb (iii); EYFP^{+}α-SMA $^{+}$F4/80^{-} cells surrounding dorsal aorta (iv). Graphs show quantification by histology of EYFP^{+}CD45^{+}F4/80^{-} and EYFP^{+}CD45^{+}F4/80^{+} cells in the embryo mesenchyme; left graph as absolute numbers and right graph as percentage of F4/80^{+} and F4/80^{-} cells on the total of EYFP^{+}CD45^{+} cells. A Dorso/Ventral orientation indicator is shown on the top right of each merged image in (A) and (B). da: dorsal aorta; l: developing limb; nt: neural tube; nc: notochord. Nuclei were stained with Hoechst in (A) and (B). Scale bars, 50 μm. (**C**) FACS analysis of E12.5 Cdh5-CREER^{T2};R26R-EYFP embryos (fetal liver was removed), showing F4/80 and CD11b expression within the EYFP^{+}CD45^{+} subset. A similar analysis was performed on YS, placenta and fetal liver. Dot plots show the gating strategy. Graph shows the percentage of F4/80^{-} CD11b^{-} and F4/80^{+}CD11b^{+} cells within the EYFP^{+}CD45^{+} population in the embryo, yolk sac, placenta and fetal liver, as quantification of FACS analyses. (**D**) Quantification by histology of EYFP^{+}α-SMA^{+} F4/80^{-} and EYFP^{+}α-SMA $^{+}$CD45^{+} cells in the embryo mesenchyme. (**E**) FACS analysis of E12.5 Cdh5-CREER^{T2}; R26R-EYFP embryos devoid of the fetal liver,

showing the percentage of α-SMA$^+$ and NG2^{lo} and ^{hi} cells within the EYFP$^+$CD45$^+$ F4/80$^-$CD11b$^-$ and EYFP$^+$CD45$^+$ F4/80$^+$ CD11b$^+$ subsets. Fluorescence minus one (FMO) controls are shown. At least 8 embryos, YS, placentas or fetal livers were pooled for each experiment in (C) and (E). At least 10 fields (20x and/or 40x) were counted for each stage for (A), (B), (D). Dot plots in (C) and (E) are representative of at least 3 independent experiments. Data in the graphs in (E) are shown as mean ± SEM. *p<0.05 vs EYFP$^+$CD45$^+$α-SMA$^+$ F4/80$^+$CD11b$^+$. * p<0.01 vs EYFP$^+$CD45$^+$NG2^{hi} F4/80$^+$CD11b$^+$.

FIGURE 4. The first wave of eVe-Cad+ derived CD41+ and CD45+ cells in the mesenchyme originates from extraembryonic hemogenic endothelium. (**A**) IF using anti-EYFP, anti-CD41 (i,ii), anti-CD45 (iii-vii), anti-CD31 (iv,vi,vii) or anti-VE-Cadherin (v) on sections of E10 YS (i) and embryos (iv) and E10.5 YS (ii,iii) and embryos (v-vii). TAM induction at E9.5. Boxed area in (vi) is shown at higher magnification in (vii). White arrows indicate labelled CD41$^+$ and CD45$^+$ HCs in the YS. Yellow arrows indicate unlabelled CD45$^+$CD31$^-$ or CD45$^+$ VE-Cadherin$^-$ HCs in the embryo. Cyan arrows indicate a EYFP$^+$ CD45$^-$ HC in the YS. (**B**) IF using anti-EYFP, anti-CD45 (i,iii-vi) and anti-CD41 (ii) on sections of E11 YS (i) and embryos (iv) and E11.5 YS (ii,iii) and embryos (v,vi). TAM induction at E10.5. Boxed area in (v) is shown at higher magnification in (vi). Yellow arrows indicate unlabelled CD45$^+$ HCs both in the embryo and YS. Cyan arrows indicate a HC EYFP$^+$ CD41$^-$ in the YS. (**C**) Quantification by histology of EYFP$^+$CD41$^+$ and EYFP$^+$CD45$^+$ cells in the YS and in the placenta at E9.5, E10.5 and E11.5. For each stage, TAM induction was performed 24 hours before collection. At least 10 fields (40x) were counted for each stage. *** p<0.001

vs the n. of $CD41^+$ or $CD45^+$ at E9.5. A Dorso/Ventral orientation indicator is shown on the top right of each merged image in the embryo. da: dorsal aorta; nt: neural tube. Nuclei were stained with Hoechst in (A) and (B). Scale bars, 50 μm.

FIGURE 5. E9.5 and E10.5 VE-Cadherin+ cells in the embryo and YS express a non-overlapping set of genes. $EYFP^+$ cells were separately sorted from E9.5 and E10.5 Cdh5-$CREER^{T2}$;R26R-EYFP embryo and yolk sac. Cre recombination was induced with TAM 24 hours before collection. A Real-Time PCR-based array analysis was performed. Positive fold changes (>3.5) represent genes more expressed in the embryo respect to the YS; negative fold changes (>3.5) represent the opposite. At least 10 embryos and YSs were pooled for each experiment. Data are representative of 3 independent experiments. Data are shown as mean ± SEM. For all datasets we have only considered genes with a fold change expression with a $p< 0.05$ (YS vs embryo).

FIGURE 6. eVE-Cad+ derived cells contribute to smooth and skeletal muscle. (**A**) IF using anti-EYFP, anti-α-SMA or anti-NG2 and anti-CD31 on E12.5 and E15.5 embryos and fetuses (transversal sections). Boxed area in the bottom panel is shown at higher magnification on the right. Arrows indicate $EYFP^+$α-SMA^+CD31^- or $EYFP^+NG2^+CD31^-$ smooth muscle cells. Quantification of $EYFP^+$α-SMA^+ $CD31^-$ and $EYFP^+$ $NG2^+$ $CD31^-$ cells was done by counting at least 10 fields (20x) for each stage. (**B**) IF using anti-EYFP, anti-α-SMA (i) or anti-MyHC (ii-iv) and anti-CD31 on E12.5, E13.5 and E15.5 transversal sections of embryos and fetuses. Arrows indicate $EYFP^+$α-SMA^+CD31^- or $EYFP^+MyHC^+CD31^-$ single-nucleated myocytes/myofibers. (**C**) IF using anti-EYFP and anti-Myogenin on E13.5 embryo

transversal sections. Arrow indicates a EYFP$^+$ Myogenin$^+$ myocyte. (**D**) IF using anti-EYFP, anti-Desmin and anti-CD31 on E17.5 or P0 hindlimb transversal (top and bottom) or longitudinal (middle) sections. Arrows indicate EYFP$^+$ Desmin$^+$ CD31$^-$ myofibers. (**E**) Confocal IF imaging of P0 hindlimb transversal sections, using anti-EYFP, anti-Desmin and anti-CD31. Arrow indicates a EYFP$^+$Desmin$^+$CD31$^-$ myofiber. (**F**) Quantification of EYFP$^+$MyHC$^+$/Desmin$^+$ CD31$^-$ myocytes or myofibers/mm^2 at E12.5, E13.5, E15.5, E17.5 and P0 in VE-Cadherin-CREER^{T2} and Cdh5-CREER^{T2} mice. At least 10 fields (20x) were counted for each stage. A Dorso/Ventral orientation indicator is shown on the top right of each merged image in the embryo/fetus. da: dorsal aorta; aa:abdominal aorta; vc:vena cava. Nuclei were stained with Hoechst. Scale bars, 50 μm (A-D) 25μm (E), except where indicated.

FIGURE 7. Isolation and in vitro characterization of eVE-Cad+ derived cells. (**A**) Dorsal aorta and vitelline artery were dissected from Cdh5-CREER^{T2};R26R-EYFP E10.5 embryos (1 TAM injection at E8.5), plated on collagen-coated dishes and cultured for 5-7 days. Phase contrast and IF using anti-EYFP and anti-CD45. White arrows indicate labelled EYFP$^+$CD45$^+$ cells in the outgrowth. Yellow arrow indicates aorta explant. (**B**) Gating strategy for FACS sorting of EYFP$^+$ cells from E12.5 Cdh5-CREER^{T2}; R26R-EYFP embryos (TAM injection at E8.5), devoid of the fetal liver. At least 8 embryos were pooled for each experiment. Dot plots are representative of n=5 independent experiments. EYFP$^+$ were subsequently cultured for 2-5 passages. A representative bright field image is shown on the right. (**C**) eVE-Cad$^+$ cells were isolated as described in (B) and exposed to differentiating stimuli. (i) eVE-Cad$^+$ cells

exposed to VEGF form an endothelial network. (ii) eVE-Cad$^+$ cells exposed to TGF-β differentiate into α-SMA$^+$ cells. IF using anti-α-SMA. (iii) eVE-Cad$^+$ cells exposed to BMP-2 become positive for alkaline phosphatase (AP). AP reaction. (iv) eVE-Cad$^+$ cells cultured in adipogenic inductive medium differentiate into adipocytes. Oil Red O staining. Note adipocytes containing red fat droplets. (v),(vi) Co-culture assay of nLacZ-eVE-Cad$^+$ cells and C2C12 myoblasts was stopped after 3 (v) or 5 days (vi). X-gal staining and IF using anti-MyHC. Arrows in (v) point to a single-nucleated X-Gal$^+$ MyHC$^+$ myoblasts. Image in (vi) shows large MyHC$^+$ myotubes containing X-Gal$^+$ nuclei. (**D**) Intra-muscular (I/M) injection of nLacZ-eVE-Cad$^+$ cells into CTX-damaged wild type or α-sarcoglycan (α-SG) KO mice. (i): Whole mount X-Gal staining of a CTX injured wild type TA muscle injected with eVE-Cad$^+$ cells. Inset at higher magnification show superficial myofibers containing X-Gal$^+$ nuclei. (ii,ii'):X-Gal staining and IF using anti-Laminin and anti-MyHC on cross-sections of the same muscle depicted in (i). X-Gal$^+$ nuclei localize centrally (white arrow) or peripherally (purple arrow) inside myofibers. (iii, iv): I/M injection of eVE-Cad$^+$ cells into α-SG KO mice. IF using anti α-SG on TA muscle cross-sections showing a cluster of regenerating α-SG$^+$ myofibers; (iii) X-Gal staining on TA muscle cross-sections showing X-Gal$^+$ nuclei in central position (white arrow) or peripherally (purple arrow) inside myofibers derived from eVE-Cad$^+$ injected cells (iv). (**E**) Gating strategy for FACS sorting of EYFP$^+$CD45$^+$F4/80$^-$CD11b$^-$ (R1), EYFP$^+$CD45$^+$ F4/80$^+$/CD11b$^+$ (R2) and EYFP$^+$CD45$^-$F4/80$^-$CD11b$^-$ (R3) subpopulations from E12.5 Cdh5-CREER^{T2}; R26R-EYFP embryos (Tamoxifen injection at E8.5), devoid of the fetal liver.

At least 8 embryos were pooled for each experiment. Dot plot is representative of n=7 independent experiments. (**F**): R1, R2 and R3 cell subpopulations were plated on collagen coated dishes in MAB permissive conditions. Photos taken after 1 passage. Only R1 ($EYFP^+CD45^+F4/80^-CD11b^-$) subpopulation generated cells with MAB morphology. (**G**) Colony forming cell assay on R1, R2 and R3 cell subpopulations. Colonies were scored after 2,4, or 7 days. R3 ($EYFP^+CD45^-$ $F4/80^-CD11b^-$) cells generated very few colonies overall. R1 ($EYFP^+CD45^+$ $F4/80^-CD11b^-$) cells generated hematopoietic colonies (including CFU-GEMM, shown in vi; and BFU-E) and colonies including adherent cells resembling a mesenchymal phenotype (iv, vi'). R2 ($EYFP^+CD45^+$ $F4/80^+CD11b^+$) cells formed mostly hematopoietic colonies (including CFU-Mac, vii; and CFU-GM, v,vii'). Graph on the right shows a quantification of the frequency of the formation of mixed hematopoietic/mesenchymal colonies (assessed by cell morphology) by the different subpopulations, normalized on the initial cell number (4 independent experiments). (**H**): Individual colonies from CFC assay (day 7) were picked and qRT-PCR analysis was performed. All data points were calculated in triplicate as gene expression relative to endogenous 28S or cyclophilin A expression. Data representative of 3 independent experiments. Data are shown as mean ± SEM. * $p<0.05$; ** $p<0.01$; *** $p<0.001$ as specified by the bar. Nuclei in (A), (C) and (D) were stained with Hoechst. Scale bars: 100 μm (C,i,iii; D,i), 50 μm (A, C,ii,iv-vi; D,ii-iii; E; F).

FIGURE S1:
Generation and recombination specificity of VE-Cadherin-CREERT2 transgenic mice.

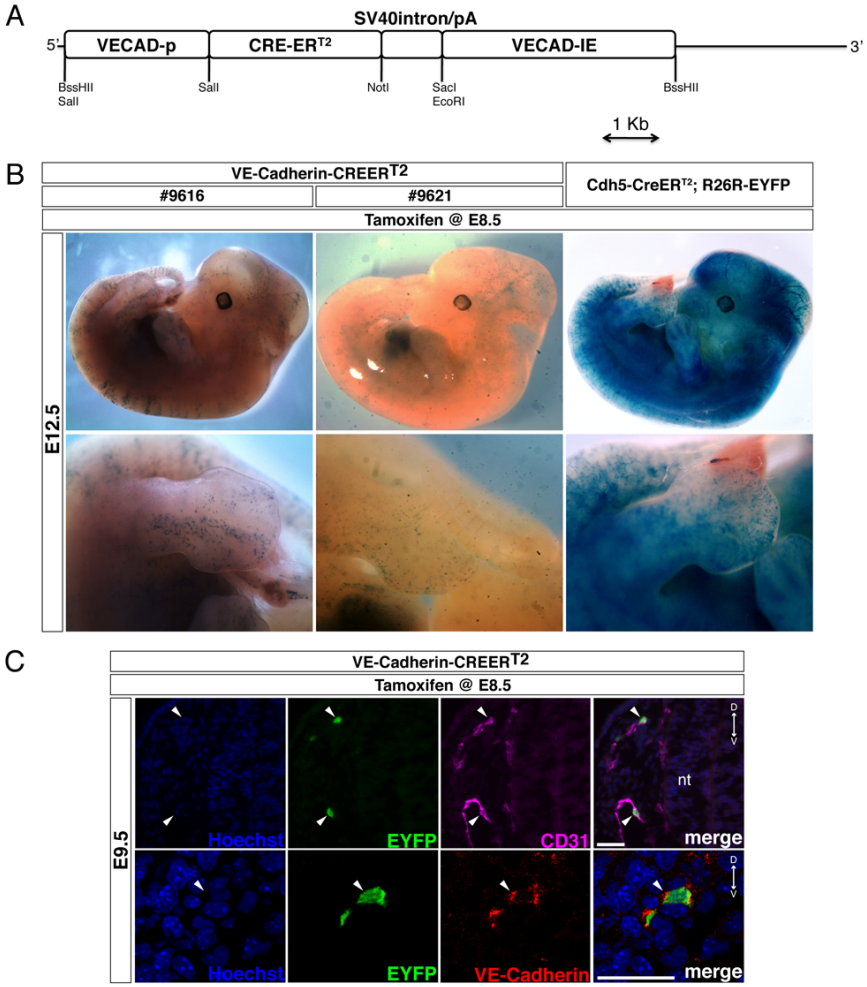

FIGURE S2:
Intra-aortic hematopoietic clusters are labelled in Cdh5-CRE-ERT2 transgenic mice by inducing Cre recombination at E8.5.

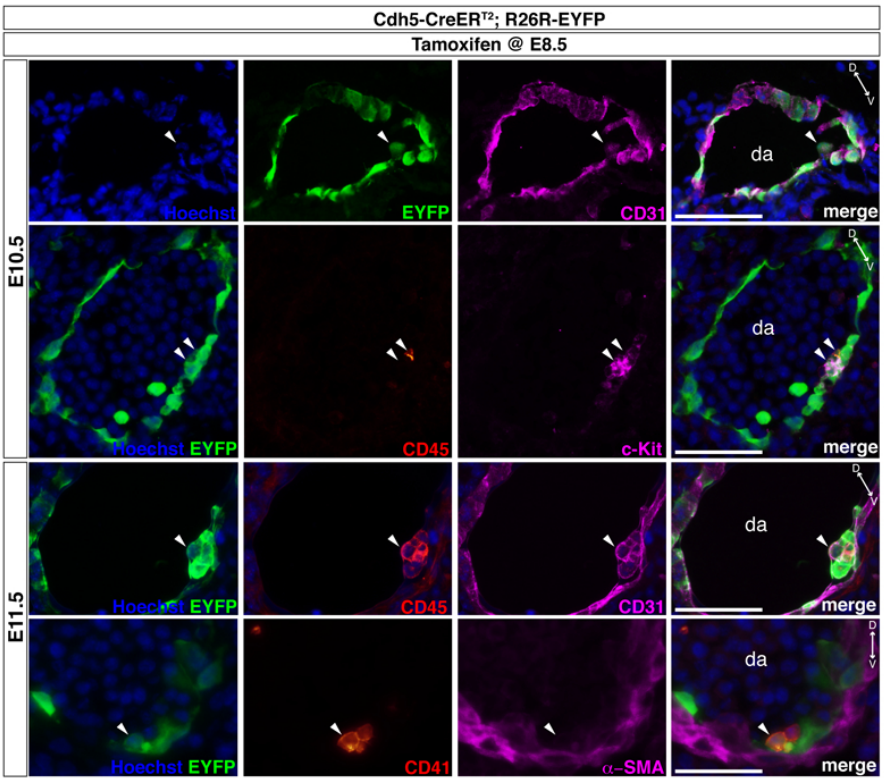

FIGURE S3:
Yolk sac eVE-Cad derived c-Kit+ hematopoietic cells are found in the mesenchyme from E10.5.

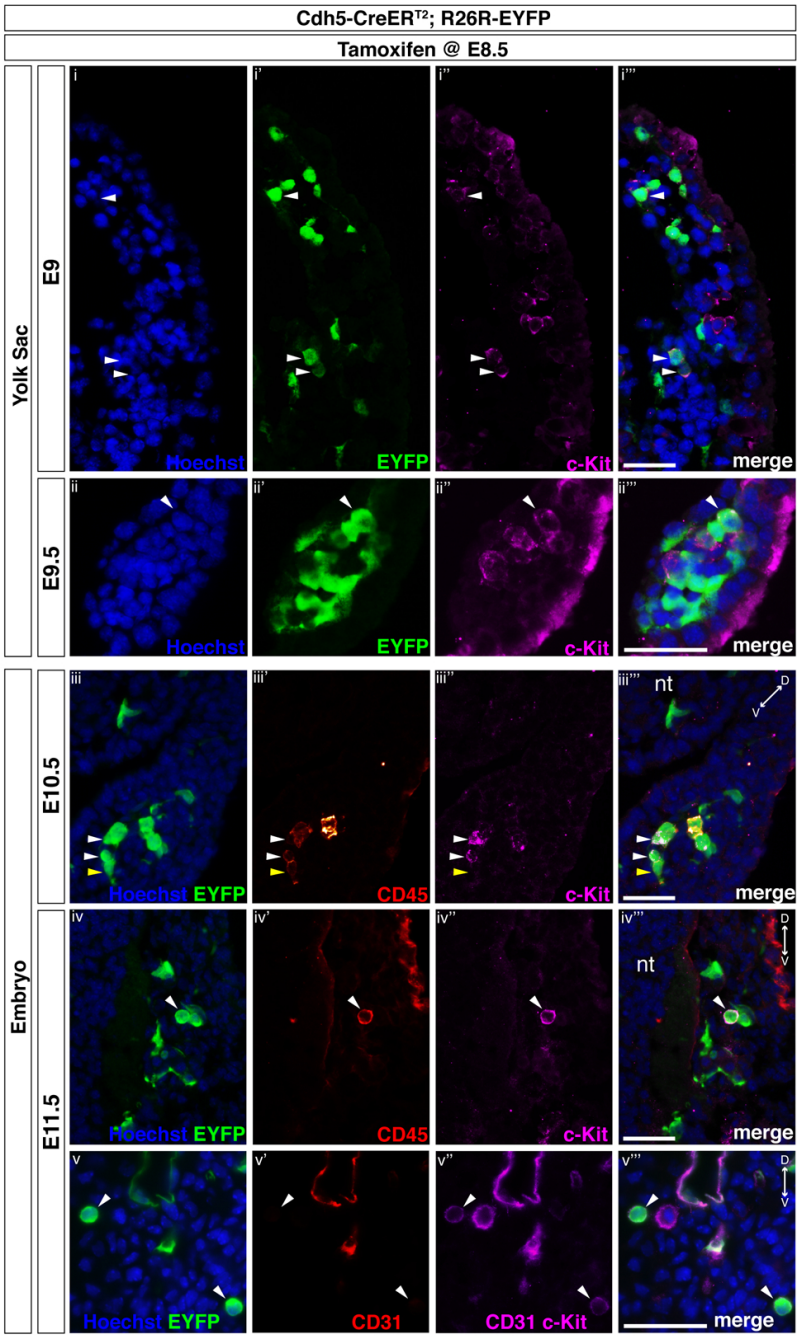

FIGURE S4:
eVE-Cad derived CD45+ and CD41+ cells are found in several anatomical locations within the mesenchyme in the embryo proper from E10.5.

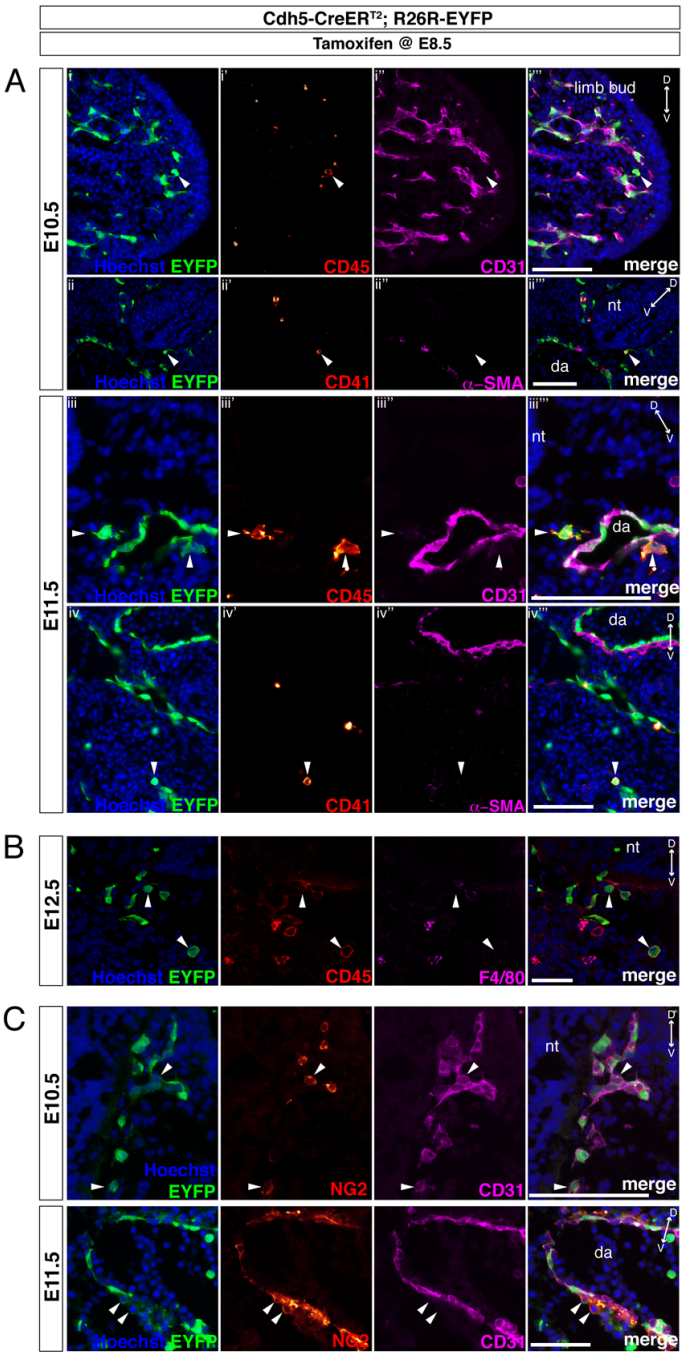

FIGURE S5:
Generation of hematopoietic cells by eVE-Cad+ progenitors in the placenta.

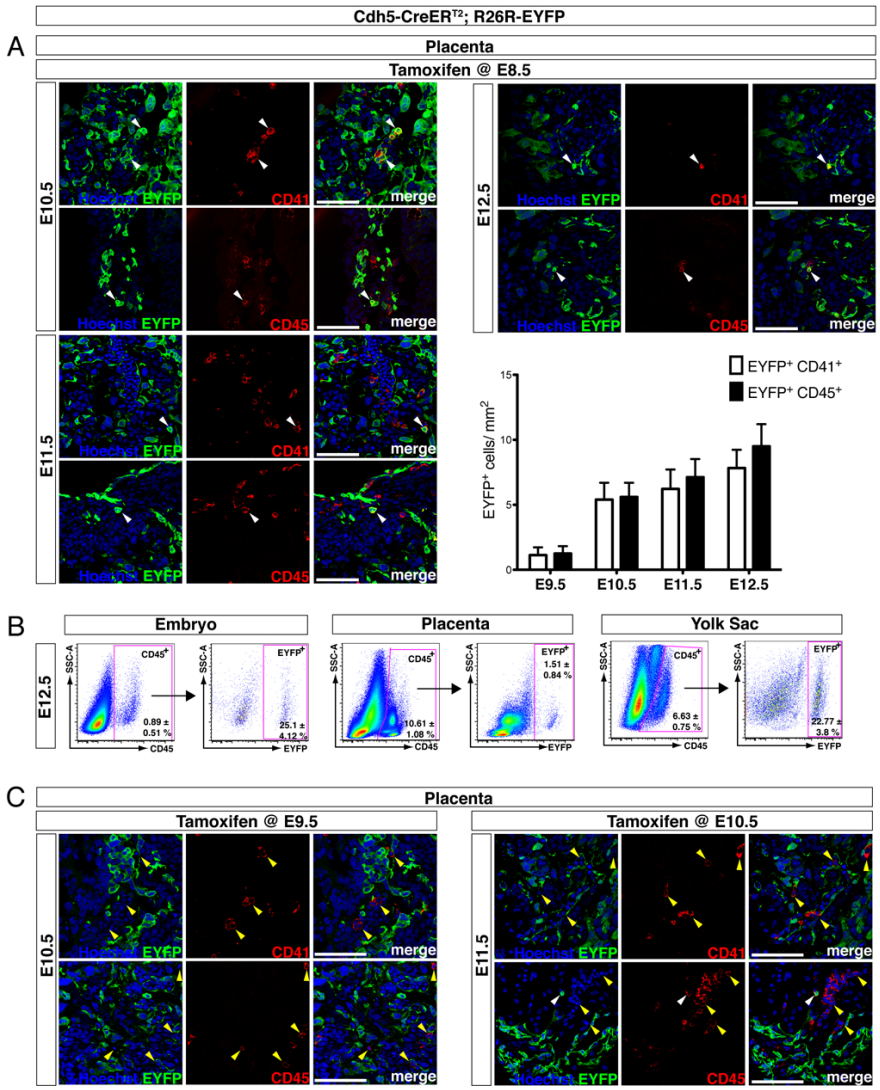

FIGURE S6:
Differential gene expression of embryo and yolk sac eVE-Cad+ cells between E9.5 and E10.5.

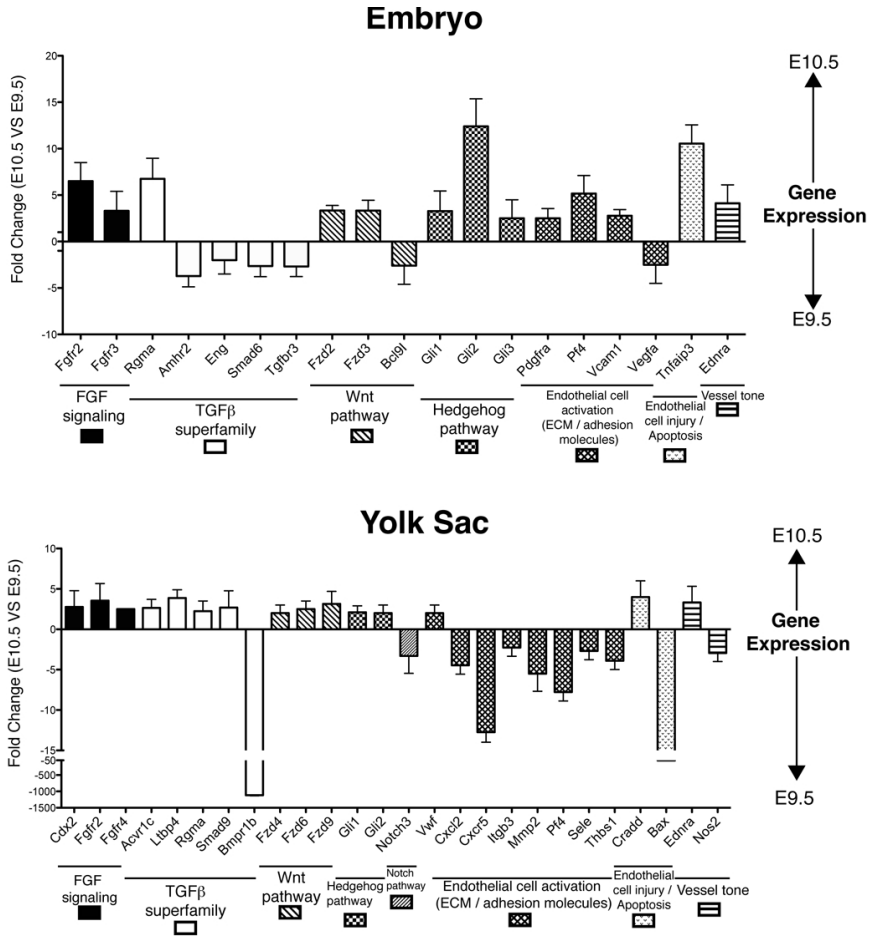

FIGURE S7:
eVE-Cad+ derived contribution to skeletal muscle development does not involve intermediate progenitors in the somites, and can be reproduced in the VE-Cadherin-CREERT2 model.

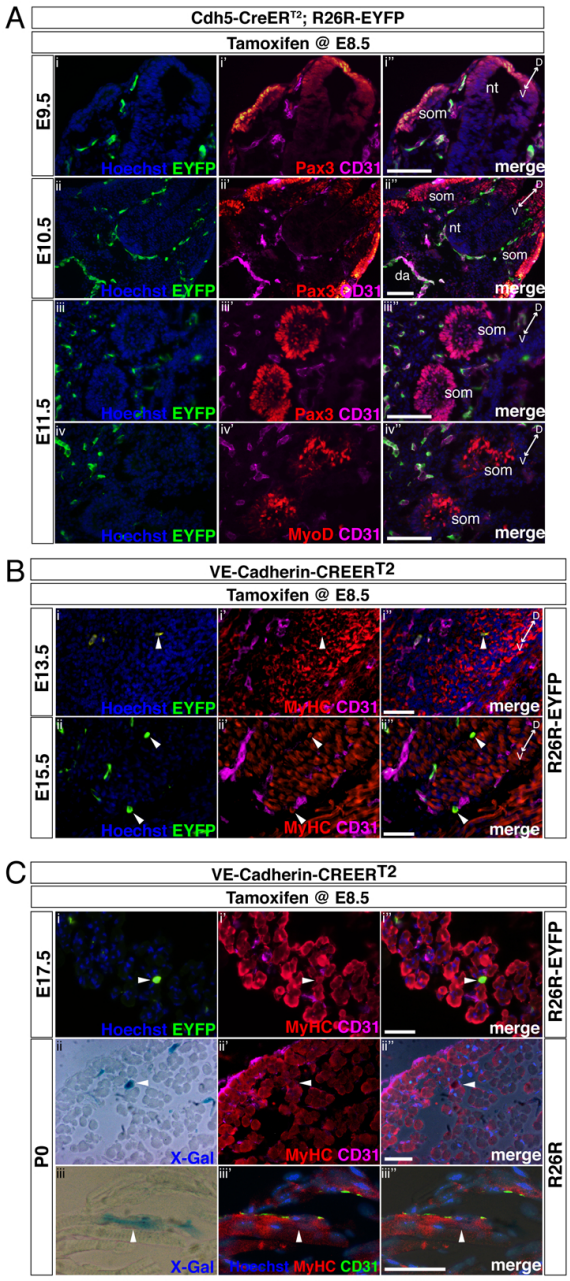

FIGURE S8:
Tracing of eVE-Cad+ derived cells in fetal mesodermal tissues.

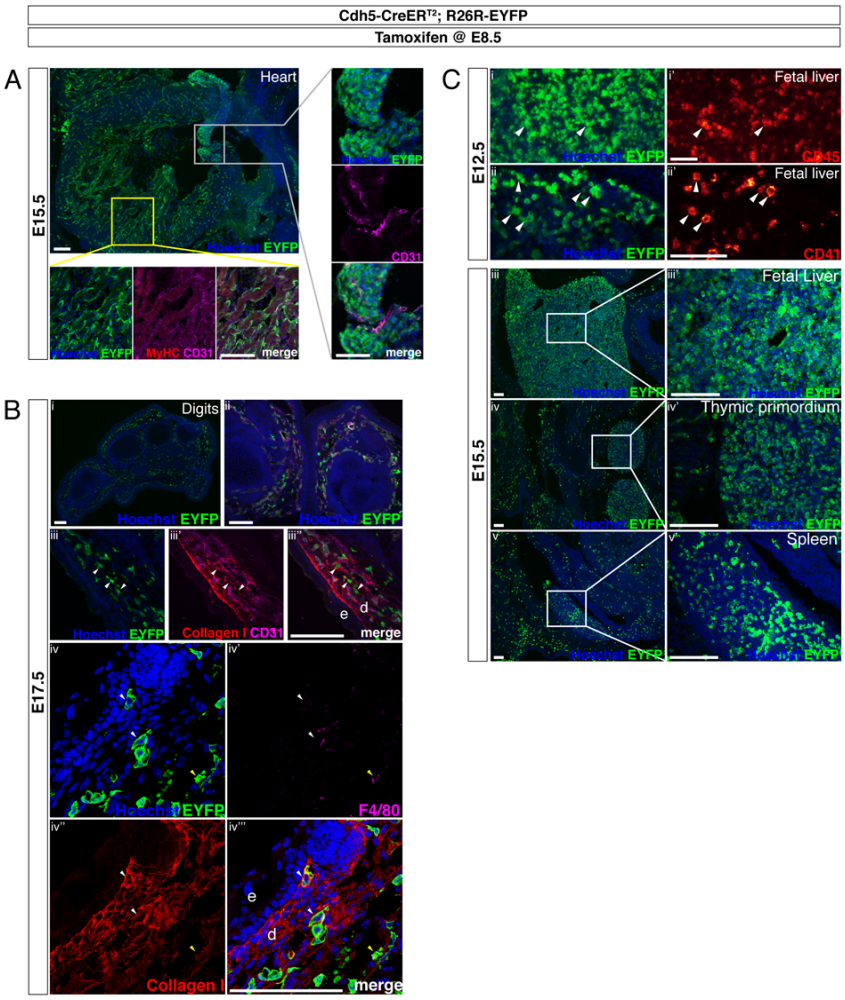

FIGURE S9:
Hemogenic endothelium derived CD31- CD45+ cells form colonies containing CD45- α-SMA+ mesenchymal cells.

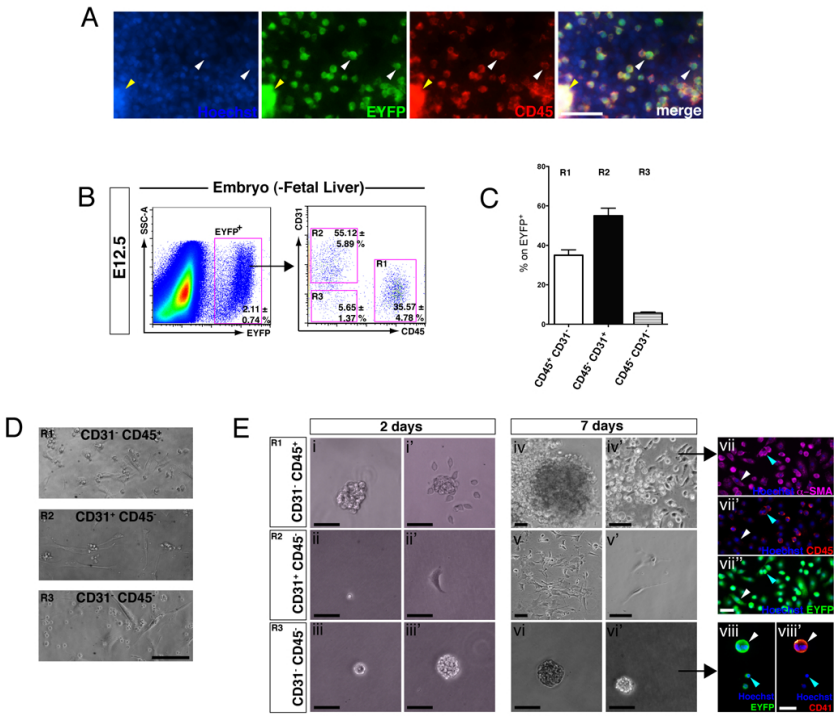

SUPPLEMENTAL INFORMATION

SUPPLEMENTAL EXPERIMENTAL PROCEDURES

Transgenic mice generation and genotyping. To generate VE-Cadherin-CREER^{T2} mice, we have produced a pBlueScript-based construct comprising a 2.5-kbp 5' flanking region of the VE-Cadherin gene (VECDp), directing endothelial specific gene expression (1, 2) of a Tamoxifen-inducible form of Cre recombinase (CREER^{T2}) (3). A 4-kbp fragment, present in the first intron of VECD gene (VECD-IE), which has been demonstrated to carry enhancer activity (4), has been cloned upstream of the CREER^{T2} transgene. A scheme of the 11 kbp fragment used for transgenic mice production is outlined in Supplementary Figure 1A. Transgenic animals were generated by injecting the purified linearized construct into the pronuclei of fertilized oocytes. A total of 7 independent transgenic lines were obtained. Those lines were tested by crossing with R26R (5) and R26R-EYFP (6) reporter mice, containing respectively a cytoplasmic lacZ gene and a cytoplasmic EYFP gene; the expression of both of them is dependent on Cre expression, as reporter genes are cloned downstream of a floxed stop cassette. 5 lines were found to express β-gal or EYFP, and 2 among them were further selected for good expression and therefore were used for subsequent experiments. Mice were kept as heterozygous, and were genotyped by using the following couples of primers: ICre2FW (5'-AGATGCCAGGACATCAGGAACCTG-3') and ICre2REV (5'-ATCAGCCACACCAGACACAGAGATC-3'), both mapping on the CRE-ER^{T2} sequence, generating a 250 bp band; VeCadFW (5'-ACAAAGGAACAATAACAGGAAACC-3'), mapping in the VECDp, and ICre2REV, generating a 1.600 bp band. Other transgenic mice used in this work have been published: Cdh5-CREER^{T2} (7); R26R (5); R26R-EYFP (6). Mice were housed at the San Raffaele Institute SPF animal facility and were kept in pathogen-free conditions. All experiments conformed to Italian law and were performed under internal regulations for animal care and handling (IACUC 355 and 489).

X-Gal staining. Whole mount X-Gal staining of dissected muscles and embryos was performed as in (8)

Antibodies for histology. Immunofluorescence analysis was done using the following antibodies: Laminin rabbit pAb, Desmin rabbit pAb, α-Smooth Muscle Actin mouse mAb (SIGMA), SGCA chicken pAb, Collagen-I mouse mAb (Abcam); NG2 rabbit pAb (Chemicon); Pax3, Pax7, Myogenin (clone IF5D) and MyHC (clone MF20) mouse mAbs (Developmental Studies Hybridoma Bank - DHSB); GFP rabbit pAb (Invitrogen) or mouse mAb (Molecular Probes); MyoD

mouse mAb (DAKO); CD45-PE rat mAb (clone 30-F11, BD), CD41-PE rat mAb (clone MWReg30, BD); CD45.2-PE mouse mAb (clone 104, BioLegend); c-Kit-APC rat mAb (clone 2B8, BD); F4/80-APC rat mAb (clone CI:A3-1, Abd Serotec); CD31/PECAM1 and VE-Cadherin rat mAb (clone MEC13.3 and clone BV13, gift from E.Dejana); Primary antibodies were detected using the appropriate secondary antibodies conjugated with AlexaFluor 488, 546, 594 or 647 (Molecular Probes).

Image acquisition and manipulation. Fluorescent and phase contrast images were taken using the following microscopes: - Nikon Eclipse E600. Image acquisition was done using the Nikon digital camera DXM1200 and the acquisition software Nikon ACT-1. - Leica AF6000. Image acquisition was performed using the DFC350 FX camera and the Leica AF600 acquisition software. - Leica TCS SP2 Laser Scanning Confocal. The imaging medium was PBS buffer; all images were recorded at room temperature. Images were assembled in panels using Adobe Photoshop CS4 or Adobe Illustrator CS4. Images showing double or multiple fluorescence were first acquired separately using appropriate filters, then the different layers were merged using Adobe Photoshop CS4.

Flow cytometry. eVE-Cad$^+$ derived cells were isolated from E9.5-E12.5 embryos. Viscera were removed for E10.5-E12.5 stages, and head and fetal liver for the E12.5 stage. Embryos were processed as described in (9). Cell sorting was performed using the MoFLo system (DAKO). FACS analysis was carried out using the BD FacsCANTO system. For all FACS analyses, single stains and fluorescence minus one (FMO) controls were used to validate the position of the gates. Data were analyzed by FlowJo software (TreeStar). The following antibodies were used for FACS analysis and cell sorting: c-Kit-APC rat mAb (clone clone 2B8, BD); F4/80-APC rat mAb (clone CI:A3-1, Abd Serotec); CD45-PE rat mAb, CD45-APC rat mAb, CD45-V450 rat mAb (clone 30-F11, BD); CD31-APC rat mAb, (clone MEC13.3, BD); CD41-PE rat mAb (clone MWReg30, BD); α-Smooth Muscle Actin mouse mAb (SIGMA); NG2 rabbit pAb (Chemicon); CD11b-APC rat mAb (clone M1/70, BioLegend); PE rat IgG isotype control; APC rat IgG isotype control (BD). When using unconjugated antibodies, the following secondary antibodies were used: Alexa Fluor 647 donkey anti-rabbit or donkey anti-mouse (Molecular Probes); PE goat anti-mouse pAb (BD). 7-Aminoactinomycin D (SIGMA) was used for dead cells detection. Mouse Fc Block (anti-mouse CD16/32-Blocks Fc-Binding; eBioscience) was used to block the Fc-mediated adherence of antibodies to mouse FcR.

Intracellular FACS analysis. To perform intracellular plus membrane FACS analysis, cells were first stained with membrane antibodies. Subsequently cells

were fixed and permeabilized with a solution of 0.1% saponin, 1% BSA in PBS. Intracellular staining (α-SMA) was then carried out.

Quantitative Real-Time PCR. Sorted EYFP$^+$ cells from E9.5-E10.5 Cdh5-CreER^{T2}; R26R-EYFP embryos, or from single colonies, were processed using RNeasy Micro kit (Qiagen). RNA was converted into cDNA using High-Capacity cDNA Reverse Transcription Kit (Applied Biosystems) according to manufacturer's instructions. Quantitative Real-Time PCR analysis was performed on cDNA using Mx3000P (Stratagene, La Jolla, CA, USA) or 7900HT FAST (Applied Biosystems) Real-Time PCR detection systems. Each cDNA sample was amplified in duplicate, using GoTaq qPCR Master Mix and GoTaq Hot Start Polymerase (Promega).

For quantitative Real Time PCR analysis, CT values greater than 37 were considered as a negative signal. Quantification was done using the comparative C_T method. 28S or cyclophilin A mRNA expression levels were used as internal control. The primers used for quantitative Real-Time PCR analysis were the following:

CD105 rev	GCTGGAGTCGTAGGCCAAGT
CD105 fw	CTGCCAATGCTGTGCGTGAA
CD31 FW	AGGGGACCAGCTGCACATTAGG
CD31 RV	AGGCCGCTTCTCTTGACCACTT
CD45 FW	CCTGCTCCTCAAACTTCGAC
CD45 RV	GACACCTCTGTCGCCTTAGC
CD71 rev	GCAAGGAAAGGATATGCAGCA
CD71 fw	GTTTCTGCCAGCCCCTTATTAT
CD73 rev	TGCTCACTTGGTCACAGGAC
CD73 fw	CAAATCCCACACAACCACTG
CD90 FW	GCCTGACAGCCTGCCTGGTG
CD90 RV	TGGAGAGGGTGACGCGGGAG
Ang1 FW	CCATGCTTGAGATAGGAACCAG
Ang1 RV	TTCAAGTCGGGATGTTTGATTT
α-SMA FW	ATTATGTTTGAGACCTTCAAT
α-SMA RV	GATGTCAATATCACACTTCAT
c-Kit FW	GGCTCATAAATGGCATGCTC
c-Kit RV	TATCTCCTCGAGAACCTTCC
NG2 fw	ACAAGCGTGGCAACTTTATC
NG2 rev	ATAGACCTCTTCTTCATATTCAT
Pax3 FW	TGAGTTCTATCAGCCGCATC
Pax3 RV	GCCTTTTTCTCGCTTTCTTC
Paraxis FW	CCCCGATTTGCTCACATACT

Paraxis RV	GTGTAAGGACCGGAGGACAA
PDGFR-β FW	CCGGAACAAACACACCTTCT
PDGFR-β RV	AACATGGGCACGTAATCTATA
Runx1 FW	AGCATGGTGGAGGTACTAGC
Runx1 RV	GGTCGTTGAATCTCGCTACC
Sox7 FW	CAGCAAGATGCTGGGAAAG
Sox7 RV	TGCATCATCCACATAGGGTCT
Tie2 FW	CGGCTTAGTTCTCTGTGGAGTC
Tie2 RV	GGCATCAGACACAAGAGGTAGG
VE-Cadherin FW	GTACAGCATCATGCAGGGCG
VE-Cadherin RV	ATTCGTATCGGATAGTGGGG
28S FW	AAACTCTGGTGGAGGTCCGT
28S RV	CTTACCAAAAGTGGCCCACTA
cyclophillin A FW	CATACGGGTCCTGGCATCTTGTCC
cyclophillin A RV	TGGTGATCTTCTTGCTGGTCTTGC

Gene expression profiling. For gene expression profiling analyses, sorted EYFP$^+$ cells from E9.5-E10.5 Cdh5-CreER^{T2}; R26R-EYFP embryos were processed using RNeasy Micro kit (Qiagen). RNA was converted into cDNA using RT^2 First Strand Kit (Qiagen). Analyses were performed using the Mouse Stem Cell Signaling and Mouse Endothelial Cell Biology RT2 Profiler™ PCR Arrays (Qiagen), according to manufacturer's instructions.

Explants and cell cultures. Dissection and culture of explants of dorsal aorta were performed as described in (10). Sorted EYFP$^+$ cells were resuspended in growth medium (DMEM 20%FBS with addition of bFGF (5 ng/mL) and β-mercaptoethanol (5mg/ml) and spotted onto calf skin collagen (SIGMA)-coated dishes. Cells were kept in 3% oxygen.

Differentiation assays. Differentiation to smooth muscle was obtained by treatment with TGF-β1 (SIGMA) and to bone-like cells by treatment with BMP-2 (Peprotech) as described in (11). Myogenic differentiation was assessed by culturing cells onto matrigel coated dishes in differentiation medium (complete medium supplemented with 2% Horse Serum – Biowhittaker) and also assessed by a co-culture assay. Sorted EYFP$^+$cells were infected with a lentiviral vector directing nLacZ expression (pRRL.sin.PPT.CMV.nLacZ.pre). Infected eVE-Cad$^+$ derived cells were cultured with a fourfold excess of unlabeled C2C12 (ATCC) myoblasts for 3-5 days. Cells were fixed with PFA 4% and stained with X-Gal and/or immunofluorescence using MyHC antibody. For endothelial network formation assay, cells were plated onto matrigel coated wells in differentiation promoting medium, with addition of VEGF 1:1000. For adipogenic differentiation, we used the STEMPRO Adipogenesis Differentiation Kit (Gibco)

according to manufacturer instructions. To confirm adipogenic differentiation, we performed an Oil Red O histochemical staining as in (11).

Colony forming cell (CFC) assay. To perform clonogenic in vitro colony forming cell assays, freshly sorted cells from E12.5 embryos were plated in a methylcellulose-based medium (M3434, StemCell Technologies). Colonies were evaluated at day 2, 4, 7 and 12. In the total CFU-C count, BFU-E (erythroid cells in the presence of megakaryocytes/MΦs), CFU-Mac (monocytes/ MΦs), CFU-GM (granulocytes and monocytes/MΦs), CFU-Mast (mast cells) and CFU-GEMM (granulocytes, monocytes/MΦs, erythroid cells and megakaryocytes) were scored. Mesenchymal-like colonies included adherent, spindle-shaped cells.

In vivo engraftment assay. Sorted eVE-Cad^{+} derived cells from E12.5-E13.5 Cdh5-CREER^{T2}; R26R-EYFP and VE-Cadherin-CREER^{T2}; R26R-EYFP embryos were cultured for 3-4 passages and infected with the pRRL.sin.PPT.CMV. nLacZ.pre lentivirus. 5–10 x 10^{5} cells were intra-muscularly injected into the TA muscle of wild type mice of the same background, which were injured with CTX 2 days before. Injected muscles were harvested 6 days later, stained for X-Gal and subsequently sectioned. eVE-Cad^{+} derived cells (either infected or not infected) were I/M injected also in TA muscles of α-sarcoglycan (α-SG) knockout mice (12). At least 5 x 10^{5} cells were injected. Mice were treated daily with Tacrolimus (subcutaneous injection, 2.5 mg/kg/day, starting 3 days before injection of cells until the end of the experiment) for immunosuppression, and were sacrificed 12 days after injection of cells. Muscles were recovered for histology.

REFERENCES TO SUPPLEMENTAL EXPERIMENTAL PROCEDURES

1. Gory S, *et al.* (1999) The vascular endothelial-cadherin promoter directs endothelial-specific expression in transgenic mice. *Blood* 93(1):184-192.
2. Breier G, *et al.* (1996) Molecular cloning and expression of murine vascular endothelial-cadherin in early stage development of cardiovascular system. *Blood* 87(2):630-641.
3. Feil R, Wagner J, Metzger D, & Chambon P (1997) Regulation of Cre recombinase activity by mutated estrogen receptor ligand-binding domains. *Biochem Biophys Res Commun* 237(3):752-757.
4. Hisatsune H, *et al.* (2005) High level of endothelial cell-specific gene expression by a combination of the 5' flanking region and the 5' half of the first intron of the VE-cadherin gene. *Blood* 105(12):4657-4663.
5. Soriano P (1999) Generalized lacZ expression with the ROSA26 Cre reporter strain. *Nat Genet* 21(1):70-71.
6. Srinivas S, *et al.* (2001) Cre reporter strains produced by targeted insertion of EYFP and ECFP into the ROSA26 locus. *BMC Dev Biol* 1:4.
7. Wang Y, *et al.* (2010) Ephrin-B2 controls VEGF-induced angiogenesis and lymphangiogenesis. *Nature* 465(7297):483-486.

8. Dellavalle A*, et al.* (2011) Pericytes resident in postnatal skeletal muscle differentiate into muscle fibres and generate satellite cells. *Nature Communications* 2:499-411.
9. Biressi S*, et al.* (2007) Intrinsic phenotypic diversity of embryonic and fetal myoblasts is revealed by genome-wide gene expression analysis on purified cells. *Dev Biol* 304(2):633-651.
10. Tonlorenzi R, Dellavalle A, Schnapp E, Cossu G, & Sampaolesi M (2007) Isolation and characterization of mesoangioblasts from mouse, dog, and human tissues. *Curr Protoc Stem Cell Biol* Chapter 2:Unit 2B 1.
11. Tagliafico E*, et al.* (2004) TGFbeta/BMP activate the smooth muscle/bone differentiation programs in mesoangioblasts. *J Cell Sci* 117(Pt 19):4377-4388.
12. Duclos F*, et al.* (1998) Progressive muscular dystrophy in alpha-sarcoglycan-deficient mice. *J Cell Biol* 142(6):1461-1471.

LEGENDS TO SUPPLEMENTAL FIGURES AND MOVIES

FIGURE S1: Generation and recombination specificity of VE-Cadherin-CREERT2 transgenic mice. (**A**) Schematic representation of the 11 kb construct used for VE-Cadherin-CREERT2 transgenic mice generation. (**B**) Whole mount X-Gal staining (dark blue) of E12.5 F1 embryos obtained by crossing VE-Cadherin-CREERT2 founders #9616 and #9621 and Cdh5-CREERT2 mice with R26R reporter line. Cre recombination was induced with 1 Tamoxifen injection at E8.5. Representative images of at least n=3 independent experiments (different litters) are shown. (**C**) Immunofluorescence (IF) using anti-EYFP and anti-CD31 or anti-VE-Cadherin on transversal sections of E9.5 VE-Cadherin-CREERT2; R26R-EYFP embryos. Nuclei were stained with Hoechst. Scale bars, 50 μm.

FIGURE S2: Intra-aortic hematopoietic clusters are labelled in Cdh5-CREERT2 transgenic mice by inducing Cre recombination at E8.5. IF using anti-EYFP, anti-CD45 or anti-CD41, and anti-CD31, anti-c-Kit or anti-α-SMA on sections of E10.5 and E11.5 Cdh5-CREERT2; R26R-EYFP embryos (1 TAM injection at E8.5). Arrows indicate heterogeneous (EYFP+ CD45+ c-Kit-,

EYFP+ CD45- c-Kit+, EYFP+ CD45+ CD31+ or EYFP+ CD41+) intra-aortic hematopoietic clusters. da:dorsal aorta. d<->v: dorso/ventral orientation indicator. Nuclei were stained with Hoechst. Scale bars, 50 μm.

FIGURE S3: Yolk sac eVE-Cad derived c-Kit+ hematopoietic cells are found in the mesenchyme from E10.5. IF using anti-EYFP, anti-c-Kit and anti-CD45 on sections of E9 - E9.5 Cdh5-CREERT2; R26R-EYFP yolk sac (top) and E10.5 – E11.5 embryos (bottom). White arrows highlight labelled EYFP+ c-Kit+ hematopoietic cells emerging from EYFP+ yolk sac vessels (top) and EYFP+ CD45+ c-Kit+ cells in the mesenchyme flanking neural tube in the embryo proper (bottom). Yellow arrow in (iii) indicates a EYFP+ CD45+ c-Kit- cell. Arrows in (v) indicate EYFP+ CD31- c-Kit+ hemopoietic cells, outside CD31+ vessels, in the mesenchyme. In the Far Red channel both CD31 and c-Kit are shown, due to the fact that the same secondary antibody recognized both primary antibodies. The c-Kit signal can be obtained by subtraction.
nt: neural tube. d<->v: dorso/ventral orientation indicator. Nuclei were stained with Hoechst. Scale bars, 50 μm.

FIGURE S4: eVE-Cad derived CD45+ and CD41+ cells are found in several anatomical locations within the mesenchyme in the embryo proper from E10.5. (**A**) IF using anti-EYFP, anti-CD45 and anti-CD31 (i,iii), or anti-CD41 and anti-α-SMA (ii,iv) on transversal sections of E10.5 (i,ii) and E11.5 (iii,iv) Cdh5-CREERT2; R26R-EYFP embryos. Arrows in (i) indicate a EYFP+ CD45+ CD31- cell in the limb bud. Arrows in (iii) indicate abluminal EYFP+ CD45+ CD31- cells close to the aorta. Arrows in (ii) and (iv) highlight EYFP+ CD41+ α-SMA- cells adjacent to the neural tube (i) or in the AGM (iv). (**B**) IF using

anti-EYFP, anti-CD45 and anti-F4/80 on transversal sections of a E12.5 Cdh5-CREERT2; R26R-EYFP embryo. Arrows indicate EYFP+ CD45+ F4/80- cells in the mesenchyme adjacent to the neural tube. (**C**) IF using anti-EYFP, anti-NG2 and anti-CD31 on transversal sections of E10.5 (top) and E11.5 (bottom) Cdh5-CREERT2; R26R-EYFP embryos. Arrows indicate EYFP+ NG2+ CD31+ cells in the mesenchyme adjacent to the neural tube (top) or perivascular EYFP+ NG2+ CD31- cells close to the dorsal aorta. da:dorsal aorta; nt:neural tube. d<->v: dorso/ventral orientation indicator. Nuclei were stained with Hoechst. Scale bars, 100 μm (A,C), 50 μm (B).

FIGURE S5: Generation of hematopoietic cells by eVE-Cad+ progenitors in the placenta. (**A**) IF using anti-EYFP and anti-CD41 or anti-CD45 on sections of E10.5-E11.5-E12.5 Cdh5-CREERT2; R26R-EYFP placentas. Cre recombination was induced with 1 TAM injection at E8.5. White arrows indicate EYFP+ CD41+ or EYFP+ CD45+ cells. Graph on the bottom shows quantification by histology of EYFP+CD45+ and EYFP+CD41+ cells in the placenta of E9.5, E10.5, E11.5, E12.5 embryos. At least 15 fields (40x, 63x) were counted for each stage. (**B**) Representative FACS analysis of E12.5 Cdh5-CREERT2; R26R-EYFP embryo, yolk sac and placenta, showing the percentage of EYFP+ cells within the CD45+ population. Cre recombination was induced with 1 TAM injection at E8.5. Data are representative of at least three independent experiments. A minimum of 8 embryos, yolk sacs or placentas were pooled for each experiment. (**C**) IF using anti-EYFP and anti-CD41 or anti-CD45 on sections of E10.5 and E11.5 Cdh5-CREERT2; R26R-EYFP placentas. Yellow arrows indicate unlabelled EYFP- CD41+ or EYFP- CD45+

cells. White arrow indicates a EYFP+ CD45+ cell. Cre recombination was induced with 1 TAM injection at E9.5 (left panel, E10.5) or E10.5 (right panel, E11.5). A minimum of 8 embryos, yolk sacs or placentas were pooled for each experiment. At least n=3 independent experiments (for each stage) were performed. Scale bars, 50 μm.

FIGURE S6: Differential gene expression of embryo and yolk sac eVE-Cad+ cells between E9.5 and E10.5. EYFP+ cells were separately sorted from E9.5 and E10.5 Cdh5-CREERT2; R26R-EYFP embryos and yolk sac. Cre recombination was induced with a single Tamoxifen injection 24 hours before collection. A Real-Time PCR-based array analysis was performed. Positive fold changes (> 3.5) represent genes more expressed at E10.5 respect to E9.5; negative fold changes (>3.5) represent the opposite. At least 10 embryos or yolk sacs, or placentas were pooled for each experiment. Data representative of n=3 independent experiments. Data are shown as mean ± SEM. For all datasets we have only considered genes with a fold change expression with a $p < 0.05$ (E9.5 vs E10.5).

FIGURE S7: eVE-Cad+ derived contribution to skeletal muscle development does not involve intermediate progenitors in the somites, and can be reproduced in the VE-Cadherin-CREERT2 model. (**A**) IF using anti-EYFP, anti-Pax3 (i-iii) or anti-MyoD (iv) and anti-CD31 on E9.5 (i), E10.5 (ii) and E11.5 (iii, iv) transversal sections of Cdh5-CREERT2; R26R-EYFP embryos. da:dorsal aorta; nt:neural tube; som:somite. (**B**) IF using anti-EYFP, anti-MyHC and anti-CD31 on transversal sections of E13.5 (i) and E15.5 (ii) VE-Cadherin-CREERT2; R26R-EYFP embryos and fetuses. Arrows indicate EYFP+ MyHC+ CD31- myocytes or myofibers. (**C**) i: IF using anti-EYFP, anti-MyHC,

and anti-CD31 on transversal sections of a E17.5 VE-Cadherin-CREERT2; R26R-EYFP hindlimb. Arrow indicates a EYFP+ MyHC+ CD31- myofiber. (ii,iii): X-Gal staining plus IF using anti-MyHC and anti-CD31 on transversal (ii) and longitudinal (iii) sections of P0 VE-Cadherin-CREERT2; R26R hindlimbs. Arrows indicate X-Gal+ MyHC+ CD31- myofibers. d<->v: dorso/ventral orientation indicator. Nuclei were stained with Hoechst. Scale bars, 50 µm.

FIGURE S8: Tracing of eVE-Cad+ derived cells in fetal mesodermal tissues. (**A**) IF using an anti-EYFP antibody on sections of Cdh5-CREERT2; R26R-EYFP fetal heart. Grey inset shows higher magnification of the heart cushions (IF using anti-EYFP and anti-CD31), which are labelled due to endothelial to mesenchymal (EMT) transition events involved in their formation. Yellow inset shows higher magnification of the myocardium (IF using anti-EYFP, anti-MyHC and anti-CD31), which is not labelled. (**B**) IF using anti-EYFP, anti-Collagen I, and anti-CD31 or anti-F4/80 on transversal sections of E17.5 Cdh5-CREERT2; R26R-EYFP forelimbs. White arrows indicate EYFP+ Collagen I+CD31- (panel iii) and EYFP+ Collagen I+ F4/80- cells (panel iv). Yellow arrow in panel iv indicates a EYFP+ F4/80+ macrophage. d: dermal layer; e: epidermis. (**C**) i,ii: IF using anti-EYFP and anti-CD45 or CD41 on transversal sections of Cdh5-CREERT2; R26R-EYFP E12.5 embryos. Fetal liver is shown. Arrows indicate labelled CD45 or CD41 cells. (iii-v): IF using anti-EYFP on transversal sections of Cdh5-CREERT2; R26R-EYFP E15.5 fetuses. Pictures show the fetal liver (iii), thymus (iv) and spleen (v). Boxed areas are shown at a higher magnification in the corresponding images on the right. Nuclei were stained with Hoechst. Scale bars, 100 µm.

FIGURE S9: Hemogenic endothelium derived CD31- CD45+ cells form colonies containing CD45- α-SMA+ mesenchymal cells. (**A**) Dorsal aortas were dissected from Cdh5-CREERT2;R26R-EYFP E11.5 embryos (1 TAM injection at E10.5), plated on collagen-coated dishes and cultured for 5-7 days. IF using anti-EYFP and anti-CD45. White arrows indicate labelled EYFP+CD45+ cells in the outgrowth. Yellow arrow indicates aorta explant. (**B**) Gating strategy for FACS sorting of EYFP+ CD31-CD45+ (R1), EYFP+CD31+ CD45- (R2) and EYFP+CD31-CD45- (R3) populations from E12.5 Cdh5-CREERT2; R26R-EYFP embryos (TAM injection at E8.5), devoid of fetal liver. At least 10 embryos were pooled for each experiment. Representative dot plots of at least n=3 independent experiments are shown. (**C**) Graph showing the percentage of sorted CD45+CD31-, CD45-CD31+ and CD45-CD31- populations on total EYFP+ cells. (**D**): R1, R2 and R3 cell subpopulations were plated on collagen coated dishes in mesoangioblast permissive conditions. Photos taken after 5 days of culture. Only R1 (EYFP+CD45+CD31-) subpopulation generated cells with mesoangioblast morphology. (**E**) Colony forming cell assay on R1, R2 and R3 cell subpopulations. Colonies were scored after 2 or 7 days. R1 (EYFP+CD45+CD31-) generated hematopoietic colonies (including CFU-GEMM -shown in iv-, BFU-E, CFU-GM, CFU-Mac, CFU-Mast) and colonies including adherent cells displaying a mesenchymal phenotype (i', iv'). When picked and cultured in mesoangioblast media, mixed colonies gave rise to EYFP+ CD45- α-SMA+ (white arrows in vii) and EYFP+

CD45+ α-SMA+ cells (cyan arrows in vii). R2 (EYFP+CD45-CD31+) cells generated overall very few colonies with endothelial morphology (v). R3 (EYFP+CD45-CD31-) cells generated few colonies as uniformly shaped aggregates (iii, vi). When picked and cultured in mesoangioblast media, those colonies grew poorly and generated bigger CD41+ (white arrows in viii) and smaller CD41- cells (cyan arrows in viii) of hematopoietic appearance, likely generated by CD41+ cells (Figure S10D,iii, vi). Only in rare cases (not shown) we detected mixed hematopoietic and mesenchymal colonies formed by CD31-CD45- cells, probably derived by EYFP+α-SMA+ expressing cells that lost CD45 expression, a rare cell population also observed in vivo at E12.5 Nuclei were stained with Hoechst. Scale bars, 50 μm (A,D, E, i-vi), 25 μm (E,vii-viii).

MOVIE S1: Reconstruction of a confocal Z-stack acquisition of immunofluorescence-stained transversal sections of E10.5 Cdh5-CREERT2; R26R-EYFP embryos (EYFP:green, CD45:red, CD31:magenta, Hoechst:blue). The central plane is shown in Fig. 3A,i. A EYFP+CD45+CD31- cell can be seen in an abluminal position respect to the dorsal aorta (arrow in Fig. 3A,i). Z-stack movie shows that the whole hematopoietic cell lies outside the blood vessel, and extends cellular processes that are in contact with the mesenchymal (or abluminal, as opposed to luminal) surface of the aorta. The movie is done with 10 sequential images, each one at a distance of 0.4 μm from the following.

MOVIE S2: Reconstruction of a confocal Z-stack acquisition of immunofluorescence-stained transversal sections of E11.5 Cdh5-CREERT2; R26R-EYFP embryos (EYFP:green, CD45:red,

CD31:magenta, Hoechst:blue). The central plane is shown in Fig. 3A,iii. Two EYFP+CD45+CD31- cells (one multi nucleated) can be seen in an abluminal position respect to the dorsal aorta (arrow in Fig. 3A,ii). Z-stack movie shows that the whole hematopoietic cells lie outside the blood vessel. Those HCs extend cellular processes that link the two of them, and the one which is closer to the vessel also displays processes that make it in contact with the mesenchymal (or abluminal, as opposed to luminal) surface of the aorta. The movie is done with 8 sequential images, each one at a distance of 0.4 μm from the following.

MOVIE S3: Reconstruction of a confocal Z-stack acquisition of immunofluorescence-stained transversal sections of E12.5 Cdh5-CREERT2; R26R-EYFP embryos (EYFP:green, Hoechst:blue). The central plane is shown in Fig. S4B,v. Movie shows that the two EYFP+CD45+F4/80- cells (indicated with arrows in Fig. S4B,v) are extra vascular and not juxtaposed to other neighbouring cells that may have interfered with immunofluorescence analysis. The movie is done with 14 sequential images, each one at a distance of 0.3 μm from the following.

MOVIE S4: Reconstruction of a confocal Z-stack acquisition of immunofluorescence-stained transversal sections of E12.5 Cdh5-CREERT2; R26R-EYFP embryos (EYFP:green, Hoechst:blue). The central plane is shown in Fig. 3B,v. Movie shows that the two EYFP+CD45+α-SMA+ cells (indicated with arrows in Fig. 3B,v) are extra vascular and not juxtaposed to other neighbouring cells that may have interfered with immunofluorescence analysis. The movie is done with 30 sequential images, each one at a distance of 0.13 μm from the following.

Chapter III

NO donor modulates embryonic endothelial progenitor fate during skeletal muscle development and regeneration

Valentina Conti[1,2], Emanuele Azzoni[1,2], Lara Campana[2], Thierry Touvier[3], Paola Zordan[2], Mario Tirone[1] and Silvia Brunelli[1,2]

[1]Dept. of Experimental Medicine, University of Milano-Bicocca, 20052 Monza, Italy; [2]Division of Regenerative Medicine, H. San Raffaele Scientific Institute, 20132, Milan, Italy; [3] E. Medea Scientific Institute, 23842 Bosisio Parini, Italy.

Manuscript in preparation

ABSTRACT

Mesoangioblasts (MABs) are multipotent progenitors with myogenic potential and able to cross endothelial barriers. MABs have been isolated from embryonic and adult vessels and, despite their current use in clinical trials, their developmental origin remains unclear. We have recently identified the *in vivo* counterpart of MABs as a subset of embryonic endothelial progenitors. Explaining the fate of these cells in normal adult skeletal muscle homeostasis and regeneration is mandatory to design tools to manipulate them *in vivo*. Nitric oxide (NO) has been shown to affect the behaviour of exogenous MABs and we investigated whether a treatment with a NO donor could influence them also *in vivo*. Here we show that cells derived from embryonic endothelial progenitors are still maintained in the adult muscle and

contribute to vessel endothelium, some interstitial cells and myofibers. These cells also contribute to circulating progenitors that can be reactivated to participate to muscle growth and regeneration after damage. This endothelial contribution to skeletal muscle fibers is increased by treatment with NO donor, both during embryogenesis and in adult mice during the regeneration process. In addition, we provide evidences for an increased vascular network observed after treatment with NO donor. Taken together, these data demonstrate that treatment with NO donors may be effective in modulating endogenous MABs *in vivo*.

INTRODUCTION

Over the last years, the existence of different stem cells with myogenic potential has been widely investigated. Besides the classical skeletal muscle progenitors represented by satellite cells, numerous multipotent and embryologically unrelated progenitors with a potential role in muscle differentiation and repair have been identified.

Mesoangioblasts (MABs) are vessel-associated progenitor cells that have been originally isolated from explants of mouse embryonic dorsal aorta and expanded and characterized *in vitro* [1]. These cells express a number of myogenic and early endothelial markers and are able to differentiate into various mesoderm cell types (such as smooth and striated muscle, bone and endothelium) both in culture or when transplanted into a host chick embryo [2]. MABs are endowed with the ability to cross the vessel wall and, when injected into the blood, they are able to reach the injured and inflamed tissues and they have been shown to significantly contribute to muscle repair when transplanted in dystrophic mice and dogs [3, 4].

These peculiar characteristics with the subsequent identification of pericytes associated with microvascular walls in the adult skeletal muscle as the human equivalent of embryonic MABs [5, 6] permitted to use these cells for cell therapy protocols. Nowadays a clinical trial with MABs for human DMD patients is indeed ongoing but, although promising, this cell therapy is still far from yielding a complete reconstitution of the skeletal muscle structure and function. Thus several research tried to boost the therapeutic efficacy of MABs. It was shown, for example, that exposure to cytokines such as high mobility group box 1 (HMGB1) and stromal cell-derived factor 1 (SDF-1) increases their homing in dystrophic muscle [7, 8]. It has also been demonstrated that a brief *ex-vivo* treatment of MABs with nitric oxide (NO) donors enhances their ability to migrate, resist death-inducing stimuli and fuse with regenerating myofibers [9] and that the treatment of dystrophic mice with a NO-releasing drug, in combination with non steroidal anti-inflammatory activity, besides slowing the progression of the disease by reducing inflammation and preventing muscle wasting, significantly enhanced the activity and proliferation of exogenously administered MABs [10].

Despite the current use of MABs in therapeutic protocols, several questions about the biology of these cells remain unsolved. So far, for example, only theoretical models have been proposed regarding their *in vivo* developmental origin [11] and also their phenotypic heterogeneity as well as their relationship with other mesoderm stem cells are not understood in detail. Unraveling these basic questions is of great importance in order to define how to correctly manipulate the fate of these cells.

Recently, in our lab, a genetic lineage tracing system based on

the cre-loxP recombinase was used to study the cell fate of a subset of endothelial cells (as VE-Cadherin-expressing cells) during normal unperturbed embryonic development (Azzoni et al., submitted – see Chapter II). We have shown that some of the cells labeled at embryonic day E8.5 (namely eVE-Cad+ cells) eventually lose endothelial specific markers and contribute to different mesodermal tissues, including smooth and skeletal muscle. eVE-Cad+ cells, if sorted and cultured *in vitro*, are able to undergo several mesodermal differentiation programs upon specific signals. Separately sorting specific subset of eVE-Cad+ cells we identified that the sub-population of labeled CD45+ cells (distinct from endothelial cells and macrophages) is the one that specifically display MAB features, both *in vitro* and *in vivo* after transplantation. These cells were also detected *in vivo* by immunofluorescence and FACS analysis and in the early embryo were almost always found in the proximity of vessels. Thus, we identified a subset of embryonic endothelial progenitors as the *in vivo* counterpart of MABs. For those reasons, our mouse model allows to investigate if a pharmacological treatment with NO donors can modulate the fate of endogenous MABs during muscle development and regeneration and, in case, which are the molecular mediators involved. Moreover our tool will allow us to assess whether NO donors modulate the fate of MABs also in adult homeostasis as well as during the process of skeletal muscle regeneration after an acute damage.

As nitric oxide donor we used molsidomine(N-ethoxycarbonyl-3-morpholino-sydnonimine), a prodrug that is enzymatically converted into its active metabolite linsidomine (3-morpholino-sydnonimine, SIN-1). Conversion of molsidomine to SIN-1 occurs primarily in the liver and release of NO from SIN-1

involves a 2-step process that occurs spontaneously and non enzymatically in the blood. Molsidomine is administered daily in the diet and its pharmacokinetics are characterized by rapid absorption and hydrolysis, requiring a short time to achieve maximal systemic concentrations of both the parent compound and SIN-1 [12]. In addition it has been demonstrated that it is possible to treat embryos through pregnant mothers.
The translation of obtained results into clinical practice could be relatively easy, considering that molsidomine has been clinically used as a vasodilatatory drug for more than 30 years, being the drug of choice for coronary heart disease [13-16].

RESULTS

Molsidomine treatment during embryonic development increases eVE-Cad+ derived contribution to myogenesis

For analysis during embryonic development, we labeled the same subset of cells (embryonic endothelial progenitors, namely eVE-Cad+) as those of the embryonic-fetal analysis described in Azzoni et al. (submitted – see Chapter II). We crossed Cdh5-CreER^{T2} mice (expressing a tamoxifen inducible Cre recombinase under the transcriptional control of the VE-Cadherin promoter) with R26R-EYFP Cre reporter mice in order to have double transgenic embryos. We induced Cre recombination in pregnant mothers with 1 single I/P injection of TAM at embryonic day E8.5, in order to avoid labeling the YS mesoderm, which transiently expresses VE-Cad at E7.5 (Fig. 1A). In case of NO donor treatment we started treating the pregnant mothers with molsidomine (at a concentration of 30mg/kg of body weight) at the beginning of the pregnancy, that is from the day when a vaginal plug was observed. The treatment continued until the recovery of the embryos/fetuses

at different developmental stages: E12.5 and the day of birth. We compared this treated embryos (MOLS) with control embryos (CTRL) collected from mice that were fed with a standard diet (Fig. 1B).

First of all we evaluated by FACS analysis the effect of molsidomine treatment on the total number of embryonic endothelial progenitors (eVE-Cad+). We prepared single cell suspension from embryos collected at E12.5, a time when we previously shown that EYFP+ labeled cells start to become a more heterogeneous population and when MABs-like cells can be found abundantly in the mesenchyme.
Embryos were deprived of the head and fetal liver, in order to enrich the mesenchymal fraction of EYFP+ cells, indeed hematopoietic cells (abundant in the fetal liver) are also labeled in our embryos.
We observed that the percentage of EYFP+ cells on the total cell population was not significantly changed by molsidomine treatment: 1.34±0.17% in CTRL embryos vs. 1.55±0.33% in MOLS embryos (Fig. 1C). This result indicates that the treatment with NO doesn't induce an increase in the proliferation of embryonic endothelial progenitors.

Concomitantly with this analysis we evaluated the effect of molsidomine on the distribution of EYFP+ cells in the two main subpopulations at this developmental stage: the endothelial (CD31+) and the leukocytic one (CD45+). Within the leukocyte population, we also determined the ratio between the macrophage (F4/80+) and non-macrophage (F4/80-) subsets. Indeed in our previous work we showed that, amongst the EYFP+ population, mesoangioblast-like cells belonged to the CD31- CD45+ F4/80- subpopulation.

First of all we observed that our treatment doesn't change the total percentage of CD31+ cells (0,80%) and CD45+ cells (1,50%) (data not shown). Analyzing the expression of these markers within the EYFP+ population, we observed no significant differences in the percentage of CD31+ cells within the EYFP+ population (18.87±2.6% vs. 18.00±0.91% in CTRL and MOLS embryos, respectively). In molsidomine treated embryos we detected a significant decrease in the percentage of EYFP+CD45+ cells (35.53±2.21% vs. 28.64±2.17%) and, consequently, a significant (p-value<0,05) increase in the number of EYFP+ cells that were negative for CD31- and CD45- (37.96±4.97% vs. 54.87±2.77%) (Fig.1D).
Regarding the leukocyte subpopulations, we observed an increase in the total number of CD45+F4/80- cells within the EYFP+ population (4.83±0.18% vs. 6.07±0.44%) in molsidomine treated embryos (Fig. 1E). This increase is also more evident by analyzing the percentage of the non-macrophage cells inside the CD45+ population, higher in molsidomine treated embryos (Fig. 1F).

Since we were mainly interested in skeletal muscle development, we decided to verify if our treatment with molsidomine during embryonic development induced at the end (i.e. in newborn mice) an increased level of myogenesis. To this end we collected total protein extract from skeletal muscle tissues of newborn mice (hind-limb and fore-limb) and we performed western blot analysis using an antibody that reacts with all anti-sarcomeric myosin antibody (MyHC). In muscles of newborn mice treated with molsidomine we detected an higher expression of sarcomeric myosin, indicating that this treatment leads to an increased level of myogenesis that results in a sort of muscle hypertrophy (Fig.

2A). From skeletal muscle tissues of the same mice we collected also RNA and we performed qPCR analysis in order to evaluate the expression of genes involved in muscle hypertrophy. In molsidomine-treated muscles we observed a clear decrease of the mRNA expression of myostatin, a negative regulator of muscle size (Fig. 2A). Nevertheless, these conditions does not result in evident differences in muscle weight between control and molsidomine-treated animals, both at early post-natal stages as well as in adult life.

Considering that sorted EYFP+ cells are rare, we decided to focus the analysis in this specific population only at the transcriptional level, evaluating if the treatment with molsidomine alters gene expression in eVE-Cad+ cells. We collected RNA of EYFP+ cells sorted from E12.5 embryos (using the same gate strategy depicted in Fig.1B) and then we performed qPCR analysis comparing gene expression panel of our treated embryos vs. control ones (Fig. 2B).
Focusing on genes involved in skeletal muscle development, we observed a general up regulation in molsidomine treated embryos. Indeed desmin, embryonic myosin heavy chain, MyoD and Myf6 mRNAs were up-regulated in EYFP+ cells obtained from molsidomine-treated embryos if compared to EYFP+ cells from control embryos.
By immunofluorescence (IF) analysis on cryosections of control and molsidomine treated embryos we evaluated the distribution of eVE-Cad+ cells and their co-localizations with skeletal muscle markers. Data obtained indicate that molsidomine treatment increases eVE-Cad+ derived contribution to skeletal muscle development. Indeed an increased number of EYFP+ myoblasts (CD31- MyHC+ cells) can be detected in sections of molsidomine treated embryos

compared to control ones (Fig. 2C and D).

By FACS analysis on E12.5 embryos we didn't detect changes in the total number of CD31+ cells and of CD31+ cells within the EYFP+ population. Also by IF analysis on embryos at the same stage we observed no impressive changes in the CD31 signal, but it was clear the presence in molsidomine-treated embryos of a more developed network of vessels. Moreover it appeared evident that in treated embryos there was an higher overlapping between the CD31 and the EYFP signals (Fig. 2E). We performed an alternate analysis of the FACS considering the percentage of EYFP+ cells within the CD31+ population and we observed that in molsidomine treated embryos there is a remarkable increase in the EYFP+ cells within the gate of the CD31+ cells: 19.05±0.9% in control embryos versus 32.34±2.8% in treated ones (Fig. 2F and G).
Interestingly, we observed by qPCR analysis (see Fig. 2B) that VEGFR-1 (Flt-1) gene expression was up-regulated in molsidomine treated embryos. The function of this receptor (expressed on endothelial cells) is particularly important during embryonic vasculogenesis. Angiopoietin-1 (Ang1) is as well an essential gene for vasculature development, is produced by non-endothelial mural cells (pericytes and vascular smooth muscle cells) and is important, in particular, for vessel maturation and stabilization. We observed that within EYFP+ cells from molsidomine treated mice this gene resulted down-regulated, as other mural cells markers, such as NG2 and PDGFRβ. Moreover, the up-regulation of α-SMA and CD90, together with the decreased expression of HSC markers such as CD45, c-Kit and Sca-1, indicates an increased fraction of myofibroblats/fibroblasts within the EYFP+ cells in embryos treated with molsidomine compared to control embryos.

In adult skeletal muscle eVE-Cad+ cells normally contribute to vessels, myofibers and interstitial cells, but not to satellite cells.

Considering our interest in the physiological contribution of embryonic mesoangioblasts in unperturbed muscle development, we investigated the fate of eVE-Cad+ derived cells that reside in skeletal muscle tissue at different post-natal and adult stages.

As a general rule, for analysis at post-natal stages we used double transgenic Cdh5-CreER^{T2}; R26R-EYFP mice when we want to perform FACS and FACS sorting analysis, while for immuno-histological analysis we crossed Cdh5-CreER^{T2} with R26R-GNZ mice, that express nuclear beta galactosidase in cells where CRE is present and active.

Regarding the pharmacological treatment, while it is demonstrated that embryos can be treated with molsidomine through the pregnant mother, it is unknown whether pups can receive the drug through their orally treated mothers during lactation. For this reason we decided to stop our analysis of the effects of a molsidomine-treatment during development of newborn mice.

FACS analysis performed on skeletal muscle tissue (anterior and posterior limb) of newborn mice revealed that molsidomine treatment doesn't significantly alter the percentage of EYFP+ cells on the total cell populations (around 1-2% both in control than treated animals). Within the EYFP+ populations we didn't detect significant differences in the endothelial subpopulation, that accounted for around the 20% of total single cells analyzed. Leukocytes accounted for the 5-8% of the total population. Within the EYFP+ cells there were no significant differences in the percentage of CD45+ cells (around 60% in

both conditions). The ratio of macrophages vs. non-macrophages leukocytes was not changed by molsidomine treatment, but with a switch compared to the situation at E12.5. Here, in newborn mice, non-macrophage leukocytes are more abundant (65%) than macrophages (35%) (Fig. 3A).

By IF analysis on sections of newborn mice we confirmed that the majority of EYFP+ cells are still endothelial cells and that, on the other side, the majority of vessels are labeled and the same was true both for control and molsidomine treated newborn mice (data not shown). Some labeled myofibers were detected in control mice and in molsidomine treated mice the endothelial contribution to myofibers was higher (Fig. 3B).
Histological examination of muscle sections by immunostaining with CD31 showed a trend for an increased vascular network in molsidomine treated mice (data not shown).

Since different cell types were generated during embryogenesis from the original eVE-Cad+ progenitors, we expected heterogeneity also in the adult progeny. Hence, we better characterized the non-endothelial cell populations, derived by embryonic eVE-Cad+ progenitors, in adult muscles at different stages by FACS and by histological analysis.
We could not find any Pax7+EYFP+ satellite cell in perinatal, juvenile or adult mice neither in control nor in molsidomine-treated mice (data not shown). A rare number of labeled myonuclei was found also in skeletal muscle of undamaged adult mice.
In addition to vessels and myofibers, skeletal muscle tissue contains different type of interstitial cells. IF and FACS analysis revealed that the undamaged post-natal muscle of our mice, labeled during embryogenesis, contained a considerable

number of EYFP+ cells which were indeed CD31- and CD45-. We tested whether these cells include subsets of NG2+ pericytes and of PW1+ interstitial cells (PICS). Surprisingly, by IF analysis, neither PW1+EYFP+ nor NG2+EYFP+ interstitial cells were found on muscle sections of juvenile mice (data not shown), even if PICS and muscle pericytes are known to be abundant in early post-natal stages where they contribute to muscle growth [5, 6, 17]. We could detect labeled NG2+ and PW1+ interstitial cells only in adult muscles. These results indicated that embryonic eVE-Cad+ precursors contribute, during unperturbed development in healthy mice, to subsets of interstitial cells only in the adult life (Fig. 3C).

By FACS analysis we determined in the adult undamaged skeletal muscle the percentage of pericytes, analyzing the expression of NG2 within the EYFP+ cells, that were negative for CD31 and CD45 markers. In control mice we detected 30% of NG2-expressing cells within the EYFP+ CD31- CD45+ cells. In undamaged muscles from mice treated with molsidomine for 20 days, this population accounted only for the 13% (Fig. 3D) and by IF analysis it was even more difficult to find colocalization of labeled cells with markers of interstitial cells (data not shown). This reduction of endothelial contribution to interstitial cells in molsidomine-treated mice maybe the outcome of the decrease already observed at embryonic stages in the mRNA expression of NG2, PDGFRβ and PW1 markers.

eVE-Cad+ derived progenitors normally participate in muscle regeneration *in vivo*.

To analyze the fate of eVE-Cad+ derived cells during the regenerative process, acute injury was induced in muscles

(TA, gastrocnemius, quadriceps and triceps brachialis) of adult mice by intra-muscular injection of cardiotoxin (CTX). Muscles were collected at different days after the induction of the damage. To evaluate the effects of treatment with molsidomine in adult mice that were injected with tamoxifen at E8.5, mice of two months of age were divided into two groups. Mice of one group were given molsidomine starting from 1 week before the damage and until the day of sacrifice. The other group served as control (Fig. 4A).

By FACS analysis on single cells suspension obtained from damaged muscles (10 days after ctx injection) we determined that EYFP+ cells account for the 10-15% of the total population both in control and in molsidomine-treated animals (Fig. 4B).
By histological analysis, we detected rare regenerating, centrally nucleated β-Gal+ myofibers at all time points analyzed, that are 7-14-21 days after one single injury. In order to evaluate whether a more severe muscle injury increases eVE-Cad+ contribution to myofiber regeneration, we performed multiple rounds of CTX injections in the same muscles with 1-week interval and we recovered muscles 1 week after the last CTX injection. In these conditions eVE-Cad+ cells contribution to muscle regeneration was slightly increased.
In mice treated with molsidomine the contribution of eVE-Cad+ cells to the regeneration process was increased compared to control mice (Fig. 4C). A precise quantification is difficult to obtain because the total contribution of eVE-Cad+ derived cells to regenerating myofiber is relatively low, with a maximum of 2-5% of all regenerating myofibers.
As in unperturbed condition, no Pax7+ cells of eVE-Cad+ origin were detected in regenerating muscle, both in control and in molsidomine-treated mice (data not shown).

Differently from healthy adult skeletal muscle, in which resident leukocytes are really rare (0.5% of the total population), in acutely damaged muscle there is an inflammation process that is characterized by a rapid and sequential invasion of leukocyte populations that persist while muscle repair occur. By FACS analysis performed 10 days after ctx injection we evaluated that the percentage of macrophages infiltrating the muscle increases, but without differences between control and molsidomine-treated mice (around 18% of the total population) (data not shown).
By histological analysis on muscles collected 7 days after injury we detect β-Gal+ macrophages, both in control mice and in molsidomine-treated mice, and this is in agreement with the extensive contribution of eVE-Cad+ derived cells to the hematopoietic system (Fig.4 D).

Together with the production of new myofibers, the regeneration of vessels is a crucial step for the restoration of a functional skeletal muscle tissue. Thus, we analyzed sections of damaged muscles from control mice and from mice treated with molsidomine during the whole period of regeneration. In addition to the more pronounced neovascularization in molsidomine-treated animals, we observed that most of eVE-Cad+ derived cells were closely associated to vessels. The majority of labeled cells were indeed CD31+ (Fig. 4E). Histological analysis of muscles collected 7 days after injury, showed that the capillary/myofibers ratio was significantly higher in molsidomine treated mice if compared with control mice. Also the capillary density (evaluated as the number of CD31+ cells/mm^2) resulted increased in molsidomine-treated mice (Fig. 4F).

eVE-Cad+ derived cells isolated from adult skeletal muscle tissue display multipotentiality *in vitro*.

To verify the multipotentiality of eVE-Cad+ derived cells resident in the skeletal muscle tissue, we isolated EYFP+ cells by fluorescence activated cell sorting from VE-Cadherin-CreER^{T2}; R26R-EYFP mice both from undamaged and damaged muscles, 7 days after ctx injection. After isolation, cells were grown in culture in conditions suited for mesoangioblasts (Fig. 5A). By IF we confirmed that isolated cells, also after some passages in culture, were indeed EYFP+ (Fig. 5B).

After infection with a lentivirus directing expression of nuclear LacZ, eVE-Cad+ derived cells were co-cultured with C2C12 murine myoblasts and some of them fused with C2C12 into multi-nucleated, MyHC+ myotubes (Fig. 5C).

Since EYFP+ cells sorted from damaged muscles were more actively proliferating, we were able to maintain them in culture for more passages and we exposed them to several differentiating stimuli, to which they responded correctly. When treated with TGFβ there was an increase in the number of αSMA+ smooth muscle cells (Fig. 5D). They formed vascular-like network when treated with VEGF (Fig. 5E) and, if cultured in adipogenic medium, some cells started accumulating lipid droplets typical of adipocytes (Fig. 5F).

Muscle resident eVE-Cad+ derived cells participate in neovessel formation, while the circulating ones contribute to muscle regeneration *in vivo*.

Since we are interested in unraveling the behavior of eVE-Cad+ derived progenitors in *in vivo* context, we decided to

investigate whether the contribution of eVE-Cad+ derived cells to regenerating myofibers observed after damage was dependent on progenitors resident in skeletal muscle, like pericytes or PW1+ cells, or on circulating progenitors. To address this issue, we performed two parallel bone marrow transplant experiments, in which we grafted bone marrow from Vecadherin-CreER^{T2}; R26R-GNZ mice (which received a TAM injection at E8.5) into C57BL/6 mice, and vice versa. After evaluating successful donor bone marrow engraftment by X-Gal staining on peripheral blood (data not shown), we performed 2 rounds of CTX damage in the same muscles, with 1-week interval, and recovered muscles 7 days after the last CTX injection. We detected donor-derived X-Gal+ nuclei inside regenerating myofibers only in C57BL/6 muscles of mice transplanted with transgenic bone marrow (Fig. 6A). X-Gal staining in the skeletal muscle of transgenic animals transplanted with C57BL/6 bone marrow was detected mostly in vessels and capillaries (Fig. 6B). We could conclude that eVE-Cad+ derived circulating progenitors, and not eVE-Cad+ derived cells resident in skeletal muscle, were able to contribute to adult muscle regeneration.

DISCUSSION

Amongst the numerous cell populations that have been recently identified as capable of participate in the regeneration process of skeletal muscle there are mesoangioblasts (MABs). These cells are associated with the microvasculature network and can be isolated both from embryonic and adult vessels. As these cells are able to cross the vessel wall, they have been used in preclinical models of systemic cell therapy for muscular dystrophies, with a significant structural and

functional recovery of skeletal muscle tissue. Thus, these cells have entered clinical experimentation for human DMD patients. Despite their use in clinical trials, in-depth studies on their developmental origin and their biological characteristics are still missing.

In our lab we set up a genetic lineage tracing murine model to label a subsets of embryonic endothelial progenitor cells, namely eVE-Cad+ cells. With an injection of tamoxifen performed at embryonic day E8.5 (temporal control) we activate the production of the CRE recombinase only in cells that are expressing the endothelium-specific gene VE-Cadherin (spatial control). The labeling is permanent so it is possible to analyze the fate of this embryonic endothelial population during development, until adulthood.

Using this lineage tracing system, combined with marker analysis in the embryo, in dorsal aorta explants and in selected sorted populations, we have recently shown (Azzoni et al., submitted – see Chapter II) that eVE-Cad+ cells contribute, in normal unperturbed development, to different mesodermal tissues, including skeletal muscle and smooth muscle. We have also demonstrated that MABs derive from embryonic endothelial progenitor cells and, more precisely, from the specialized subpopulation of differentiated endothelial cells that have hematopoietic potential, that is the hemogenic endothelium. These data revealed for the first time that the *in vitro* and *in vivo* myogenic and multi-lineage differentiation capability of vessel-associated stem cells (such as MABs) are not a cell culture or transplantation artefact, but rather an expression of a differentiation potential that takes part also during normal development.

Our genetic model allowed us to study here the responsiveness of endothelial progenitor cells to specific molecules and signalling pathways. The fine understanding of mechanisms that guide the fate choice of these endogenous progenitors could indeed open the way to design tools for *in vivo* manipulation of endogenous MABs fate in the embryo and, more interesting, clinically, also in adult life. In order to determine whether a pharmacological treatment with nitric oxide could activate endogenous progenitors and, possibly, push them to undergo specifically the myogenic program, we analyzed the effects of a treatment with molsidomine, a well known nitric oxide donor drug.
The role of NO in early myogenesis has been poorly investigated to date. A recent paper showed that treatment with molsidomine of a-SG null pregnant mice has beneficial effects during embryonic myogenesis, resulting in a recovery of Pax7+ cells loss in treated embryos compared to untreated dystrophic ones. The authors also showed that nitric oxide stimulated satellite cells proliferation via signaling pathways requiring Vangl2 and cGMP and that this delays the reduction of the satellite cells pool observed during repetitive-acute and chronic damages, favoring muscle regeneration [18].

In our work, we analyzed the effects of molsidomine treatment during embryogenesis on wt embryos and newborn mice, in which a subset of endothelial progenitor cells (eVE-Cad+) were permanently labeled during embryonic day E8.5. We didn't detect an increase in the total number of eVE-Cad+ cells, at both stages analyzed and we thus concluded that NO doesn't affect the proliferation rate of these endothelial cells, as it did with satellite cells.

Molsidomine-treatment during embryogenesis led in newborn mice to a moderate skeletal muscle hypertrophy, with increased expression of myosin heavy chain (at the protein level) and decreased transcription of myostatin, a member of the transforming growth factor-β superfamily and a negative regulator of muscle growth and regeneration.
Within eVE-Cad+ derived cells we observed a greater contribution to myoblasts in molsidomine-treated embryos as early as E12.5. By mRNA expression analysis we demonstrated that also mRNA expression level of myogenic genes was higher in eVE-Cad+ derived cells from treated embryos and by IF we detected more EYFP labeled myoblasts. This higher contribution of endothelial cells to myogenesis during embryonic development resulted in a slightly increased number of eVE-Cad+ derived myofibers of newborn mice.

This treatment also resulted in a remarkable effect on the vascular network organization. Endothelial progenitor cells are indeed responsible for the angiogenetic process as well as for vessel remodeling occurring during perinatal growth. Angiogenesis include vessel sprouting, endothelial cell bridging and/or intussusception, while post-natal vessel remodeling involves changes in endothelial cell phenotype and structural alterations, without the formation of new blood vessels. In both cases, endothelial cells secrete growth factors that attract pericytes that, surrounding the vessel wall, promote vessel maturation and stabilization. When vessels lose pericytes, they become hemorrhagic and hyperdilated, which leads to pathological conditions, such as edema.
We observed that molsidomine treated embryos vessels have a more developed structure. eVE-Cad+ derived cells seems to participate directly to vessel production, rather than to vessel

stabilization. Indeed, we observed a reduction of expression of pericyte/mural marker within eVE-Cad+ cells. It should be of interest to further study the effect of molsidomine treatment during embryogenesis and the outcome observed in newborn mice. In particular it is important to study effects on the behavior of pericytes. The analysis of some histological features, such as the pericyte coverage of vessel, is absolutely necessary to verify if the better vessel network observed in molsidomine treated animals is also normally functional. Indeed, it should be noticed that, amongst the animals treated with molsidomine during embryogenesis and collected as newborn, we obtained some mice suffering of edema.

In our mice, we never detected labeled satellite cells. Moreover, despite we confirmed that molsidomine treatment increased the total number of Pax7+ cells [18], we didn't detect labeled Pax7+ cells, both for treatment during embryogenesis and during adult skeletal muscle regeneration. This means that the effect of molsidomine is confined to an increased proliferation of satellite cells and do not involve recruitment of eVE-Cad+ derived cells to this subset of cells.

Isolation of other types of vessel-associated stem cells from the adult muscle, with multilineage mesodermal or myogenic differentiation potential, has been reported in the last few years [19]. These include pericyte-derived cells [5], PICS [17] and perivascular cells [20]. In particular, postnatal muscle pericytes differentiate into muscle fibres and generate satellite cells [6]. In adult animals, other than a small number of eVE-Cad+ derived muscle fibers, we detected labeling also in subsets of pericytes and PICs. These results imply that the subsets of eVE-Cad+ derived pericytes and PW1+ interstitial cells in the

adult are not myogenic as the AP+ pericytes [6]. In animals treated with molsidomine there was a significant decrease in eVE-Cad+ cells contribution to interstitial cells (pericytes/mural cells) and this was evident also during early embryogenesis.

Regarding the endothelial contribution to myofiber during the regeneration process we analyzed adult skeletal muscle after acute muscle injury induced by intra-muscular injection of cardiotoxin. We have shown that eVE-cad+ derived cells are able to contribute to the regeneration process and that treatment with molsidomine during the whole period of regeneration increased their contribution to new myofibers as well as to the neoangiogenetic process, a crucial step for the complete recovery of a functional tissue.

From adult injured muscles, we were able to sort eVE-Cad+ derived cells and we demonstrated their *in vitro* mesodermal multipotentiality. These cells were indeed responsive to TGFβ and VEGF signals and when co-cultured with myoblasts they fuse to form multinucleated myotubes. This capacity reflects that of eVE-Cad+ derived cells sorted from embryos (Azzoni et al., submitted - see Chapter II) and resembles the classical behavior of mesoangioblasts isolated from embryonic dorsal aortas or from post-natal/adult vessels.

Besides postnatal pericytes and PICs, cells from adult bone marrow participate in the regeneration of damaged skeletal myofibers at low frequency [21] that increases with muscle damage [22]. Using a bone marrow transplantation (BMT) approach, we have demonstrated that the main players in eVE-Cad+ derived contribution to adult skeletal muscle regeneration are indeed circulating progenitors and not

resident cells, thus confirming that, in the adult, satellite cells are the main source of resident stem cells necessary for acute injury-induced muscle regeneration [23, 24]. This does not exclude the possibility that other types of myogenic cells that do not express Pax7 during muscle homeostasis can participate in muscle regeneration in the presence of a favourable niche, of which satellite cells appear to be the most critical component. These data fit our results, if we hypothesize that eVE-Cad+ derived circulating myogenic progenitors contribute to muscle regeneration by fusing to regenerating myofibers, rather than transiting through a Pax7+ intermediate, which is fully consistent with what we observe *in vivo*. eVE-Cad+ derived cells could possibly function as “alternative” progenitors, to be recruited to the skeletal muscle lineage in case of emergency, when muscle damage is too severe to be repaired only with canonical muscle progenitors.

In conclusion, we have demonstrated that cells derived from embryonic endothelium (eVE-Cad+ cells) are still maintained in the adult muscle and contribute to vessel endothelium and to interstitial cells that are developmentally unrelated to the myogenic PICs and muscle pericytes.
Most importantly, we found that eVE-Cad+ cells also contribute to circulating progenitors that are able to be reactivated to participate to muscle growth and regeneration after damage, as part of their normal fate.
Moreover, we showed that treatment with molsidomine during embryonic development effectively increased the contribution of eVE-Cad+ cells to skeletal muscle fibers and that treatment during the regeneration process in adult mice was also effective in increasing their contribution to newly formed skeletal muscle fibers. Furthermore, we demonstrated that

molsidomine administration leads to an increased vascular network, both in case of embryonic treatment as well as in adult life during tissue regeneration.

Taken together, these data could represent the starting point for analysis of endothelial progenitor cells contribution to skeletal muscle fibers and vessels in mice with a dystrophic phenotype. The combination of these studies with pharmacological treatment with molsidomine could shed light on the behaviour of endogenous endothelial progenitors and how to modulate their fate according to different needs. In parallel, it remains decisive the analysis of putative environmental cues acting in the pathological muscle milieu in order to minimize the detrimental effects on the effectiveness of the transplanted stem cells as well as on the survival and proliferation/differentiation efficacy of endogenous stem cells, such as satellite cells or endogenous MABs.
Recently, satellite cells were established as being responsible and absolutely required for muscle regeneration. The possibility that unorthodox myogenic progenitors could be useful for cell therapy-based strategies remains. Results obtained with additional analysis in this direction, indeed, should be used to understand how to stimulate endogenous multipotent endothelial progenitors to undergo specific fate choice. This should be of importance in perspectives of combining cell therapy with exogenous transplanted cells and pharmacological approaches to yield synergic therapeutic effects.

MATERIALS AND METHODS

Animals and Treatment Mice were housed in the pathogen-free facility at our Institution and treated in accordance with the European Community guidelines and with the approval of the Institutional Ethical Committee. Transgenic mice used in this work have been published: Cdh5-CREER^{T2} (Benedito et al, 2009); R26R-EYFP (Srinivas et al, 2001); R26R-GNZ (Stoller et al, 2008). Cre activity was induced in the embryo at E8.5 by one single intra-peritoneal injection in pregnant females with 2 mg/25 gr of body weight of Tamoxifen (TAM) (SIGMA; 10 mg/mL in corn oil). Since tamoxifen administered during early gestation (i.e. E8.5) results in the inability of pregnant mother to deliver pups, a cesarean section was always required for delivery and newborn mice were cross-foster to lactating dams. Standard diet (STD) or a diet containing 3 mg/kg of (1-ethoxy-N-(3-morpholino-5-oxadiazol-3-iumyl)-methanimidate (molsidomine) was prepared based on the daily food intake measured for these animals (Brunelli et al. 2007). No significant differences in food intake and weight gain were observed among the experimental groups.

Embryos and foetuses Mouse embryos were collected after natural overnight matings. Fertilization was considered to take place at 6 a.m. For histological analysis, dissected E12.5 embryos were fixed for 2 hours with a 4% solution of paraformaldehyde (PFA) in PBS at 4°C. Embryos were washed in PBS and dehydrated/cryoprotected with passages in PBS solutions with increasing sucrose concentration (10% for 1 hour, 20% for 1 hour, 30% overnight). Embryos were finally embedded in OCT and sectioned using a Leica 1850UV cryostat (8µM sections were made). P0 newborns were dissected and skin was removed. Anterior and posterior limbs were further dissected, fixed, dehydrated and embedded similarly to E12.5 embryos.

X-Gal staining To perform X-Gal staining, muscle sections were fixed with a 4% solution of paraformaldehyde (PFA) in PBS at 4°C for 5'. After that, samples were washed in PBS and incubated in X-Gal staining solution (1 mg/ml 5-bromo-4-chloro-3-indolyl-β-D- galactosidase, 5 mM K4Fe(CN)6, 5 mM K3Fe(CN)6, 2 mM MgCl2 in PBS) for 2-3 hours at 37°C or O/N at RT.

Immunofluorescence and antibodies. Muscles were frozen in isopentane cooled by liquid nitrogen or embedded in OCT and 8um thick slices were obtained by cryostat sectioning. Frozen sections of muscles were fixed with 4% PFA at 4°C. Immunofluorescence was carried out as in [10]. Immunofluorescence analysis was done using the following antibodies: Laminin chicken anti-mouse (Abcam), α-Smooth Muscle Actin mouse mAb (SIGMA), NG2 rabbit pAb (Chemicon); Pax7 and MyHC (clone MF20) mouse mAbs (Developmental Studies Hybridoma Bank - DHSB); GFP rabbit pAb (Invitrogen) or mouse mAb (Molecular Probes);

PW1 rabbit anti-mouse (1:3000, gift from D. Sassoon); CD68 monoclonal mouse anti-mouse (1:100, Abd Serotec); CD31/PECAM1 and VE-Cadherin rat mAb (clone MEC13.3 and clone BV13, gift from E.Dejana); Primary antibodies were detected using the appropriate secondary antibodies conjugated with AlexaFluor 488, 546, 594 or 647 (Molecular Probes).

Immunohistochemistry Endogenous peroxidases were blocked by treating the sections with a solution of H2O2 30% in methanol for 30'. Sections were then permeabilized by incubation in a solution of 0.2% Triton, 1% BSA in PBS for 30' at room temperature, and subsequently blocking was done by incubation in donkey serum 10% in PBS for 30' at RT. Sections were incubated overnight with primary antibody at 4°C and washed in PBS. Treatment with a biotinylated secondary antibody (DAKO) for 1 hour at RT was followed by ABC Elite Kit (Vectastain). Enzymatic reaction with SIGMAFAST DAB (3,3′-Diaminobenzidine tetrahydrochloride) (SIGMA) to reveal the signal was followed under observation at the microscope and stopped when signal reached the desired intensity.

Flow cytometry Single cell suspension were prepared from E12.5 embryos deprived of viscera and head and fetal liver and processed as described in [25]. Muscles from adult mice were processed as described (Pessina et al., 2012). Cell sorting was performed using the MoFLo system (DAKO). FACS analysis was performed using the BD FacsCANTO system (data were analyzed using the FCS software). A primary gate based on the physical parameters (forward and side light scatter, FSC and SSC, respectively) was always set to exclude dead cells or small debris. The following antibodies were used for FACS analysis and cell sorting: F4/80-APC rat mAb (clone CI:A3-1, Abd Serotec); CD45-Pecy7 rat mAb; CD31-APC rat mAb, (clone MEC13.3, BD) or CD31-PE; NG2 rabbit pAb (Chemicon); CD11b-APC rat mAb (clone M1/70, BioLegend); PE rat IgG isotype control; APC rat IgG isotype control (BD). When using unconjugated antibodies, the following secondary antibody was used: Alexa Fluor 647 donkey anti-rabbit (Molecular Probes). 7-Aminoactinomycin D (SIGMA) was used for dead cells detection. Mouse Fc Block (anti-mouse CD16/32-Blocks Fc-Binding; eBioscience) was used to block the Fc-mediated adherence of antibodies to mouse FcR.

Differentiation assays Differentiation to smooth muscle was obtained by treatment with TGF-β1 (SIGMA) as described in [26]. For endothelial network formation assay, cells were plated onto matrigel coated wells in differentiation promoting medium, with addition of VEGF 1:1000. For adipogenic differentiation, we used the STEMPRO Adipogenesis Differentiation Kit (Gibco) according to manufacturer instructions. Myogenic differentiation was assessed by co-culture with C2C12 myoblasts. Sorted EYFP+ cells were infected with a

lentiviral vector directing nLacZ expression (pRRL.sin.PPT.CMV. nLacZ.pre). Infected eVE-Cad+ derived cells were cultured with a fourfold excess of unlabeled C2C12 (ATCC) myoblasts for 3-5 days on matrigel coated dishes in differentiation medium (complete medium supplemented with 2% Horse Serum, Biowhittaker). Cells were fixed with PFA 4% and stained with X-Gal and/or immunofluorescence using MyHC antibody.

Muscle regeneration assays For *in vivo* regeneration process an acute injury was performed on adult mice (age 6-8 weeks) by intra-muscularly injecting 50μl of 15μM cardiotoxin (CTX, SIGMA) in TA and triceps brachialis or 50μl of 50μM CTX in gastrocnemius and quadriceps. For the multiple damage experiments, CTX was injected on the same muscles two or three times with a temporal interval of 7 days. Mice were sacrificed 5, 7, 10 or 15 days after the CTX injection. Muscles were collected and processed for different analysis. In case of drug treatment on adult mice, it was started 1 week before CTX injection and continued until sacrifice.

Bone marrow transplantation (BMT) Bone marrow from femurs and tibia of Vecadherin-CreER^{T2}; R26R-GNZ mice (TAM injected at E8.5) was harvested and cell suspensions were produced. Approximately 10^7 cells were transplanted by tail vein injection into lethally irradiated C57BL/6 8-wk old mice, which were purchased from Charles River Laboratories. The opposite experiment was also performed, in which the donors were C57BL/6 mice and the recipients were lethally irradiated Vecadherin-CreER^{T2}; R26R-GNZ mice TAM injected at E8.5. Efficiency of the transplantation procedure was assessed 5 weeks later by X-Gal staining on cytospin preparations of peripheral blood.

Quantitative Real-Time PCR RNA collected from muscle tissues using RNeasy Mini (or Micro) kit (Quiagen) or the TRIzol protocol (Invitrogen) was converted into double-stranded cDNA using the High-Capacity cDNA Reverse Transcription Kit (Applied Biosystems) according to manufacturer's instructions. Quantitative Real-Time PCR analysis was performed on cDNA using 7900HT FAST (Applied Biosystems) Real-Time PCR detection systems. Each cDNA sample was amplified in duplicate, using GoTaq qPCR Master Mix and GoTaq Hot Start Polymerase (Promega). Quantification was done using the comparative C_T method and cyclophilin A mRNA expression levels were used as internal control. The primers used for quantitative Real-Time PCR analysis were the following:

DESMIN	fw: AATAAGAACAACGATGCGCTG
DESMIN	rev: CTGGCTTACAGCACTTCATGT
eMHC	fw: TGAAGAAGGAGCAGGACACCAG
eMHC	rev: CACTTGGAGTTTATCCACCAGATCC

MYOD	fw: ACGGCTCTCTCTGCTCCTTT
MYOD	rev: GTAGGGAAGTGTGCGTGCT
MYF6	fw: ATTCTTGAGGGTGCGGATTT
MYF6	rev: CTGGGGAGTTTGCGTTCCT
PAX7	fw: GACTCGGCTTCCTCCATCTC
PAX7	rev: AGTAGGCTTGTCCCGTTTCC
VEGFR1	fw: ACCTGTCCAACTACCTCAAGAGC
VEGFR1	rev: CCTGGTTCCAGGCTCTCTTTCTT
DRP1	fw: CGACTTTGCTGATGCCTGT
DRP1	rev: GTTGCCTGTTGTTGGTTCCT
IGF-1	fw: CTCTGCTTGCTCACCTTCAC
IGF-1	rev: CTCATCCACAATGCCTGTCT
PW1	fw: CCAAAAAGCCATCCCACA
PW1	rev: TCCCTTCATAACCCCTCTCC
SCA-1	fw: TTACCCATCTGCCCTCCTAA
SCA-1	rev: GGTCTGCAGGAGGACTGAGC
MST	fw: GGTGCACAAGATGAGTATGC
MST	rev: AGCCTGAATCCAACTTAGGC
CD45	fw: CCTGCTCCTCAAACTTCGAC
CD45	rev: GACACCTCTGTCGCCTTAGC
CD90	fw: GCCTGACAGCCTGCCTGGTG
CD90	rev: TGGAGAGGGTGACGCGGGAG
Ang1	fw: CCATGCTTGAGATAGGAACCAG
Ang1	rev: TTCAAGTCGGGATGTTTGATTT
α-SMA	fw: ATTATGTTTGAGACCTTCAAT
α-SMA	rev: GATGTCAATATCACACTTCAT
c-Kit	fw: GGCTCATAAATGGCATGCTC
c-Kit	rev: TATCTCCTCGAGAACCTTCC
NG2	fw: ACAAGCGTGGCAACTTTATC
NG2	rev: ATAGACCTCTTCTTCATATTCAT
Pax3	fw: TGAGTTCTATCAGCCGCATC
Pax3	rev: GCCTTTTTCTCGCTTTCTTC
PDGFR-β	fw: CCGGAACAAACACACCTTCT
PDGFR-β	rev: AACATGGGCACGTAATCTATA
Sox7	fw: CAGCAAGATGCTGGGAAAG
Sox7	rev: TGCATCATCCACATAGGGTCT
cyclophillin A	fw: CATACGGGTCCTGGCATCTTGTCC
cyclophillin A	rev: TGGTGATCTTCTTG CTGGTCTTGC

Protein extracts and immunoblot analysis Muscles tissue from adult mice were homogenized as described in (Pessina et al., 2012). The membranes were probed using the following antibodies (Abs): anti-sarcomeric myosin MyHC (Developmental Studies Hybridoma Bank) and anti-calnexin (Genetex Inc, San Antonio, TX, USA), used as an internal control.

Image acquisition and manipulation Fluorescent and phase contrast images were taken using the following microscopes: - Nikon Eclipse E600. Image acquisition was done using the Nikon digital camera DXM1200 and the acquisition software Nikon ACT-1. - Leica AF6000. Image acquisition was performed using the DFC350 FX camera and the Leica AF600 acquisition software. - Leica TCS SP2 Laser Scanning Confocal. The imaging medium was PBS buffer; all images were recorded at room temperature. Images were assembled in panels using Adobe Photoshop CS4 or Adobe Illustrator CS4. Images showing double or multiple fluorescence were first acquired separately using appropriate filters, then the different layers were merged using Adobe Photoshop CS4.

Statistical analysis Data were analyzed with Microsoft Excel 12.2.3 and GraphPad Prism 5. Values are expressed as means ± SEM. To assess statistical significance, two-tailed Student's t-tests were used. Statistical probability values of <0.05 were considered significant.

REFERENCES

1. De Angelis, L., et al., Skeletal myogenic progenitors originating from embryonic dorsal aorta coexpress endothelial and myogenic markers and contribute to postnatal muscle growth and regeneration. J Cell Biol, 1999. 147(4): p. 869-78.
2. Minasi, M.G., et al., The meso-angioblast: a multipotent, self-renewing cell that originates from the dorsal aorta and differentiates into most mesodermal tissues. Development, 2002. 129(11): p. 2773-83.
3. Sampaolesi, M., et al., Cell therapy of alpha-sarcoglycan null dystrophic mice through intra-arterial delivery of mesoangioblasts. Science, 2003. 301(5632): p. 487-92.
4. Sampaolesi, M., et al., Mesoangioblast stem cells ameliorate muscle function in dystrophic dogs. Nature, 2006. 444(7119): p. 574-9.
5. Dellavalle, A., et al., Pericytes of human skeletal muscle are myogenic precursors distinct from satellite cells. Nat Cell Biol, 2007. 9(3): p. 255-67.
6. Dellavalle, A., et al., Pericytes resident in postnatal skeletal muscle differentiate into muscle fibres and generate satellite cells. Nat Commun, 2011. 2: p. 499.
7. Palumbo, R., et al., Extracellular HMGB1, a signal of tissue damage, induces mesoangioblast migration and proliferation. J Cell Biol, 2004. 164(3): p. 441-9.
8. Galvez, B.G., et al., Complete repair of dystrophic skeletal muscle by mesoangioblasts with enhanced migration ability. J Cell Biol, 2006. 174(2): p. 231-43.

9. Sciorati, C., et al., Ex vivo treatment with nitric oxide increases mesoangioblast therapeutic efficacy in muscular dystrophy. J Cell Sci, 2006. 119(Pt 24): p. 5114-23.
10. Brunelli, S., et al., Nitric oxide release combined with nonsteroidal antiinflammatory activity prevents muscular dystrophy pathology and enhances stem cell therapy. Proc Natl Acad Sci U S A, 2007. 104(1): p. 264-9.
11. Cossu, G. and P. Bianco, Mesoangioblasts-vascular progenitors for extravascular mesodermal tissues. Curr Opin Genet Dev, 2003. 13(5): p. 537-42.
12. Rosenkranz, B., B.R. Winkelmann, and M.J. Parnham, Clinical pharmacokinetics of molsidomine. Clin Pharmacokinet, 1996. 30(5): p. 372-84.
13. Majid, P.A., et al., Molsidomine in the treatment of patients with angina pectoris. N Engl J Med, 1980. 302(1): p. 1-6.
14. Detry, J.M., et al., Hemodynamic effects of molsidomine at rest and during submaximal and maximal exercise in patients with coronary artery disease limited by exertional angina pectoris. Am J Cardiol, 1981. 47(1): p. 109-15.
15. Karsch, K.R., et al., Haemodynamic effects of molsidomin. Eur J Clin Pharmacol, 1978. 13(4): p. 241-5.
16. Guerchicoff, S., et al., Acute double blind trial of a new anti-anginal drug: molsidomine. Eur J Clin Pharmacol, 1978. 13(4): p. 247-50.
17. Mitchell, K.J., et al., Identification and characterization of a non-satellite cell muscle resident progenitor during postnatal development. Nat Cell Biol, 2010. 12(3): p. 257-66.
18. Buono, R., et al., Nitric oxide sustains long-term skeletal muscle regeneration by regulating fate of satellite cells via signaling pathways requiring Vangl2 and cyclic GMP. Stem Cells, 2012. 30(2): p. 197-209.
19. Peault, B., et al., Stem and progenitor cells in skeletal muscle development, maintenance, and therapy. Mol Ther, 2007. 15(5): p. 867-77.
20. Crisan, M., et al., A perivascular origin for mesenchymal stem cells in multiple human organs. Cell Stem Cell, 2008. 3(3): p. 301-13.
21. Ferrari, G., Muscle Regeneration by Bone Marrow-Derived Myogenic Progenitors. Science, 1998. 279(5356): p. 1528-1530.
22. Palermo, A.T., et al., Bone marrow contribution to skeletal muscle: a physiological response to stress. Dev Biol, 2005. 279(2): p. 336-44.
23. Lepper, C., T.A. Partridge, and C.M. Fan, An absolute requirement for Pax7-positive satellite cells in acute injury-induced skeletal muscle regeneration. Development, 2011. 138(17): p. 3639-46.
24. Sambasivan, R., et al., Pax7-expressing satellite cells are indispensable for adult skeletal muscle regeneration. Development, 2011. 138(17): p. 3647-56.
25. Biressi, S., et al., Intrinsic phenotypic diversity of embryonic and fetal myoblasts is revealed by genome-wide gene expression analysis on purified cells. Developmental Biology, 2007. 304(2): p. 633-651.
26. Tagliafico, E., et al., TGFbeta/BMP activate the smooth muscle/bone differentiation programs in mesoangioblasts. J Cell Sci, 2004. 117(Pt 19): p. 4377-88.

Figure 1: Effect of molsidomine treatment during embryogenesis on eVE-Cad+ derived cells

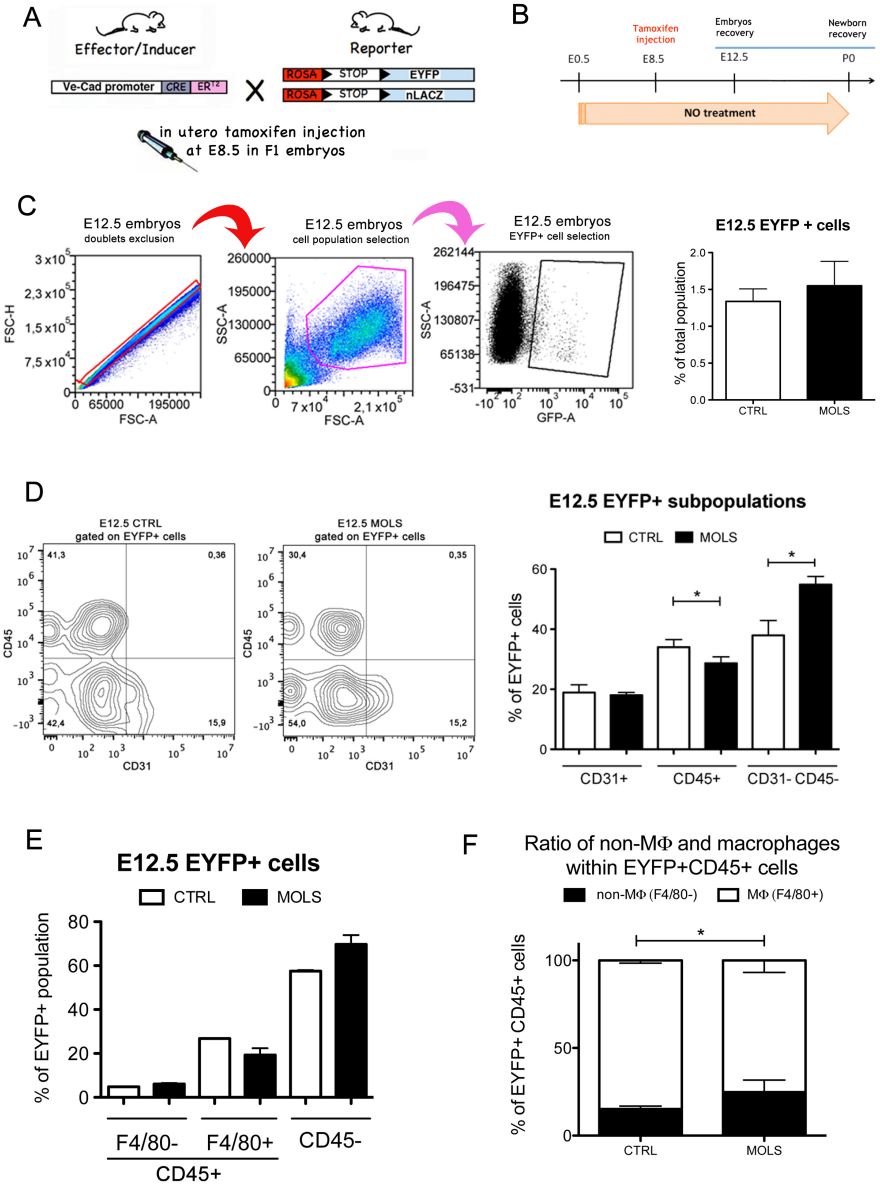

Figure 2: Molsidomine treatment during embryonic development increases eVE-Cad+ derived cells contribution to myogenesis

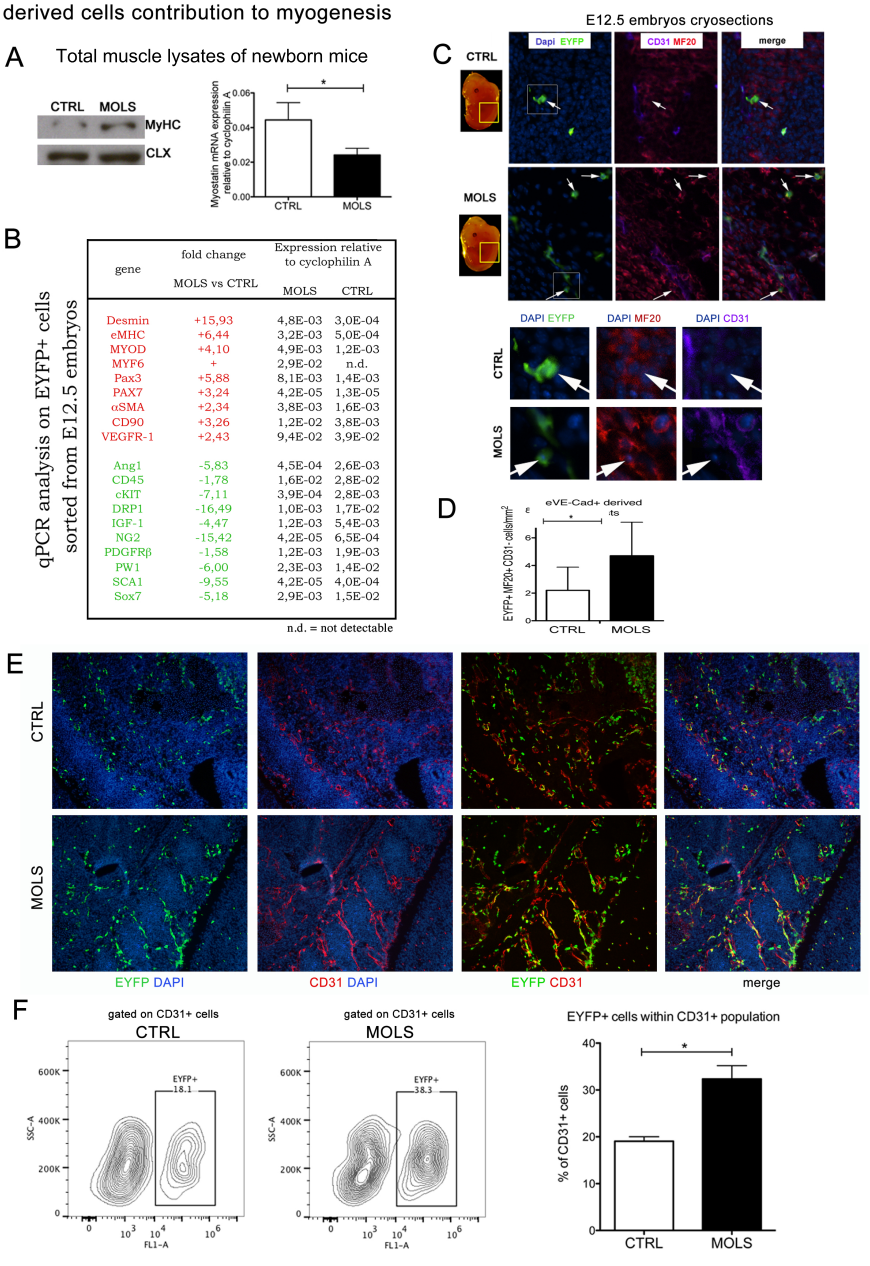

gene	fold change MOLS vs CTRL	Expression relative to cyclophilin A MOLS	CTRL
Desmin	+15,93	4,8E-03	3,0E-04
eMHC	+6,44	3,2E-03	5,0E-04
MYOD	+4,10	4,9E-03	1,2E-03
MYF6	+	2,9E-02	n.d.
Pax3	+5,88	8,1E-03	1,4E-03
PAX7	+3,24	4,2E-05	1,3E-05
αSMA	+2,34	3,8E-03	1,6E-03
CD90	+3,26	1,2E-02	3,8E-03
VEGFR-1	+2,43	9,4E-02	3,9E-02
Ang1	-5,83	4,5E-04	2,6E-03
CD45	-1,78	1,6E-02	2,8E-02
cKIT	-7,11	3,9E-04	2,8E-03
DRP1	-16,49	1,0E-03	1,7E-02
IGF-1	-4,47	1,2E-03	5,4E-03
NG2	-15,42	4,2E-05	6,5E-04
PDGFRβ	-1,58	1,2E-03	1,9E-03
PW1	-6,00	2,3E-03	1,4E-02
SCA1	-9,55	4,2E-05	4,0E-04
Sox7	-5,18	2,9E-03	1,5E-02

Figure 3: eVE-Cad+ derived cells contributes to myonuclei and interstitial cells in post-natal undamaged skeletal muscle

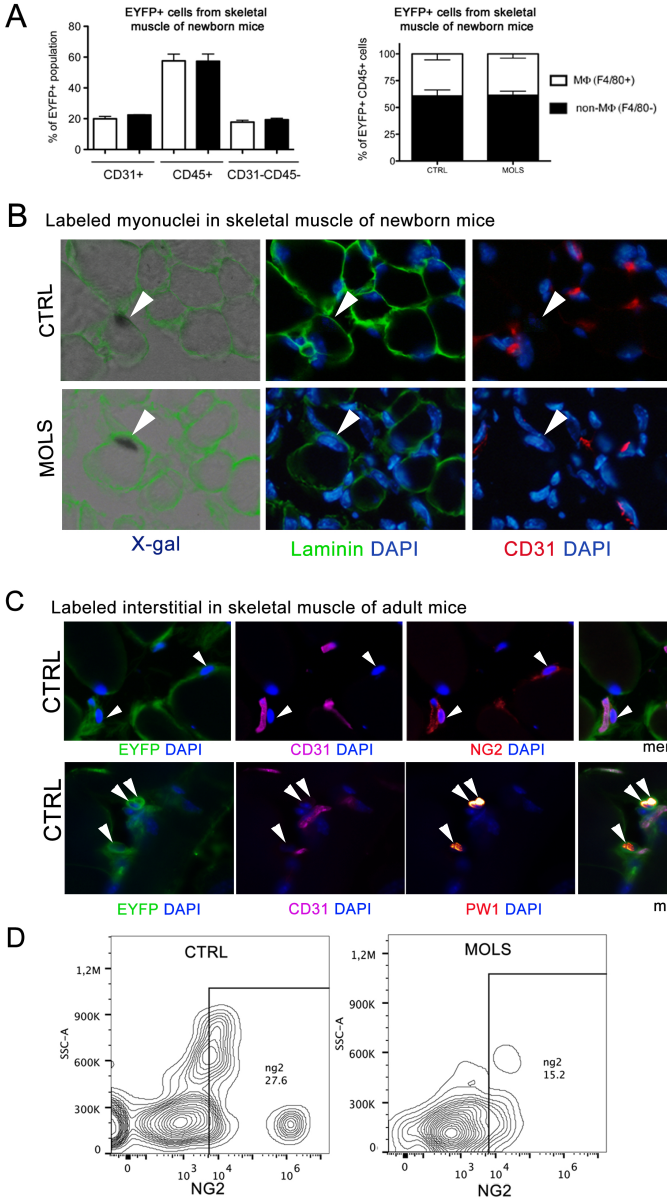

Figure 4: Molsidomine treatment increases eVE-Cad+ derived cells contribution to skeletal muscle regeneration

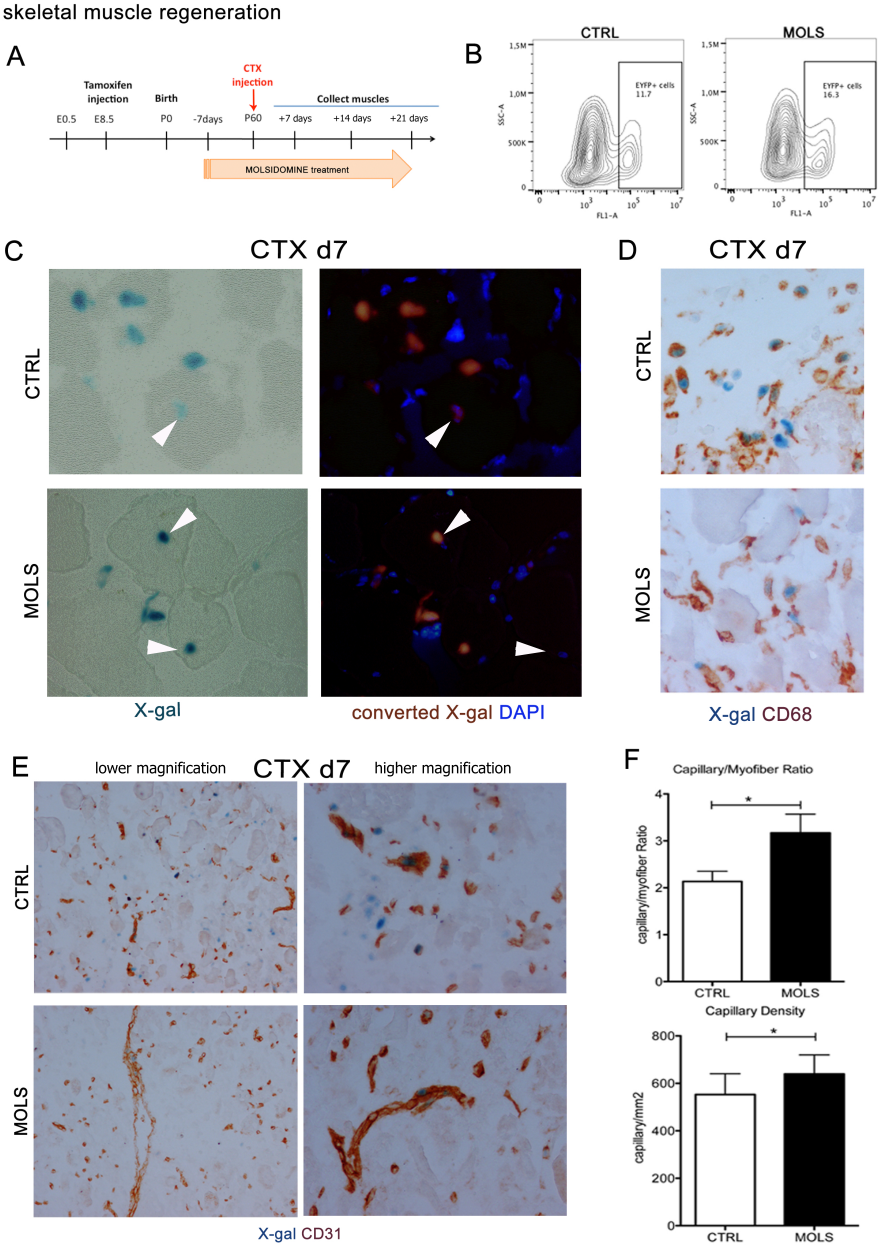

Figure 5: eVE-Cad+ derived cells from adult muscles are multipotent in vitro

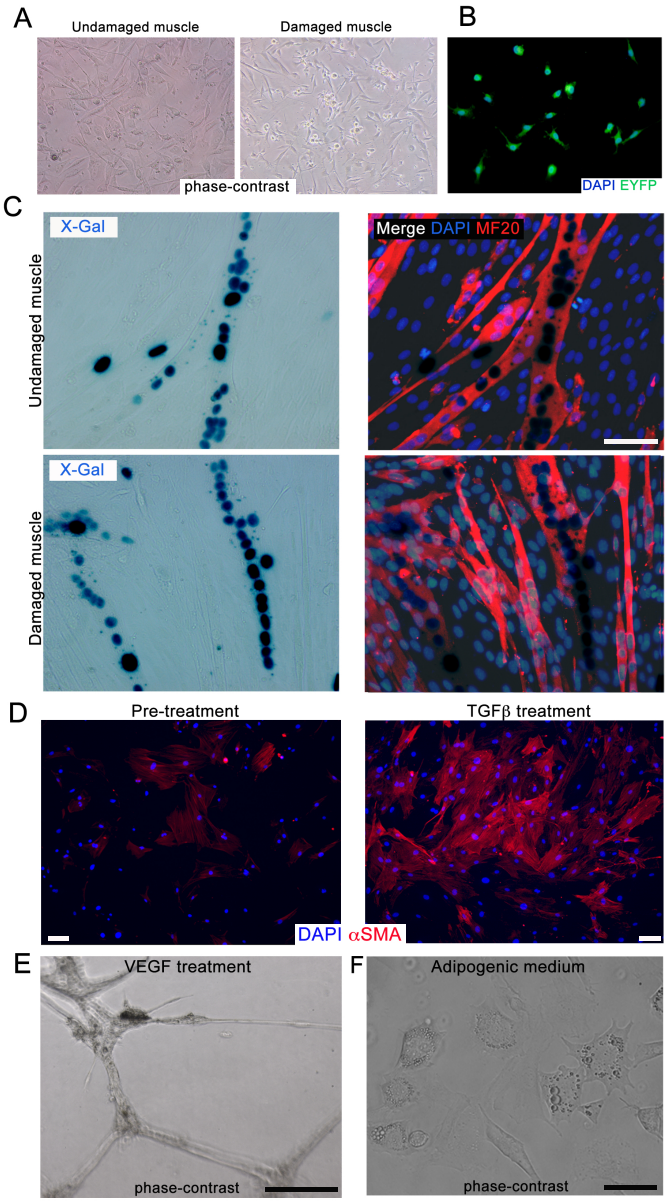

Figure 6: Circulating eVE-Cad+ derived cells contribute to skeletal muscle regeneration, while the resident ones contributes to vessel and capillaries.

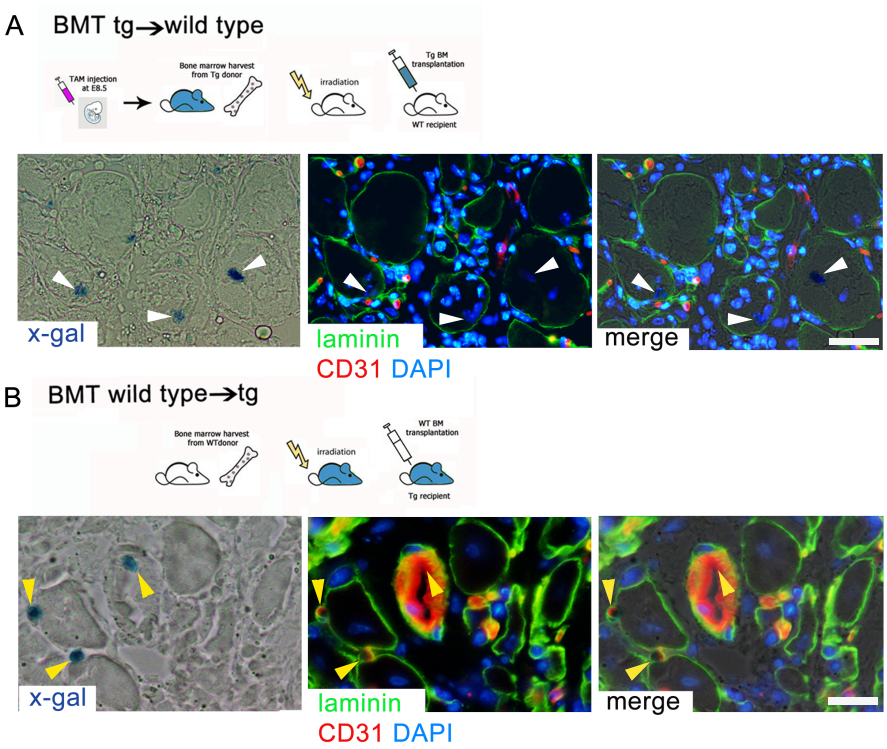

LEGENDS TO FIGURES

Figure 1. Effect of molsidomine treatment during embryogenesis on eVE-Cad+ derived cells. (**A**)Scheme of the general approach used to obtain double transgenic mice Cdh5-CreER^{T2};R26R-EYFP or Cdh5-CreER^{T2};R26R-GNZ and the time of tamoxifen induction. (**B**)Scheme of the protocol for pharmacological treatment with molsidomine during embryogenesis. (**C**)**Left**: General gating strategy used for FACS analysis on single cells suspension from E12.5 Cdh5-CREER^{T2}; R26R-EYFP embryos, devoided of the head and fetal liver. **Right**: Graph representing the percentage of EYFP+ cells obtained by FACS analysis on single cells suspension from E12.5 embryos. (**D**)**Left**: FACS analysis on single cells suspension from E12.5 embryos showing the percentage of CD45+ and CD31+ cells within the EYFP+ subset. **Right**: Graph representing results obtained with at least 8 control and 8 molsidomine-treated embryos. *p-value<0,05. (**E**)Graph representing results obtained by FACS analysis on single cells suspension from E12.5 embryos showing the percentage of CD45+ and F4/80+ or F4/80-cells within the EYFP+ subset. (**F**)Graph representing the ratio of F4/80+ and F4/80- cells within the EYFP+CD45+ population obtained by FACS analysis on E12.5 embryos. * p-value<0,05.

Figure 2. Molsidomine treatment during embryogenesis increases eVE-Cad+ derived cells contribution to myogenesis. (**A**) **Left**: Representative western blot analysis of myosin heavy chain expression in total muscle lysates of ctrl and molsidomine-treated of newborn mice. CLX was used as

internal loading control. **Right**: qPCR analysis on total muscle lysates of the same mice using primers specific for myostatin. Data were calculated in triplicate as gene expression relative to endogenous cyclophilin A expression. Data are represented as the mean±S.E.M. of at least 5 control and 5 molsidomine-treated newborn mice. (**B**)qPCR analysis on EYFP+ cells FACS sorted from E12.5 embryos, devoided of the head and fetal liver. A list of primers used is present in material and methods. Data were calculated in triplicate as gene expression relative to endogenous cyclophilin A expression and are shown as fold change between molsidomine-treated embryos versus control ones as well as gene expression relative to endogenous cyclophilin A expression. A 1.5-fold-change cut off was defined, thus only transcripts with a fold change greater than 1.5 (i.e., <-1.5 or >+1.5) were considered biologically real. Red genes are unregulated in molsidomine-treated embryos and green genes are down regulated in embryos treated with molsidomine compared to control embryos. (**C**)Immunofluorescence (IF) with Hoechst, anti-EYFP, anti-MyHC (MF20) and anti-CD31 on sagittal sections of E12.5 embryos. Arrows indicate EYFP+ MyHC+ CD31- single-nucleated myocytes/myofibers. Scale bar: 25 μm. (**D**)Graph showing quantification of EYFP+MyHC+CD31+ myocytes or myofibers/mm^2 at E12.5 embryos. (**E**)IF with Hoechst, anti-EYFP and anti-CD31 on sagittal sections of E12.5 embryos. Scale bar: 50 μm. (**F**)**Left**: FACS analysis on single cells suspension from E12.5 embryos showing the percentage of EYFP+ cells within the CD31+ subset. **Right**: Graph representing results obtained with at least 8 control and 8 molsidomine-treated embryos. * p-value<0,05.

Figure 3. eVE-Cad+ derived cells contributes to myonuclei and interstitial cells in post-natal undamaged skeletal muscle. (**A**)**Left**: Graph representing results obtained by FACS analysis on single cells suspension from skeletal muscles of newborn mice showing the percentage of CD45+ and CD31+ cells within the EYFP+ subset. **Right**: Graph representing the ratio of F4/80+ and F4/80- cells within the EYFP+CD45+ population obtained by FACS analysis on single cells suspension from skeletal muscles of newborn mice. (**B**)X-Gal staining plus IF with Hoechst, anti-Laminin and anti-CD31 antibodies on transversal sections P0 newborn mice. Arrows indicate labelled (X-Gal+) myonuclei. Scale bar: 50 μm. (**C**)**Top**: Cross-sections of adult (P60) muscles immunostained with Hoechst, anti-EYFP, anti-CD31 and anti-NG2. Arrows point to EYFP+ NG2+ CD31- pericytes. **Bottom**: Cross-sections of adult (P60) muscles immunostained with Hoechst, anti-EYFP, anti-CD31 and anti-PW1. Arrows point to interstitial EYFP+ PW1+ CD31- cells. Scale bar: 25 μm. (**D**)FACS analysis on single cells suspension from adult muscles showing the percentage of NG2+ cells within the EYFP+ CD31- CD45- population in undamaged muscles from control mice and mice treated with molsidomine for 20 days.

Figure 4. Molsidomine treatment increases eVE-Cad+ derived cells contribution to skeletal muscle regeneration. (**A**)Scheme representing the protocol of pharmacological treatment with molsidomine during adult skeletal muscle regeneration induced by intramuscular injection of cardiotoxin (CTX). (**B**)FACS analysis on single cells suspension from damaged

adult muscles showing the percentage of EYFP+ cells. (**C**)X-Gal staining plus IF with Hoechst on transversal sections of adult Tibialis Anterior muscles collected 7 days after damage. Arrows indicate labelled (X-Gal+) myonuclei inside regenerating myofibers. Scale bar: 25 μm. (**D**)Immunohistochemistry (IHC) on transversal sections of adult Tibialis Anterior muscles collected 7 days after damage stained for β-gal and anti-CD68. Scale bar: 25 μm. (**E**) IHC on transversal sections of adult Tibialis Anterior muscles collected 7 days after damage stained for β-gal and anti-CD31. Scale bar: 100 μm (left), 25 μm (right). (**F**)Graphs represent capillary/myofiber ratio and capillary density obtained by quantification of IF with anti-CD31 and anti-laminin on transversal sections of adult Tibialis Anterior muscles collected 7 days after damage.

Figure 5 eVE-Cad+ derived cells from adult skeletal muscle are multipotent in vitro. (**A**)EYFP+ cells were FACS sorted from adult undamaged and damaged muscles and cultured in vitro on collagen coated dishes in MAB permissive conditions. Representative phase contrast images are shown. Scale bar: 50 μm. (**B**)Representative IF with Hoechst and anti-EYFP on cells sorted from damaged muscles after 2 passages in culture. Scale bar: 50 μm. (**C**)Cells were infected with pRRL.sin.PPT.CMV.nLacZ.pre lentivirus and co-cultured with C2C12 in low serum-medium to induce myogenic differentiation. Co-culture assay was stopped after 5 days. Images show X-gal staining plus IF with Hoechst and anti-MHC (MF20) antibody. Images show large MHC+ myotubes containing many X-Gal+ nuclei. Scale bar: 50 μm. (**D**)Cells

from adult damaged muscles exposed to TGF-β for 5 days differentiate extensively in smooth muscle actin (αSMA) positive cells. IF with Hoechst and anti-αSMA antibody in untreated cells (left) and in cells after TGF-β treatment (right). Scale bar: 50 μm. (**E**)Cells from adult damaged muscles exposed to VEGF form an endothelial network. A representative phase contrast image is shown. Scale bar: 25 μm. (**F**)Cells from adult damaged muscles cultured in adipogenic inductive medium differentiate into adipocytes. A representative phase contrast image is shown in which adipocytes containing fat droplets in the cytoplasm are recognizable. Scale bar: 25 μm.

Figure 6. Circulating eVE-Cad+ derived cells contributes to skeletal muscle regeneration, while the resident ones contributes to vessel and capillaries. (**A**)**Top**: Scheme representing the protocol of BMT in which bone marrow from Cdh5-CreER^{T2}; R26R-NZG mice was transplanted into C57BL/6 recipients. **Bottom**: X-Gal staining plus IF with Hoechst, anti-laminin and anti-CD31 on TA injured with 2 cycles of CTX (at day 0 and 7) and recovered at day 14. White arrows indicate labelled (X-Gal+) myonuclei inside regenerating myofibers. Scale bar: 25 μm. (**B**)**Top**: Scheme representing the protocol of BMT in which bone marrow from C57BL/6 mice was transplanted into Cdh5-CreER^{T2}; R26R-NZG recipients. **Bottom**: X-Gal staining plus IF with Hoechst, anti-laminin and anti-CD31 on TA injured with 2 cycles of CTX (at day 0 and 7) and recovered at day 14. Yellow arrows indicate labelled (X-Gal+) nuclei of capillaries and vessels (CD31+). Scale bar: 25 μm.

Chapter IV

Necdin enhances muscle reconstitution of dystrophic muscle by vessel-associated progenitors, by promoting cell survival and myogenic differentiation.

Patrizia Pessina[1*], Valentina Conti[1*], Rossana Tonlorenzi[2], Thierry Touvier[3], Raffaella Meneveri[2], Giulio Cossu[2,4] and Silvia Brunelli[1,2]

[1]Dept. of Experimental Medicine, University of Milano-Bicocca, Monza, Italy; [2]Division of Regenerative Medicine, H. San Raffaele, Milan, Italy; [3]E. Medea Scientific Institute, Lecco, Italy and [4]Dept. of Biology, University of Milano, Milan, Italy.

*These authors equally contributed to this paper

Cell Death & Differentiation 19, 827-838 (May 2012)

Necdin enhances muscle reconstitution of dystrophic muscle by vessel associated progenitors, by promoting cell survival and myogenic differentiation.

Patrizia Pessina[1§], Valentina Conti[1§], Rossana Tonlorenzi[2], Thierry Touvier[3], Raffaella Meneveri[1], Giulio Cossu[2,4] and Silvia Brunelli[1,2*]

[1]Dept. of Experimental Medicine, University of Milano-Bicocca, 20052, Monza, Italy; [2]Division of Regenerative Medicine, H. San Raffaele Scientific Institute, 20132, Milan, Italy; [3] E. Medea Scientific Institute, 23842, Bosisio Parini, Lecco, Italy; [4]Dept. of Biology, University of Milano, 20130 Milan, Italy

§These authors equally contributed to the work

*Corresponding author

Silvia Brunelli

Dept. of Experimental Medicine, University of Milano-Bicocca, 20052 Monza, Italy and Division of Regenerative Medicine, H. San Raffaele Scientific Institute, 20132, Milan, Italy

Tel, +390264488308; +390226435066

brunelli.silvia@hsr.it

Running title: necdin optimizes mesoangioblasts engraftment in the dystrophic muscle

Keywords: necdin, muscle dystrophy, stem cells, apoptosis, differentiationAbbreviations: Ab: antibody; αSMA: alpha Smooth Muscle Actin; α-SG: alpha sarcoglycan; DMD: Duchenne Muscular Dystrophy; GFP: Green Fluorescence Protein; MABs: mesoangioblasts; PDGFR: Platelet Derived Growth Factor; TA: Tibialis Anterior; TGFβ: Transforming Growth Factor beta; TNFα: Tumor Necrosis Factor alpha.

ABSTRACT

Improving stem cell therapy is a major goal for the treatment of muscle diseases, where physiological muscle regeneration is progressively exhausted. Vessel-associated stem cells, such a mesoangioblasts, appear to be the most promising cell type for the cell therapy for muscular dystrophies and have been shown to significantly contribute to restoration of muscle structure and function in different muscular dystrophy models. Here we report that MAGE protein necdin enhances muscle differentiation and regeneration by

mesoangioblasts. When necdin is constitutively over-expressed, it accelerates their differentiation and fusion in vitro and it increases their efficacy in reconstituting regenerating myofibres in the α-sarcoglycan dystrophic mouse. Moreover, necdin enhances survival when mesoangioblasts are exposed to cytotoxic stimuli that mimic the inflammatory dystrophic environment. Taken together, these data demonstrate that overexpression of necdin may be a crucial tool to boost therapeutic applications of mesoangioblasts in dystrophic muscle.

INTRODUCTION

Adult mammalian skeletal muscle is a stable tissue with slow turnover. Nonetheless, it has the ability to complete a rapid and extensive regeneration in response to severe damage generated by direct trauma or genetic defects. Local cues lead to the activation of quiescent myogenic precursors, the satellite cells, that form new myofibers and reconstitute a contractile function [1]. A fraction of activated cells returns to a quiescent state, in order to maintain a more or less constant pool of satellite cells. This self-maintenance mechanism cannot however compensate for the chronic loss of myonuclei throughout lifetime, as reflected by the reduction in

satellite cell number with aging, or by their depletion due to continuous activation of muscle repair in dystrophic muscles [2]. Indeed, in the most severe forms of muscular dystrophy, such as Duchenne muscular dystrophy (DMD), muscle regeneration is progressively exhausted, leading the patient to complete paralysis and death. Therapeutic approaches based on exogenous stem cell administration have been proposed with success in animal models of the disease. In particular, the mesoangioblasts [3] are a population of vessel-associated stem cells that have been shown to contribute to muscle repair when transplanted in dystrophic mice and dogs [4, 5].

Despite the identification of mesoangioblasts as potential sources of skeletal muscles, and the experimental evidence that they can be used to support *in vivo* skeletal myogenesis, the molecular mechanism regulating their growth, survival and differentiation into skeletal muscle remain largely unexplored. Designing tools to boost these processes may be a crucial step toward the optimization of cell therapy, and many genes and molecules are now being investigated in order to manipulate their fate.

Amongst these molecules, necdin may be one ideal candidate. Necdin (Ndn) is a member of melanoma antigen-encoding gene (MAGE) protein family [6]. It is a maternally imprinted gene that maps on a

chromosomal region known to be deleted in patients suffering from the Prader–Willi syndrome (PWS) [7]. Necdin null mice exhibit some of the features of PWS patients, and the absence of necdin impairs differentiation and maturation of hypothalamic neurons [8, 9].

In skeletal muscle necdin plays a pivotal role in tissue differentiation and maintenance [10, 11]. In particular, we provided the first evidence that this protein is required for proper myoblast differentiation, for the normal postnatal muscle fiber growth, and for the efficient repair upon muscle injury [10]. We showed that necdin acts at different levels: it cooperates with MyoD to promote the transcriptional activation of myogenin; in addition, it exerts a pro-survival, anti-apoptotic action counteracting the cytotoxic effect of several apoptotic agents [10]. Furthermore we recently showed, in a mouse model and in human patients, that necdin counteracts muscle wasting specifically induced by cachexia, a pathology in which atrophy is associated with tumor load [12, 13]. In this context, necdin exerts its protecting effect by interfering with TNFα-activated signalling at various levels and it is associated with a regenerative response of the muscle to wasting.

These evidences prompted us to investigate whether necdin function could be exploited to improve the performance of vessel-associated stem/progenitor cells in dystrophic skeletal muscle regeneration. We

demonstrate here that necdin is indeed able to accelerate and enhance myogenic differentiation of mesoangioblasts and to increase cell survival, thus leading to a more efficient reconstitution of the dystrophic muscle.

RESULTS

Characterization of necdin overexpressing mesoangioblasts.

We isolated mesoangioblasts from biopsies of muscles of adult (6 months old) C57 mice exactly according to [14] (Fig 1A). Proliferating mesoangioblasts (wt MABs) express very low level of necdin, therefore to study its role in these cells we generated a cell line that over-expresses necdin constitutively: we produced a lentiviral vector expressing necdin under the constitutive PGK promoter and eGFP under the CMV promoter in opposite orientation, to infect wt mesoangioblasts (NDNMABs) (Fig 1B). As a control, we transduced the same cells with the lentiviral vector expressing only eGFP (GFPMABs). Cells were FACS sorted for the GFP expression (around 80% of the total number of cells did express GFP) and after 2 passages both NDNMABs and GFPMABs express high level of GFP fluorescent signal by immunofluorescence or FACS analysis (Fig.1B and not shown). qPCR analysis show that NDNMABs express necdin

around 0,018 fold respect to GAPDH and more than 3000 folds respect to GFPMABs (Fig 1C-Suppl. Fig. 1A). Western blot analysis shows indeed a greater expression of necdin in NDNMABs, respect to GFPMABs (Fig. 1D).

Proliferation curve demonstrated that all cells, transduced or not, grow at the same rate (Fig. 1E).

FACS, RT-PCR and qPCR analysis confirmed that the three populations retained mesoangioblasts markers (CD34, Sca1, α7 integrin) and express pericytes markers (NG2, PDGFR and αSMA), without significant differences (Fig.1F-H, Suppl. Fig.1B). Likewise none express endothelial markers, such as VE-cadherin, nor Pax7, marker of satellite cells derived myoblasts (Fig 1G, Suppl. Fig.1B).

Mesoangioblasts have been demonstrated to differentiate efficiently in different cell types. We therefore tested the ability of GFPMABs and NDNMABs to respond to smooth muscle and adipogenic differentiation cues. Induction by TGFβ led to an high and comparable smooth muscle differentiation frequency in the two populations as seen by the presence of a comparable number of αSMA positive cells with smooth muscle morphology (Fig. 2A-B), and by the increased expression of smooth muscle myosin (smMHC) and

Smoothelin, as differentiation proceeds (Fig. 2C). We also show that the levels of Msx2, a gene we have previously described to cooperate with necdin in smooth muscle differentiation of mesoangioblasts [15], do indeed increase over time (Fig.2C).

After treatment with an adipogenesis inducing medium, NDNMABs showed a number of terminally differentiated, Oil-Red positive-cells, that is comparable to that of GFPMABs (Fig 2D-E), but interestingly NDNMABs cells expressed a decreased level of adipogenic markers (AP2 and PPARγ) at all time points (Fig. 2F), suggesting that Necdin slows adipogenic differentiation of mesoangioblasts.

Necdin accelerates mesoangioblast cells myogenic differentiation and fusion

Unlike their embryonic counterpart, mesoangioblasts derived from adult muscle are able to differentiate in skeletal muscle cells spontaneously, without the need of co-culture with myoblasts and yet they differ from satellite cells because do not express Pax7 [14, 16] (Fig. 1G, Suppl. Fig.1B). Skeletal muscle differentiation was induced by culturing NDNMABs and GFPMABs in muscle-differentiation medium (Fig. 3A) and fusion index was calculated to compare their differentiation potential: NDNMABs showed a higher fusion index

(NDNMABs: 54%; GFPMABs: 26%), with the progressive appearance of an increased number of myotubes with more nuclei over time, and in particular with more than 10 nuclei at 6 days (Fig. 3B-C).

Enhanced differentiation potential of mesoangioblasts over-expressing necdin, may depend on a different level of expression of myogenic factors leading to an increased expression of muscle specific cytoskeletal proteins, and/or decreased cell death. We first analyzed the expression of MyoD, Myogenin and Myosin Heavy C,hain during a time course skeletal muscle differentiation.

Protein and RNA were extracted from GFPMABs and NDNMABs at the beginning of differentiation (T0) and after three (T3) and six (T6) days. The increased fusion index we observed in NDNMABs was accompanied by increased expression of Myogenin and MyHC, both at RNA and protein levels (Fig 3D-F), indicating that necdin accelerates myogenic differentiation by promoting the expression of myogenic factor and then of specific cytoskeletal proteins. MyoD RNA but not protein levels appear slightly increased in NDNMABs at T3 and T6. Necdin levels in GFPMABs remain the same over time, while it appears that viral mediated necdin expression in NDNMABs

increases at T3 and then decrease at T6, both at RNA and protein level (Fig. 3D-F). In C2C12 myoblasts we have described that necdin binds to the myogenin promoter and therefore cooperates to the transcription of this gene [10]. We investigated whether this mechanism of action was conserved in mesoangioblast differentiation. Chromatin immunoprecipitation was performed on NDNMABs as in [10]. We found indeed that necdin was equally able to bind this DNA sequence that was precipitated by anti-necdin antibody (Fig. 3G), indicating that this maybe one direct mechanism of action leading to enhanced myogenic differentiation of NDNMABs.

Necdin protects mesoangioblasts from cell death

An important aspect of the acute and chronically damaged muscle is that it originates a pro-apoptotic microenvironment in which cytokines such as TNFα, and reactive oxygen species, generated both by the necrotic fibers and cells of the immune system infiltrating the muscle [17], that may contribute to the limited effect of myogenic cells transplantation.

Our previous studies revealed that necdin acts as a pro-survival factor in muscle cells [10]. We investigated whether necdin has the same role

also on mesoangioblasts cells. Proliferating GFPMABs and NDNMABs were exposed either to Stauroporine (2 μM) for 3h or overnight to the reactive oxygen species arsenic trioxide (As_2O_3) (20 μM). After treatment, we evaluated cell death by measuring Propidium Iodide (PI) incorporation by FACS.

Fig. 4 A-B (and Suppl. Fig. 2A) shows dot plots relative to representative experiments. Three populations can be clearly distinguished: GFP^+ PI^- cells (live cells); GFP^+ PI^{low} cells (cells that start to loose the membrane integrity and in which, consequently, the PI is only present in the citoplasm) and GFP^- PI^{high} cells (dead cells that have lost GFP expression because of the complete loss of membrane integrity and in which the PI is intercalated in the DNA).

We analyzed and plotted (Fig. 4C-D) the number of dead cells (GFP^- PI^{high}) and we observed that NDNMABs showed a 35% increase in cell vitality respect to GFPMABs.

In addition to the marked reduction of the GFP^- PI^{high} population, we also observed a reduction in the number of the GFP^+ PI^{low} population. In particular, after staurosporine treatment, NDNMABs showed a 30% decrease and, after As_2O_3 treatment, a 50% decrease of the apoptosing cell population, if compared with GFPMABs. These data confirmed

that over-expressing necdin mesoangioblasts resist better to the different apoptotic treatments used, thus demonstrating that necdin plays a crucial role in cell survival also in vessel associated myogenic progenitors.

Necdin promotes mesoangioblasts-mediated muscle reconstitution *in vivo*.

These encouraging results *in vitro* led us to investigate whether necdin could optimize mesoangioblast contribution to muscle repair *in vivo*, in a murine model of muscular dystrophy, the α-sarcoglycan (α-SG$^{-/-}$) null mice.

We performed intra-muscular injections of GFPMABs and NDNMABs in the Tibialis Anterior (TA), quadriceps (QUAD) or gastrocnemius (GASTRO) of 4 months old a-SG$^{-/-}$ mice. We injected 5x10^5 cells in 50 ml of physiological solution (TA) and 7x10^5 cells in 70 ml of physiological solution (QUAD and GASTRO). In order to have an internal control, we injected GFPMABs in the right muscles and NDNMABs mesoangioblasts in left muscles of the same mouse.

24h (12 mice), and 14 days (21 mice) after the injections, mice were sacrificed and muscles were collected. RNA and proteins were extracted for Real time PCR and western blot analysis respectively.

Alternatively muscles were either digested for FACS analysis or crysectioned to perform immunofluorescence.

We first detected the ability of mesoangioblasts to survive in the inflammatory microenvironment of dystrophic muscles. To this end, we transplanted GFPMABs or NDNMABs in muscles of alpha-sarcoglycan null mice, we sacrificed them 24 hours later and we collected treated muscles for subsequent experiments (Suppl. Fig. 3A).

Since *in vivo* necrotic mesoangioblasts, that have lost the GFP expression, can't be discriminated anymore from other host-cells, we focused our analysis on the detection of early and late stages of apoptosis.

We combined TUNEL assay with immunofluorescence against GFP. Counting on muscle serial sections, we demonstrated that muscle transplanted with NDNMABs contained a decreased number of apoptosing $Tunel^{+}GFP^{+}$ cells, respect to control mesoangioblasts (Fig. 5A-B).

We collected mRNA from muscles injected with mesoangioblasts and we evaluated the number of surviving and transcriptionally active mesoangioblasts by qPCR using specific primers for GFP. We normalized the level of GFP messenger in each injected-muscle

sample with that corresponding to the total input of injected cells. We demonstrated that muscles treated with NDNMABs showed a greater GFP expression, indicating a higher survival level of these cells, and we can indirectly estimate the number of dead mesoangioblasts that are no longer detectable in the muscle (Fig. 5C).

Moreover we performed a FACS analysis on single cells dissociated from the transplanted muscles and we evaluated the amount of apoptotic mesoangioblasts as the number of GFP positive cells that are also positive for 7-amino-actinomycin D (7AAD). We demonstrated that muscles injected with GFPMABs contained almost double the amount of $GFP^{+}7AAD^{+}$ respect to NDNMABs injected muscles (Fig. 5D-E and Suppl. Fig.2B).

All these data are in agreement with the *in vitro* results, indicating that overexpression of necdin confers to mesoangioblasts a higher resistance to cell death.

We therefore determined the ability of these cells to regenerate new muscle fibers by evaluating the restoration of α-SG expression in regenerating fibers. We performed immunofluorescence staining for α-SG on cryosections of TA muscle of α-$SG^{-/-}$ mice treated with intra-

muscular injections of GFPMABs and NDNMABs and wt or α-SG$^{-/-}$ mice as controls. Sections from mice treated with NDNMABs showed higher number of α-SG positive fibers (Fig. 6A). Some of the MABs that do not contribute to the new regenerating fibers, remain in the interstitial space between fibers, together with other cells, such as macrophages, that infiltrate the dystrophic muscle (Suppl. Fig. 3B-C). Accordingly, muscles treated with NDNMABs showed a higher level of α-SG expression respect to muscles treated with GFPMABs both as RNA, as revealed by Real Time-PCR analysis (Fig. 6B) and as protein, measured by Western blot (Fig. 6C).

DISCUSSION

There is actually no cure for muscular dystrophies, although many strategies are entering clinical experimentation. Among these stem cell therapy is an attractive approach and research in this direction has moved very rapidly in the last years. Stem cell populations with myogenic potential can be isolated from multiple regions of the body [18, 19]. Until now, mesoangioblasts appear to fulfil most these features [3, 14, 16] and shown to significantly contribute to restore muscle structure

and function in mouse and dog models of muscular dystrophy [4, 5, 20], still protocol optimization for cell therapy is still ongoing, and different drug and gene therapy approaches have been investigated to improve their clinical outcome.

For example, the treatment of dystrophic mice with nitric oxide plus NSAIDs [21] and/or the treatment of mesoangioblasts with NO, SDF1, S1P or HMGB1 improved to different levels and with different mechanisms either homing or survival of mesoangioblasts in skeletal muscle, increasing their therapeutic effectiveness [22-25].

Here we demonstrate that the efficacy of mesoangioblasts cells to reconstitute dystrophic muscle is improved by the expression of the MAGE protein necdin. Importantly when necdin is over-expressed, both the myogenic differentiation and survival of mesoangioblasts were enhanced both *in vitro* and *in vivo*.

We have previously shown that necdin has an important role in skeletal muscle differentiation and maintenance by satellite-derived myoblasts in different conditions of muscle damage or wasting [10, 12], therefore we constitutively over-expressed necdin in adult mesoangioblasts. We found that necdin, when overexpressed in mesoangioblasts, causes a higher fusion rate *in vitro*, suggesting that necdin is required to increase their differentiation potential by

promoting new myofiber growth and fusion. To understand the molecular mechanisms that regulate this process, we first investigated if necdin could act on transcriptional pathways, as we already demonstrated for satellite-derived myoblasts [10]. In myoblast cultures from the gain of function transgenic mice (MlcNec) increased expression correlates with an increased fusion index and with changes in the expression of different myogenic markers, including myogenin and sarcomeric myosin. In particular we found that necdin acts through a transcriptional regulation of myogenin, in cooperation with MyoD. Here we found that in mesoangioblast cells triggered to differentiate into skeletal muscle, an increased expression of necdin led to an accelerated myogenesis and to a higher rate of fusion. This correlates with higher levels of myogenin and skeletal myosin, suggesting that necdin play a similar role in controlling the action of myogenic regulatory factors. We indeed demonstrate that this effect maybe linked to a direct transcriptional action of necdin, since it is able to bind to the same promoter sequence of the Myogenin gene, as it does in myoblasts [10].

Most importantly necdin did not trigger myogenic differentiation alone, but only when a differentiation stimuli is provided. This is of great importance since ideally the stem cells should differentiate only

upon reaching the damaged muscle, where the environment of the remodeling tissue can trigger myogenic differentiation. Therefore cells overexpressing necdin, even at very high levels, but in conditions that do not favour differentiation, and in absence of other myogenic regulatory factors behave as controls, in terms of proliferation and expression of specific molecular markers.

Furthermore, the differentiation enhancement is limited to skeletal myogenesis: smooth muscle differentiation is not affected. This is in agreement with what we described previously: necdin is indeed involved in smooth muscle differentiation of mesoangioblasts but only in combination with the transcription factor Msx2 [15], that is not expressed in proliferating mesoangioblast, nor GFPMABs nor NDNMABs, but that is moderately upregulated upon smooth muscle differentiation stimuli (e.g. TGF-β).

We also observed that a similar amount of terminally differentiated adipocytes (Oil Red O positive cells) are present at the end of the treatment with an adipogenic differentiation medium, whether necdin is overexpressed or not. Interestingly, time course analysis of adipogenic markers shows that overexpression of necdin decreases their level of expression. Necdin inhibition of adipogenic differentiation of pre-adypocytes has been previously described [26, 27],

but no data are available on the co-factor that may cooperate with necdin in this process, and more experiments will be required to get more insight into this issue. There is evidence that in the aged or dystrophic muscle mesenchymal progenitors distinct from satellite cells contribute to ectopic fat cell formation in degenerating skeletal muscle, in aging or dystrophy [28]. It is also still unclear whether this environment could trigger adipogenic conversion of myogenic precursors, therefore leading to an additional muscle loss [29]. It would be of great importance to get more insights into the role of necdin in this fate choice, since overexpression of necdin could not only lead to an increased myogenic differentiation of endogenous or transplanted myogenic precursors, but at the same time inhibit their adipogenic differentiation.

Necdin has been also demonstrated to play a role as anti-apoptotic protein. In particular, we demonstrated that necdin interacts both with caspase-3 and caspase-9 pathways in satellite cells [10]. Since the reduced ability of mesoangioblasts to resist the cytotoxic environment existing in the damaged muscle maybe one of the main reasons for their partial effect, we tested this possibility by exposing mesoangioblasts to a cytotoxic stimulus and found that necdin protects mesoangioblasts from cell death.

In agreement with these results in vitro, we showed that mesoangioblasts overexpressing necdin, when delivered in α-sarcoglycan null (α-SG$^{-/-}$) mice, are able to better survive in the cytotoxic dystrophic environment. More interestingly, it provides a greater contribution to muscle repair, as demonstrated by an increased expression of α-SG and restoration of α-SG expressing muscle fibers. We show that some undifferentiated mesoangioblasts, both GFPMABs and NDNMABs, are retained in the interstitium of the dystrophic muscle, where other cells are present, in particular macrophages [17].

We think our results open a new way to manipulate mesoangioblasts fate. Recently a Human Artificial chromosome vector (HAC vector) has been manipulated to contain the entire human dystrophin gene including its entire transcriptional regulatory elements (DYS-HAC) [30]. This DYS-HAC was stably maintained in mice and cultured human cells, and mice derived from ES containing this HAC were expressing the transgene. This system, whether successfully applied to the mesoangioblast mediated stem cell therapy approach, could be additionally exploited to contain not only dystrophin, but also a series of other genes, to optimize the feature of the stem cells. In this light

necdin could provide transplanted cells with the ability to better survive and to differentiate efficiently when in the appropriate conditions, without interfering with their properties, and to contribute to an optimal skeletal muscle reconstitution.

One critical concern on the use of necdin in the optimization of stem cell therapy is the potential tumorigenic risk. Many proteins of the MAGE family, in particular those belonging to Type I (MAGE A, B, and C) are characterized by a wide expression in a variety of malignant tumors, and are being considered as highly attractive targets for cancer immunotherapy [31]. However, other than this association, little is known regarding their functions in cell activities and in tumor initiation and progression. Necdin is on the other hand a member of Type II proteins that are expressed in normal tissues. Necdin has been also suggested playing a role as a tumor suppressor gene [32]. Long term studies on mice overexpressing necdin or on immunodeficient mice injected with cells overexpressing necdin will be certainly required to address this issue.

Detailed studies on the molecular mechanism of the effect of necdin in myogenic stem cells and in general in muscle regeneration are on their way to further enhance its action, that may be a crucial step towards

the optimization of cell therapy by mesoangioblasts or other stem cells.

MATERIALS AND METHODS

Mesoangioblasts cell culture and in vitro differentiation

Mesoangioblasts (MABs) were isolated and cultured exactly as previously described in [14]. Specifically, adult-derived murine mesoangioblasts were isolated from muscular biopsies of a 6-month-old C57BL/6 mouse hind legs. After dissecting both the tibialis anterior and rinse them in PBS with Ca^{2+}–Mg^{2+} to remove residual blood, they were carefully cleaned from adipose and connettive tissues, trying to identify portions of interstitial tissue containing small vessels. The fragments were minced in 1-2mm pieces and transferred on collagen type I-coated dishes and and incubated at 37ºC, 5% CO_2 and 5% O_2 in proliferation medium consisting of Dulbecco's modified Eagle's medium (DMEM) supplemented with 20% fetal bovine serum, 2mM L-glutamine, 1mM sodium pyruvate, 100 IU ml^{-1} penicillin and 100 mg ml^{-1} streptomycin. After 5-8 days at 37ºC, besides initial outgrowth of adherent cells, mainly consisting of large and flat fibroblasts, mesoangioblasts could be discerned as small,

poorly adhering and very refractile cells. The mixed population was enzimatically dissociated by collagenase/dispase treatment and cloned by limiting dilution in 96-multiwell dishes. After 7–10 days first clones of cells were distinguishable and propagated in proliferation medium. After few passages most of the clones adopted a large, flat morphology and underwent proliferative senescence. However, few clones retained a small, refractile, morphology with the ability to proliferate for at least 40 passages.

MABs were induced to differentiate to smooth muscle as described in [33] and to induce the adipogenic differentiation the STEMPRO® Adipogenesis Differentiation Kit (GIBCO) was used, according to the manufacture's protocol. After 10 days, cells were washed in PBS, fixed in 4% PFA for 5 minutes at room temperature and subsequently incubated with Oil-Red-O solution, as previously described [14]. The proportion of cells differentiating in each different cell type was calculated by counting the cells expressing the appropriate differentiation markers against the total number of cells. The average number was determined by counting cells in at least ten microscopic fields (170-200 cell/field), in at least five independent experiments.

MABs derived from adult muscle can spontaneously differentiate into multinucleated skeletal myotubes when cultured onto matrigel coated plastic support in differentiation promoting medium (complete medium supplemented with 2% Horse Serum).

Lentiviral vector preparation and mesoangioblasts transduction

The control GFP lentiviral vector and the necdin lentiviral vector (in pCCL.sin.cPPT.SV40polyA.eGFP.minCMV.hPGK.Wpre) were generated and prepared as described in [10].

Viral titer was determined by GFP fluorescence infecting HeLa cells with serial dilution of the virus. The final MOI was 10^7 TU/ml. After 24 h in culture, MABs were transduced with a MOI of 100 in proliferation medium overnight. The next day, the medium was changed and cells were maintained in proliferation medium for one passage and then subjected to fluorescence-activated cell sorting (FACS) for GFP-positive cells.

We generated 6 different lines overexpressing Necdin and 4 control lines. Necdin expression in NDNMABs ranged from 0,003 to 0,018 fold GAPDH expression (Supplementary Fig. 1A) and expression was 834 to 4938 fold the expression in GFPMABs. Necdin expression in

GFPMABs ranged from 0,000004 to 0,000006 fold GAPDH expression (average Ct, GFPMABs: 31; NDNMABs: 20; GAPDH: 13). Since in a preliminary analysis we did not observe toxicity, and the effect on proliferation, differentiation or survival in vitro was similar, we have decided to further characterize a single line for each construct.

Generation of the Growth Curve

MABs from the different genotypes were seeded at a density of $2x10^3$ cells per cm^2 of surface area in 6 well plates or T25 flasks in duplicate. Cell number was assessed by direct cell count and viable cells were judged by Trypan blue dye (Sigma) exclusion. The duplicate plates were counted every 24 hours and the results were plotted on a logarithmic scale.

Flow cytometry analysis

The monoclonal antibodies used for this analysis were the following: anti-α7integrin-PE (MBL); anti-Sca1-APC and anti-CD34-Alexa 647 (eBioscience).

MABs were harvested, washed twice with PBS, resuspended in blocking solution (10% FBS in PBS) and incubated for 15 minutes at

room temperature. Subsequently, cells ($2x10^5$ per tube) were incubated with various combinations of conjugated-antibodies for 45 minutes at 4°C in the dark, according to the manufacture's recommendations. The background level was estimated by omitting the primary antibody. After PBS washing cells were fixed in 1% PFA before FACS analysis.

Cell analysis was performed on at least 10.000 events for each sample and determined using the Accuri® C6 Flow Cytometer® System equipped with a blue (488 nm) and a red (640 nm) laser, two scatter detectors, and four fluorescence detectors with interference filters optimized for the detection of FITC, PE, PerCP-Cy5.5 and APC. The analysis was performed using the Accuri CFlow® software. A primary gate based on physical parameters (forward and side light scatter, FSC and SSC, respectively) was set to exclude dead cells or small debris.

Immunofluorescence

Immunofluorescence on cell cultures and cryosections was performed according to [15], using antibodies specific for sarcomeric myosin MF20, alpha-smooth muscle actin (α-SMA, Sigma), laminin

(Abcam), GFP (Chemicon International), Necdin (Upstate), CD68 (AbDSerotec) and alpha-sarcoglycan (Anti-SGCA, Sigma). For fluorescence detection, appropriate secondary antibodies conjugated with either Alexa 488 (green; Invitrogen) or Alexa 594 (red; Invitrogen) or Alexa 647 (purple, Invitrogen) were used. Nuclei were stained with Hoechst.

To compare the ability of MABs from the different genotypes to fuse and differentiate into multinucleated myotubes, we evaluated both the relative fusion index, counting the number of MHC-positive myotubes, calculated as the number of nuclei per cell, after 3 and 6 days in the differentiating medium, as well as the absolute fusion index, calculated as the percentage of MHC-positive nuclei over the total number of nuclei after 6 days in differentiation medium. An average value was determined by counting cells (500-700 cells/field) in at least ten microscopic fields. Results were expressed as mean ± s.e.m. of five independent experiments.

RT-PCR

RNA (1-2 μg) collected from cells or tissues using RNeasy Mini (or Micro) kit (Quiagen) or the TRIzol protocol (Invitrogen) was

converted into double-stranded cDNA using the cDNA synthesis kit "High Capacity Reverse Transcription Kit" (Applied Biosystem), according to the manufacturer's instructions.

RT-PCRs were performed using the GoTaq Mix (Promega) for GAPDH (5′ TTCACCACCATGGAGAAGGC 3′ FW; 5′ GGCATGGACTGTGGTCATGA 3′ REV); CD34 (5′ ACCACACCAGCCATCTCAG 3′ FW; 5′ TAGATGGCAGGCTGGACTTC 3′ REV); NG2 (5′ ACAAGCGTGGCAACTTTATC 3′ FW; 5′ ATAGACCTCTTCTTCATATTCAT 3′ REV); PDGFRβ (5′ CCGGAACAAACACACCTTCT 3′ FW; 5′ AACATGGGCACGTAATCTATA 3′ REV); Sca1 (5′ TTACCCATCTGCCCTCCTAA 3′ FW; 5′ GGTCTGCAGGAGGACTGAGC 3′ REV); αSMA (5′ CTGACAGAGGCACCACTGAA 3′ FW; 5′ CATCTCCAGAGTCCAGCACA 3′ REV); VE-Cadherin (5′ GTACAGCATCATGCAGGGCG 3′ FW; 5′ ATTCGTATCGGATAGTGGGG 3′ REV); Pax7 (5′ GACTCGGCTTCCTCCATCTC 3′ FW; 5′ AGTAGGCTTGTCCCGTTTCC 3′ REV).

Real-time quantitative PCR (qPCR) was carried out with a real-time PCR system (Mx3000P; Stratagene). Each cDNA sample was amplified in triplicate by using the SYBR Green Supermix (Bio-Rad Laboratories) for cyclophillin A (5' CATACGGGTCCTGGCATCTTGTCC 3' FW;5' TGGTGATCTTCTTGCTGGTCTTGC 3' REV), GAPDH (5' CACCATCTTCCAGGAGCGAG 3'FW; 5' CCTTCTCCATGGTGGTGAAGAC 3'REV), Necdin (5' GGTGAAGGACCAGAAGAGGA 3' FW; 5' TGGGCATACGGTTGTTGAG 3' REV), CD34 (5' ACCACACCAGCCATCTCAG 3' FW; 5' TAGATGGCAGGCTGGACTTC 3' REV), NG2 (5' ACAAGCGTGGCAACTTTATC 3' FW; 5' ATAGACCTCTTCTTCATATTCAT 3' REV), PDGFRβ (5' CCGGAACAAACACACCTTCT 3' FW; 5' AACATGGGCACGTAATCTATA 3' REV), Sca1 (5' TTACCCATCTGCCCTCCTAA 3' FW; 5' GGTCTGCAGGAGGACTGAGC 3' REV), αSMA (5' CTGACAGAGGCACCACTGAA 3' FW; 5' CATCTCCAGAGTCCAGCACA 3' REV), Pax7 (5'

GACTCGGCTTCCTCCATCTC 3’ FW; 5’ AGTAGGCTTGTCCCGTTTCC 3’ REV), Ve-cadherin (5’ GTACAGCATCATGCAGGGCG 3’ FW; 5’ ATTCGTATCGGATAGTGGGG 3’ REV), Smoothelin (5’ ATCTGATTCTCCCGTGGTTG 3’ FW; 5’ CTGCTTCTTGTGGGAGGAAG 3’ REV), smMHC (5’ GCAGAAGGCTCAGACCAAAG 3’ FW; 5’ TATCCAGAATGCCCAGGAAG 3’ REV), msx2 (5’ CCATATACGGCGCATCCTACC 3’ FW; 5’ CAACCGGCGTGGCATAGAG 3’ REV), aP2 (5’ TCACCTGGAAGACAGCTCCT 3’ FW; 5’ AATCCCCATTTACGCTGATG 3’ REV), PPARγ (5’ AGACAACGGACAAATCACCA 3’ FW; 5’ TGGACACCATACTTGAGCAGA 3’ REV), MyoD (5’ ACGGCTCTCTCTGCTCCTTT 3’ FW; 5’ GTAGGGAAGTGTGCGTGCT 3’ REV), Myogenin (5’ GACATCCCCCTATTTCTACCA 3’ FW; 5’ GTCCCCAGTCCCTTTTCTTC 3’ REV), MHC (5’ GGCCAAAATCAAAGAGGTGA 3’ FW; 5’ CGTGCTTCTCCTTCTCAACC 3’ REV), GFP (5’ ACAAGCAGAAGAACGGCATC 3’ FW; 5’

CGGTCACGAACTCCAGCA 3' REV), α-SG (5' CTTGTGGGTCGTGTGTTTGT 3' FW; 5' GGTGAGCGTGGTAGGTGAGT 3' REV).

Quantification has been performed using the ΔCt method using as reference gene cyclophillin A or GAPDH, or the Livak method for relative gene expression analysis, using as reference value the value of WTMABs or GFPMABs.

Chromatin immunoprecipitation

ChIP assay was performed as previously described [10] on 6×10^6 of over-expressing Necdin mesoangioblasts grown in differentiating medium for 3 days.

The input DNA was an aliquot of the supernatant from the centrifuged sonicate (DNA size range: 200–1,000 bp). The chromatin was immunoprecipitated with normal rabbit IgG (Santa Cruz Biotechnology, Inc.), rabbit anti-HA (Santa Cruz Biotechnology, Inc.) and rabbit anti-necdin (Upstate Biotechnology). PCRs were performed on the purified immunoprecipitated DNA with GoTaq (Promega) and the primers used were myogenin (5′-GAATCACATGTAATCCACTGGA-3′ FW, 5′-ACGCCAACTGCTGGGTGCCA-3′ REV), β-actin (5′-

GCTTCTTTGCAGCTCCTTCGTTG-3′ FW, 5′-TTTGCACATGCCGGAGCCGTTGT-3′ REV).

Cell resistance to cell death

MABs from the different genotypes were incubated with or without 2μM staurosporine for 3 hours or with or without 20μM As_2O_3 overnight. Cells were detached and stained with Propidium Iodide (PI) according to the kit's manufacturer's instructions and analyzed by flow cytometry as described [24].

Protein extracts and immunoblot analysis

Muscles tissue were homogenized or cells were scraped in 20 mM Tris-HCl pH 8.8, 5 mM EDTA, 10% glycerol, 50mM NaF, 1% Triton X-100 and protease inhibitor cocktail (Sigma) and centrifuged for 10 minutes at 13.000 rpm at 4°C to discard cellular debris. After electrophoresis, proteins (30-40 μg) were electrophoretically transferred to nitro-cellulose filters and antigens revealed by the respective primary Abs and the appropriate secondary Abs, as already described [10]. The antibodies used were: anti-Necdin (Upstate Biotechnology), anti-MyoD (DAKO), anti-sarcomeric myosin MF20 and anti-myogenin (from Developmental Studies Hybridoma Bank),

anti-alpha-sarcoglycan (Novocastra) and, to normalize protein levels, anti-β–tubulin (Covance) and anti-glyceraldehyde 3-phosphate dehydrogenase (GAPDH) mAb (from Biogenesis).

***In vivo* reansplantation**

4-months-old α-sarcoglycan null (a-SG$^{-/-}$) mice were injected by intra-muscular delivery with $5x10^5$ (for tibialis anterior) or with $7x10^5$ mouse MABs (for quadriceps and gastrocnemius) and animals were sacrificed 14 days after transplantation. Different muscles were collected for real-time PCR or frozen in isopentane cooled by liquid nitrogen for histological analysis.

***In vivo* Cell Survival Assay**

To identify MABs undergoing apoptosis in vivo, we performed, together with GFP immunofluorescence, TUNEL test using the ApopTag® Red In Situ Apoptosis Detection Kit (Chemicon International) according to the manufacturer's instructions, on cryostat sections of OCT-embedded muscles of alpha-sarcoglycan null mice recovered 24 hours after mesoangioblasts intra-muscular injection.

Tissue digestion and flow cytometric analysis of cell death.

Muscles of alpha-sarcoglycan null mice were recovered 24 hours after mesoangioblasts intra-muscular injection and finely minced. Each sample underwent four cycles of enzymatic digestion at 37^{o}C for 10 minutes in the presence of 3.5 mg/ml dispase (Invitrogen) and 0.5 mg/ml collagenase type V (Sigma-Aldrich). The single cell suspension was filtered to remove tissue debris. The isolated cells were harvested and resuspended in PBS 10% FBS. Cells were stained with 10 μg/ml of 7-amino-actinomycin D (7AAD, Sigma-Aldrich) . Cell analysis was performed on at least 10.000 events for each sample and determined using the Accuri® C6 Flow Cytometer® System. The analysis was performed using The Accuri CFlow® software. A primary gate based on physical parameters (forward and side light scatter, FSC and SSC, respectively) was set to exclude dead cells or small debris.

Image acquisition and manipulation

Images in fluorescence and phase contrast have been taken on the Nikon microscope Eclipse E600, (lenses Plan Fuor: 4x/013, 10x/0.33, 20x/0.50, 40x/0.75) or on the Leica AF6000. Images have been acquired using the NIKON digital camera DXM1200, and the acquisition software NIKON ACT-1, or using the DFC350 FX digital

camera and the Leica AF600 acquisition software, imaging medium, PBS buffer, room temperature. Images were assembled in panels using Adobe Photoshop 7.0. Images showing double fluorescence were first separately acquired using the different appropriate filters, the two layers then merged with Adobe Photoshop 7.0.

Acknowledgements

This work has benefited from research funding from Telethon (GGP07013), the Italian Ministry of University and Research (PRIN 2009), the European Community's Seventh Framework Programme in the project ENDOSTEM (Grant agreement number 241440) to SB, and OPTISTEM (Grant agreement number 223098) to GC. We are also grateful to Jordi Diaz-Manera for technical help.

References

1. Zammit PS, Partridge TA, Yablonka-Reuveni Z. The skeletal muscle satellite cell: the stem cell that came in from the cold. *J Histochem Cytochem* 2006; **54**(11)**:** 1177-91.

2. Conboy IM, Rando TA. Aging, stem cells and tissue regeneration: lessons from muscle. *Cell Cycle* 2005; **4**(3)**:** 407-10.

3. Minasi MG, Riminucci M, De Angelis L, Borello U, Berarducci B, Innocenzi A *et al.* The meso-angioblast: a multipotent, self-renewing cell that originates from the dorsal aorta and differentiates into most mesodermal tissues. *Development* 2002; **129**(11)**:** 2773-83.

4. Sampaolesi M, Blot S, D'Antona G, Granger N, Tonlorenzi R, Innocenzi A *et al.* Mesoangioblast stem cells ameliorate

muscle function in dystrophic dogs. *Nature* 2006; **444**(7119)**:** 574-9.

5. Sampaolesi M, Torrente Y, Innocenzi A, Tonlorenzi R, D'Antona G, Pellegrino MA *et al.* Cell therapy of alpha-sarcoglycan null dystrophic mice through intra-arterial delivery of mesoangioblasts. *Science* 2003; **301**(5632)**:** 487-92.

6. Barker PA, Salehi A. The MAGE proteins: emerging roles in cell cycle progression, apoptosis, and neurogenetic disease. *J Neurosci Res* 2002; **67**(6)**:** 705-12.

7. Cassidy SB. Prader-Willi syndrome. *J Med Genet* 1997; **34**(11)**:** 917-23.

8. Gerard M, Hernandez L, Wevrick R, Stewart CL. Disruption of the mouse necdin gene results in early post-natal lethality. *Nat Genet* 1999; **23**(2)**:** 199-202.

9. Muscatelli F, Abrous DN, Massacrier A, Boccaccio I, Le Moal M, Cau P *et al.* Disruption of the mouse Necdin gene results in hypothalamic and behavioral alterations reminiscent of the human Prader-Willi syndrome. *Hum Mol Genet* 2000; **9**(20)**:** 3101-10.

10. Deponti D, Francois S, Baesso S, Sciorati C, Innocenzi A, Broccoli V *et al.* Necdin mediates skeletal muscle regeneration by promoting myoblast survival and differentiation. *J Cell Biol* 2007; **179**(2)**:** 305-19.

11. Kuwajima T, Taniura H, Nishimura I, Yoshikawa K. Necdin interacts with the Msx2 homeodomain protein via MAGE-D1 to promote myogenic differentiation of C2C12 cells. *J Biol Chem* 2004; **279**(39)**:** 40484-93.

12. Sciorati C, Touvier T, Buono R, Pessina P, Francois S, Perrotta C *et al.* Necdin is expressed in cachectic skeletal muscle to protect fibers from tumor-induced wasting. *J Cell Sci* 2009; **122**(Pt 8)**:** 1119-25.

13. Pessina P, Conti V, Pacelli F, Rosa F, Doglietto GB, Brunelli S *et al.* Skeletal muscle of gastric cancer patients expresses genes involved in muscle regeneration. *Oncol Rep* 2010; **24**(3)**:** 741-5.

14. Tonlorenzi R, Dellavalle A, Schnapp E, Cossu G, Sampaolesi M. Isolation and characterization of mesoangioblasts from mouse, dog, and human tissues. *Curr Protoc Stem Cell Biol* 2007; **Chapter 2:** Unit 2B 1.

15. Brunelli S, Tagliafico E, De Angelis FG, Tonlorenzi R, Baesso S, Ferrari S *et al.* Msx2 and necdin combined activities are required for smooth muscle differentiation in mesoangioblast stem cells. *Circ Res* 2004; **94**(12)**:** 1571-8.

16. Dellavalle A, Sampaolesi M, Tonlorenzi R, Tagliafico E, Sacchetti B, Perani L *et al.* Pericytes of human skeletal muscle are myogenic precursors distinct from satellite cells. *Nat Cell Biol* 2007; **9**(3)**:** 255-67.

17. Brunelli S, Rovere-Querini P. The immune system and the repair of skeletal muscle. *Pharmacol Res* 2008; **58**(2)**:** 117-21.

18. Peault B, Rudnicki M, Torrente Y, Cossu G, Tremblay JP, Partridge T *et al.* Stem and progenitor cells in skeletal muscle development, maintenance, and therapy. *Mol Ther* 2007; **15**(5)**:** 867-77.

19. Cossu G, Biressi S. Satellite cells, myoblasts and other occasional myogenic progenitors: possible origin, phenotypic features and role in muscle regeneration. *Semin Cell Dev Biol* 2005; **16**(4-5)**:** 623-31.

20. Gargioli C, Coletta M, De Grandis F, Cannata SM, Cossu G. PlGF-MMP-9-expressing cells restore microcirculation and efficacy of cell therapy in aged dystrophic muscle. *Nat Med* 2008; **14**(9)**:** 973-8.

21. Brunelli S, Sciorati C, D'Antona G, Innocenzi A, Covarello D, Galvez BG *et al.* Nitric oxide release combined with nonsteroidal antiinflammatory activity prevents muscular

dystrophy pathology and enhances stem cell therapy. *Proc Natl Acad Sci U S A* 2007; **104**(1)**:** 264-9.

22. Donati C, Cencetti F, De Palma C, Rapizzi E, Brunelli S, Cossu G *et al.* TGFbeta protects mesoangioblasts from apoptosis via sphingosine kinase-1 regulation. *Cell Signal* 2009; **21**(2)**:** 228-36.

23. Palumbo R, Galvez BG, Pusterla T, De Marchis F, Cossu G, Marcu KB *et al.* Cells migrating to sites of tissue damage in response to the danger signal HMGB1 require NF-kappaB activation. *J Cell Biol* 2007; **179**(1)**:** 33-40.

24. Sciorati C, Galvez BG, Brunelli S, Tagliafico E, Ferrari S, Cossu G *et al.* Ex vivo treatment with nitric oxide increases mesoangioblast therapeutic efficacy in muscular dystrophy. *J Cell Sci* 2006; **119**(Pt 24)**:** 5114-23.

25. Galvez BG, Sampaolesi M, Brunelli S, Covarello D, Gavina M, Rossi B *et al.* Complete repair of dystrophic skeletal muscle by mesoangioblasts with enhanced migration ability. *J Cell Biol* 2006; **174**(2)**:** 231-43.

26. Zhu N-L, Wang J, Tsukamoto H. The Necdin-Wnt pathway causes epigenetic peroxisome proliferator-activated receptor gamma repression in hepatic stellate cells. *Journal of Biological Chemistry* 2010; **285**(40)**:** 30463-30471.

27. Tseng Y-H, Butte AJ, Kokkotou E, Yechoor VK, Taniguchi CM, Kriauciunas KM *et al.* Prediction of preadipocyte differentiation by gene expression reveals role of insulin receptor substrates and necdin. *Nature Cell Biology* 2005; **7**(6)**:** 601-611.

28. Uezumi A, Fukada S-i, Yamamoto N, Takeda Sai, Tsuchida K. Mesenchymal progenitors distinct from satellite cells contribute to ectopic fat cell formation in skeletal muscle. *Nature Cell Biology* 2010; **12**(2)**:** 143-152.

29. Biressi S, Rando TA. Heterogeneity in the muscle satellite cell population. *Seminars in cell & developmental biology* 2010.

30. Hoshiya H, Kazuki Y, Abe S, Takiguchi M, Kajitani N, Watanabe Y *et al.* A highly stable and nonintegrated human artificial chromosome (HAC) containing the 2.4 Mb entire human dystrophin gene. *Mol Ther* 2009; **17**(2)**:** 309-17.

31. Weber J. Immunotherapy for melanoma. *Curr Opin Oncol* 2011; **23**(2)**:** 163-9.

32. Chapman EJ, Knowles MA. Necdin: a multi functional protein with potential tumor suppressor role? *Mol Carcinog* 2009; **48**(11)**:** 975-81.

33. Tagliafico E, Brunelli S, Bergamaschi A, De Angelis L, Scardigli R, Galli D *et al.* TGF{beta}/BMP activate the smooth muscle/bone differentiation programs in mesoangioblasts. *J Cell Sci* 2004; **117**(Pt 19)**:** 4377-4388.

Figure 1

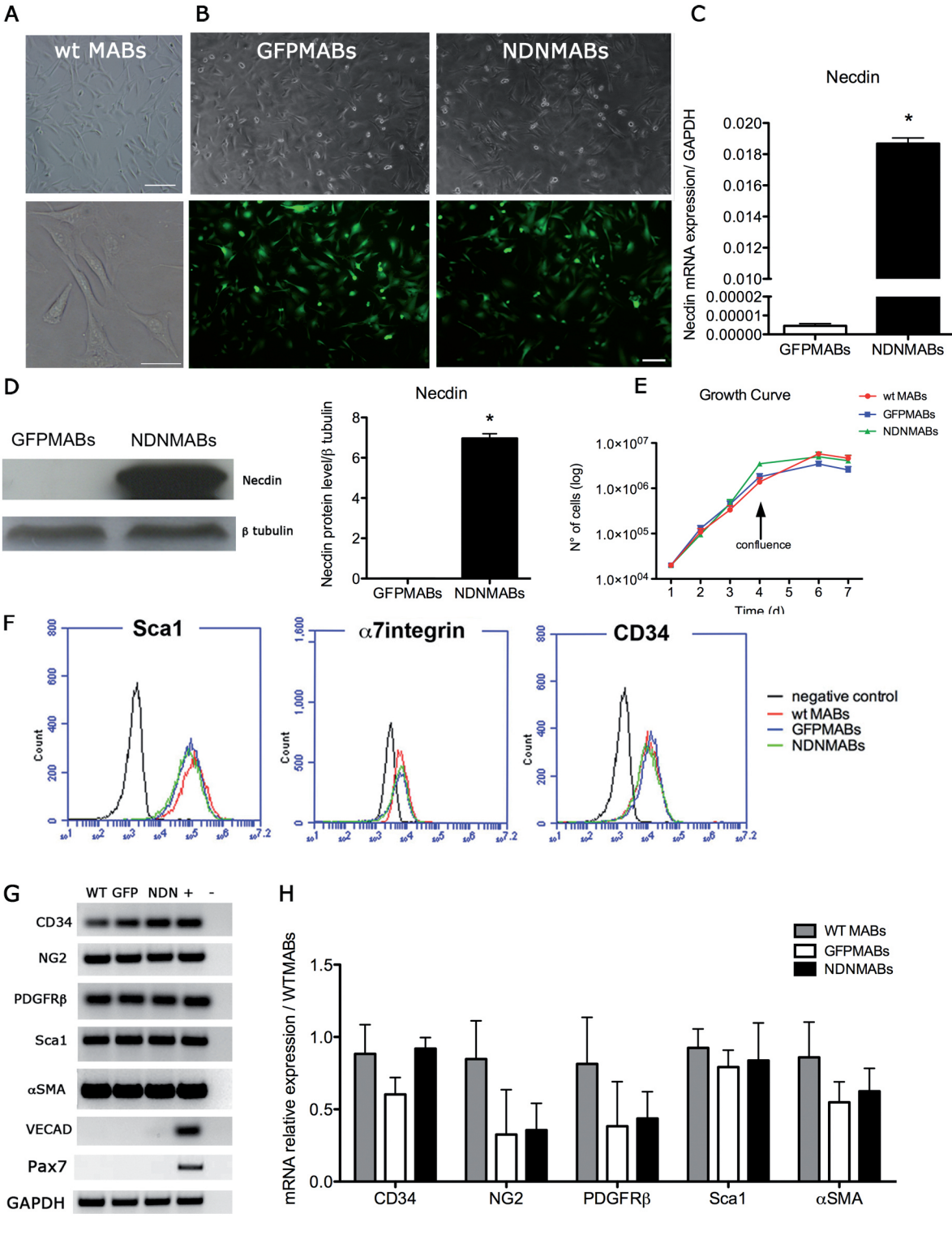
A
B
C
wt MABs
GFPMABs
NDNMABs
Necdin
Necdin mRNA expression/ GAPDH
0.020
0.018
0.016
0.014
0.012
0.010
0.00002
0.00001
0.00000
*
GFPMABs
NDNMABs
D
E
GFPMABs
NDNMABs
Necdin
β tubulin
Necdin protein level/β tubulin
Growth Curve
wt MABs
GFPMABs
NDNMABs
N° of cells (log)
confluence
Time (d)
F
Sca1
α7integrin
CD34
Count
negative control
wt MABs
GFPMABs
NDNMABs
G
H
WT GFP NDN + -
CD34
NG2
PDGFRβ
Sca1
αSMA
VECAD
Pax7
GAPDH
mRNA relative expression / WTMABs
WT MABs
GFPMABs
NDNMABs
CD34
NG2
PDGFRβ
Sca1
αSMA

Figure 2

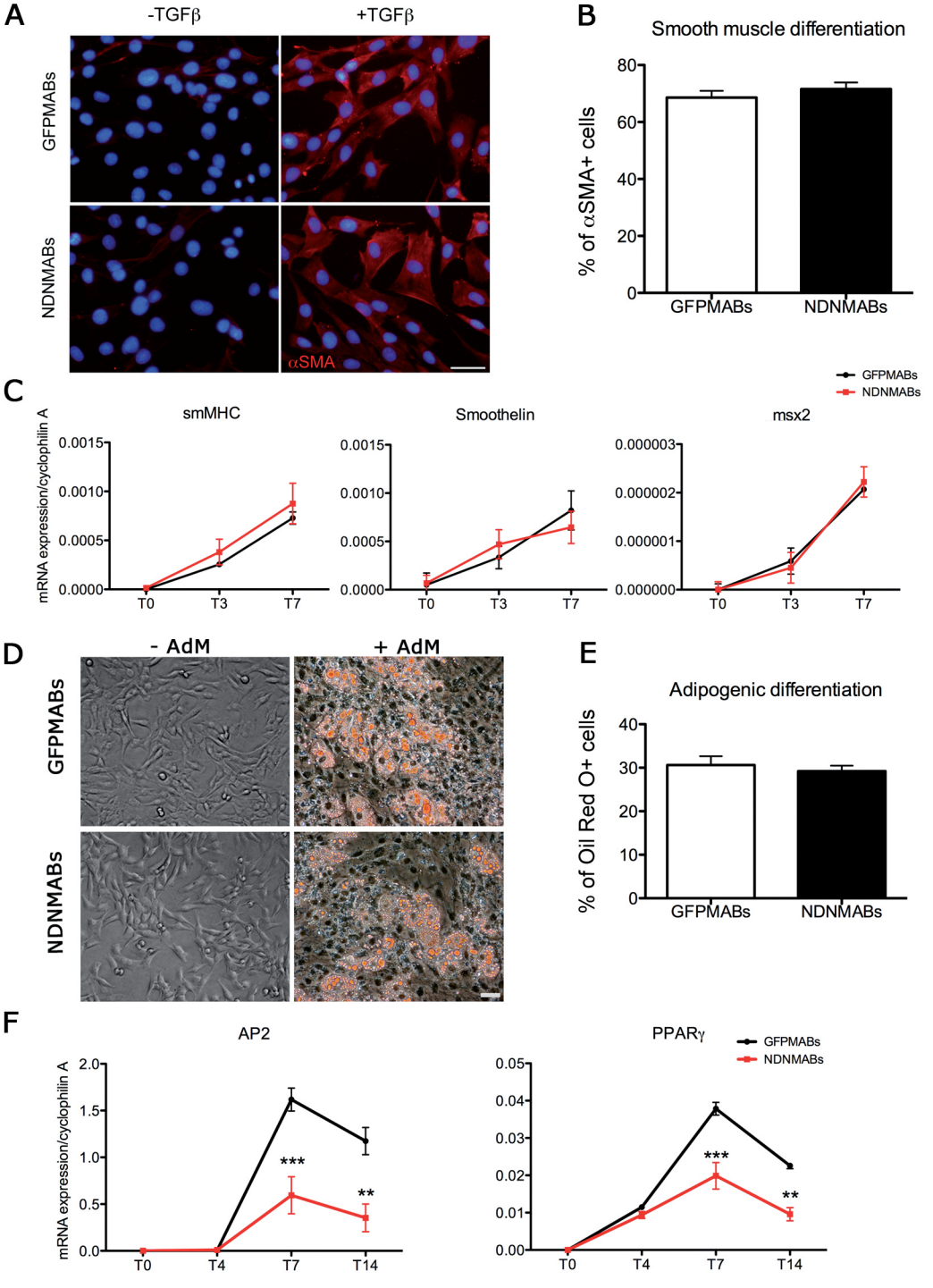
A
-TGFβ
+TGFβ
GFPMABs
NDNMABs
αSMA
B
Smooth muscle differentiation
% of αSMA+ cells
80
60
40
20
0
GFPMABs
NDNMABs
C
GFPMABs
NDNMABs
smMHC
Smoothelin
msx2
mRNA expression/cyclophilin A
0.0015
0.0010
0.0005
0.0000
0.000003
0.000002
0.000001
0.000000
T0
T3
T7
D
- AdM
+ AdM
GFPMABs
NDNMABs
E
Adipogenic differentiation
% of Oil Red O+ cells
40
30
20
10
0
GFPMABs
NDNMABs
F
AP2
PPARγ
GFPMABs
NDNMABs
mRNA expression/cyclophilin A
2.0
1.5
1.0
0.5
0.0
0.05
0.04
0.03
0.02
0.01
0.00
***
**
T0
T4
T7
T14

Figure 3

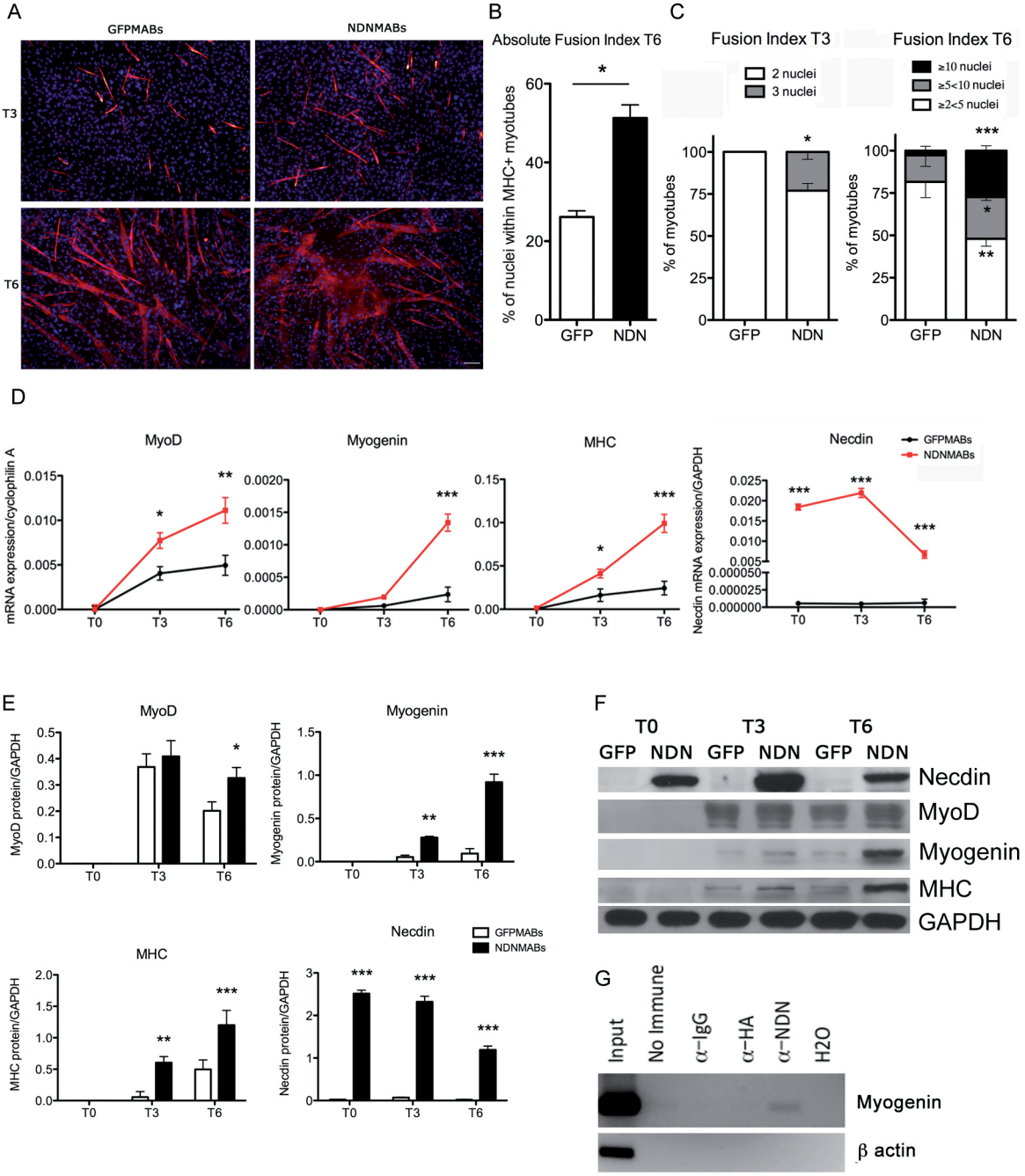
A
GFPMABs
NDNMABs
T3
T6
B
Absolute Fusion Index T6
% of nuclei within MHC+ myotubes
GFP
NDN
C
Fusion Index T3
Fusion Index T6
2 nuclei
3 nuclei
≥10 nuclei
≥5<10 nuclei
≥2<5 nuclei
% of myotubes
D
MyoD
Myogenin
MHC
Necdin
GFPMABs
NDNMABs
mRNA expression/cyclophilin A
Necdin mRNA expression/GAPDH
T0
T3
T6
E
MyoD protein/GAPDH
Myogenin protein/GAPDH
MHC protein/GAPDH
Necdin protein/GAPDH
F
T0
T3
T6
GFP
NDN
Necdin
MyoD
Myogenin
MHC
GAPDH
G
Input
No Immune
α-IgG
α-HA
α-NDN
H2O
Myogenin
β actin

Figure 4

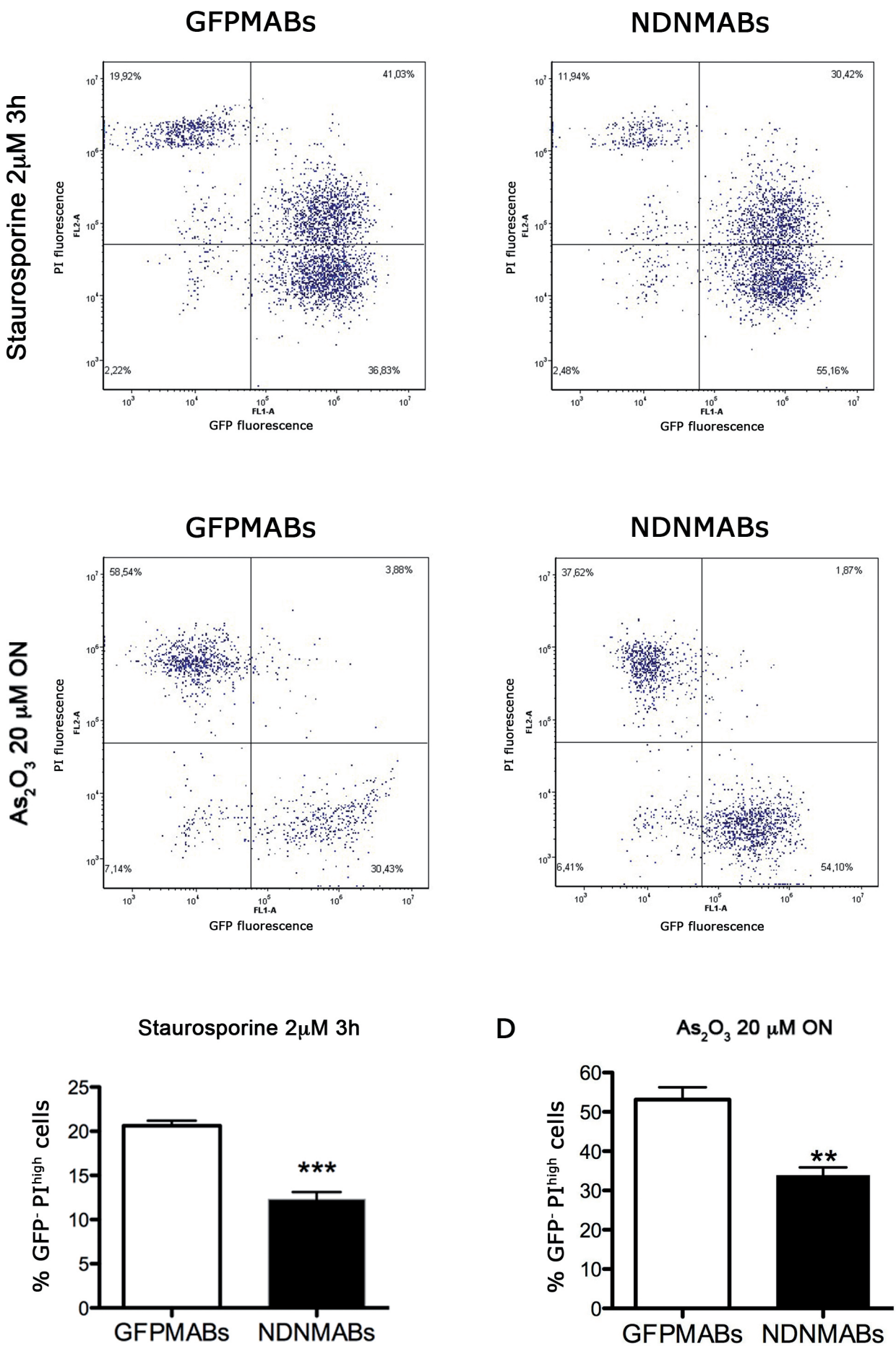
A
GFPMABs
NDNMABs
Staurosporine 2μM 3h
19,92%
41,03%
2,22%
36,83%
11,94%
30,42%
2,48%
55,16%
PI fluorescence
FL2-A
FL1-A
GFP fluorescence
B
GFPMABs
NDNMABs
As2O3 20 μM ON
58,54%
3,88%
7,14%
30,43%
37,62%
1,87%
6,41%
54,10%
C
Staurosporine 2μM 3h
% GFP- PIhigh cells
***
GFPMABs
NDNMABs
D
As2O3 20 μM ON
**

Figure 5

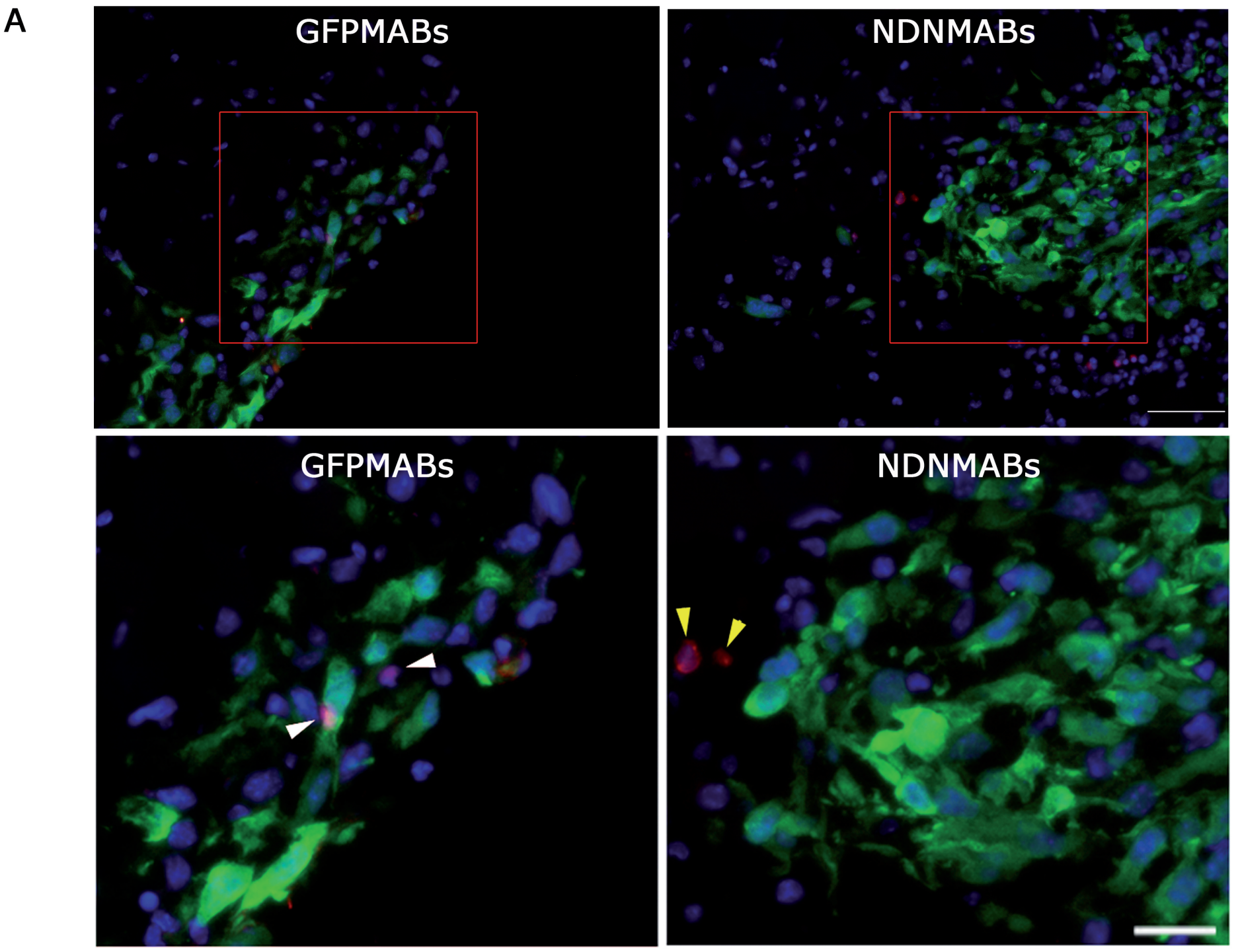
A
GFPMABs
NDNMABs
GFPMABs
NDNMABs

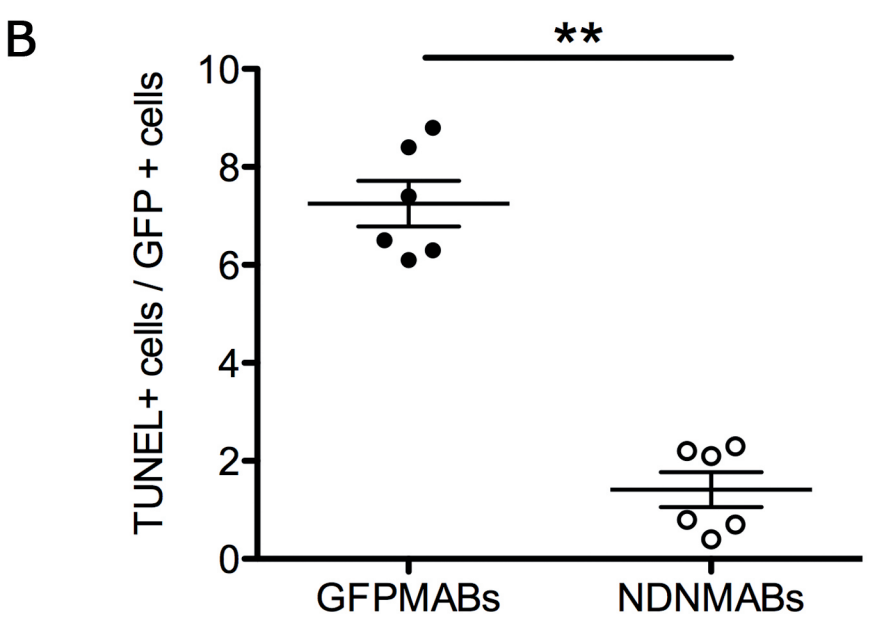
B
**
TUNEL+ cells / GFP + cells
10
8
6
4
2
0
GFPMABs
NDNMABs

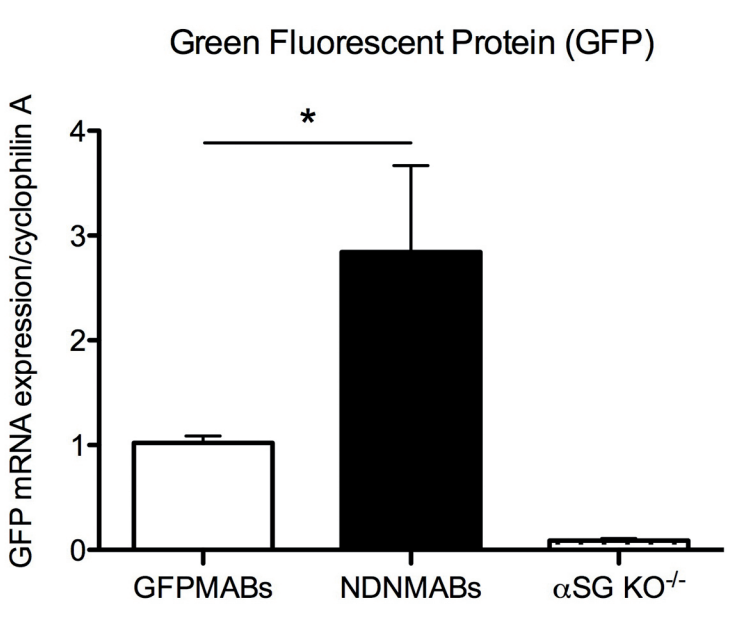
C
Green Fluorescent Protein (GFP)
*
GFP mRNA expression/cyclophilin A
4
3
2
1
0
GFPMABs
NDNMABs
αSG KO-/-

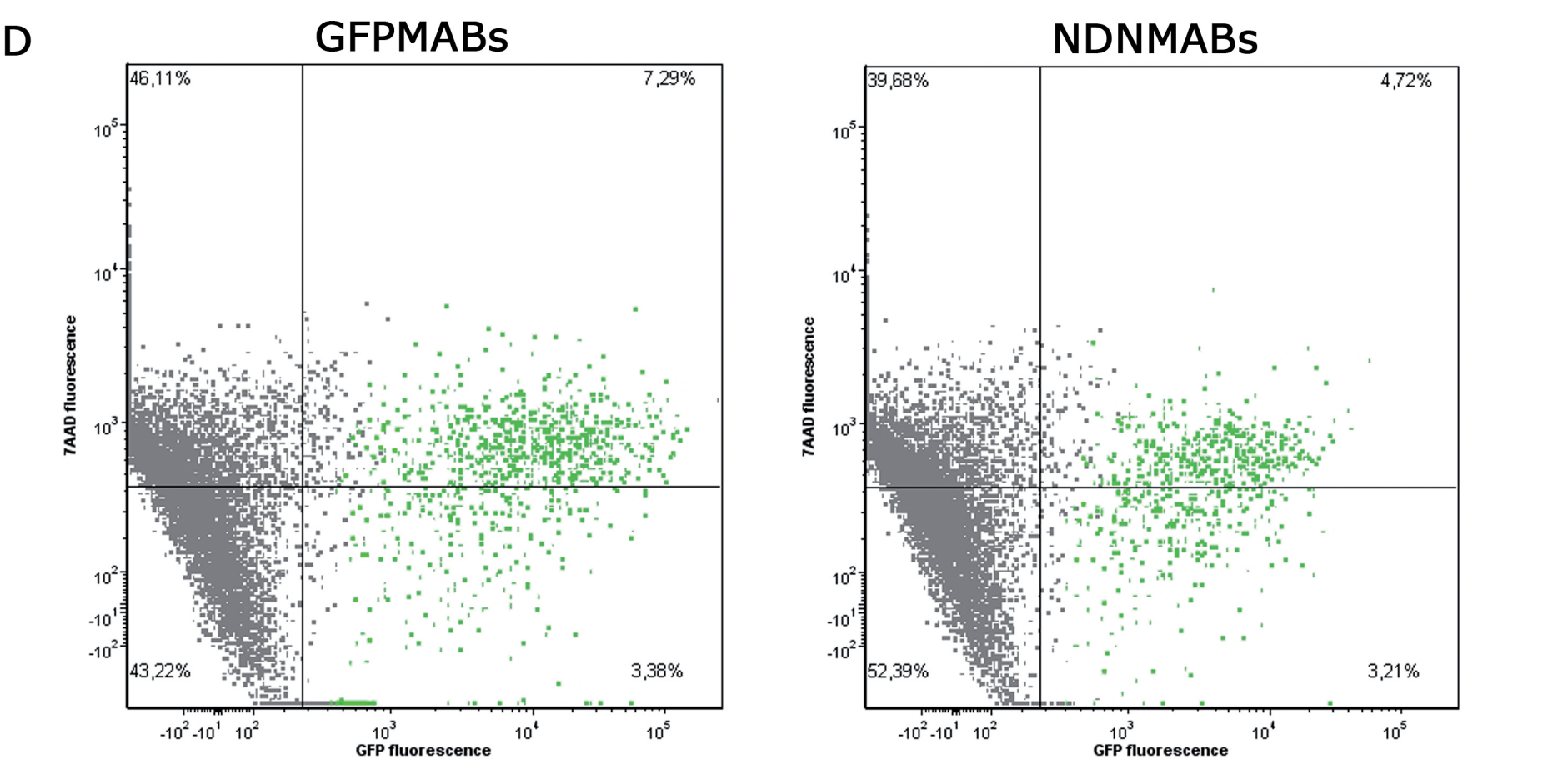
D
GFPMABs
NDNMABs
46,11%
7,29%
43,22%
3,38%
39,68%
4,72%
52,39%
3,21%
7AAD fluorescence
GFP fluorescence

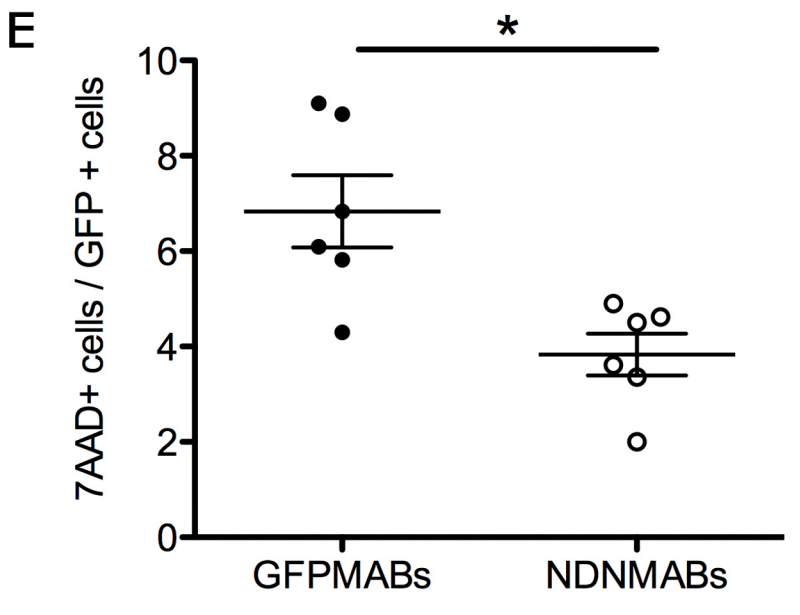
E
*
7AAD+ cells / GFP + cells
10
8
6
4
2
0
GFPMABs
NDNMABs

Figure 6

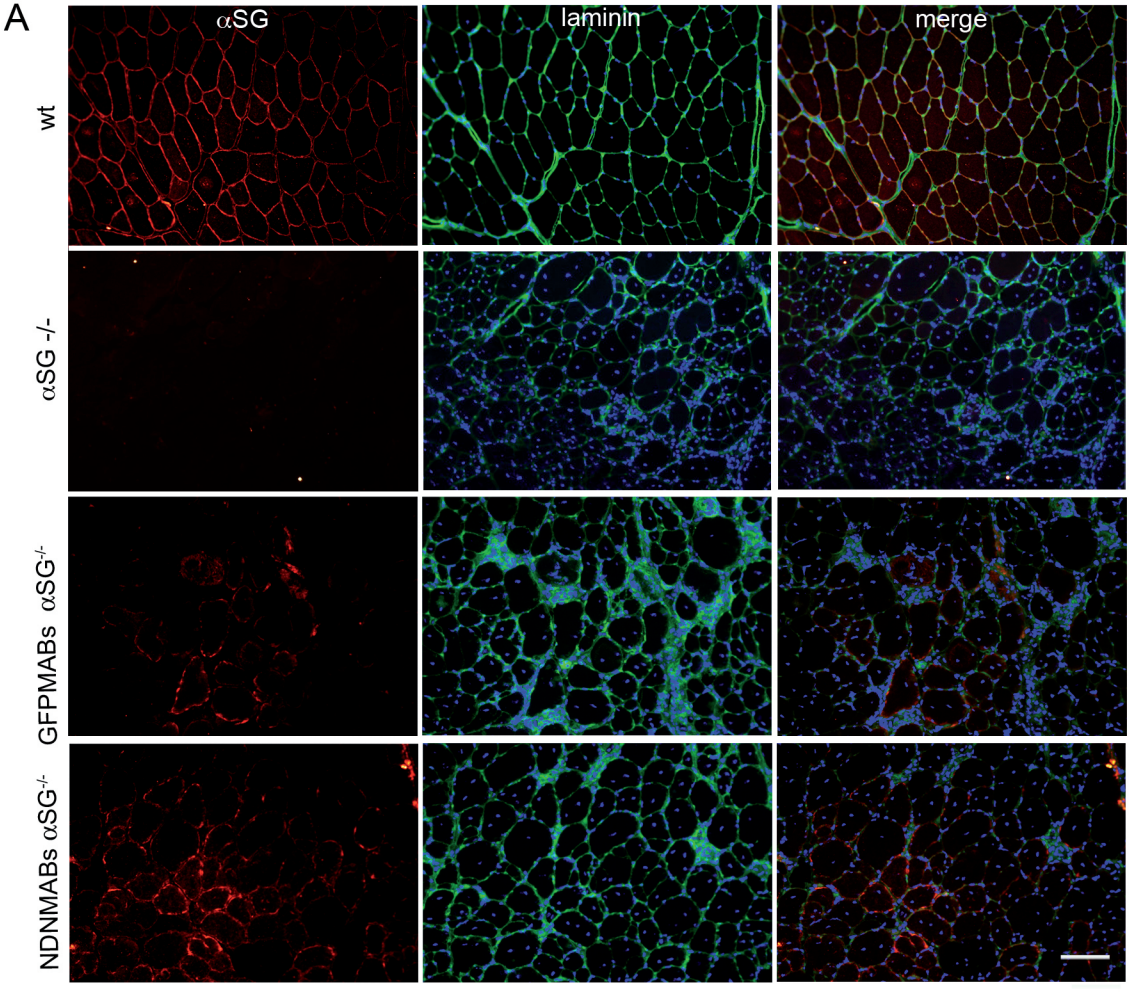
A
αSG
laminin
merge
wt
αSG -/-
αSG-/- GFPMABs
αSG-/- NDNMABs

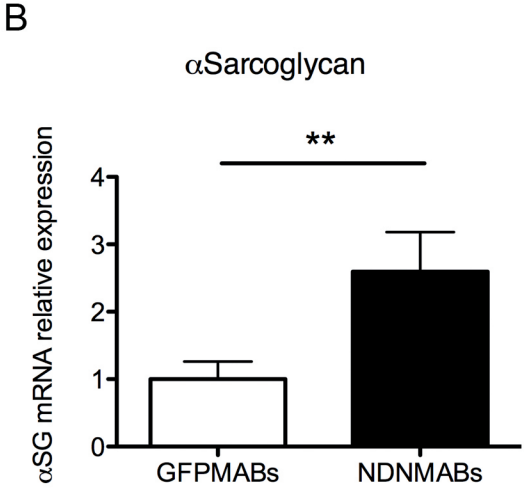
B
αSarcoglycan
αSG mRNA relative expression
**
4
3
2
1
0
GFPMABs
NDNMABs

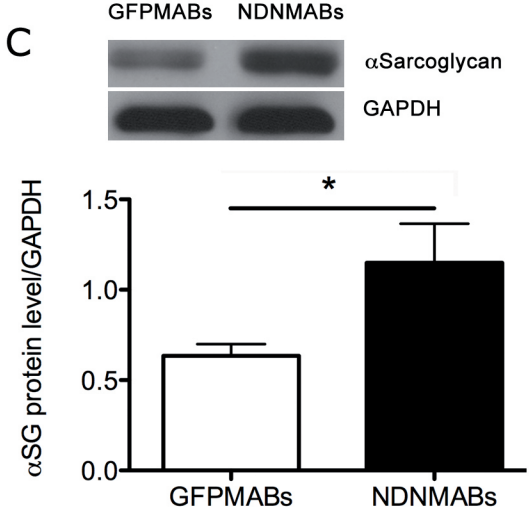
C
GFPMABs
NDNMABs
αSarcoglycan
GAPDH
αSG protein level/GAPDH
*
1.5
1.0
0.5
0.0
GFPMABs
NDNMABs

Figure Legends

Figure 1. Generation and characterization of mesoangioblasts overexpressing necdin. (A) Phase-contrast morphology of proliferating adult-derived MABs (wt MABs). Top and bottom images show different magnifications. Scale bar: 100 μm (top) and 50 μm (bottom). (B) Mesoangioblasts were transduced with a recombinant lentivirus expressing only GFP (GFPMABs) (left column) as a control or with recombinant lentivirus to over-express necdin constitutively (NDNMABs) (right column). GFP fluorescence was evaluated 24h after the infection. Top row: bright field images; bottom row: fluorescence microscopy images. Scale bar: 100 μm. (C) Necdin mRNA level was measured by qPCR and expressed as fold increase versus GAPDH. Error bars represent s.e.m. of five independent experiments; *$p<0.001$ vs GFPMABs. (D) Representative western blot analysis of necdin expression in GFPMABs and NDNMABs (left). Results from five independent experiments were quantified by densitometry analysis (right) and expressed as fold increase over b-tubulin. *$p<0.05$ vs GFPMABs. (E) Growth curves of wt MABs, GFPMABs and NDNMABs plotted on a logarithmic scale: the lines are for the most part overlapping, indicating that there was no significant change in the growth rates of the newly generated MABs

lines compared to wt MABs. Viable cells were counted every 24 hours for 7 days. Results were expressed as mean ± s.e.m. of duplicate samples of five independent experiments. (F) Flow cytometric analysis of the three lines of mesoangioblasts using SCA1, α7integrin and CD34 antibodies. Black line is a negative control. (G) RT-PCR and (H) qPCR on proliferating cells using primers specific for typical MABs markers in order to compare wt MABs (wt), GFPMABs (GFP) and NDNMABs (NDN). In H all data points were calculated in triplicate as gene expression relative to the expression of WTMABs. Data are represented as the mean ± s.e.m of five independent experiments.

Figure 2. Necdin partially influence adipogenic but not smooth muscle differentiation of mesoangioblasts (A) Smooth muscle differentiation was induced by treating mesoangioblasts with 5ng/ml of TGFβ for seven days. Immunofluorescence with an antibody specific for αSMA (red) was performed on control and TGFβ-treated GFPMABs (top) and NDNMABs (bottom). Nuclei were stained with Hoechst (blue). Scale bar: 100 μm. (B) Histogram representing the percentage of αSMA positive TGFβ-treated mesoangioblasts over the

total number of cells. An average value was determined by counting cells in at least ten microscopic fields (150-190 cell/field). Results were expressed as mean ± s.e.m. of five independent experiments. (C) qPCR on cells undergoing smooth muscle differentiation 0, 3 and 7 days after addition of the differentiation medium (T0, T3, T7), using primers specific for smMHC, smoothelin and msx2. All data points were calculated in triplicate as gene expression relative to endogenous cyclophilin A expression. Data are represented as the mean ± s.e.m of five independent experiments.

(D) Adipogenic differentiation was induced by treating cells with a specifically-formulated medium for up to 14 days (AdM). Confirmation of terminal adipogenesis differentiation was made by the Oil Red O staining, that highlights lipidic vacuoles in the cytoplasm. Scale bars: 100 μm (E) Histogram representing the percentage of mesoangioblasts positive for Oil Red O staining, after treatment with the adipogenic medium, over the total number of cells. An average value was determined by counting cells in at least ten microscopic fields (170-200 cell/field). Results were expressed as mean ± s.e.m of five independent experiments. $^{**}p<0.005$, $^{***}p<0.0005$. (F) qPCR on cells undergoing adipogenic differentiation, at day 0, 4, 7 and T14 after addition of the

differentiation medium (T0, T4, T7, T14) using primers specific for the adipocyte marker aP2 and PPARγ. All data points were calculated in triplicate as gene expression relative to endogenous cyclophilin A expression. Data are represented as the mean ± s.e.m of five independent experiments; $**p<0.01$, $***p<0.001$.

Figure 3. Necdin enhances myogenic differentiation (A) Skeletal muscle differentiation assay. GFPMABs (left column) and NDNMABs (right column) were cultured for three (T3, top row) and six (T6, bottom row) days in differentiating medium (DMEM with 2% Horse Serum). Immunofluorescence was performed with a specific antibody against Myosin Heavy Chain (MF20) (red). Nuclei were stained with Hoechst (blue). Scale bar: 100 μm. (B) Absolute fusion index was determined at T6 counting the percentage of MHC-positive nuclei over the total number of nuclei. An average value was determined by counting cells in at least ten microscopic fields (500-700 cells/field). Results were expressed as mean ± s.e.m. of five independent experiments. $*p<0.05$. (C) Relative fusion index was determined at three (T3, left) and six (T6, right) days in differentiating medium by counting the number of MHC-positive myotubes, according to the number of nuclei per cell. Results were expressed as

the mean ± s.e.m. of five independent experiments. *p<0.05, **p<0.005, ***p<0.0005. (D) Time course of skeletal muscle differentiation was evaluated by qPCR analysis for MyoD, Myogenin, MHC and necdin expression in GFPMABs and NDNMABs. All data points were calculated in triplicate as gene expression relative to endogenous cyclophilin A (for MyoD, Myogenin and MHC) or GAPDH (for Necdin) expression. Data are represented as the mean ± s.e.m of five independent experiments. *p<0.05; **p<0.01, ***p<0,001. (E-F) Western blot analysis with specific antibodies against MyoD, myogenin, MHC and Necdin in GFPMABs and NDNMABs at different time points during skeletal muscle differentiation. GAPDH protein level was used as an internal loading control. Graphs (E) show mean values ± s.e.m. obtained from the ratio of densitometric values of protein/GAPDH bands on the blot of the same experiments. Data are representative of five independent experiments. *p<0.05; **p<0.01, ***p<0,001. The western in panel (F) shows a representative experiment. (G) Soluble chromatin was prepared from cultures of NDNMABs differentiated for 72h in differentiating medium, and immunoprecipitated with an antibodies specific for necdin. Parallel extracts were exposed to rabbit IgG and to rabbit HA as control for nonspecific precipitation of chromatin.

Precipitated genomic DNA was analyzed by PCR, using primers designed to amplify sequences in the myogenin promoter. Input refers to DNA input control in which PCR amplification was performed before immunoprecipitation. A sample where no antibody was used for immunoprecipitation was run in parallel (no Immune).

Figure 4. Necdin expression confers an improved cell survival *in vitro* Cell death of GFPMABs and NDNMABs was induced by treating cells with staurosporine (2 μM) for three hours (A-C) or As2O3 (20μM) overnight (B-D). Percentage of dead cells (GFP^- PI^{high}) and apoptosing cells (GFP^+ PI^{low}) was evaluated by FACS analysis, measuring Propidium Iodide (PI) incorporation. (A-B) Dot plots relative to representative experiments. (C-D) Charts representing the number of dead cells (GFP^- PI^{high}) after staurosporine (C) or As2O3 (D). Error bars represent means ± s.e.m. of six independent experiments. $^{**}p<0.005$, $^{***}p<0.0005$.

Figure 5. Necdin expression increases engrafted mesoangioblasts survival *in vivo* (A-B) $5x10^5$ MABs were injected intra-muscularly into tibialis anterior of 4-month-old a-sarcoglycan null (α-$SG^{-/-}$) mice.

After 24 hours muscles were collected and OCT-embedded. Cryosections of GFPMABs-injected (left column) or NDNMABs-injected (right column) muscles were stained for TUNEL (red) and Hoechst (blue) and immunofluorescence was performed using a GFP specific antibody (green). Top and bottom rows show different magnifications. Scale bars: 50 μm (top) and 25 μm (bottom). (B) The graph shows the number of TUNEL+ GFP+ cells over the total number of GFP+ cells. An average value was determined by counting cells in at least ten microscopic fields (100-150 GFP-positive cells/field). Values shown are the means ± s.e.m. of experiments on 6 animals. $^{**}p<0.001$ vs GFPMABs-injected muscles. (C) GFPMABs or NDNMABs ($7x10^5$) were injected intra-muscularly into the gastrocnemius of 4-month-old α-$SG^{-/-}$ mice. After 24 hours muscles were collected and the number of surviving and transcriptionally active mesoangioblasts was evaluated by qPCR using specific primer for GFP. Data were calculated by comparing the level of GFP messenger in each injected-muscle sample with that corresponding to the total input of injected cells. All data points were calculated in triplicate as gene expression relative to endogenous cyclophilin expression. Values shown are the means ± s.e.m. of experiments on 6 animals per group. $^{*}p<0.05$ vs GFPMABs-injected muscles. (D)

Muscles of α-SG$^{-/-}$ mice intra-muscularly injected with mesoangioblasts were digested to single cell suspension and cells were stained with 7-amino-actinomycin D (7AAD). FACS analysis was performed in order to quantify the amount of apoptotic mesoangioblasts (7AAD positive cells) within the population of the GFP positive cells. (E) The graph shows the percentage of 7AAD+ cells over the total number of GFP+ cells. Values shown are the means ± s.e.m. of experiments on 6 animals. *p<0.01 vs GFPMABs-injected muscles.

Figure 6. Necdin expression leads to an improved mesoangioblasts mediated reconstitution of the dystrophic muscle. (A) Immunofluorescence with specific antibodies for α-SG (red) and Laminin (green) on sections of Tibialis Anterior of α-SG$^{-/-}$ mice (n=21) sacrificed 14 days after intra-muscular injection of 5x10^5 mesoangioblasts. Nuclei were stained with Hoechst (blue). The panel shows immunofluorescence on Tibialis Anterior of wt mouse, α-SG$^{-/-}$ mouse and α-SG$^{-/-}$ mice injected with GFPMABs or NDNMABs. Representative sections are shown. Scale bar: 100 μm. (B) α-SG expression, evaluated by qPCR, in quadriceps of α-SG$^{-/-}$ mice injected

with $7x10^5$ GFPMABs or NDNMABs. All data points were calculated in triplicate as α-SG expression relative to muscles injected with GFPMABs. The values indicated in the chart are the means ± s.e.m. of experiments on 14 animals. $^{**}p<0.005$ vs GFPMABs-injected muscles. (C) Western blot analysis with an antibody specific for α–sarcoglycan on muscles of α-$SG^{-/-}$ mice sacrificed 14 days after intra-muscular injection of $7x10^5$ mesoangioblasts. GAPDH protein level was used as an internal loading control. Graph shows mean values ± s.e.m. obtained from the ratio of the densitometric values of protein/GAPDH bands of experiments on 10 animals. The image shows a representative experiment. $^{*}p<0.01$ vs GFPMABs-injected muscles.

Supplementary figure 1. (**A**) Necdin expression in the different lines of infected mesoangioblasts (6 lines overexpressing Necdin and 4 control lines) was determined by qPCR. All data points were calculated in triplicate as gene expression relative to endogenous GAPDH expression.The graph is representative of six independent experiments. (**B**) qPCR analysis with primers specific for CD34, NG2, PDGFRβ, Sca1, αSMA, Pax7 and VE-cadherin. cDNA from total embryo (day E13.5) was used as a positive control. All data points were calculated in triplicate as fold change respect to endogenous cyclophilinA expression. Data are represented as the mean ± s.e.m of five independent experiments.

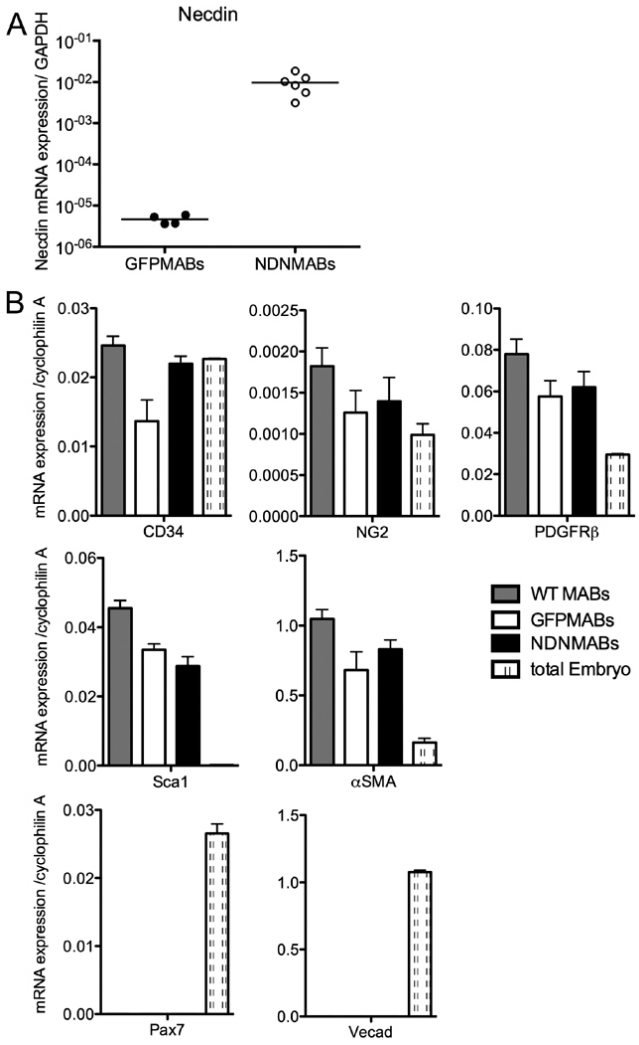

Supplementary figure 2. (**A**) Flow cytometry-gating strategy for the *in vitro* analysis. After specific death-inducing treatments, MABswere detached and stained with Propidium Iodide (PI). On the basis of physical parameters (forward and side light scatter, FSC and SSC) a gate was set to exclude aggregates (R1) and subcellular debris (R2). Quadrant boundaries were set using appropriate positive and negative controls.**(B)**Flow cytometry-gating strategy for the *in vivo* analysis.Single cell suspension from dissociated muscles was firstly gated to exclude undesired large particles and clusters of cells (R1). In R1, gating was performed by excluding subcellular debris from a plot of light scatter characteristics (R2). In the R2 population GFP fluorescence was plotted against 7AAD fluorescence. Quadrant boundaries were set using appropriate positive and negative controls.

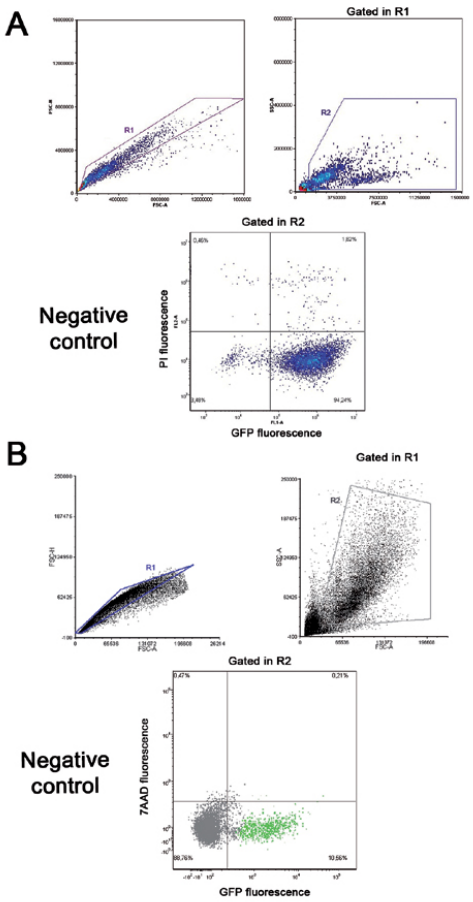

Supplementary figure 3. (**A**) Immunofluorescence with specific antibodies against GFP (top panel, green) or Necdin (bottom panel, green) on sections of tibialis anterior of aSG$^{-/-}$mice injected with 5x10^{5}GFPMABs orNDNMABs and sacrificed the day after the injection. Nuclei were stained with Hoechst (blue). Scale bars: 50 µm (top panel) and 100 µm (bottom panel). (**B**) Immunofluorescence with an antibody specific for GFP (green) on sections of tibialis anterior of aSG$^{-/-}$mice injected with 5x10^{5}GFPMABs orNDNMABs and sacrificed 14 days later. Nuclei were stained with Hoechst (blue). Scale bar: 25µm. (**C**) Immunofluorescence with an antibody specific for the pan monocyte/macrophage marker CD68 (red) on sections of tibialis anterior of wt mouse, aSG$^{-/-}$ mouse and of aSG$^{-/-}$mice injected with GFPMABs or NDNMABsand sacrificed 14 days after intra-muscular injection of 5x10^5 mesoangioblasts. Nuclei were stained with Hoechst (blue). The panel shows representative sections. Scale bar: 25 µm.

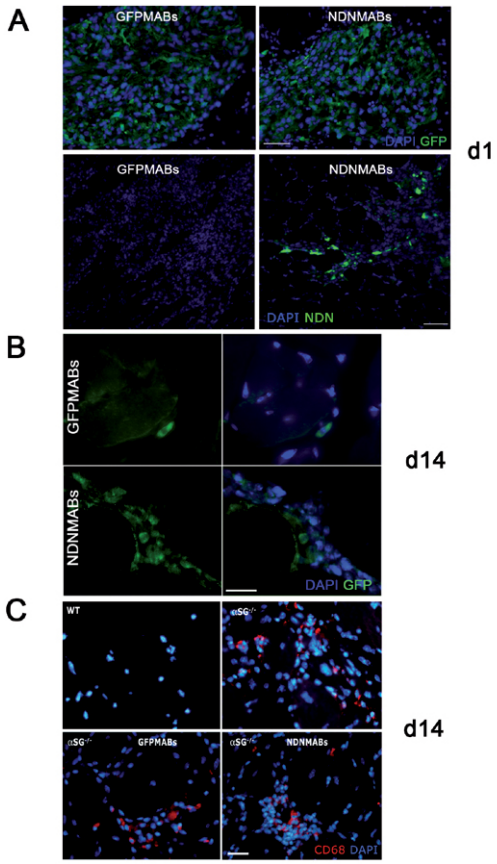

Chapter V. Final Discussion

5.1. Summary

Regeneration of skeletal muscle is sustained by production of new myofibers and satellite cells are indispensable for this process. However, a variety of non-satellite cell types can also participate in skeletal muscle regeneration in the adult. There is much interest in understanding the biology of these progenitors because of their potential use in clinical applications for degenerative diseases such as muscular dystrophies (MD). At the moment the best candidates are mesoangioblasts (MABs). Understanding the basic biology of these cells is mandatory to develop treatment to improve their regenerative potential. To unveil their native identity and physiological role, we used a lineage tracing strategy to label embryonic endothelial progenitors and we demonstrated that haemogenic endothelium harbors a population of progenitors that physiologically contributes to several mesodermal lineages during development, representing the in vivo counterpart of MABs. By following the fate of these cells until adulthood we showed that these cells contribute to subset of myogenic progenitors and take part in muscle regeneration. By using the same genetic system, we analyzed the effects of a pharmacological treatment based on a nitric oxide-donor on the fate of these cells during embryogenesis and during adult regeneration, showing an increased endothelial contribution to myogenesis in both cases.

Moreover, combining current pre-clinical protocols for MABs transplantation with genetic manipulation, we demonstrated that over-expression of the MAGE protein Necdin promotes their survival and myogenic differentiation, resulting in an improved therapeutic efficacy.

5.2. Translational significance and future perspectives

Muscular dystrophies (MD), a heterogeneous group of inherited disorders characterized by progressive muscle wasting and weakness, are one of the most diffuse pathologies with the most frequent form, the Duchenne muscular dystrophy (DMD), affecting around 1 in 3,500 boys worldwide.

Following the identification of dystrophin as the gene responsible for DMD[1], the genes responsible for the large majority of MD have been identified. Nevertheless a resolutive therapy for MD is still lacking, although several different experimental approaches have been attempted.

At present, therapy of MD is based on symptomatic treatment and supportive care: the current treatment consists of glucocorticoid administration, characterized by clinically significant adverse effects.

In the last decades, gene and cell therapy become of great interest in this field of research: in gene therapy, mutated genes are replaced with normal ones, while in stem cell therapy diseased cells are replaced with healthy cells. Although these approaches raised hopes for new treatments for MD, it seems that one single approach is not sufficient to obtain great results (mainly due to the large volume and wide distribution of the target tissue) and that a definitive cure for MD is likely to emerge as a combination of more approaches.

The introduction of stem cells into the field of health sciences become clinically more feasible after the demonstration that, not only embryonic/fetal tissues, but also adult tissues contain cells capable of self-renewal and terminal differentiation. Another important discovery was that adult stem cell residing in a specific tissue are not already committed to one or a few

lineages but can also generate cells of unrelated types. These two concepts together opened new important perspectives.

The treatment of a patient with cell therapy approach can be done in two ways: heterologous/allogeneic transplant and autologous transplant. Both strategies have specific advantages and pitfalls: with the first strategy the patient need to be immunosuppressed to avoid the rejection of exogenous cells; in the second case cells derived from the patients need to be manipulated *in vitro* to correct the genetic defect.

The first approaches of cell therapy for MD were based on satellite cells (SCs), the highly myogenic resident stem cell of the muscle. SCs have been isolated and cultured in vitro, and to be transplanted in vivo they need to be delivered via intramuscular injections, because they lack the ability to cross the muscle endothelium when delivered systemically.

In 1990 the first SC transplant in a DMD patient showed safety and dystrophin production[2]. This promising result triggered a rapid series of clinical trials of SC transplantation for DMD patients. However, although there were no adverse effects, these clinical trials produced very limited positive results and, unfortunately, no clinical benefit[3-14].

In the following years, several research identified three problems that were responsible for the limited results observed: (i) the rapid death of most of the SCs in the first 3 days after transplantation[15-17]; (ii) the fact that SCs do not migrate more than 200 μm away from the intramuscular injection trajectory, implying a huge number of injections to be performed in order to treat a complete muscle[18] and (iii) the described immune responses toward the injected SCs, observed also in the case of major histocompatibility locus coincidence, that led to complete rejection in less that 2

weeks[19,20]. Moreover, it was shown that cyclosporine, used for immunosuppression in several clinical trials, induces apoptosis of the myoblasts at the time of their differentiation[21,22]. Many researches are now ongoing in order to find solutions to overcome these problems. Autologous transplantation of unmodified SCs has recently shown good results in preclinical work in the case of MD affecting only few muscles, such as oculopharyngeal MD[23]. In this cases SCs are isolated from nonaffected muscles and this protocol has entered clinical experimentation.

Considering all the possible impeding factors, the ideal stem cell population for the use in cell therapy protocols for MD needs to satisfy some requisites. It should be present in easily accessible postnatal tissues, expandable in vitro without losing intrinsic characteristics, easily transducible with viral vectors, able to extravasate and reach the damaged skeletal muscle from the blood flow, allowing systemic injections and, of course, able to differentiate into skeletal muscle cells in vivo with high efficiency.

The demonstration that multipotent cell types (different from SCs) can differentiate into skeletal muscle *in vitro* or *in vivo* has created an alternative possibility for the cell therapy of MD. In the last years several progenitors endowed with myogenic potential were identified both in skeletal muscle (pericytes, endothelial cells and interstitial cells) and in other tissues (such as BM or adipose-tissue). These cells have been shown to participate, after transplantation to newly formed myofibers and some of them eventually enter the SC pool.

Amongst these are mesoangioblasts (MABs), mesoderm-derived stem cells associated with small vessels and originally described in the mouse embryonic dorsal aorta. Similar though

not identical cells have been later identified and characterized from postnatal small vessels of mice, rats, dogs and humans. Embryonic and adult MABs have in common the expression of pericyte markers, the anatomical location, the ability to self-renew in culture and to differentiate into various types of mesodermal lineages upon proper culture conditions[24,25]. Preclinical studies in both dystrophic mice and dogs[26,27] provided evidence that MABs have the capacity to functionally ameliorate the dystrophic phenotype. Based on these data, human allogeneic HLA-identical MABs are in a phase I/II clinical trial for the treatment of pediatric DMD patients.

Nowadays, MABs are thus the only cell type, in addition to SCs, that has reached clinical experimentation. However, several points about the biology of these cells are not understood in detail. So far, for example, only theoretical models have been proposed for their *in vivo* developmental origin[28] and still no insights have been given on their role during normal unperturbed development and during physiological and pathological tissue remodelling *in vivo* as well as on their relationship with other mesoderm stem cells. Unraveling these basic questions is of great importance in order to define how to correctly manipulate the fate of these cells and optimize their *in vivo* recruitment and mobilization.

To investigate the role of endothelial derived progenitors *in vivo*, my lab used the cre-loxP recombinase system, crossing a transgenic mouse expressing a tamoxifen inducible Cre recombinase (CRE-ER^{T2}) under the transcriptional control of the VE-Cadherin promoter (specifically active in endothelial progenitors and differentiated endothelial cells[29,30]) to different reporter mice (Rosa26-EYFP or Rosa26-GNZ floxed).

By supplying tamoxifen in utero at embryonic day 8.5 we were able to permanently label a subset of embryonic endothelial progenitors (namely eVE-Cad+ cells) and follow their fate during normal skeletal muscle development and maturation as well as during regeneration after cardiotoxin-induced acute injury. Thus, this model offers a lineage map of cells that at one time (i.e. at E8.5) had expressed VE-Cadherin.

With this system, in our study, we demonstrated, for the first time, the developmental origin of embryonic MABs as a population of cells derived from the haemogenic endothelium. These results strongly prove that the *in vitro* and *in vivo* myogenic and multi-lineage differentiation potential of MABs are not an artifact, but rather an expression of a real differentiation potential that takes part also during normal development (Azzoni et al., submitted – see Chapter II).

Since cell therapy with MABs, although promising, is still far from yielding a complete reconstitution of the skeletal muscle structure and function, it clearly requires improvement, particularly if we consider that human MABs have a finite lifespan in culture and a large number of cells is needed to treat each patient. Thus in the last years a huge amount of research have been done in order to boost the therapeutic efficacy of MABs, acting on different aspects of their biology, such as migration, homing, engraftment and survival within damaged muscles as well as activation, expansion and commitment toward myogenic lineage. To this end, several studies combined cell transplantation with either cell conditioning or genetic manipulation.

Exposure to specific cytochines or chemokines have been described to specifically influence MABs behaviour. For example, treatment with NO, sphingosine-1phosphate (S1P),

stromal-derived factor 1 (SDF1), tumor necrosis factor α (TNFα), HMGB1 or adiponectin improved to different levels and with different mechanisms either proliferation, survival, homing in skeletal muscle and myogenic differentiation of MABs, increasing their therapeutic efficacy[31-35].

About approaches based on genetic manipulation, it has been shown that MABs transfected with vectors leading to the expression of α4 integrin (a key molecule that control rolling and extravasation of leukocytes and other stem cells and that is not expressed by MABs) significantly improves their migration[33]. Other approaches have evaluated the effects of the loss of proteins normally expressed by MABs. For example it has been shown that lack of PW1 dramatically inhibits MABs ability to differentiate in muscle, leading to a defective ability to rescue muscle in dystrophic mice.

In this regard, in our paper (see Chapter IV) we have shown that the MAGE protein Necdin leads to a more efficient reconstitution of the dystrophic muscle by MABs, by promoting their survival and by enhancing their myogenic differentiation. In particular, we found that Necdin acts through a transcriptional regulation of myogenin, in cooperation with MyoD[36].

Another kind of approach that is gaining importance in these years aims at the development of new strategies to activate and mobilize the endogenous stem cells, as an alternative to exogenous stem cell transplantation. Ideally therapeutic approaches based on endogenous stem cell stimulation have distinct advantage since they involve minimal manipulation, do not present problems related to the immune response and are less invasive. Moreover, they would be significantly less expensive and thus affordable to public health systems. While

approaches based on exogenous stem cells have been intensely explored, less is known about the possibility of using endogenous stem cells as a therapeutic strategy but increasing the number of these cells within the regenerating muscle as well as enhancing their activation, mobilization and homing are expected to be beneficial to obtain optimal conditions for muscular recovery.

In addition to the re-activation of the satellite cells, these approaches target also the endogenous vascular associated progenitors (VAPs) (that includes MABs/pericytes and smooth muscle cell progenitors) because these cells are critical to the regeneration process at different levels. They can contribute to muscle regeneration by improving neo-vascularization after damage (thus providing oxigenation and nourishment to the regenerating myofibers), by maintaning an appropriate and hospitable stem cell niche for the satellite cells and by directly contributing to new fibers by direct myogenic differentiation.

The tight physical association between SCs and capillaries raised hypotesis of a continuos interplay between SCs, endothelial cells and VAPs after tissue damage to set up coordinated processes of angiogenesis and myogenesis in a functional manner[37]. Endothelial cell progenitors have been usually considered to originate from the bone marrow, enter the circulation and eventually incorporate in proliferating vessels and in regions of vascular injury. However, indirect evidence suggests that endothelial cell and VAPs may also be present in the mature vasculature[38].

First attempts to directly target endogenous stem cells focused on the use of molecules that have been already shown to modify, at least *in vitro*, muscle and vasculature progenitor

cells, such as nitric oxide, HMGB1, Cripto, specific deacetylase inhibitors, and their analogs.

In our lab, we wanted to analyze the effects of NO on skeletal myogenesis occuring during normal embryonic development as well on skeletal muscle regeneration and to this end we took advantage of the previously described lineage tracing system. As nitric oxide donor we used molsidomine, a direct NO donor belonging to the group of the sydnonimines and already used in humans for the chronic treatment of stable angina. Since the effect of NO on embryonic myogenesis has not been investigated in detail, we firstly demonstrated that the treatment with molsidomine during the whole embryonic development resulted, in newborn mice, into a sort of skeletal muscle hypertophy and this was observed both at the transcriptional and the traslational level. Indeed we observed a decrease of myostatin mRNA (a negative regulator of the muscle mass) and an increased exression of sarcomeric protein (structural protein of the sarcomere).

Then our work focused on the analysis of the effects of molsidomine on the specific population of embryonic endothelial progenitors (eVE-Cad+ cells), that normally contribute to the development to several mesodermal tissues (including smooth and skeletal muscle) and that include cells that we identified as the *in vivo* counterpart of embryonic mesoangioblasts (Azzoni et al., submitted – see chapter II).

In our study, we observed that, after treatment with molsidomine, as early as in E12.5 embryos there is an increased contribution of eVE-Cad+ cells to skeletal myogenesis. Of importance, this increase was accompanied by a decrease of the eVE-Cad+ cells contribution to interstial cells, such as pericytes.

In adult mice, during normal homeostasis, we showed the presence of eVE-Cad+ derived myofibers and interstitial cells (pericytes and PICs), but not satellite cells. Moreover eVE-Cad+ derived cells sorted from adult muscle and cultured *in vitro* were still multipotent and able to give rise, in addition to endothelial networks, also to myotubes, αSMA+ smooth muscle cells and adipocytes.

During the process of muscle regeneration, we proved that eVE-Cad+ derived cells contribute to new myofibers. Most importantly, using a bone marrow transplantation approach, we were able to demonstrate that eVE-Cad+ derived circulating progenitors are responsible of the contribution to new myofibers, while resident eVE-Cad+ derived cells contribute to the development/maturation of the vascular network.

In adult mice treated with molsidomine during the regeneration process, we observed an increased number of labeled myofibers and a better vascular network. These two aspects are both of fundamental importance, indeed the vascular stem cell niche itself has a role in tissue homeostasis and perivascular stem cells as well the vessels themselves contribute to tissue renewal. Our lineage tracing model is a very useful tool because cells that we label represent a subset of endogenous multipotent progenitors that can be ideal target to improve tissue recovery, because they can contribute to skeletal muscle and to neo-angiogenesis. The importance of neo-angiogenesis for tissue homeostasis and repair led to the idea that manipulating these processes could offer therapeutic opportunities for several diseases, including MD, and all informations obtained by these reserches will be surely useful for the definition of a pharmacological treament protocol for MD. Indeed the decrease in muscle perfusion and the resultant

tissue ischemia is a critical component of the mechanisms that leads to myofiber death in MD.

The next step in our study will be to perform lineage tracing studies in mouse models of MD in order to follow the fate of endogenous endothelial progenitors in a context of chronic damage. This will allow us to analyze the effect of molsidomine on the fate of these endogenous stem cells in a situation in which the normal components of the skeletal muscle tissue (myofibers and vessels) are altered.

In addition, several evidences indicate that inflammation plays an important role for the pathogenesis of the dystrophic muscle. Our genetic tool will allow us to verify if treatment with molsidomine can help balancing the pro- versus anti-inflammatory responses, in the perspective of creating a favourable milieu for the subsequent endogenous stem cells activation. It has been already shown that treatment of dystrophic mice with nitric oxide donors in combination with nonsteroidal antiinflammatory drugs (NSAID) has significant and persistent therapeutic effects, through actions on both muscle preservation and regeneration[39,40]. These results suggested that NO together with inhibition of inflammation synergized to yield a novel effective therapy in MD.

In conclusion, given the role of NO in the regulation of skeletal muscle function and its possible effects on endogenous VAPs, suggested from our study, we can postulate that NO treatment could be effective in enhancing the regeneration process, acting on several target cells and with different mechanisms. Thus, the pharmacological approach with NO donor drugs may constitute a solid basis for combinatorial therapies in association with stem cell and, possibly, gene therapy approaches to obtain an enhanced therapeutic benefit.

5.3. References

1. Hoffman EP, Brown RH Jr, Kunkel LM. *Dystrophin: the protein product of the Duchenne muscular dystrophy locus.* Cell. 1987;**51**(6):919-28.
2. Law PK, Bertorini TE, Goodwin TG, Chen M, Fang QW, Li HJ, Kirby DS, Florendo JA, Herrod HG, Golden GS. *Dystrophin production induced by myoblast transfer therapy in Duchenne muscular dystrophy*. Lancet. 1990;**336**(8707):114-115.
3. Law PK, Goodwin TG, Fang QW, Chen M, Li HJ, Florendo JA, Kirby DS. *Myoblast transfer therapy for Duchenne muscular dystrophy*. Acta Paediatr Jpn. 1991; **33**(2):206-215.
4. Law PK, Goodwin TG, Fang Q, Duggirala V, Larkin C, Florendo JA, Kirby DS, Deering MB, Li HJ, Chen M, et al. *Feasibility, safety, and efficacy of myoblast transfer therapy on Duchenne muscular dystrophy boys.* Cell Transplant. 1992; **1**(2-3):235-244.
5. Huard J, Roy R, Bouchard JP, Malouin F, Richards CL, Tremblay JP. *Human myoblast transplantation between immunohistocompatible donors and recipients produces immune reactions.* TransplantProc. 1992;**24**(6):3049-3051.
6. Karpati G, Ajdukovic D, Arnold D, Gledhill RB, Guttmann R, Holland P, Koch PA, Shoubridge E, Spence D, Vanasse M, et al. *Myoblast transfer in Duchenne muscular dystrophy*. Ann Neurol. 1993;**34**(1):8-17.
7. Gussoni E, Pavlath GK, Lanctot AM, Sharma KR, Miller RG, Steinman L, Blau HM. *Normal dystrophin transcripts detected in Duchenne muscular dystrophy patients after myoblast transplantation*. Nature. 1992; **356**(6368):435-438.
8. Tremblay JP, Malouin F, Roy R, Huard J, Bouchard JP, Satoh A, Richards CL. *Results of a triple blind clinical study of myoblast transplantations without immunosuppressive treatment in young boys with Duchenne muscular dystrophy.* Cell Transplant. 1993;**2**(2):99-112.
9. Morandi L, Bernasconi P, Gebbia M, Mora M, Crosti F, Mantegazza R, Cornelio F. *Lack of mRNA and dystrophin expression in DMD patients three months after myoblast transfer*. Neuromuscul Disord. 1995; **5**(4):291-295.
10. Mendell JR, Kissel JT, Amato AA, King W, Signore L, Prior TW, Sahenk Z, Benson S, McAndrew PE, Rice R, et al. *Myoblast transfer in the treatment of Duchenne's muscular dystrophy.* N Engl J Med. 1995;**333**(13):832-838.
11. Miller RG, Sharma KR, Pavlath GK, Gussoni E, Mynhier M, Lanctot AM, Greco CM, Steinman L, Blau HM. *Myoblast implantation in Duchenne muscular dystrophy: the San Francisco study.* Muscle Nerve. 1997; **20**(4):469-478.
12. Skuk D, Goulet M, Tremblay JP. *Use of repeating dispensers to increase the efficiency of the intramuscular myogenic cell injection procedure*. Cell Transplant 2006;**15**(7):659-663.
13. Neumeyer AM, Cros D, McKenna-Yasek D, Zawadzka A, Hoffman EP, Pegoraro E, Hunter RG, Munsat TL, Brown RH Jr. *Pilot study of myoblast transfer in the treatment of Becker muscular dystrophy*. Neurology. 1998; **51**(2):589-592.
14. Partridge T. *The current status of myoblast transfer*. Neurol Sci. 2000; **21**(suppl 5):S939-S942.
15. Huard J, Acsadi G, Jani A, Massie B, Karpati G. *Gene transfer into skeletal muscles by isogenic myoblasts.* Hum Gene Ther 1994; **5**: 949-958.

16. Fan Y, Maley M, Beilharz M, Grounds M. *Rapid death of injected myoblasts in myoblast transfer therapy.* Muscle Nerve. 1996;**19**(7):853-860.
17. Guérette B, Skuk D, Célestin F, Huard C, Tardif F, Asselin I, Roy B, Goulet M, Roy R, Entman M, Tremblay JP. *Prevention by anti-LFA-1 of acute myoblast death following transplantation.* J Immunol. 1997;**159**(5):2522-2531.
18. Skuk D, Roy B, Goulet M, Tremblay JP. *Successful myoblast transplantation in primates depends on appropriate cell delivery and induction of regeneration in the host muscle*. Exp Neurol. 1999;**155**(1):22-30.
19. Huard J, Roy R, Bouchard JP, Malouin F, Richards CL, Tremblay JP. *Human myoblast transplantation between immunohistocompatible donors and recipients produces immune reactions*. TransplantProc. 1992;**24**(6):3049-3051.
20. Guerette B, Asselin I, Vilquin JT, Roy R, Tremblay JP. *Lymphocyte infiltration following allo- and xenomyoblast transplantation in mice.* Transplant Proc 1994; **26**(6): 3461.
21. Hardiman O, Sklar RM, Brown RH Jr. *Direct effects of cyclosporin A and cyclophosphamide on differentiation of normal human myoblasts in culture*. Neurology 1993; **43**: 1432-1434
22. Hong F, Lee J, Song JW, Lee SJ, Ahn H, Cho JJ, et al. (2002). *Cyclosporine blocks muscle differentiation by inducing oxidative stress and by inhibiting the peptidylprolyl-cis-trans-isomerase activity of cyclophilin A: cyclophilin A protects myoblasts from cyclosporine-induced cytotoxicity*. FASEB J. 2002; **16**(12):1633-1635
23. Perie S, Mamchaoui K, Mouly V, et al. *Premature proliferative arrest of cricopharyngeal myoblasts in oculo-pharyngeal muscular dystrophy: therapeutic perspectives of autologous myoblast transplantation*. Neuromuscul Disord 2006;**16**:770-781.
24. De Angelis L, Berghella L, Coletta M, Lattanzi L, Zanchi M, Cusella De Angelis MG, et al. *Skeletal myogenic progenitors originating from embryonic dorsal aorta coexpress endothelial and myogenic markers and contribute to postnatal muscle growth and regeneration*. The Journal of Cell Biology. 1999;**147**(4), 869-878.
25. Minasi MG, Riminucci M, De Angelis L, Borello U, Berarducci B, Innocenzi A, et al. *The meso-angioblast: a multipotent, self-renewing cell that originates from the dorsal aorta and differentiates into most mesodermal tissues.* Development. 2002;**129**(11):2773-83
26. Sampaolesi M, Torrente Y, Innocenzi A, Tonlorenzi R, D'antona G, Pellegrino MA, et al. *Cell therapy of alpha-sarcoglycan null dystrophic mice through intra-arterial delivery of mesoangioblasts*. Science. 2003, **301**(5632), 487-492.
27. Sampaolesi M, Blot S, D'antona G, Granger N, Tonlorenzi R, Innocenzi A, et al. *Mesoangioblast stem cells ameliorate muscle function in dystrophic dogs.* Nature. 2006; **444**(7119), 574-579.
28. Cossu G, & Bianco P. *Mesoangioblasts-vascular progenitors for extravascular mesodermal tissues.* Current Opinion in Genetics & Development. 2003;**13**(5), 537-542.
29. Breier G, Breviario F, Caveda L, Berthier R, Schnürch H, Gotsch U, Vestweber D, Risau W, Dejana E. *Molecular cloning and expression of murine vascular*

endothelial-cadherin in early stage development of cardiovascular system. Blood, 1996; **87**(2):p.630-41.

30. Gory S, Vernet M, Laurent M, Dejana E, Dalmon J, Huber P. *The vascular endothelial-cadherin promoter directs endothelial-specific expression in transgenic mice.* Blood,1999; **93**(1):p.184-92.
31. Sciorati C, Galvez BG, Brunelli S, Tagliafico E, Ferrari S, Cossu G, & Clementi E. *Ex vivo treatment with nitric oxide increases mesoangioblast therapeutic efficacy in muscular dystrophy*. Journal of Cell Science. 2006; **119**(Pt 24), 5114-5123.
32. Donati C, Cencetti F, Nincheri P, Bernacchioni C, Brunelli S, Clementi E, et al. *Sphingosine 1-Phosphate Mediates Proliferation and Survival of Mesoangioblasts*. Stem Cells. 2007; **25**(7), 1713-1719.
33. Galvez BG, Sampaolesi M, Brunelli S, Covarello D, Gavina M, Rossi B, et al. *Complete repair of dystrophic skeletal muscle by mesoangioblasts with enhanced migration ability*. The Journal of Cell Biology. 2006; **174**(2), 231-243.
34. Palumbo R, Sampaolesi M, De Marchis F, Tonlorenzi R, Colombetti S, Mondino A, et al. *Extracellular HMGB1, a signal of tissue damage, induces mesoangioblast migration and proliferation*. The Journal of Cell Biology. 2004;**164**(3), 441-449.
35. Fiaschi T, Tedesco FS, Giannoni E, Diaz-Manera J, Parri M, Cossu G, & Chiarugi P. *Globular adiponectin as a complete mesoangioblast regulator: role in proliferation, survival, motility, and skeletal muscle differentiation.* Molecular Biology of the Cell. 2010;**21**(6), 848-859.
36. Pessina P, Conti V, Tonlorenzi R, Touvier T, Meneveri R, Cossu G, & Brunelli S. *Necdin enhances muscle reconstitution of dystrophic muscle by vessel-associated progenitors, by promoting cell survival and myogenic differentiation.* Cell Death Differ. 2012; 19(**5**):827-38
37. Christov C, Chretien F, Abou-Khalil R, Bassez G, Vallet G, Authier FJ, Bassaglia Y, Shinin V, Tajbakhsh S, Chazaud B et al. *Muscle satellite cells and endothelial cells: close neighbors and privileged partners*. Mol. Biol. Cell 2007; **18**, 1397-1409.
38. Grenier G, Scime A, Le Grand F, Asakura A, Perez–Iratxeta C, Andrade-Navarro MA, Labosky PA, Rudnicki MA. *Resident endothelial precursors in muscle, adipose, and dermis contribute to postnatal vasculogenesis*. Stem Cells 2007; **25**:3101-3110.
39. Brunelli S, Sciorati C, D'Antona G, Innocenzi A, Covarello D, Galvez BG, Perrotta C, Monopoli A, Sanvito F, Bottinelli R, et al. *Nitric oxide release combined with nonsteroidal antiinflammatory activity prevents muscular dystrophy pathology and enhances stem cell therapy*. Proc Natl Acad Sci U S A. 2007;**104**(1):264-9.
40. Sciorati C, Buono R, Azzoni E, Casati S, Ciuffreda P, D'Angelo G, Cattaneo D, Brunelli S, Clementi E. *Co-administration of ibuprofen and nitric oxide is an effective experimental therapy for muscular dystrophy, with immediate applicability to humans*. Br J Pharmacol. 2010; **160**(6):1550-60.

Chapter VI - List of Publications

◊ **Skeletal muscle of gastric cancer patients expresses genes involved in muscle regeneration.**

Patrizia Pessina, Valentina Conti, Fabio Pacelli, Fausto Rosa, Giovan Battista Doglietto, Silvia Brunelli, Maurizio Bossola.

Oncology Reports. 2010; 24(3):741-745.

◊ **Necdin enhances muscle reconstitution of dystrophic muscle by vessel-associated progenitors, by promoting cell survival and myogenic differentiation.**

Patrizia Pessina*, Valentina Conti*, Rossana Tonlorenzi, Thierry Touvier, Raffaella Meneveri, Giulio Cossu and Silvia Brunelli.

*these authors contributed equally to this work

Cell Death and Differentiation 2012 May; 19(5):827-38.

◊ **Hemogenic endothelium generates mesoangioblasts that contribute to several mesodermal lineages in vivo.**

Emanuele Azzoni, Valentina Conti, Arianna Dellavalle, Lara Campana, Ralf H. Adams, Giulio Cossu, Silvia Brunelli.

Under revision in PNAS.

Chapter VII – Acknowledgments

"It's not the adventure that matters as much

as who you spend it with."

Ed eccoci arrivati all'ultima pagina di questa lunga tesi. Sembra quasi un sogno ma ormai ci siamo… e la mia vita da post-doc sta per cominciare. Tante cose sono cambiate in questi ultimi tre anni e fra tutte, soprattutto, sono cambiata molto IO. Quindi voglio spendere qualche parola per ringraziare tutte le persone che hanno contribuito a questo cambiamento.

Non si può certo non iniziare dal mio capo, Silvia – grazie per avermi dato sempre fiducia in tutti questi anni e per avermi dato varie possibilità di crescere, non solo lavorativamente.

Grazie ad Elisabetta Dejana – come "mio mentor" durante questi tre anni mi ha più volte dimostrato che la vera passione per questo lavoro non si perde per strada.

Grazie a Giulio Cossu, a Rossella Gallli e ai rispettivi lab members, con i quali ho condiviso non solo gli spazi fisici del lab, ma anche tutto quello che gira attorno alle lunghe giornate "San Raffaeliane".

Un grazie speciale a Thierry e Paola – siete dei colleghi e delle persone fantastiche! Spero di continuare a lavorare con voi per molto ancora!

Grazie anche a Stephanie e Cristina – nonostante sia mancata la quotidianità della vita del lab, causa sedi distaccate, è sempre stato bello confrontarsi con voi su argomenti scientifici e non (e questo vale tutt'ora).

Grazie a Mario, il mio primo (e per ora unico) studente - sei stato veramente di grande aiuto per me e per il mio lavoro. Il tuo carattere gioioso ha reso più allegre le giornate in lab, e questo non è da poco, e non da meno sono stati i dolci fantastici con cui ci hai deliziato.

Voglio ringraziare tutti quelli con cui ho lavorato/collaborato in questi anni e, in particolare, quelle persone che, da più o meno lontano, si sono continuate a dimostrare sempre pronte ad un consulto scientifico e ad uno scambio di saluti e idee, tra cui Patrizia, Elena, Lara, Lucia, Rossana, Laura, Gonzalo, Sara, Diego, Emilie, Andrea…

Grazie al Prof. Biondi e ad Elisabetta Paccagnini, perchè hanno saputo organizzare al meglio il programma annuale di questo corso di dottorato, rendendolo assolutamente valido e costruttivo. E… un grazie ai miei colleghi del DIMET, in particolare Alice e Irene – a quando la prossima gita in treno?

Beh… a questo punto credo proprio di poter passare a ringraziare le persone che mi hanno accompagnato in questi tre anni fuori dal lab (eh sì… ho avuto una vita anche fuori dal lab!)

Innanzitutto grazie alla mia stupenda famiglia – più passa il tempo più mi rendo conto di quanto siete i genitori e i fratelli migliori che mi sarebbero potuti capitare. Non vi cambierei mai!

Un grazie ai miei parenti, zie, zii, cugini e cugine con mariti/fidanzati e figli - Siete persone splendide con le quali è sempre piacevole condividere momenti di vita! Un pensiero va anche a chi, purtroppo, in questi anni è mancato… Nonna e zii… siete e sarete sempre nel mio cuore. Grazie per tutto quello che avete fatto per me!

Un grazie ai miei veri amici, con cui ho vissuto attimi indimenticabili: Tania (più che attimi… l'amicizia di una vita); Lucia, Gabriele, Alessio, Luciano (il nostro viaggio in Argentina è stato un'avventura veramente fantastica, unica, irripetibile); Adriana & Carlo, Veronica & Enrico, Serena & Mauro... grazie per tutte le volte che vi ho sentiti vicini, siete fantastici.

E… per concludere in bellezza… un immenso grazie a Dario, per tutto, perché "You're simply the best, Better than all the rest, Better than anyone, Anyone I've ever met" – Ti amo!